

DTIC FILE COPY

(4)

AD-A201 894

RD & E

C E N T E R

Technical Report

No. 13337

FAILURE ANALYSIS OF THE LOWER REAR BALL JOINT ON THE

HIGH-MOBILITY MULTIPURPOSE

WHEELED VEHICLE (HMMWV)

AUGUST 1988

DTIC
ELECTE
NOV 30 1988
S D
E

James Aardema
U.S. Army Tank-Automotive Command
ATTN: AMSTA-RYA
Warren, MI 48397-5000

By

APPROVED FOR PUBLIC RELEASE:
DISTRIBUTION IS UNLIMITED

U.S. ARMY TANK-AUTOMOTIVE COMMAND
RESEARCH, DEVELOPMENT & ENGINEERING CENTER
Warren, Michigan 48397-5000

88 11 30 001

NOTICES

This report is not to be construed as an official Department of the Army position.

Mention of any trade names or manufacturers in this report shall not be construed as an official endorsement or approval of such products or companies by the U.S. Government.

Destroy this report when it is no longer needed. Do not return it to the originator.

Best Available Copy

REPRODUCTION QUALITY NOTICE

This document is the best quality available. The copy furnished to DTIC contained pages that may have the following quality problems:

- **Pages smaller or larger than normal.**
- **Pages with background color or light colored printing.**
- **Pages with small type or poor printing; and or**
- **Pages with continuous tone material or color photographs.**

Due to various output media available these conditions may or may not cause poor legibility in the microfiche or hardcopy output you receive.

☐

If this block is checked, the copy furnished to DTIC contained pages with color printing, that when reproduced in Black and White, may change detail of the original copy.

Unclassified
SECURITY CLASSIFICATION OF THIS PAGE

REPORT DOCUMENTATION PAGE				Form Approved OMB No. 0704-0188		
1a. REPORT SECURITY CLASSIFICATION Unclassified			1b. RESTRICTIVE MARKINGS			
2a. SECURITY CLASSIFICATION AUTHORITY			3. DISTRIBUTION / AVAILABILITY OF REPORT Approved for Public Release: Distribution is Unlimited			
2b. DECLASSIFICATION / DOWNGRADING SCHEDULE						
4. PERFORMING ORGANIZATION REPORT NUMBER(S)			5. MONITORING ORGANIZATION REPORT NUMBER(S) 13337			
6a. NAME OF PERFORMING ORGANIZATION U.S. Army Tank-Automotive Command		6b. OFFICE SYMBOL (If applicable) AMSTA-RY	7a. NAME OF MONITORING ORGANIZATION U.S. Army Tank-Automotive Command			
6c. ADDRESS (City, State, and ZIP Code) Warren, MI 48397-5000			7b. ADDRESS (City, State, and ZIP Code) Warren, MI 48397-5000			
8a. NAME OF FUNDING / SPONSORING ORGANIZATION		8b. OFFICE SYMBOL (If applicable)	9. PROCUREMENT INSTRUMENT IDENTIFICATION NUMBER			
8c. ADDRESS (City, State, and ZIP Code)			10. SOURCE OF FUNDING NUMBERS			
			PROGRAM ELEMENT NO.	PROJECT NO.	TASK NO.	WORK UNIT ACCESSION NO.
11. TITLE (Include Security Classification) Failure Analysis of the Lower Rear Ball Joint on the High-Mobility Multipurpose Wheeled Vehicle (HMMWV)						
12. PERSONAL AUTHOR(S)						
13a. TYPE OF REPORT Final		13b. TIME COVERED FROM 87 May TO 87 Oct		14. DATE OF REPORT (Year, Month, Day) 1988 August		15. PAGE COUNT
16. SUPPLEMENTARY NOTATION						
17. COSATI CODES			18. SUBJECT TERMS (Continue on reverse if necessary and identify by block number)			
FIELD	GROUP	SUB-GROUP	Simulation, DADS, HMMWV, Suspension, Ball Joints, Dynamics.			
19. ABSTRACT (Continue on reverse if necessary and identify by block number)						
<p>Tests of the HMMWV M1037 S-250 Shelter Carrier conducted at Aberdeen Proving Grounds (APG) and the Nevada Automotive Test Center (NATC) have resulted in failures of the lower rear ball joints. A three-dimensional computer model of the HMMWV Shelter Carrier, including all suspension and steering components, was developed using the DADS methodology to calculate the position, velocity, and acceleration as well as the forces and torques at critical points on the vehicle and at suspension elements while the vehicle is negotiating the NATC course. The results give the magnitude of the forces acting on the joint and also provide the scenario of leading to the failure.</p> <p>The joint angle between the ball joint stud and the ball joint housing was calculated to determine if an interference condition occurred.</p>						
20. DISTRIBUTION / AVAILABILITY OF ABSTRACT <input checked="" type="checkbox"/> UNCLASSIFIED/UNLIMITED <input type="checkbox"/> SAME AS RPT. <input type="checkbox"/> DTIC USERS				21. ABSTRACT SECURITY CLASSIFICATION Unclassified		
22a. NAME OF RESPONSIBLE INDIVIDUAL James Aardema				22b. TELEPHONE (Include Area Code) (313) 574-5032		22c. OFFICE SYMBOL AMSTA-RYA

TABLE OF CONTENTS

Section	Page
1.0. INTRODUCTION.....	12
2.0. OBJECTIVE.....	13
3.0. CONCLUSION.....	14
4.0. RECOMMENDATIONS.....	14
5.0. DISCUSSION.....	15
5.1. <u>Vehicle Description</u>	15
5.2. <u>Vehicle Properties</u>	15
5.2.1. Weight.....	18
5.2.2. CG.....	18
5.2.3. Moment of Inertia.....	18
5.3. <u>Suspension</u>	18
5.3.1. Suspension Description.....	18
5.3.2. Wheel Kingpin Inclination.....	18
5.3.3. Wheel Caster.....	27
5.3.4. Wheel Camber.....	27
5.3.5. Wheel Alignment.....	29
5.3.6. Springs.....	29
5.3.7. Shock Absorbers.....	34
5.3.8. Friction.....	39
5.3.9. Auxiliary Roll Stiffness.....	40
5.3.10. Tires.....	40
5.3.11. Run Flat Device.....	42
5.3.12. Ball Joints.....	42
5.4. <u>Steering</u>	44
5.4.1. Steering Description.....	44
5.5. <u>Terrain</u>	44
5.5.1. Course Profile Description.....	44
5.6. <u>Dynamic Analysis</u>	44
5.6.1. HMMWV Model.....	50
5.6.2. Program Enhancements.....	50
5.6.3. Post Processing.....	50
5.6.4. Dynamic Results.....	56
5.7. <u>Static Analysis</u>	127
5.7.1. Heavy Duty Right Rear Suspension Model.....	127
5.7.2. Results.....	138
LIST OF REFERENCES.....	145
SELECTED BIBLIOGRAPHY.....	147
APPENDIX A. MONROE AUTO EQUIPMENT SHOCK ABSORBER TEST REPORT LO1349.....	A-1

TABLE OF CONTENTS (Continued)

Section	Page
APPENDIX B. UNIVERSITY OF MICHIGAN TRANSPORTATION INSTITUTE LETTER DATED July 23, 1985.....	B-1
APPENDIX C. GOODYEAR TIRE DATA.....	C-1
APPENDIX D. NATC TERRAIN DATA.....	D-1
APPENDIX E. DYNAMIC ANALYSIS VEHICLE INPUT DATA FILE.....	E-1
APPENDIX F. STATIC ANALYSIS INPUT DATA FILE.....	F-1
DISTRIBUTION LIST.....	Dist-1



Accession For	
NTIS GRA&I	<input checked="" type="checkbox"/>
DTIC TAB	<input type="checkbox"/>
Unannounced	<input type="checkbox"/>
Justification	
By	
Distribution/	
Availability Codes	
Dist	Avail and/or Special
A-1	

LIST OF ILLUSTRATIONS

Figure	Title	Page
5-1.	HMMWV M1037 and M1042 S250 Shelter Carriers.....	17
5-2.	Front Left Suspension, Front View.....	21
5-3.	Front Left Suspension, Left Side View.....	22
5-4.	Front Left Suspension, Top View.....	23
5-5.	Rear Left Suspension, Rear View.....	24
5-6.	Rear Left Suspension, Left Side View.....	25
5-7.	Rear Left Suspension, Top View.....	26
5-8.	Static Toe Angle Calculations.....	32
5-9.	Front Shock Absorber Curve.....	37
5-10.	Heavy Duty Rear Shock Absorber Curve.....	38
5-11.	Longitudinal Slip Versus Longitudinal Force Coefficient Curve.....	43
5-12.	Steering Left Side, Top View.....	46
5-13.	Steering Right Side, Top View.....	47
5-14.	Steering Left Side View.....	48
5-15.	Steering Stops.....	49
5-16.	Chassis CG Vertical Position.....	57
5-17.	Chassis CG Vertical Global Velocity.....	58
5-18.	Chassis CG Vertical Global Acceleration.....	59
5-19.	Chassis Global Pitch Angle.....	60
5-20.	Chassis Pitch Local Velocity.....	61
5-21.	Chassis Pitch Local Acceleration.....	62
5-22.	Chassis Global Roll Angle.....	63
5-23.	Chassis Roll Local Velocity.....	64

LIST OF ILLUSTRATIONS (Continued)

Figure	Title	Page
5-24.	Chassis Roll Local Acceleration.....	65
5-25.	Chassis Global Yaw Angle.....	67
5-26.	Chassis Yaw Local Velocity.....	68
5-27.	Chassis Yaw Local Acceleration.....	69
5-28.	Front Left Spring Force.....	70
5-29.	Front Right Spring Force.....	71
5-30.	Rear Left Spring Force.....	72
5-31.	Rear Right Spring Force.....	73
5-32.	Front Left Shock Length.....	74
5-33.	Front Right Shock Length.....	75
5-34.	Rear Left Shock Length.....	76
5-35.	Rear Right Shock Length.....	77
5-36.	Front Left Shock Metal to Metal Force.....	78
5-37.	Front Right Shock Metal to Metal Force.....	79
5-38.	Rear Left Shock Metal to Metal Force.....	80
5-39.	Rear Right Shock Metal to Metal Force.....	81
5-40.	Front Left Shock Velocity.....	82
5-41.	Front Right Shock Velocity.....	83
5-42.	Rear Left Shock Velocity.....	84
5-43.	Rear Right Shock Velocity.....	85
5-44.	Front Left Shock Force.....	86
5-45.	Front Right Shock Force.....	87
5-46.	Rear Left Shock Force.....	88
5-47.	Rear Right Shock Force.....	89

LIST OF ILLUSTRATIONS (Continued)

Figure	Title	Page
5-48.	Front Left Tire Deflection.....	90
5-49.	Front Right Tire Deflection.....	91
5-50.	Rear Left Tire Deflection.....	92
5-51.	Rear Right Tire Deflection.....	93
5-52.	Front Left Tire Run Flat Force.....	95
5-53.	Front Right Tire Run Flat Force.....	96
5-54.	Rear Left Tire Run Flat Force.....	97
5-55.	Rear Right Tire Run Flat Force.....	98
5-56.	Front Left Tire Normal Force.....	99
5-57.	Front Right Tire Normal Force.....	100
5-58.	Rear Left Tire Normal Force.....	101
5-59.	Rear Right Tire Normal Force.....	102
5-60.	Front Left Tire Slip Angle.....	103
5-61.	Front Right Tire Slip Angle.....	104
5-62.	Rear Left Tire Slip Angle.....	105
5-63.	Rear Right Tire Slip Angle.....	106
5-64.	Front Left Tire Lateral Force.....	107
5-65.	Front Right Tire Lateral Force.....	108
5-66.	Rear Left Tire Lateral Force.....	109
5-67.	Rear Right Tire Lateral Force.....	110
5-68.	Upper Front Left Ball Joint Tensile Force.....	111
5-69.	Upper Front Left Ball Joint Shear Force.....	112
5-70.	Upper Front Right Ball Joint Tensile Force.....	113
5-71.	Upper Front Right Ball Joint Shear Force.....	114

LIST OF ILLUSTRATIONS (Continued)

Figure	Title	Page
5-72.	Upper Rear Left Ball Joint Tensile Force.....	115
5-73.	Upper Rear Left Ball Joint Shear Force.....	116
5-74.	Upper Rear Right Ball Joint Tensile Force.....	117
5-75.	Upper Rear Right Ball Joint Shear Force.....	118
5-76.	Lower Front Left Ball Joint Tensile Force.....	119
5-77.	Lower Front Left Ball Joint Shear Force.....	120
5-78.	Lower Front Right Ball Joint Tensile Force.....	121
5-79.	Lower Front Right Ball Joint Shear Force.....	122
5-80.	Lower Rear Left Ball Joint Tensile Force.....	123
5-81.	Lower Rear Left Ball Joint Shear Force.....	124
5-82.	Lower Rear Right Ball Joint Tensile Force.....	125
5-83.	Lower Rear Right Ball Joint Shear Force.....	126
5-84.	Upper Front Left Ball Joint Angle.....	128
5-85.	Upper Front Right Ball Joint Angle.....	129
5-86.	Upper Rear Left Ball Joint Angle.....	130
5-87.	Upper Rear Right Ball Joint Angle.....	131
5-88.	Lower Front Left Ball Joint Angle.....	132
5-89.	Lower Front Right Ball Joint Angle.....	133
5-90.	Lower Rear Left Ball Joint Angle.....	134
5-91.	Lower Rear Right Ball Joint Angle.....	135
5-92.	Static Vertical Tire Force.....	139
5-93.	Static Vertical and Forward Longitudinal Forces.....	140
5-94.	Static Vertical and Rearward Longitudinal Forces.....	141
5-95.	Static Vertical and Outward Lateral Forces.....	142

LIST OF ILLUSTRATIONS (Continued)

Figure	Title	Page
5-96.	Static Vertical and Inward Lateral Forces.....	143
5-97.	Static Vertical, Forward Longitudinal, and Outward Lateral Forces.....	144

LIST OF TABLES

Table	Title	Page
5-1.	HMMWV Weight Characteristics Summary.....	16
5-2.	Weights for Vehicle Components.....	19
5-3.	Vehicle Center of Gravity Location.....	19
5-4.	Chassis Sprung Mass Center of Gravity Location.....	20
5-5.	Vehicle Moments of Inertia.....	20
5-6.	Kingpin Angle and Kingpin Offset.....	28
5-7.	Caster Angle and Caster Offset.....	28
5-8.	Camber Angle.....	30
5-9.	Front Toe-In Alignment Specifications.....	31
5-10.	Rear Toe-Out Alignment Specifications.....	31
5-11.	Static Toe Angle.....	31
5-12.	Spring Usage.....	33
5-13.	Spring Characteristics.....	35
5-14.	Required Order of Body Input Data.....	41
5-15.	Maximum Allowable Ball Joint Angle.....	45
5-16.	Coordinate Reference Frames.....	51
5-17.	DADS Elements.....	52
5-17.	DADS Elements (Continued).....	53
5-18.	Subroutines Modified or Added.....	54
5-18.	Subroutines Modified or Added (Continued).....	55
5-19.	DADS Elements.....	136
5-20.	Static Loading Combinations and Directory Locations.....	137

1.0. INTRODUCTION

This report prepared by the Analytical and Physical Simulation Branch of the System Simulation Division, U.S. Army Tank-Automotive Command (TACOM) details a dynamic analysis of the High-Mobility Multipurpose Wheeled Vehicle (HMMWV). Tests of the HMMWV M1037 S-250 Shelter Carrier conducted at Aberdeen Proving Grounds (APG) and at the Nevada Automotive Test Center (NATC) have resulted in failures of the lower rear ball joints. This ball joint connects the rear wheel assembly to the rear suspension lower control "A" arm. Failure of the joint causes the vehicle to become instantaneously inoperable.

The HMMWV dynamic response resulting from negotiating the bump course used in the NATC tests was analyzed. Analysis of the vehicle's dynamic response included the position, velocity, and acceleration of various parts of the vehicle as well as the forces that act upon the vehicle. Position, velocity, and acceleration provide the complete dynamic history of the vehicle while the forces and torques are used to determine component loading.

Analysis of the HMMWV employs the Dynamic Analysis and Design System (DADS) computer-based methodology to generate and solve the vehicle's equations of motion.

2.0. OBJECTIVE

The objective of the dynamic analysis was to use a three-dimensional computer model of the HMMWV M1037 S-250 Shelter Carrier using the DADS methodology to calculate the position, velocity, and acceleration as well as the forces and torques at critical points on the vehicle and at the suspension elements while the vehicle is negotiating an obstacle course.

The obstacle course at NATC was chosen for the dynamic simulation because of the failures of the rear ball joints while negotiating this course and because the course was surveyed, which gave an accurate geometrical course description. Seven obstacles ranging from 13 to 22 inches high, spaced approximately 1-1/2 to 2 wheel-base lengths apart, comprise the course. The vehicle speed just before entering the test course was approximately 15 miles per hour. This speed was also used during the simulation.

This analysis also calculated the joint angle between the ball joint stud and the housing to determine if interference occurred.

The simulation results provide a dynamic history of the vehicle response while negotiating the course. These results give the magnitude of the forces acting on the joint and also provide the scenario of events leading to the failure.

A static force analysis was also performed on the right rear suspension unit to determine the magnitude of the joint forces under a given loading condition. Forces applied to the wheel included a combination of vertical, lateral, and longitudinal forces acting at the wheel and road interface. The static analysis results provide the sensitivity of the rear suspension unit to externally applied forces.

3.0. CONCLUSION

The dynamic simulation results showed that both the front and the rear wheels left the ground frequently while the HMMWV negotiated the NATC course. Large forces were generated in the suspension elements when the vehicle returned to the ground. Furthermore, greater forces were produced at the right rear suspension unit because the center of gravity (CG) location is rearward and to the right of the vehicle. The large forces are generated when the shock absorber exceeds the travel limits, causing metal-to-metal contact within the internal shock components. Also at this time the tire run-flat insert makes contact with the tire carcass due to large tire deflections. When these events occur the suspension unit is essentially locked up, thus generating large reaction forces.

Simulation results also showed that the largest tensile and shear forces occurred within the right rear ball joint when the right rear wheel strikes the ground after clearing the first obstacle. Video tapes of the tests at NATC showed failure to occur at the same location within the course.

The analysis also showed that the angle between the ball joint stud and the housing did not exceed the recommended angular motion limits and no interference occurred.

The static analysis showed that the rear suspension units are very sensitive to a combination of forward longitudinal forces and outward lateral forces along with the vertical support forces applied to wheel. Under these conditions the magnitude of the shear force component in the lower ball joint increases greatly with only small increases in the externally applied forces. This loading condition could occur when the inside rear wheel leaves the ground while negotiating a turn or a bump and simultaneously power is applied to the wheels. When the wheel returns to the ground, vertical and lateral forces would be created along with a forward longitudinal force due to the power applied to the wheels. Under these conditions large shear forces would be generated in the lower ball joint.

4.0. RECOMMENDATIONS

Based upon the simulation results the following recommendations will improve the life of the ball joint:

- Modify the shock absorber characteristics within the hydraulic bump stop region to provide more dissipative forces. This in turn will decrease the frequency of exceeding the shock travel limits, decrease the velocity of the suspension prior to reaching metal-to-metal contact, and decrease the impact reaction forces if metal-to-metal contact does occur.
- In addition to, or as an alternative to the previous recommendation, install rubber bump stops external to the shock absorber will also decrease the velocity of the suspension elements before the shock makes metal-to-metal contact.
- Modify the size or the stiffness of the run-flat insert. If the run-flat radius were smaller, then the probability of the tire carcass making contact with the device during large tire deflections would decrease. A less stiff or "softer" device would generate smaller reaction forces when contact does occur.
- Distribute the load such that the center of gravity is located closer to the vehicle center thus distributing the forces more evenly between the suspension units.
- Increase the size of the ball joint stud.
- Change the material composition and hardness of the ball joint stud.

5.0. DISCUSSION

5.1. Vehicle Description

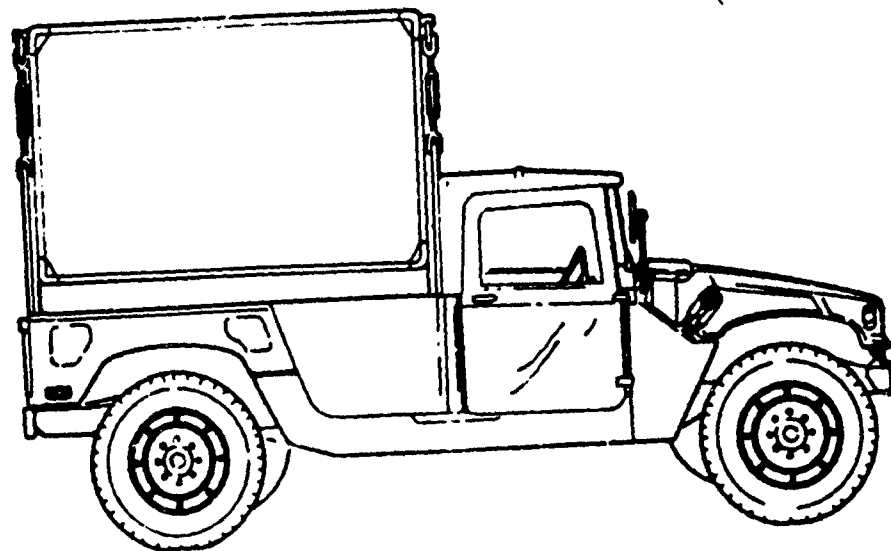
The HMMWV is designed to provide combat, combat support, and combat service support roles. The HMMWV is capable of accepting various body configurations to accommodate weapon systems, 1-1/4-ton utility cargo, and ambulance roles. A high degree of mobility is required in both off-road and on-road travel. The 4X4 wheeled common chassis includes a 145-hp diesel engine, automatic transmission, power steering, and run-flat tires. Table 5-1, supplied by AM General, gives the HMMWV weight characteristics for each model.

The purpose of the M1037 and M1042 models is for securing and transporting the S250 electrical equipment shelter. The M1042 model, which has a winch, can be used for recovery operations. Figure 5-1 shows the M1037 and M1042 models. The M1037 model was used for this analysis.

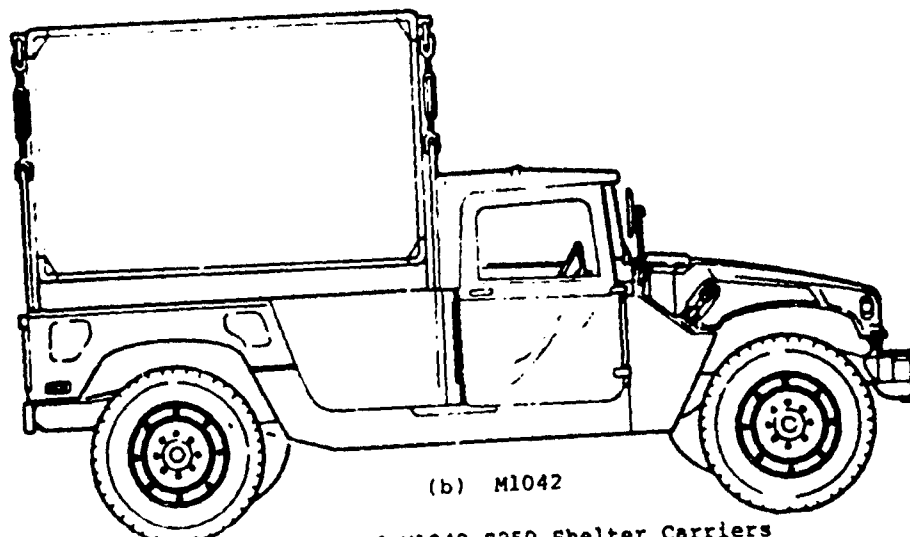
5.2. Vehicle Properties

Table 5-1. HMMWV Weight Characteristics Summary

Model No.	Model Description	Camber of Gravity		Curb Height	Front Axle		Rear Axle		All-terrain Pay Load	Contract Cost
		GVW	GVW		Weight	Netting	Weight	Netting		
4090	Truck, Utility	57.7"	29.9"	5062 Lbs	2900 Lbs	3350 Lbs	2300 Lbs	4350 Lbs	2500 Lbs	7700 Lbs
4090B	Truck, Utility	55.8"	29.7"	5109 Lbs	3052 Lbs	3400 Lbs	2275 Lbs	4300 Lbs	2375 Lbs	7700 Lbs
4090C	Truck, Utility	61.2"	32.6"	5913 Lbs	3111 Lbs	3550 Lbs	2940 Lbs	4650 Lbs	2140 Lbs	8300 Lbs
4090D	Truck, Utility	61.2"	32.6"	6040 Lbs	3170 Lbs	3550 Lbs	2925 Lbs	4640 Lbs	2025 Lbs	8300 Lbs
4090E	Truck, Utility	64.1"	32.9"	6340 Lbs	3046 Lbs	3725 Lbs	3172 Lbs	4675 Lbs	1942 Lbs	8600 Lbs
4090F	Truck, Utility	62.4"	32.3"	6081 Lbs	3060 Lbs	3400 Lbs	3100 Lbs	4080 Lbs	1830 Lbs	8000 Lbs
4090G	Truck, Utility	62.1"	33.1"	5922 Lbs	3060 Lbs	3400 Lbs	3112 Lbs	4080 Lbs	1830 Lbs	8000 Lbs
4090H	Truck, Utility	60.3"	32.9"	5940 Lbs	3060 Lbs	3400 Lbs	3030 Lbs	4340 Lbs	2113 Lbs	8000 Lbs
4090I	Truck, Utility	61.2"	32.9"	6372 Lbs	3046 Lbs	3725 Lbs	3111 Lbs	4675 Lbs	1942 Lbs	8600 Lbs
4090J	Truck, Utility	61.5"	32.6"	6400 Lbs	3030 Lbs	3400 Lbs	3093 Lbs	4300 Lbs	1642 Lbs	8400 Lbs
4090K	Truck, Utility	61.6"	30.4"	5206 Lbs	2834 Lbs	3362 Lbs	2509 Lbs	3234 Lbs	1642 Lbs	8400 Lbs
4090L	Truck, Utility	59.6"	30.3"	5413 Lbs	2834 Lbs	3362 Lbs	2509 Lbs	3234 Lbs	1642 Lbs	8400 Lbs
4090M	Truck, Utility	61.6"	30.4"	5206 Lbs	2834 Lbs	3362 Lbs	2509 Lbs	3234 Lbs	1642 Lbs	8400 Lbs
4090N	Truck, Utility	61.6"	30.4"	5206 Lbs	2834 Lbs	3362 Lbs	2509 Lbs	3234 Lbs	1642 Lbs	8400 Lbs
4090O	Truck, Utility	61.6"	30.4"	5206 Lbs	2834 Lbs	3362 Lbs	2509 Lbs	3234 Lbs	1642 Lbs	8400 Lbs
4090P	Truck, Utility	61.6"	30.4"	5206 Lbs	2834 Lbs	3362 Lbs	2509 Lbs	3234 Lbs	1642 Lbs	8400 Lbs
4090Q	Truck, Utility	61.6"	30.4"	5206 Lbs	2834 Lbs	3362 Lbs	2509 Lbs	3234 Lbs	1642 Lbs	8400 Lbs
4090R	Truck, Utility	61.6"	30.4"	5206 Lbs	2834 Lbs	3362 Lbs	2509 Lbs	3234 Lbs	1642 Lbs	8400 Lbs
4090S	Truck, Utility	61.6"	30.4"	5206 Lbs	2834 Lbs	3362 Lbs	2509 Lbs	3234 Lbs	1642 Lbs	8400 Lbs
4090T	Truck, Utility	61.6"	30.4"	5206 Lbs	2834 Lbs	3362 Lbs	2509 Lbs	3234 Lbs	1642 Lbs	8400 Lbs
4090U	Truck, Utility	61.6"	30.4"	5206 Lbs	2834 Lbs	3362 Lbs	2509 Lbs	3234 Lbs	1642 Lbs	8400 Lbs
4090V	Truck, Utility	61.6"	30.4"	5206 Lbs	2834 Lbs	3362 Lbs	2509 Lbs	3234 Lbs	1642 Lbs	8400 Lbs
4090W	Truck, Utility	61.6"	30.4"	5206 Lbs	2834 Lbs	3362 Lbs	2509 Lbs	3234 Lbs	1642 Lbs	8400 Lbs
4090X	Truck, Utility	61.6"	30.4"	5206 Lbs	2834 Lbs	3362 Lbs	2509 Lbs	3234 Lbs	1642 Lbs	8400 Lbs
4090Y	Truck, Utility	61.6"	30.4"	5206 Lbs	2834 Lbs	3362 Lbs	2509 Lbs	3234 Lbs	1642 Lbs	8400 Lbs
4090Z	Truck, Utility	61.6"	30.4"	5206 Lbs	2834 Lbs	3362 Lbs	2509 Lbs	3234 Lbs	1642 Lbs	8400 Lbs



(a) M1037



(b) M1042

Figure 5-1. HMMWV M1037 and M1042 S250 Shelter Carriers

5.2.1. Weight. The simulated HMMWV M1037-MSE S-250 Shelter Carrier had a reported total gross vehicle weight (GVW) of 8,719 pounds. AM General Division of LTV Aerospace and Defense Company, manufacturers of the vehicle, provided the weights of the suspension components. Table 5-2 gives the weight of the chassis sprung mass and the weight of the suspension elements.

5.2.2. CG. The CG location for the HMMWV M1037-MSE S-250 Shelter Carrier as located from behind the front wheels, the vehicle center, and the ground are given in Table 5-3. By subtracting the weight of each suspension component such as the upper and lower control arms and the wheels, the CG location for the chassis sprung mass was calculated. The calculated chassis sprung mass CG location is given in Table 5-4.

5.2.3. Moment of Inertia. Exact measurements for the moment of inertia for the HMMWV M1037-MSE S-250 Shelter Carrier have not been conducted. However, moment of inertia measurements for the TOW weapons carrier with the TOW system (GVW 6,393 lbs) were conducted during Group 1 vehicle tests. The roll, pitch, and yaw moments of inertia are given in Table 5-5. The moment of inertia for the chassis sprung mass will be less than the total vehicle moment of inertia because the chassis sprung mass does not include the suspension elements. Since the HMMWV shelter carrier has a GVW greater than the TOW weapon carrier, the moments of inertia presented in Table 5-5 were used for the shelter carrier chassis sprung mass.

5.3 Suspension

5.3.1. Suspension Description. Four independent double "A" arm suspension units are used on the HMMWV, one for each wheel. Both the upper "A" arm and the lower "A" arm are attached at the chassis frame and at the wheel assembly. Rear radius rods and front tie rods, connected between the chassis frame and the wheel assembly, control the static toe angle and the wheel steer direction. A coil spring and a shock absorber are mounted between the chassis and each lower control arm. Figures 5-2 through 5-7 show the suspension geometry and dimensions for each front and rear suspension units and the steering components.

5.3.2. Wheel Kingpin Inclination. The kingpin inclination angle is defined as the angle in front elevation between the steering axis and vertical. The kingpin offset is defined as the horizontal distance at the ground in front elevation between the point where the steering axis intersects the ground and the center of tire contact.¹

Kingpin inclination angle provides a self-aligning moment when a wheel is steered. During steering a wheel is turned around the kingpin axis, which causes both sides of the vehicle to lift. This lifting action creates an unstable condition. When the vehicle tries to regain the low, stable position, a self-aligning moment is created. The moments generated are zero at zero steer angle, and with a steer angle, the

Table 5-2. Weights for Vehicle Components

Item	Weight
Chassis Spring Mass	7,747 pounds
Lower Control Arm	36 pounds each
Upper Control Arm	12 pounds each
Wheel Assembly	195 pounds each
Total gross vehicle weight	8,719 pounds

Table 5-3. Vehicle Center of Gravity Location

Direction	Location
Fore-Aft	81.70 inches
Right Side	0.52 inches
Vertical	46.00 inches

Table 5-4. Chassis sprung mass center of gravity location

Direction	Location
Fore-Aft	83.800 inches
Right Side	0.585 inches
Vertical	49.684 inches

Table 5-5. Vehicle moments of inertia

Axis	Inertia
Roll	13,320 lb-inch-sec**2
Pitch	52,680 lb-inch-sec**2
Yaw	56,280 lb-inch-sec**2

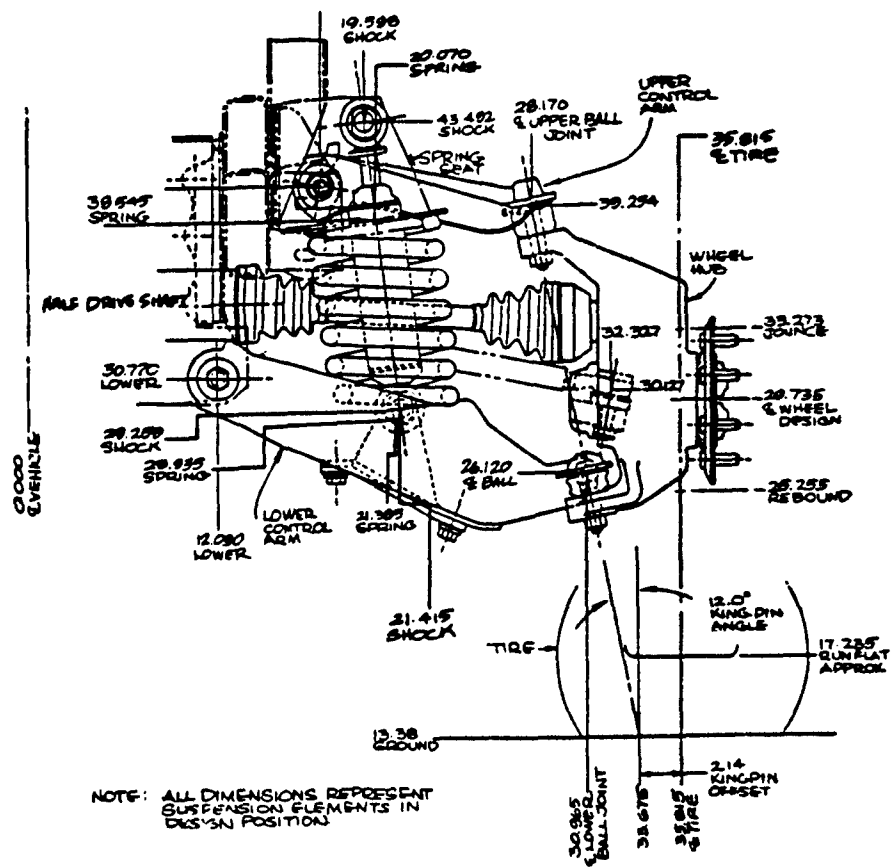
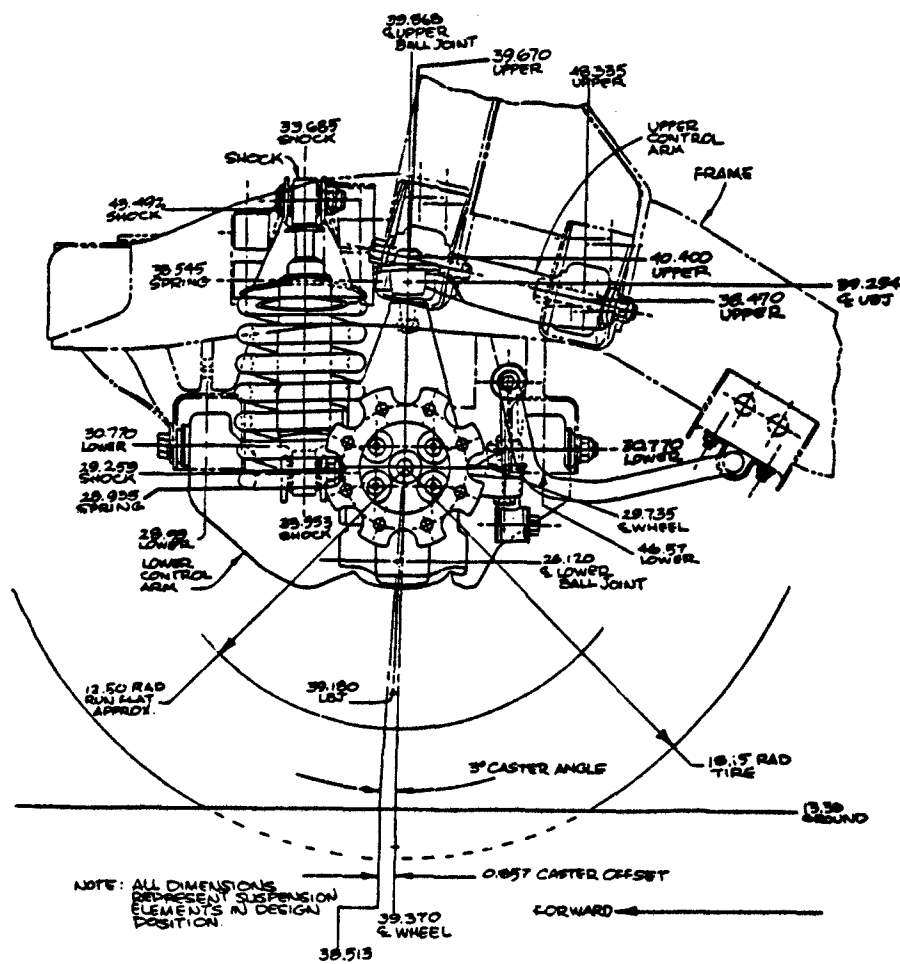


Figure 5-2. Front Left Suspension, Front View



**FRONT LEFT SUSPENSION
LEFT SIDE VIEW**

Figure 5-3. Front Left Suspension, Left Side View

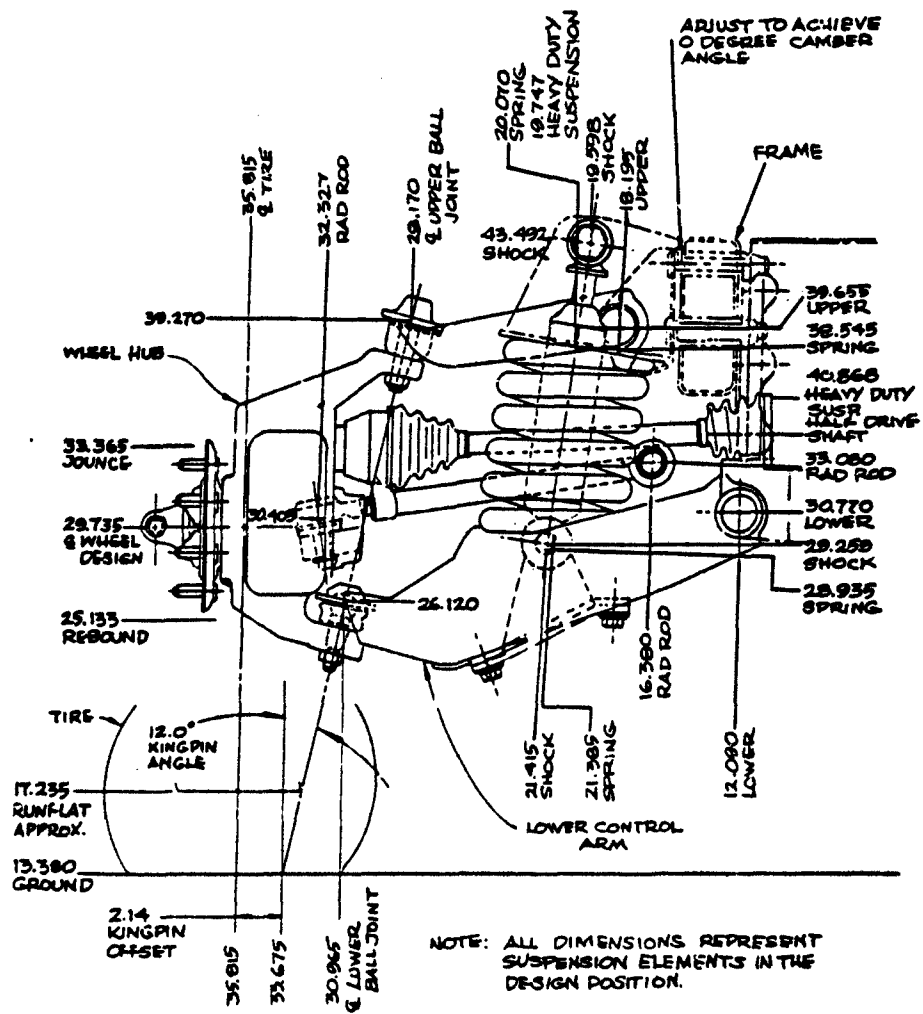


Figure 5-5. Rear Left Suspension, Rear View

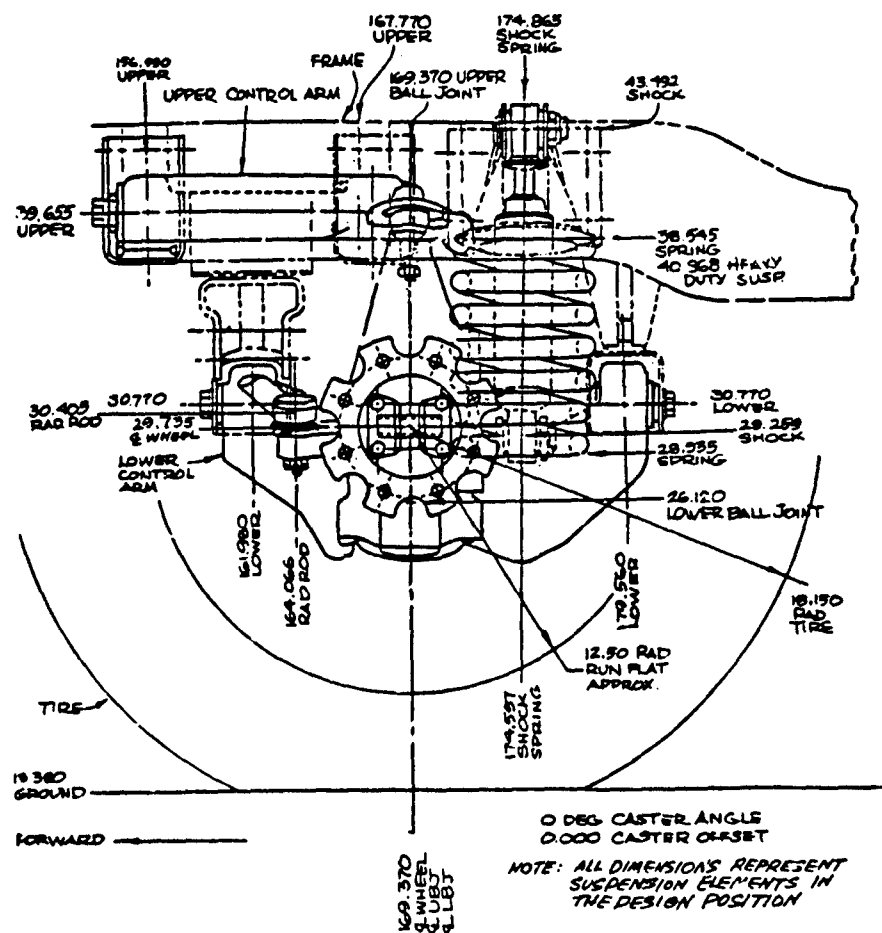


Figure 5-6. Rear Left Suspension, Left Side View

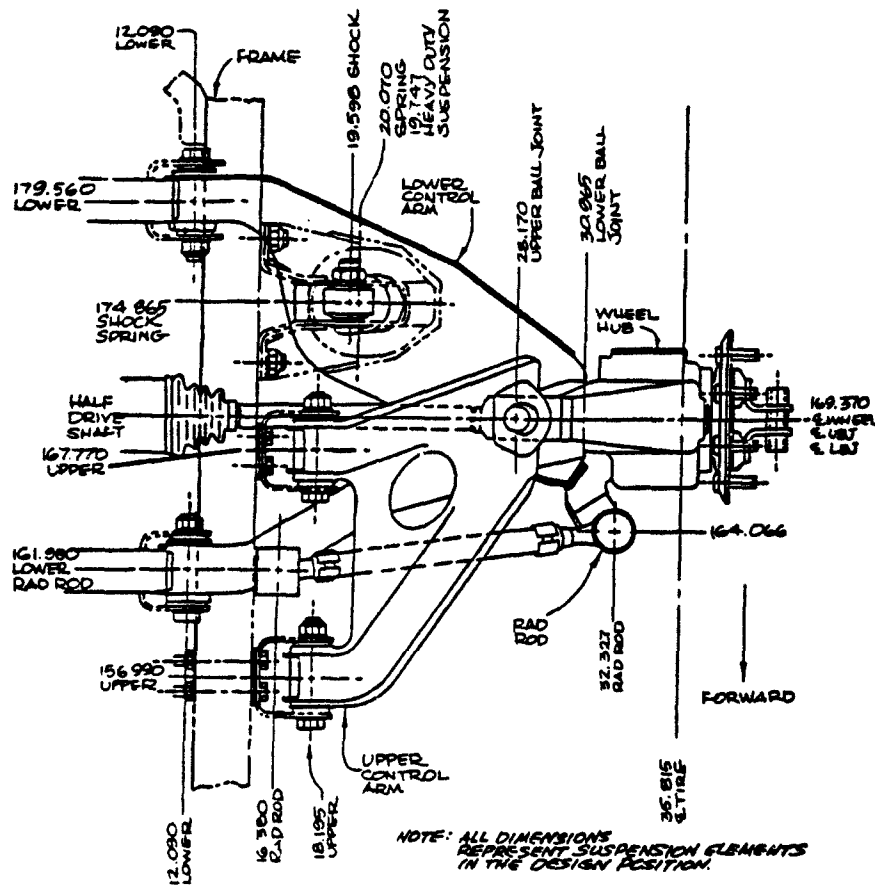


Figure 5-7. Rear Left Suspension, Top View

moments on both the left and right wheels act together. The net centering moment is proportional to the load but independent of the left and right load distribution.²

The actual turning center of a steered wheel is at the kingpin offset point. Steering motion of the wheel around this point requires both wheel sliding and rotation.³

The kingpin inclination angle and the kingpin offset for the HMMWV front and rear suspension units at the design position are given in Table 5-6.

5.3.3. Wheel Caster. Caster angle is defined as the angle in side elevation between the steering axis and vertical. Caster angle is considered positive when the steering axis is inclined rearward (in the upward direction) and negative when the steering axis is inclined forward.⁴

Caster offset is defined as the distance in side elevation between the points where the steering axis intersects the ground and the center of tire contact. The offset is considered positive when the intersection point is forward of the tire contact center and negative when it is rearward.⁵

Caster is used for the self-aligning steering effect it produces. With an applied steer angle, one side of the axle lifts and the other side drops. This axle roll will cause the left and right wheel loads to vary with steer angle in an amount dependent on the roll stiffness at the axle and on other factors. The total caster restoring torque is symmetric about the zero steer angle point and would equal zero if no load imbalance on the wheels is assumed. The total torque at zero steer angle will not be zero if a load imbalance exists, and the vehicle will experience a steering "pull" in normal straight ahead driving. During normal cornering at a given speed, the load transfer to the outside wheel produces a torque, via the caster, which attempts to steer the vehicle into the turn.

The caster angle and the caster offset for the HMMWV front and rear suspension units at the design position are given in Table 5-7. The tolerance on the caster angle given in Table 5-7 is plus or minus 1.5 degrees.

5.3.4. Wheel Camber. Wheel camber angle is defined as the inclination of the wheel plane to vertical. Camber angle is considered positive when the wheel leans outward at the top and negative when it leans inward.

A cambered wheel would follow a circular rolling path if not restricted. However, the direction of travel of a cambered wheel on a vehicle deviates from its natural rolling path, creating a slip angle and consequently a lateral cornering force. Values of this force are relatively small.⁶

Table 5-6. Kingpin Angle and Kingpin Offset

Suspension Unit	Kingpin Angle	Kingpin Offset
Front	12 degrees	2.14 inches
Rear	12 degrees	2.14 inches

Table 5-7. Caster Angle and Caster Offset

Suspension Unit	Caster Angle*	Caster Offset
Front	3 degrees	0.857 inches
Rear	0 degrees	0.000 inches

*Tolerance on the Caster Angle is Plus or Minus 1.5 Degrees

The wheel camber angle has only secondary effects on the steering behavior of a vehicle. A camber angle can be chosen to achieve axial bearing loads and to change the kingpin offset distance. The selection of camber angle is normally dominated by tire wear. Too high a camber angle promotes excessive tire wear.

The camber angle for the HMMWV front and rear suspension units at the design position are given in Table 5-8. The tolerance on the camber angle given in Table 5-8 is plus 1.50 degrees or minus 0.50 degrees.

The camber angle on the HMMWV is adjusted by inserting spacers between the chassis frame and the upper control arm mounting bracket. Adding spacers increases the camber angle while removing spacers decreases the camber angle.

5.3.5. Wheel Alignment. Static toe-in or toe-out of a pair of wheels at a specified wheel load or relative position of the wheel center with respect to the chassis sprung mass is the difference in the transverse distances between the wheel planes taken at the extreme rear and front points of the tire tread. When the distance at the rear of the wheel is greater, the wheels are "toed-in"; and where smaller, the wheels are "toed-out."¹⁰

The wheel toe angle combined with the vehicle drive direction forms a tire slip angle, creating a side-thrust capacity for absorbing side shocks from the road and eliminating steering wheel flutter known as "shimmy." Too-high toe-in angles result in excessive tire wear and high rolling resistance.

The front toe-in alignment specifications and the rear toe-out alignment specifications shown in Table 5-9 and Table 5-10 respectively can be found in Technical Manual TM 9-2320-280-20, pages 8-13 through 8-22.

The wheel toe-in angle and toe-out angle can be calculated from the tire measurements explained in the Technical Manual and shown in Figure 5-8. The tire radius in the free condition is 18.15 inches.

The static toe-in and toe-out angles for the HMMWV front and rear suspension units at the design position are given in Table 5-11. The wheel toe-in angle and the wheel toe-out angle are used as input to the wheel body orientation angle (ANGLE.3) about the global Z axis. The effects of the wheel toe-in or toe-out angle can be seen in the tire slip angles and the resulting lateral forces and aligning torques on each wheel.

5.3.6. Springs. Constant rate coil springs are used in each suspension unit. The springs are placed between the lower control arm and the chassis frame. The spring attachment points are shown in Figures 5-2 through 5-7. Table 5-12 gives the spring usage for several vehicle models. The HMMWV M1037 S-250 Shelter Carrier has a heavy duty rear suspension unit and uses the heavy duty spring (5597913). The chassis

Table 5-8. Camber Angle

Suspension Unit	Camber Angle*
Front	0 degrees
Rear	0 degrees

*Tolerance on the Camber Angle is Plus 1.5 or Minus 0.5 Degrees

Table 5-9. Front Toe-In Alignment Specifications

Vehicle Model	Toe-In
M998, M1025, M1026, M1035 M1038, M1043, M1044	7/16 inch \pm 1/8 inch (11 mm \pm 3 mm)
M966, M996, M997, M1036 M1037, M1042, M1045, M1046	5/16 inch \pm 1/8 inch (8 mm \pm 3 mm)

Table 5-10. Rear Toe-Out Alignment Specifications

Vehicle Model	Toe-Out
M998, M1025, M1026, M1035 M1038, M1043, M1044	7/16 inch \pm 1/8 inch (11 mm \pm 3 mm)
M966, M996, M997, M1036 M1037, M1042, M1045, M1046	5/16 inch \pm 1/8 inch (8 mm \pm 3 mm)

Table 5-11. Static Toe Angle

Suspension Unit	Static Toe	Static Toe Angle
Front	Toe-In 7/16 inch	0.00430 radians
Rear	Toe-Out 7/16 inch	0.00430 radians

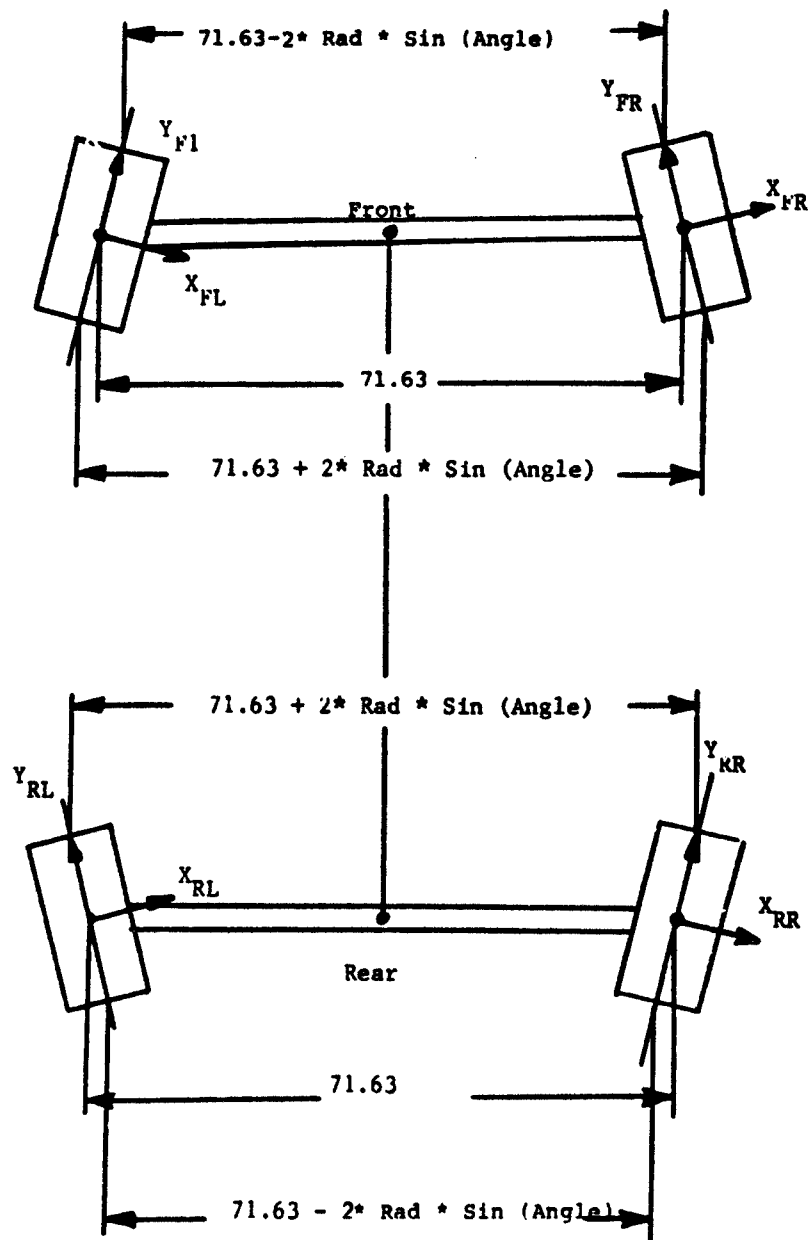


Figure 5-8. Static Toe Angle Calculations

Table 5-12. Spring Usage

Vehicle	Model	Front Springs	Rear Springs
Cargo/Troop Carrier	M998	5579473	5579471
Armament Carrier	M1043	5579473	5579471
TOW W/C	M966	5579473	5579471
S250 Shelter Carrier	M1037	5579473	5597913
Maxi-Ambulance	M997	5579473	5597913
Mini-Ambulance	M996	5579473	5597913
L119 8600 GVW	M998	5594500	5594499
L119 9300 GVW	M998	5594500	5594996

attachment point for the heavy duty rear suspension unit is different from the chassis attachment point for the standard rear suspension units. The front suspension units have spring (5579473). Table 5-13 shows the spring characteristics.

5.3.7. Shock Absorbers. Shock absorbers are used in each suspension unit to provide dissipative forces. The shock absorbers are placed inside the spring elements and are connected between the lower control arms and the chassis frame. The shock absorber attachment points are shown in Figures 5-2 through 5-7. The HMMWV M1037 S-250 Shelter Carrier has heavy duty suspension units in the rear and uses shock absorbers 12340072 (5590597). The front suspension units are equipped with shock absorbers 12340071 (5590327).

The shock absorbers provide a damping force proportional to the relative velocity between the shock piston rod and the shock piston cylinder. The HMMWV shock absorber has three ranges of operation -a midstroke region and two hydraulic bump stop regions. Hydraulic bump stops are built into the shocks near the end of travel in each direction to increase the damping force before metal-to-metal contact occurs.

Shock absorber hydraulic bump stops are engaged at:

COMPRESSED LENGTH AT START OF ENGAGEMENT = 13.76 INCHES
EXTENDED LENGTH AT START OF ENGAGEMENT = 15.85 INCHES

Shock absorber metal-to-metal contact occurs at:

COMPRESSED LENGTH AT METAL TO METAL CONTACT = 12.76 INCHES
EXTENDED LENGTH AT METAL TO METAL CONTACT = 16.48 INCHES

The tolerance on the above dimensions is plus or minus one-eighth of an inch.

When metal-to-metal contact occurs a large force proportional to the metal-to-metal penetration is generated in the shock. Metal-to-metal penetration represents the deflection and the buckling of the internal shock absorber components. The metal-to-metal contact force was calculated using a linear stiffness value of 150,000 lbs per inch of penetration. There are no data or test results to support this stiffness value but this value was assumed and based upon the material yield limits.

The hydraulic bump stops have no stiffness characteristics. If the shock is within the bump stop region and at rest (0 velocity), then there are no forces generated in the shock. The only time the shock can exert a force is when there is a relative velocity or when metal-to-metal contact occurs. When the bump stop region is encountered the shock's effective piston area is increased. As a result of increasing the effective area, the shock damping forces are also increased. Test Report L013497 produced by Monroe Auto Equipment for AM General gives the damping forces

Table 5-13. Spring Characteristics

Spring Number	5579471	5579473	5597913	5594500	5594499	5594996
Location	Rear Normal	Front	Rear Heavy Duty	Front	Rear	Rear
Nominal Spring Rate (lbs/inch)	1,728	954	2,108	954	2,108	2,520
Spring Rate Tolerance (lbs/inch)	69.1	38.2	84.3			
Nominal Design Load (lbs)	4,726	3,491	6,388	2,982	5,705	6,515
Design Load Tolerance (lbs)	94.5	69.8	127.75			
Height at Design Load (inches)	9.70	9.70	12.00	9.70	12.00	12.00
Free Height (inches)	12.43	13.36	15.03	12.93	14.71	14.59
Wire Diameter (inches)	1.044	0.904	1.173	0.904	1.173	1.219
Solid Height	6.50	6.03	8.44			

at three different frequencies throughout each shock absorber region. A copy of the Monroe Test Report L013497 is included in Appendix A.

The shock absorber tests described in Test Report L013497 cycled the shock in each region with a 1.5-inch stroke using a haversine signal input. The haversine signal function used in the test is given by the function:

$$f(x) = 1.50*1/2*(1-\cos(wt))$$

$$f'(x) = 0.75*w*\sin(wt)$$

The maximum velocity obtained by the shock during the test is $(0.75*w)$.

Figure 5-9 shows the resulting force versus velocity curves for the front shock absorber, 12340071, at 30-, 85-, and 170-cycles-per-minute frequency in each operating region. Figure 5-10 shows the resulting force versus velocity curves for the heavy duty rear shock absorber, 12340072, at 30-, 85-, and 170-cycles-per-minute frequency in each operating region. The force values plotted on the curves are the average values obtained during the test and have a tolerance of plus or minus 25%.

The DADS Translational Spring Damper Acuator (TSDA) element was used to model the shock absorber. Since the shock absorber has several operating regions and different damping coefficients in each region, the DADS code had to be expanded to perform the correct calculations for each operating region. Subroutine FRC10.FOR was modified to call USER_TSDA.FOR. Shock calculations were performed in the USER_TSDA.FOR routine. The logic of USER_TSDA.FOR routine requires that the spring and shock input data in the *.FM3 file be entered in a specified order. The four springs must be defined in TSDA elements 1 through 4. The front shock absorbers must be defined in TSDA elements 5 and 6 while the rear shock absorbers must be defined in TSDA elements 7 and 8.

The function routine called CUBIC1.FOR was written to provide a smooth transition, within the tolerance of the shock absorber, between the three operating regions. The discontinuities between the operating regions severely slow down the numerical integration algorithm by forcing it to take smaller step sizes at the discontinuity. The use of CUBIC1 speeds up the simulation.

The properties of the CUBIC1 function are as follows:

$$\begin{aligned}f(0) &= 0.0 \\f(1) &= 1.0 \\f'(0) &= f'(1) = 0.0\end{aligned}$$

The CUBIC1 function used to model the transitions between the different operating regions is derived below.

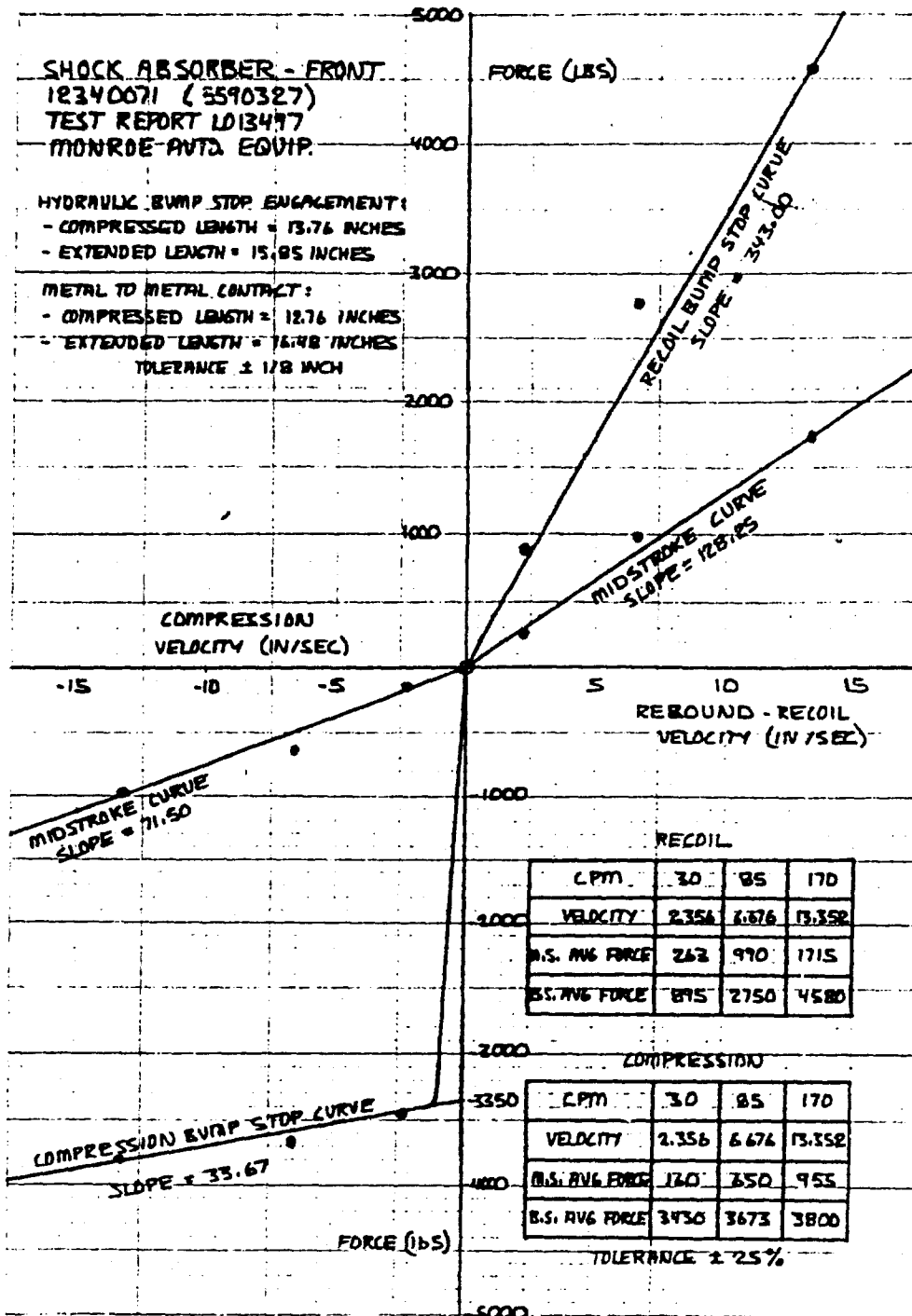


Figure 5.9. Front Shock Absorber Curve

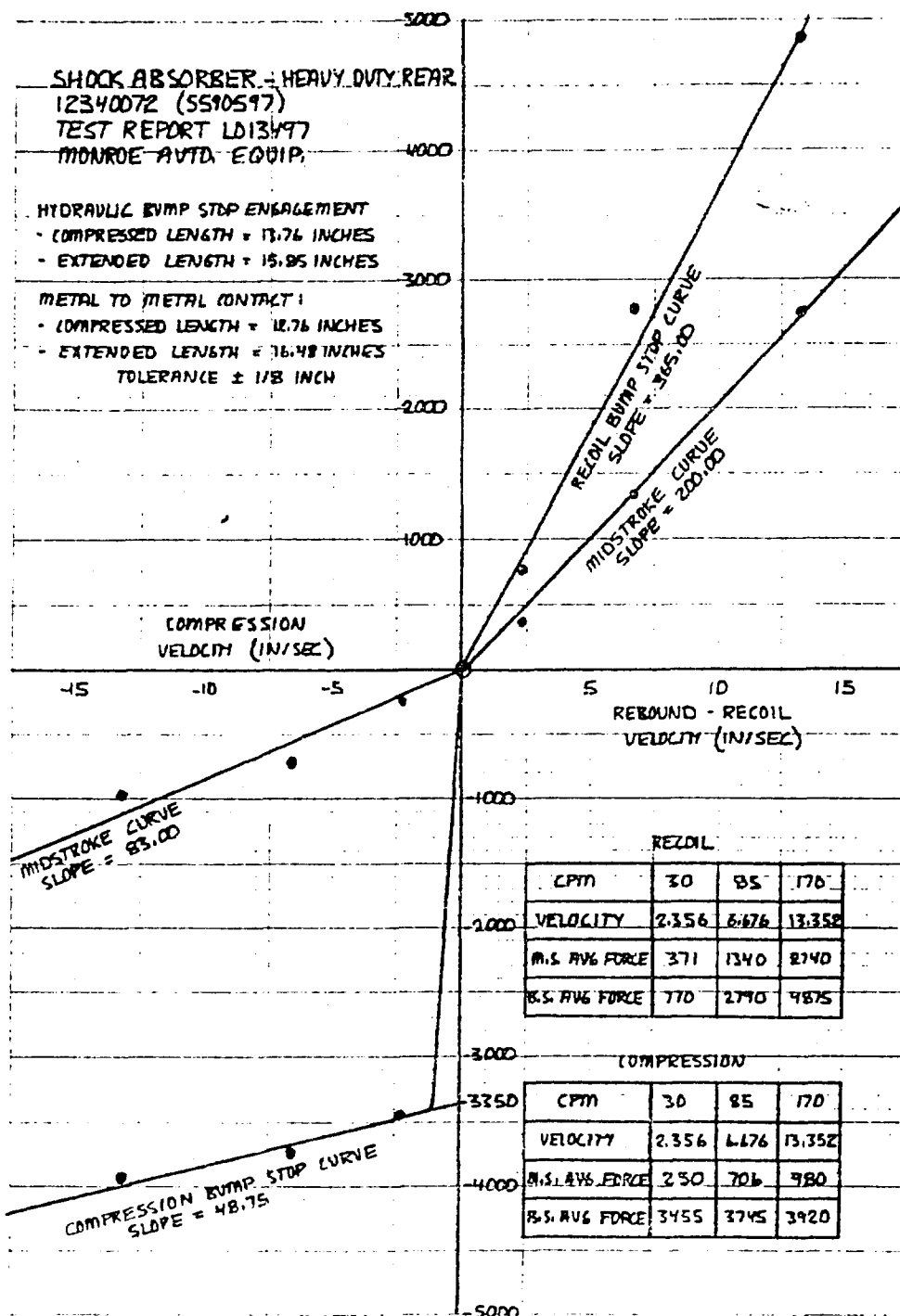


Figure 5.10. Heavy Duty Rear Shock Absorber Curve

$$f(x) = a(x^{**3}) + b(x^{**2}) + cx + d$$

$$f'(x) = 3a(x^{**2}) + 2bx + c$$

$$f(0) = 0 = d$$

$$f(1) = a + b + c = 1$$

$$f'(0) = 0 = c$$

$$f'(1) = 3a + 2b = 0$$

$$b = 3$$

$$a = -2$$

The resulting function is shown below.

$$\text{CUBIC1: } f(x) = -2(x^{**3}) + 3(x^{**2}) \text{ for } 0 \leq x \leq 1$$

$$f'(x) = -6(x^{**2}) + 6(x) \text{ for } 0 \leq x \leq 1$$

5.3.8. Friction. Coulomb friction in the suspension units plays a role in the suspension forces and was included in the HMMWV model. The friction forces for each suspension unit were assumed to act along the shock absorber. These forces were calculated in subroutine USER TSDA.FOR and added to the system in the TSDA element describing each shock absorber. The University of Michigan Transportation Research Institute (UMTRI) conducted a parameter measurement study of a HMMWV vehicle and found that the coulomb friction in the front suspension unit is 106 lbs and the coulomb friction in the rear suspension unit is 112 lbs. Because the friction forces act in different directions depending on the direction of motion, coulomb friction was modeled using a cubic function. A copy of the UMTRI test results is given in Appendix B.

The function routine CUBIC.FOR was written to model coulomb friction. This type of force, like other frictional forces, is not linear and is independent of the contact area and the magnitude of the relative velocity as long as motion exists.

The properties of the CUBIC function are as follows:

$$f(-1) = -1.0$$

$$f(0) = 0.0$$

$$f(1) = 1.0$$

$$f'(-1) = f'(1) = 0.0$$

The CUBIC routine provides a smooth transition between the range $f(-1)$ and $f(1)$. Discontinuities severely slow down the numerical integration algorithm by forcing it to take smaller step sizes at the discontinuity. The use of CUBIC speeds up the simulation by eliminating the discontinuity associated with frictional-type forces.

The CUBIC routine used for modeling coulomb friction is derived below.

$$f(x) = a(x^{**3}) + b(x^{**2}) + cx + d$$

$$f'(x) = 3a(x^{**2}) + 2bx + c$$

$$f(0) = 0 = d$$

$$f(1) = a + b + c = 1$$

$$f(-1) = -a + b - c = -1$$

$$2b = 0$$

$$f'(1) = 3a + c = 0$$

$$f'(-1) = 3a + c = 0$$

$$6a + 2c = 0$$

$$a = -1/2$$

$$c = 3/2$$

$$\text{CUBIC: } f(x) = -1/2(x^{**3}) + 3/2(x) \text{ for } -1 \leq x \leq 1$$

$$f'(x) = -3/2(x^{**2}) + 3/2 \text{ for } -1 \leq x \leq 1$$

5.3.9. Auxiliary Roll Stiffness. A roll stabilization bar is connected between the two front lower control arms. The rear suspension units are not equipped with a roll stabilization bar. A rotation of the vehicle sprung mass about the fore-aft axis with respect to a transverse axis joining the lower control arms at their center of gravity is defined as suspension roll. Given a suspension roll angle, an auxiliary roll stabilization force is generated by the roll stabilization bar at each lower control arm.

Parameter measurements of the HMMWV conducted by UMTRI determined the vertical roll stiffness. At a nominal wheel load of 1,500 pounds the vertical stiffness at the wheel was measured with both the roll stabilization bar active and with the roll stabilization bar disconnected. Comparing the two vertical stiffness, UMTRI determined that the auxiliary roll stiffness at the wheel was 54 pounds per inch. A copy of the UMTRI test results is given in Appendix B.

The roll stabilization bar calculations are performed in the DADS TACOM-TIRE force element subroutine FRC36.FOR. The logic of FRC36.FOR routine requires that the chassis and front lower control arms input data in the *.FM3 file be entered in the order specified in Table 5-14.

Subroutine FRC36.FOR also requires that the Auxiliary roll stiffness dimensions be given as pounds of force per suspension roll in radians at the lower control arm center of gravity.

5.3.10. Tires. For this analysis Goodyear bias-type tires 36X12.50 LT Wrangler II were used. Tire pressures of 20 pounds per square inch (psi) on the front and 30 psi on the rear are maintained on the HMMWV 1037 S250 Shelter Carrier Vehicle. Goodyear Tire Company provided the Tire Normal Force Displacement Curve, the Lateral Force versus Slip Angle and

Table 5-14. Required Order of Body Input Data

Body Element Number	Element Name
1	Chassis
2	Lower Front Left Control Arm
3	Lower Front Right Control Arm

Vertical Load Curve, and the Aligning Torque versus Slip Angle and Vertical Load Curve at several operating pressures. All of this data are included in Appendix C. The vertical load curves at 20 psi and 30 psi were used in this analysis. The lateral force and aligning torque curves were not used in this analysis because the data was only measured up to 6 degrees of tire slip. For this analysis tire slip angles may reach 12 degrees or more and it is not valid to extrapolate the data to that degree.

Lateral tire force characteristics were also measured by UMTRI and are given in Appendix B. The lateral force data measured by UMTRI are valid up to 16 degrees of tire slip. For this reason the UMTRI lateral force data were used for this analysis. Unfortunately UMTRI did not measure tire aligning torque characteristics, therefore the aligning torque data was set to zero for this analysis.

Longitudinal forces for the turning wheel are based upon longitudinal tire slip and vertical normal force. When the tire is rolling more rapidly or less rapidly than the angular spin velocity then a longitudinal slip is generated. Tire slip means that this tire is being distorted and does not necessarily imply that sliding exists between the tire tread rubber and the roadway. The longitudinal force coefficient curve relating the ratio between longitudinal force and vertical normal force to longitudinal slip is shown in Figure 11.

The DADS TACOM-TIRE element, module 36, was used to model the tire. The tire force calculations are performed in the subroutine TIREF.FOR. These forces were then transferred to FRC36.FOR where they were appended to their respective body elements.

5.3.11. Run-Flat Device. Run-flat devices are inserted inside each wheel to allow operation of the vehicle in case of a flat tire. The run-flat system consists of a two-piece, bolt-on die cast magnesium inner tire support. The surface acting as a support during run-flat conditions is 3.5 inches wide. The run-flat device radius is approximately 12.50 inches. The free radius of the tire is 18.15 inches. Assuming that the tire carcass is 1 inch thick, a tire deflection of more than 4.65 inches would create contact between the run-flat insert device, the tire carcass, and the road. When contact occurs the run-flat device would generate forces proportional to the penetration into the run-flat device to help support the vehicle.

The stiffness of the run-flat device was assumed to be 10,000 pounds per inch of penetration and the dissipative forces associated with the device were assumed to be zero. The run-flat calculations are performed in subroutine TIREF.FOR.

5.3.12. Ball Joints. To determine if the ball joint stud made an interference contact with the ball joint housing, the relative angle between the ball joint housing and the ball joint stud was calculated.

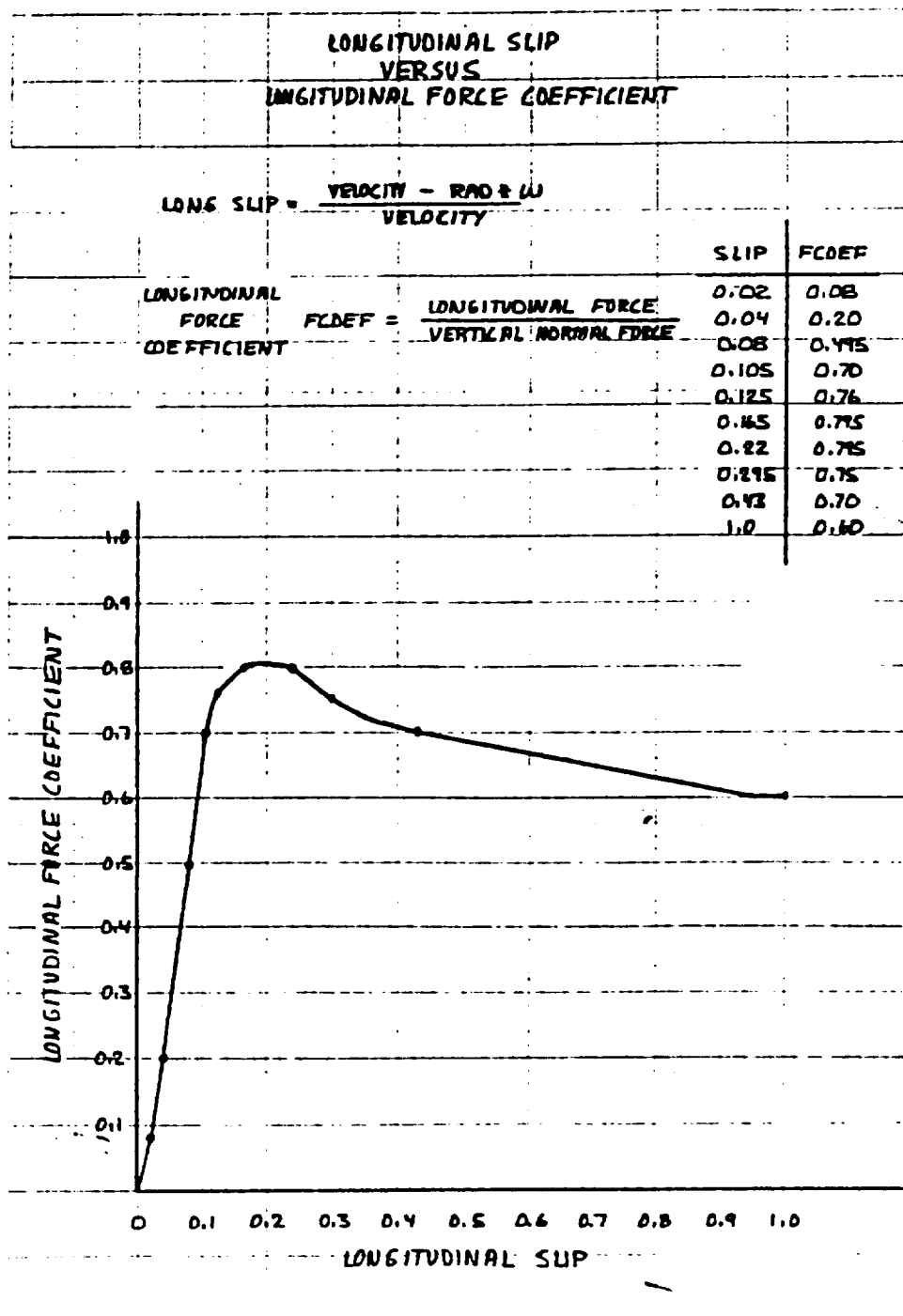


Figure 5-11. Longitudinal Slip Versus Longitudinal Force Coefficient Curve

The maximum allowable angle between the stud and housing for the upper and lower joints is given in Table 5-15.

The DADS spherical joint element was used to calculate the relative angle between the stud and the housing. A unit joint axis on the control arm was defined to be perpendicular to the ball joint housing. With the suspension unit in the design position, this unit joint axis represents a global rotation of 12.00 degrees and a rotation of 3.00 degrees. A unit joint axis on the ball joint stud or wheel hub assembly was defined along the kingpin axis. Since both joint axis are unit vectors, taking the dot product between the housing joint axis and the stud joint axis will determine the relative angle. The DADS code was expanded to calculate the relative angle. The subroutine MM15.FOR was modified to call FRC15.FOR. Subroutine FRC15.FOR uses the joint axis to calculate the relative joint angle.

If the forces in the spherical joints are calculated in the joint coordinate system described above, then the forces along the unit joint axis on the ball joint stud would represent tensile or compression loading. Shear force can be calculated from the force components perpendicular to the ball joint stud axis.

5.4. Steering

5.4.1. Steering Description. The HMMWV is equipped with power assisted steering. The power steering assembly is located at the left-hand side. The power steering pump is a Saginaw Steering Gear model 125. The power steering pump is a belt driven vane-type pump with a rated capacity of 2.6 GPM at 1,500 rpm. The steering gear make and model is Saginaw Steering Gear model 708. The steering gear is a recirculating ball, worm, and nut device with a 13/16:1 ratio. Figures 5-12 through 5-14 show the steering geometry and dimensions.

Steering limits are determined by steering stops located on the wheel hub assembly and the lower control arm. Steering stops are adjusted to limit steering at 36.00 degrees for the inside steered wheel. Figure 5-15, taken from TM 9-2320-280-20, pages 6-36 and 6-37, shows the steering stop angle.

For this analysis the steering input command was constantly equal to zero throughout the simulation.

5.5. Terrain

5.5.1. Course Profile Description. Vehicle tests at NATC were conducted over a manmade test course with seven obstacles. A survey of the test course profile is given in Appendix D. This NATC course profile description was used for this HMMWV ball joint analysis.

5.6. Dynamic Analysis

Table 5-15. Maximum Allowable Ball Joint Angle

Ball Joint	Maximum Allowable Angle
Lower	19.5 Degrees
Upper	30.0 Degrees

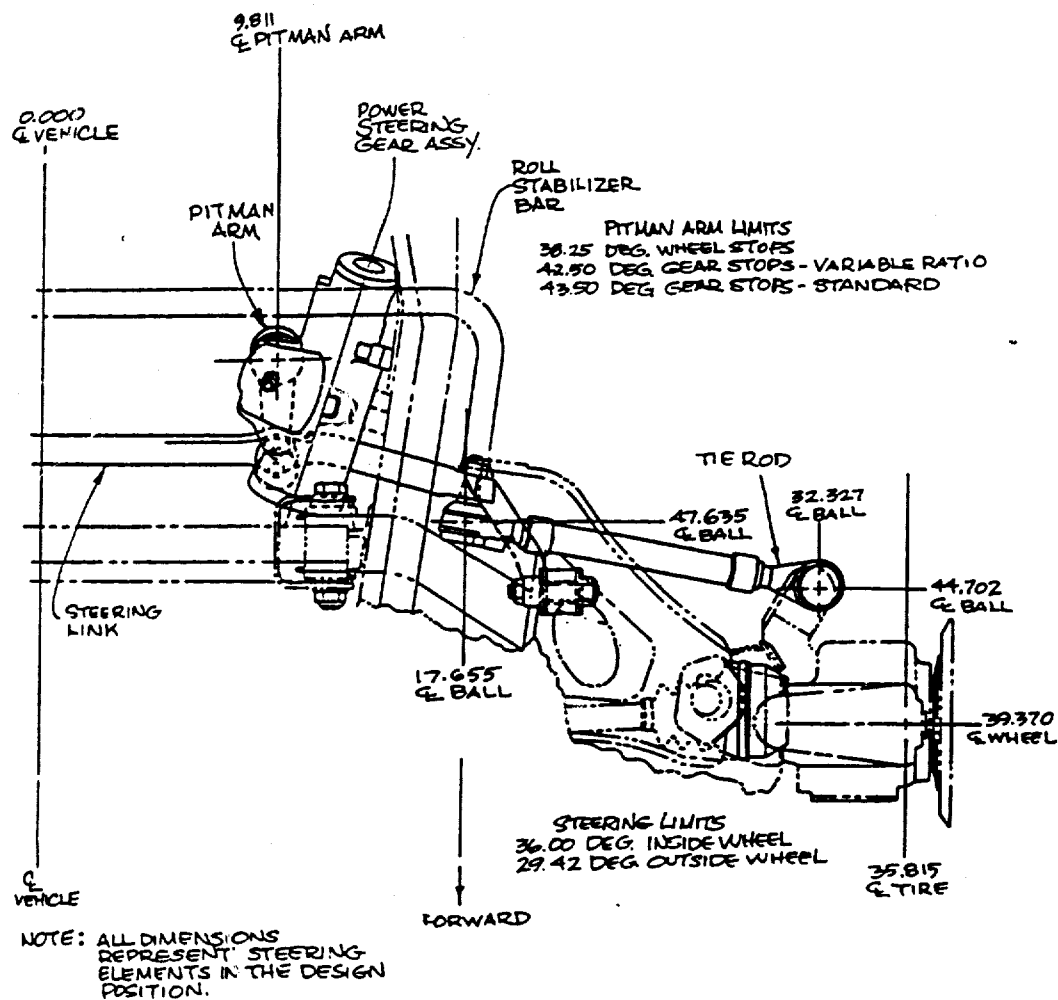


Figure 5-12. Steering Left Side, Top View

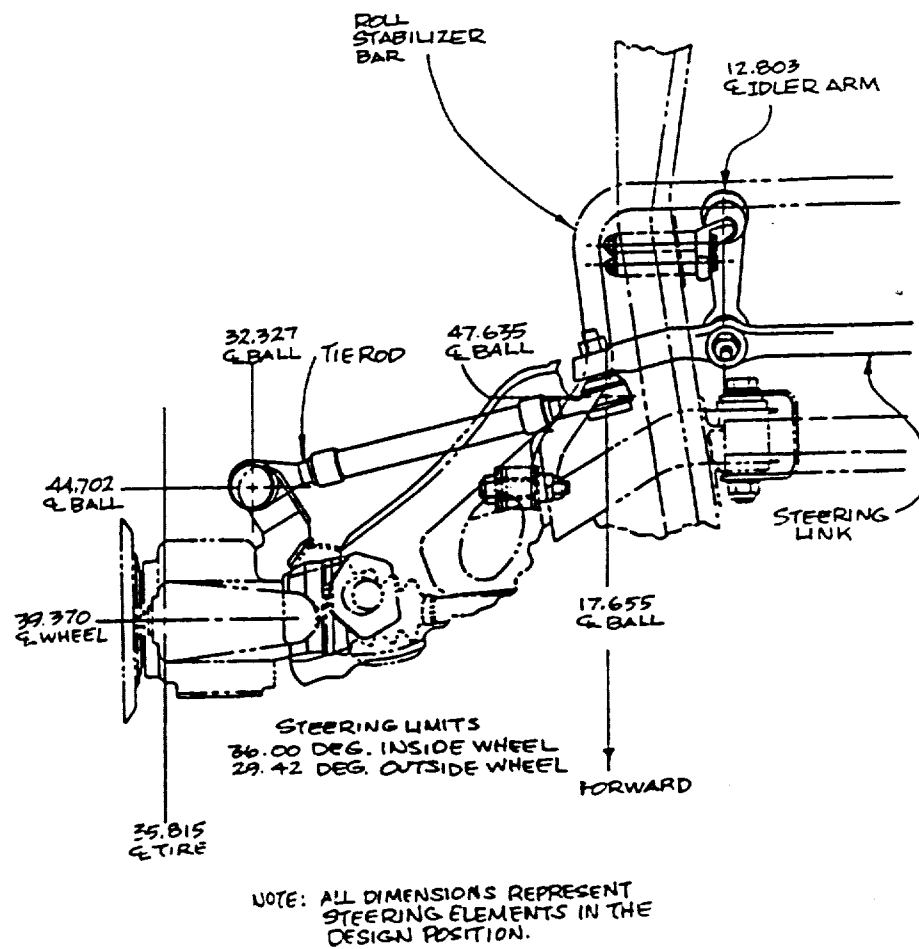
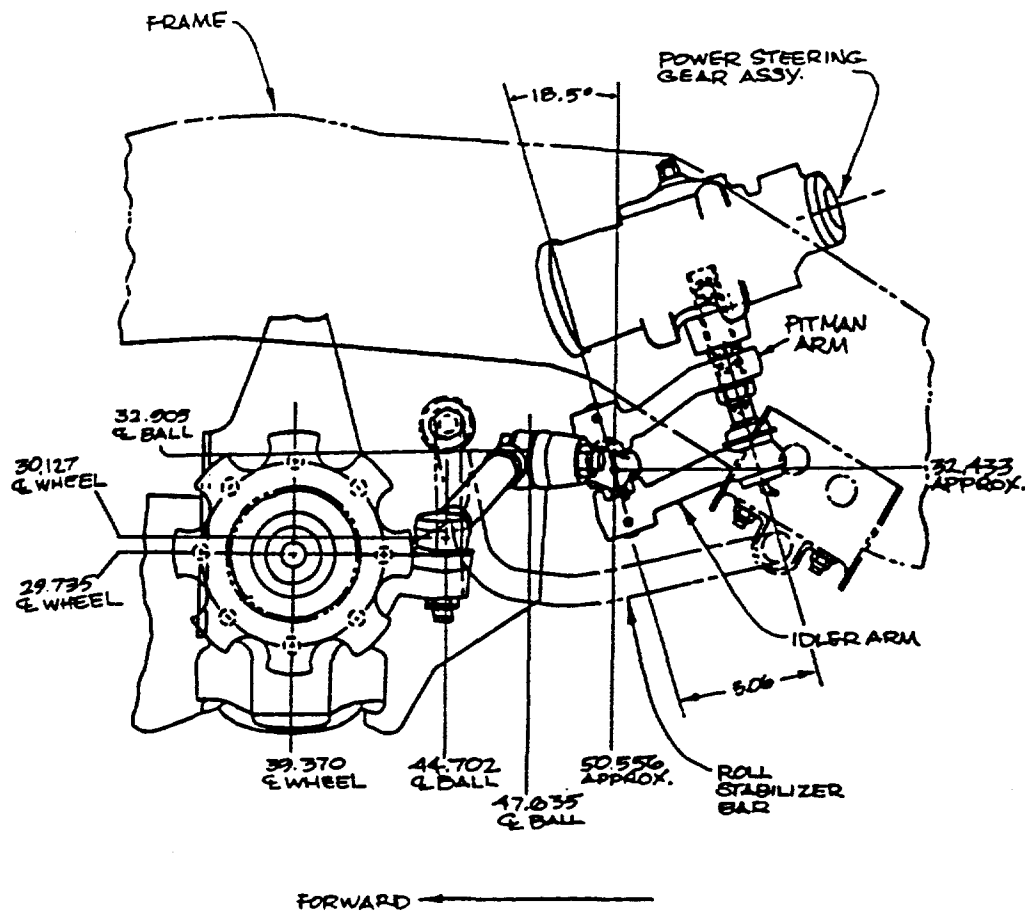


Figure 5-13. Steering Right Side, Top View



NOTE: ALL DIMENSIONS REPRESENT ELEMENTS
IN THE DESIGN POSITION.

Figure 5-14. Steering, Left Side View

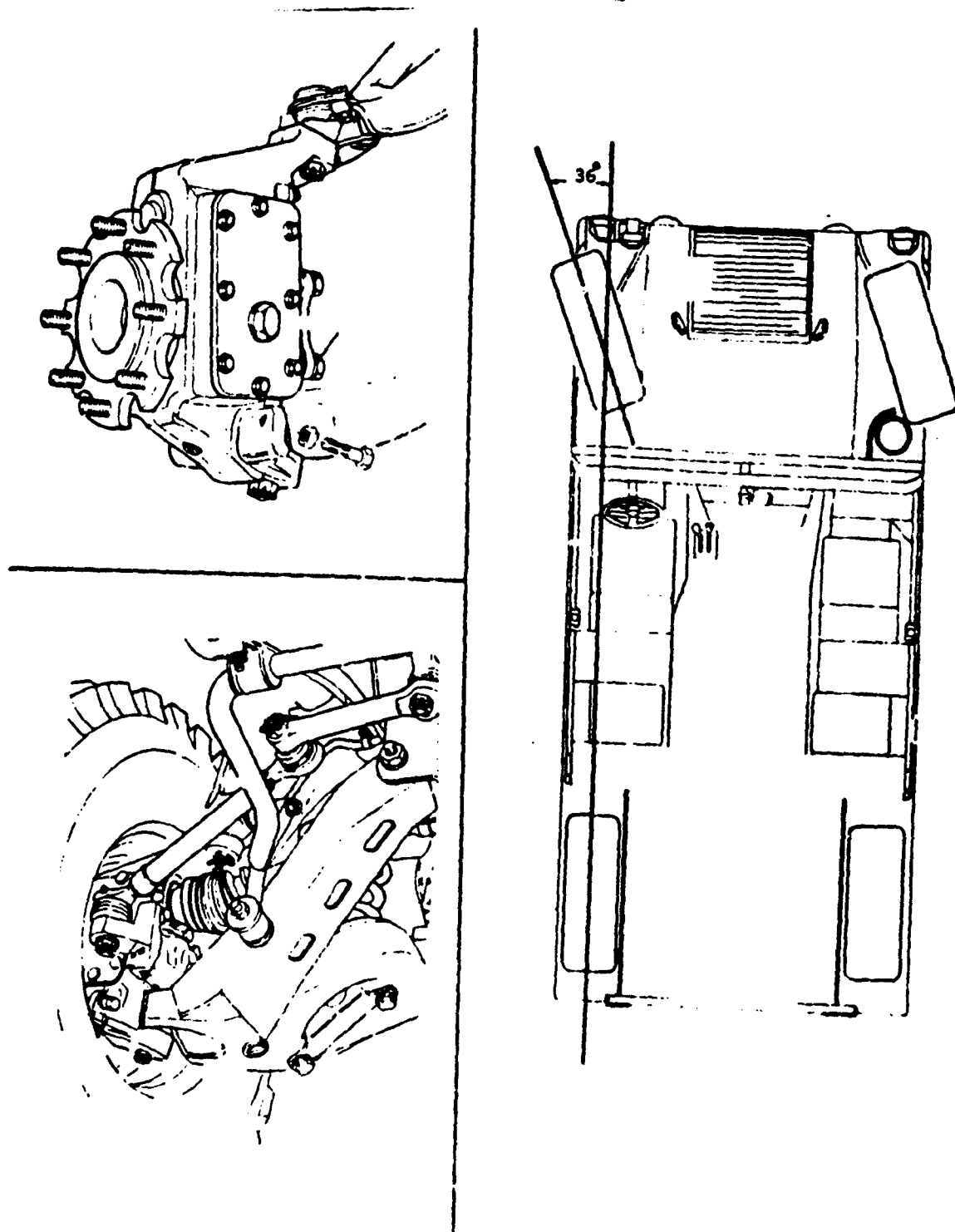


Figure 5-15. Steering Stop

5.6.1. HMMWV Model. The purpose of this dynamic analysis is to simulate the vehicle's dynamic response from negotiating the NATC course. The initial vehicle speed was 15 mph for this analysis, the same as the actual speed employed at the vehicle tests conducted at NATC. During the simulation there was no simulated driver response to braking, acceleration, or steering.

The analysis of the HMMWV employed the DADS methodology. The computer program builds a mathematical model of the system from a set of data input and calculates the position, velocity, and acceleration of various parts of the vehicle as well as the forces that act in the vehicle.

DADS contains a large library of mechanical elements that can be used to build a vehicle model. These elements include bodies, joints and other constraints, and force-and-torque producing elements. The HMMWV vehicle model was created using the three-dimensional version. All vehicle input data were described relative to a global reference frame located on the ground.

The coordinate reference frames used in this analysis are shown in Table 5-16.

The DADS elements listed in Table 5-17 were used to describe the HMMWV vehicle. A complete list of all the vehicle data can be found in the *.VB3 verbatim file and the *.INP user input data file listed in Appendix E. The data files are placed in the directory [AARDEMA.DADS3D.HMMWV.1037.HIGHCG.NATC]. To run the program in batch mode, execute command file *.SBM which will submit the job. To run the program interactively, execute the command file *.COM.

5.6.2. Program Enhancements. Several additions and modifications were made to the DADS code to more accurately model the vehicle characteristics and to provide easy access to output data. Table 5-18 lists the subroutines that were added or modified and a brief description of their purpose.

The source code additions and modifications are placed in the directory [AARDEMA.DADS3D.HMMWV.SOURCE] on the VAX8800 computer. All user common blocks are placed in the directory [AARDEMA.DADS3D.HMMWV.COMMON]. Command file COMP.COM was used to compile each subroutine. All object code are placed in the directory [AARDEMA.DADS3D.HMMWV.OBJECT]. The modified subroutines are then replaced in the object code libraries ANALYSIS.OLB, MOD3D.OLB, and USER3D.OLB by the command file LIB_REPLACE.COM. Command file LINK_DADS3D_HMMWV.COM is used to link all the subroutines and create an executable code. The executable code and mapping files are placed in the directory [AARDEMA.DADS3D.HMMWV.EXE].

5.6.3. Post Processing. The DADS post processor program provides a means of plotting and writing the simulation results. However, not all of the necessary information is available when user-written subroutines are implemented. For this reason an array named UPLOTT was implemented

Table 5-16. Coordinate Reference Frames

Axis	Description
X - Axis	Right Side
Y - Axis	Forward
Z - Axis	Vertical

Table 5-17. DADS Elements

DADS ELEMENT	ELEMENT NAME	DESCRIPTION
HEADER	HEADER	Comments
SYSTEM	SYSTEM.DATA	Simulation Parameters
DYNAMIC	DYNAMIC.DATA	Simulation Parameters
DISTANCE.CONSTRAINT	TIE-ROD.FL	Front Left Tie Rod
DISTRANCE.CONSTRAINT	TIE-ROD.FR	Front Right Tie Rod
DISTANCE.CONSTRAINT	RAD-ROD.RL	Rear Left Rad Rod
DISTANCE.CONSTRAINT	RAD-ROD.RR	Rear Right Rad Rod
TACOM-TIRE	TIRE.FL	Front Left Tire
TACOM-TIRE	TIRE.FR	Front Right Tire
TACOM-TIRE	TIRE.RL	Rear Left Tire
TACOM-TIRE	TIRE.RR	Rear Right Tire
TSDA	SPRING.FL	Front Left Spring
TSDA	SPRING.FR	Front Right Spring
TSDA	SPRING.RL	Rear Left Spring
TSDA	SPRING.RR	Rear Right Spring
TSDA	SHOCK.FL	Front Left Shock
TSDA	SHOCK.FR	Front Right Shock
TSDA	SHOCK.RL	Rear Left Shock
TSDA	SHOCK.RR	Rear Right Shock
REVOLUTE.JOINT	REV.LFL	Lower Front Left
REVOLUTE.JOINT	REV.LFR	Lower Front Right
REVOLUTE.JOINT	REV.LRL	Lower Rear Left
REVOLUTE.JOINT	REV.LRR	Lower Rear Right
REVOLUTE.JOINT	REV.UFL	Upper Front Left
REVOLUTE.JOINT	REV.UFR	Upper Front Right
REVOLUTE.JOINT	REV.URL	Upper Rear Left
REVOLUTE.JOINT	REV.URR	Upper Rear Right
REVOLUTE.JOINT	PITMAN.REV	Pitman Arm to Chassis
REV-SPHR	IDLER.ARM	Steering Link to Chassis
SPHERICAL	SPH.LFL	Lower Front Left Ball Joint
SPHERICAL	SPH.LFR	Lower Front Right Ball Joint
SPHERICAL	SPH.LRL	Lower Rear Left Ball Joint
SPHERICAL	SPH.LRR	Lower Rear Right Ball Joint
SPHERICAL	SPH.UFL	Upper Front Left Ball Joint
SPHERICAL	SPH.UFR	Upper Front Right Ball Joint
SPHERICAL	SPH.URL	Upper Rear Left Ball Joint
SPHERICAL	SPH.URR	Upper Rear Right Ball Joint
UNIVERSAL	PITMAN.UNIV	Steering Link to Pitman Arm

Table 5-17. DADS Elements (Continued)

DADS ELEMENT	ELEMENT NAME	DESCRIPTION
BODY	CHASSIS	Chassis
BODY	ARM.LFL	Lower Front Left
BODY	ARM.LFR	Lower Front Right
BODY	ARM.LRL	Lower Rear Left
BODY	ARM.LRR	Lower Rear Right
BODY	ARM.UFL	Upper Front Left
BODY	ARM.UFR	Upper Front Right
BODY	ARM.URL	Upper Rear Left
BODY	ARM.URR	Upper Rear Right
BODY	WHEEL.FL	Front Left
BODY	WHEEL.FR	Front Right
BODY	WHEEL.RL	Rear Left
BODY	WHEEL.RR	Rear Right
BODY	PITMAN.ARM	Steering Arm
BODY	STEERING.LINK	Steering Link
INITIAL CONDITION	INIT.CHASSIS.ORIEN	Chassis Orientation
INITIAL CONDITION	INIT.CHASSIS.X	Chassis X
INITIAL CONDITION	INIT.CHASSIS.Y	Chassis Y
INITIAL CONDITION	INIT.CHASSIS.Z	Chassis Z
INITIAL CONDITION	INIT.WHEEL.FL	Front Left Wheel Z
INITIAL CONDITION	INIT.WHEEL.FR	Front Right Wheel Z
INITIAL CONDITION	INIT.WHEEL.RL	Rear Left Wheel Z
INITIAL CONDITION	INIT.WHEEL.RR	Rear Right Wheel Z
DRIVER	DRIVER	Steering Command
CURVE	TIRE.COEF	Tire Longitudinal Slip Coefficient
CURVE	BIAS.TIRE.20PSI	Tire Vertical Force @ 20 psi
CURVE	BIAS.TIRE.30PSI	Tire Vertical Force @ 30 psi
CURVE	TRAJECTORY	Steering Trajectory

Table 5-18. Subroutines Modified or Added

SUBROUTINE	DESCRIPTION
ATB.FOR	Multiplies a 3X3 matrix "A" by a 3X3 matrix "B".
BLOCKD.FOR	Modified the size of the TIRE and ITIRE arrays for the TACOM tire model and set the record length for the input data.
CARPET.FOR	Calculates the lateral force and the aligning torque as a function of slip and normal force given in the tire carpet plot data.
CUBIC.FOR	Provides a smoothing function to model coulomb friction. See section 5.3.8 titled "Friction" for more information.
CUBIC1.FOR	Provides a smoothing function to model transitions between events. See section 5.3.7 titled "Shock Absorbers" for more information.
DADS.FOR	Added the TACOM-TIRE element to the DADS element library.
EXEUNT.FOR	Added the closing of the movie file *.MOV, the shared file *.SHR, the user input file *.INP, and the auxillary output file *.AUX.
FRC10.FOR	Added a call to the user written subroutine USER-TSDA.FOR to calculate shock forces. These forces, called UFORCE, were add to the total force in the TSDA element.
FRC15.FOR	Calculate the angle between the ball joint stud axis and the ball housing axis.
FRC36.FOR	Calculate tire dynamics and appends tire forces to the wheel bodies. Performs speed controller calculations and performs roll stabilization bar calculations.
IN36.FOR	Modified to read element number 36 which contains TACOM-TIRE data. Also added a call to subroutine USET.FOR to read in additional tire and terrain data.

Table 5-18. Subroutines Modified or Added (Continued)

SUBROUTINE	DESCRIPTION
IN49.FOR	Modified to get the number of driver differential equations used by the relative angle type driver. The number is stored in variable NDRVDE.
JNCTN.FOR	Added MM36 to the external call list and added the GOTO call for MM36.
MAINB.FOR	Added the opening and sharing of the movie file *.MOV, the shared file *.SHR, the user input file *.INP, and the auxillary user output file *.AUX.
MM03.FOI	Modified the call list to RPT03.FOR to include the user differential variable arrays UDE and DUDE.
MM15.FOR	Added the call to FRC15.FOR.
MM36.FOR	This subroutine is called by JNCTN for TACOM tire information. It call IN36 to read input data, MOVE36 to set initial conditions for the user differential equation, FRC36 to calculate tire dynamics and tire forces, and RPT03 to report data to output file. The size of NY and NYTOT are increased for integrating the tire rotational accelertions and velocities.
MOVE36.FOR	Sets the initial conditions for the user differential equations.
RPT03.FOR	Added code to write out animation data to the movie file and the shared file.
RPT36.FOR	Reports TACOM-TIRE results to the output file *.OUT.
SURF.FOR	Calculates the elevation of a point in a grid pattern which describes the terrain surface.
TIREF.FOR	Calculates tire forces for the TACOM tire model.
USER_TSDA.FOR	Calculates shock absorber forces.
USET.FOR	Reads in additional data from the user input file *.INP.

into the user-written subroutines to store the required user information. At each report interval the contents of UPL0T are written to the user output file *.AUX.

After the simulation is successfully completed the additional user data can be extracted from the *.AUX file by executing the EXTRACT.EXE file located in the directory [AARDEMA.DADS3D.HMMWV.EXE]. This data can be plotted by using the DADS post processor.

Shear forces within each ball joint are obtained by writing the joint perpendicular force components to an output file using the DADS post processor and then using the program SHEAR.EXE located in the directory [AARDEMA.DADS3D.HMMWV.EXE] to calculate the shear force. A plot of the shear forces can be made using the DADS post processor.

The commands for extracting the user data from the UPL0T arrays are contained in the command file EXTRACT.COM. By executing this command file the data will be stored in the files *.DAT and can be plotted using the EXC command in the DADS post processor.

Many of the commands for plotting vehicle data and user data have been automated. By executing the command file PLOT.COM at a Tektronix terminal with a hard copy machine, the plots will automatically be created.

5.6.4. Dynamic Results. The following simulation results are for the HMMWV negotiating the NATC course at 15 mph.

Figures 5-16 through 5-18 show the chassis center of gravity vertical position, velocity, and acceleration. The chassis position data have a vertical offset of 13.38 inches because the ground elevation, as defined by the original vehicle layout drawings, is equal to 13.38 inches. This is clearly shown in Figures 5-2 through 5-7. The maximum vertical acceleration of 5.6 G's occurs when the rear wheels strike the ground after clearing the first obstacle.

Figures 5-19 through 5-21 show the chassis pitch angle, pitch velocity, and pitch acceleration. Positive pitch represents the vehicle front coming upwards. The maximum positive pitch acceleration occurs when the front wheels strike the ground after negotiating the first obstacle. The maximum negative pitch occurs while the front wheels are off the ground, after negotiating the second obstacle, and while at the same time the rear wheels are striking the ground after clearing the first obstacle. At this time the only contact the vehicle has with the ground is by the rear wheels.

Figures 5-22 through 5-24 show the chassis roll angle, roll velocity, and roll acceleration. Positive roll indicates that the vehicle is leaning on the right side. At the end of the simulation, where the course is flat, the vehicle settles out to a positive roll angle. This is a result of the CG being on the right side of the vehicle.

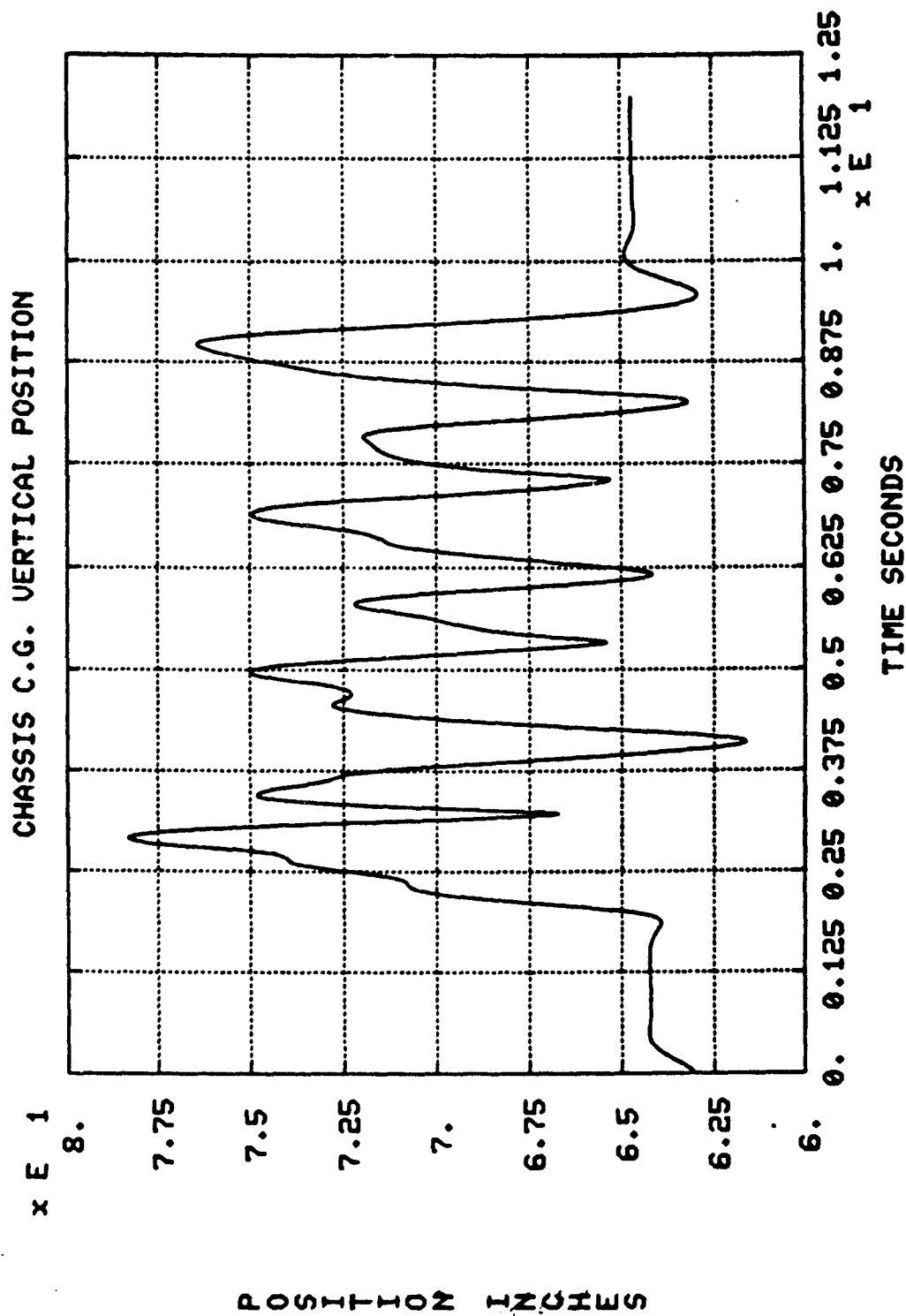


Figure 5-16. Chassis C.G. Vertical Position

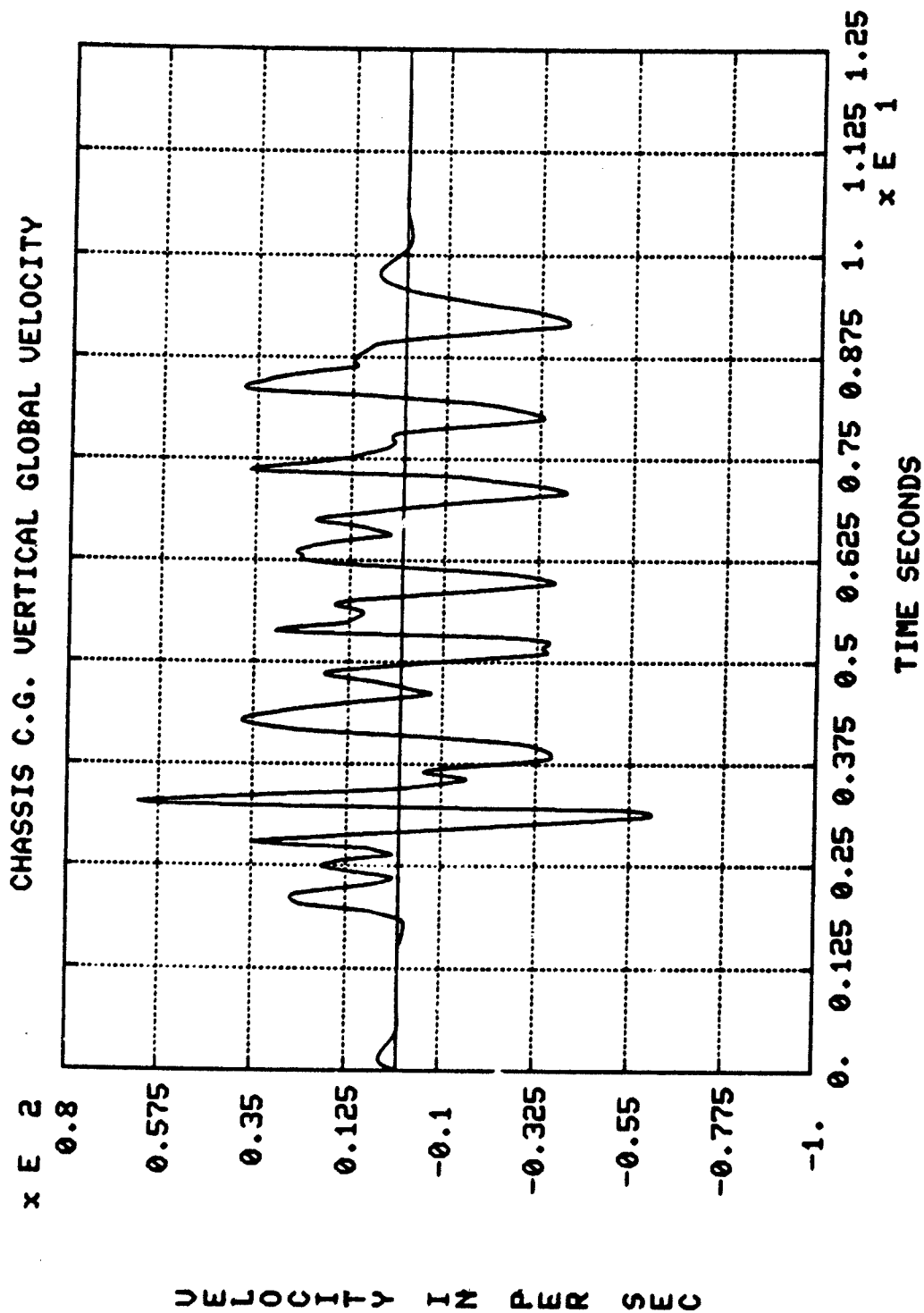


Figure 5-17. Chassis CG Vertical Global Velocity

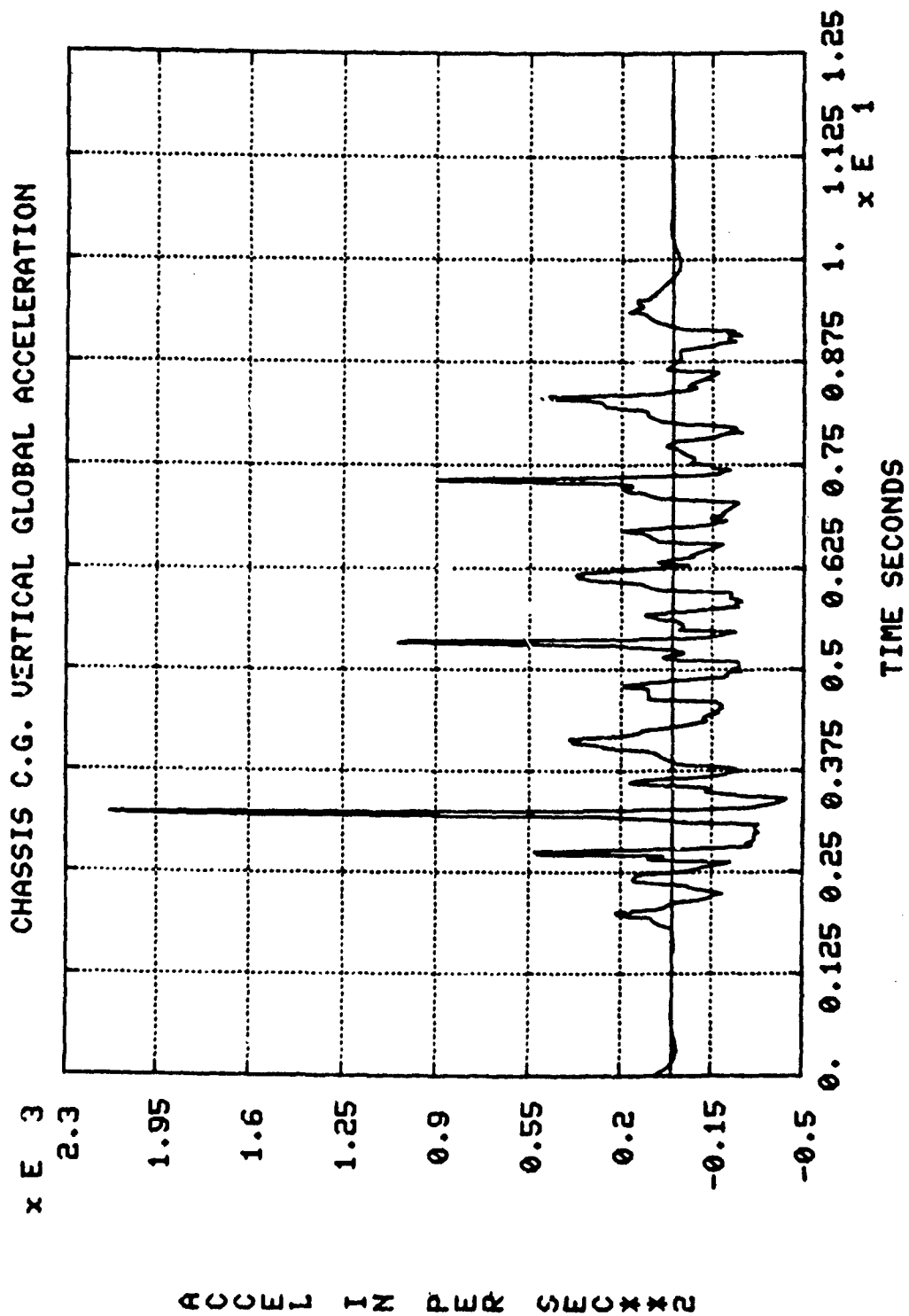


Figure 5-18. Chassis CG Vertical Global Acceleration

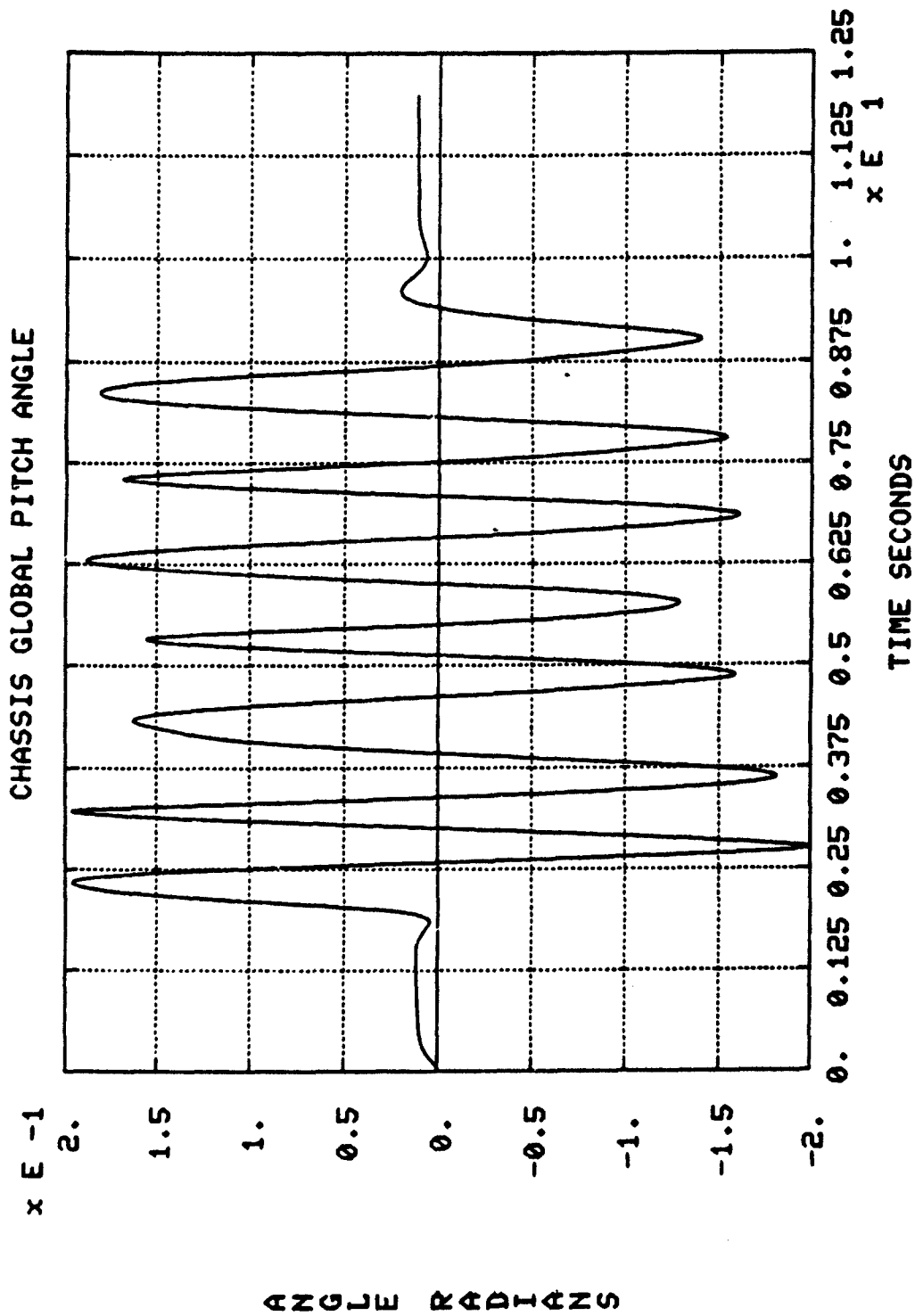


Figure 5-19. Chassis Global Pitch Angle

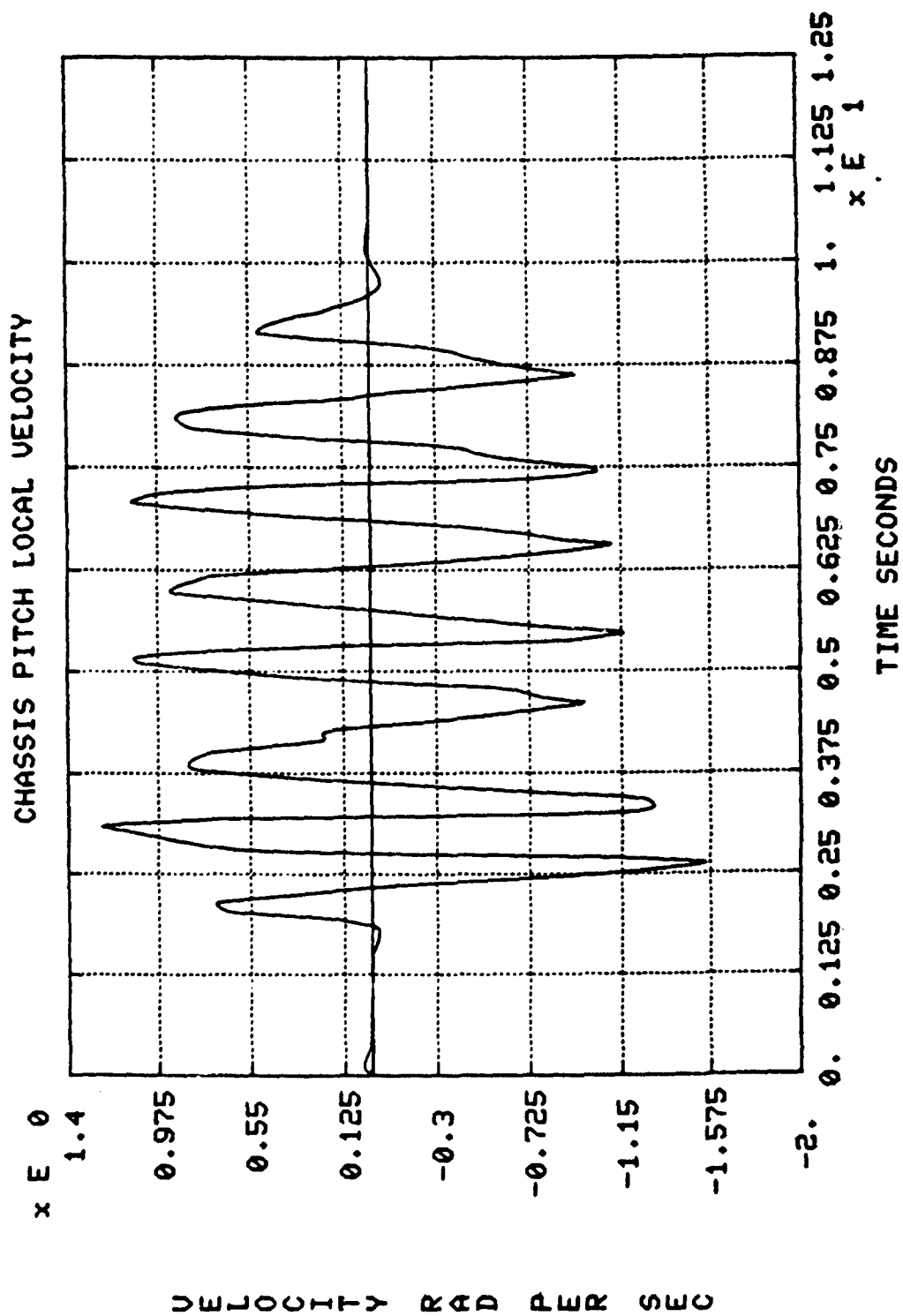


Figure 5-20. Chassis Pitch Local Velocity

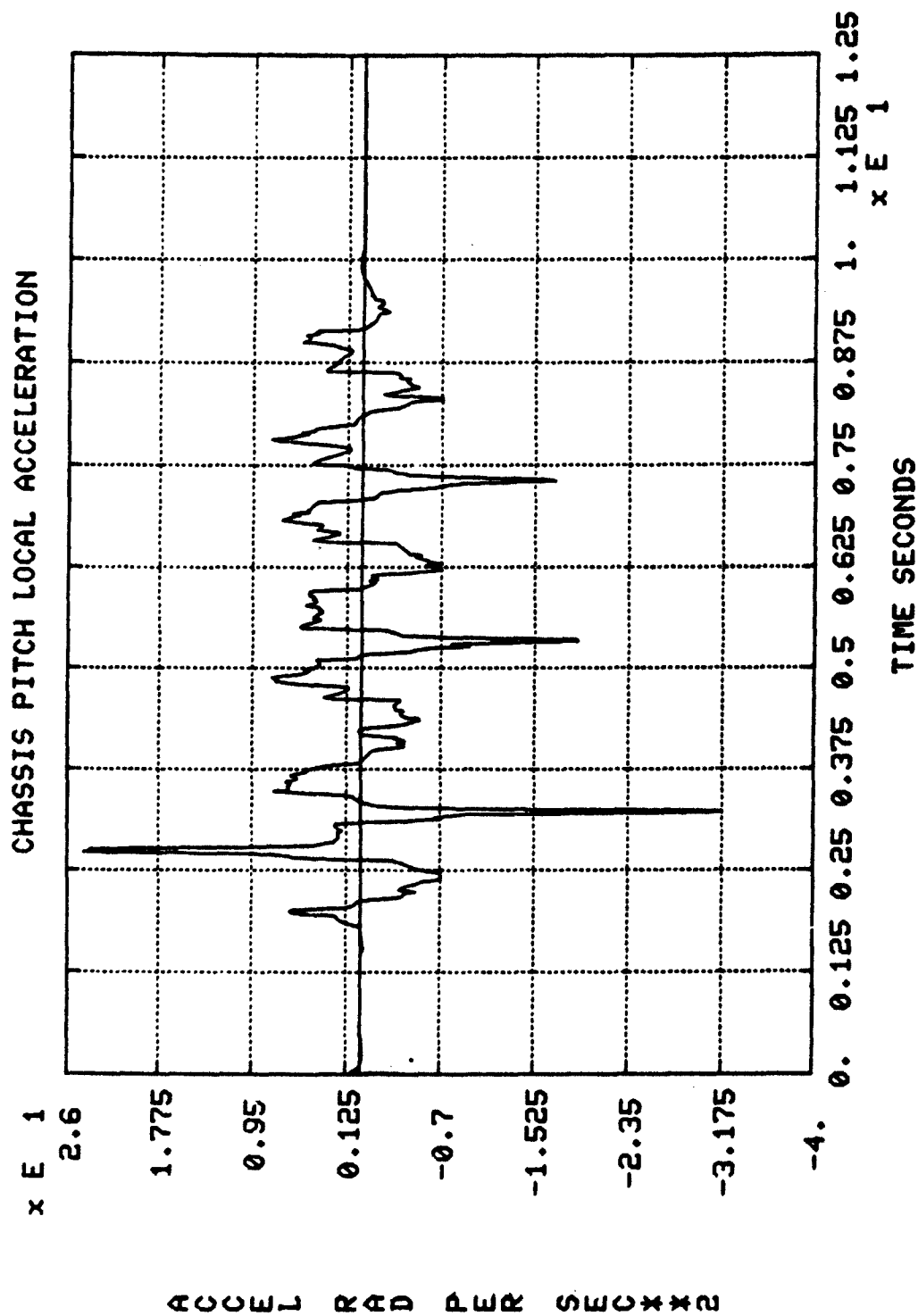


Figure 5-21. Chassis Pitch Local Acceleration

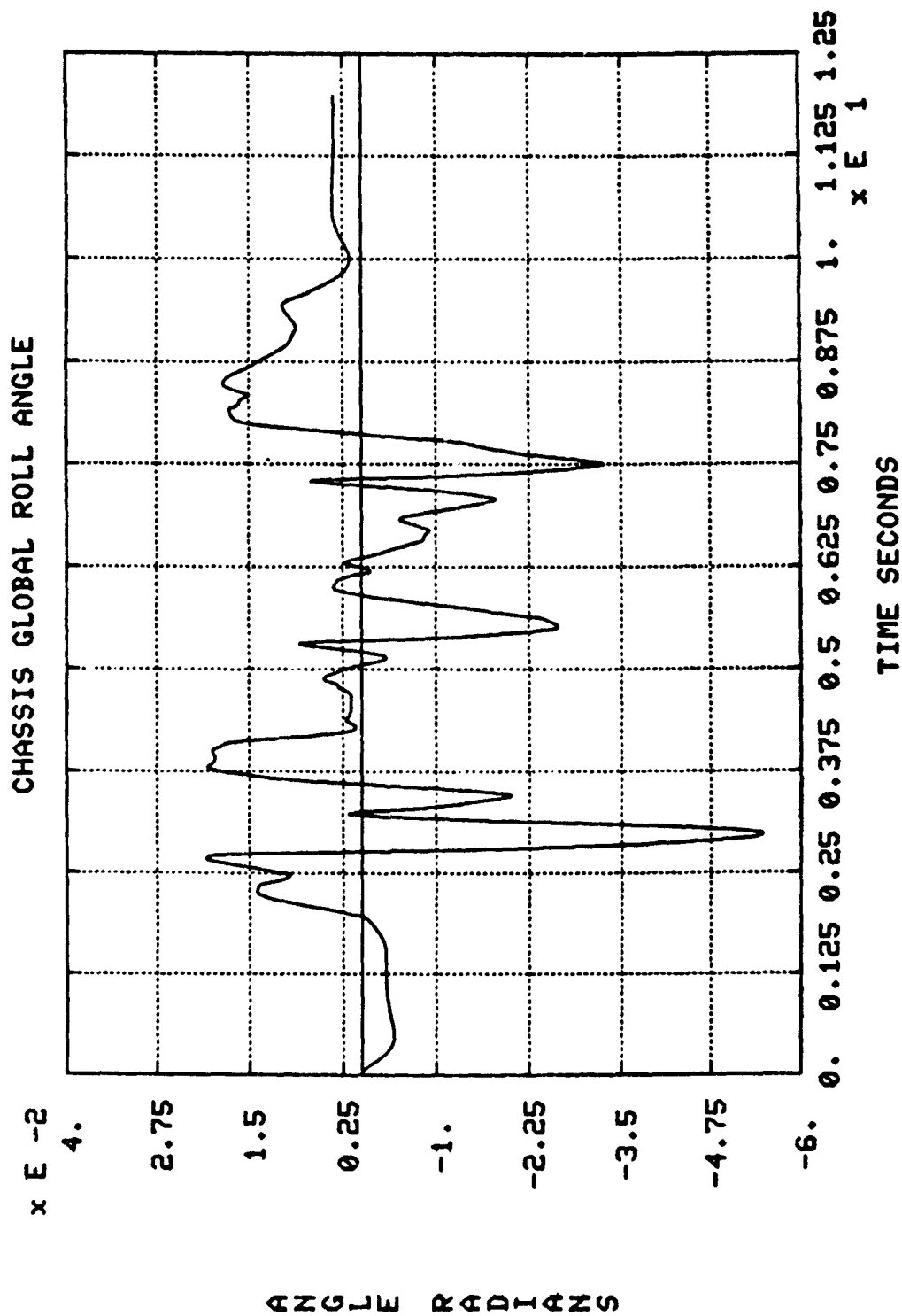


Figure 5-22. Chassis Global Roll Angle

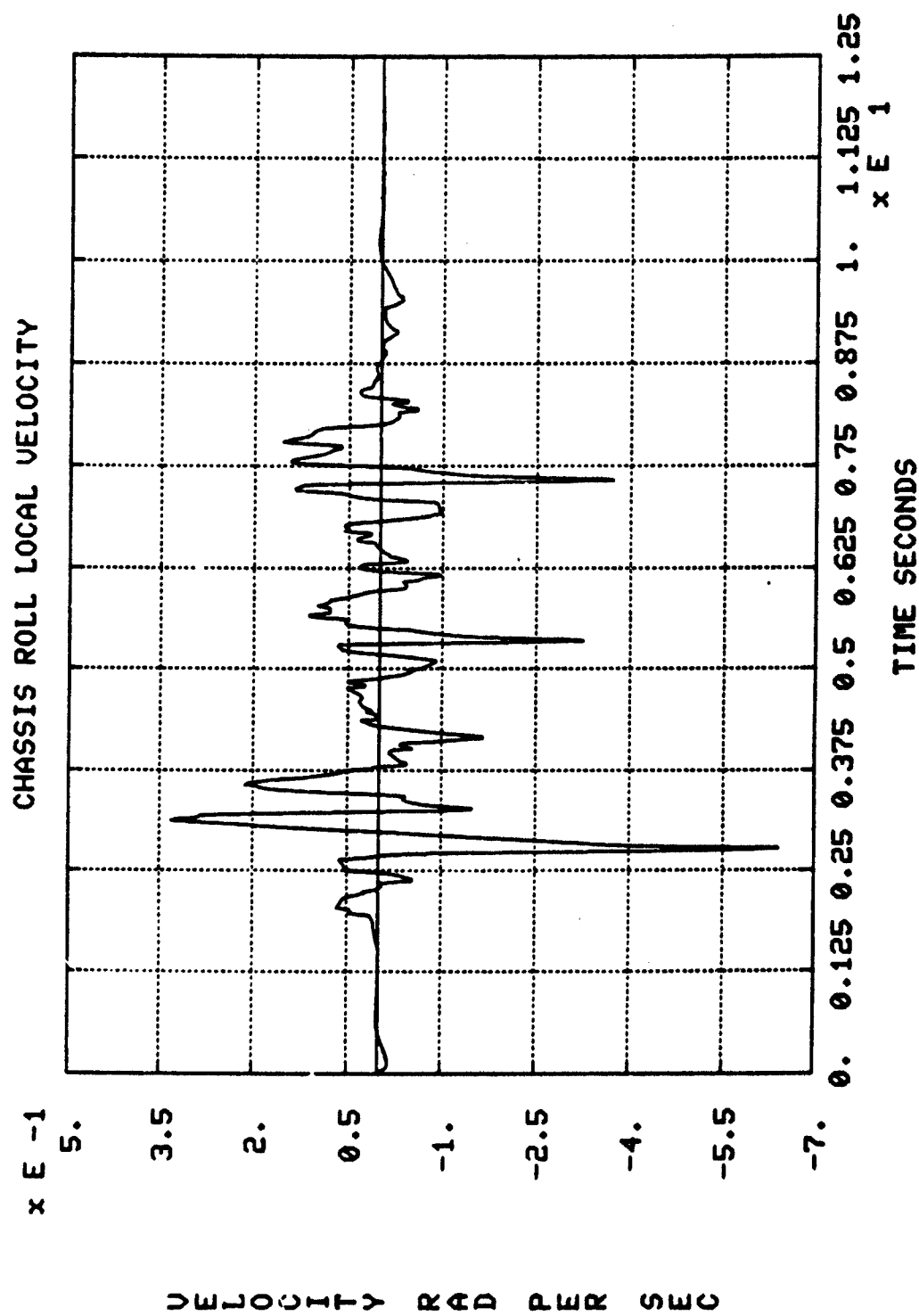


Figure 5-23. Chassis Roll Local Velocity

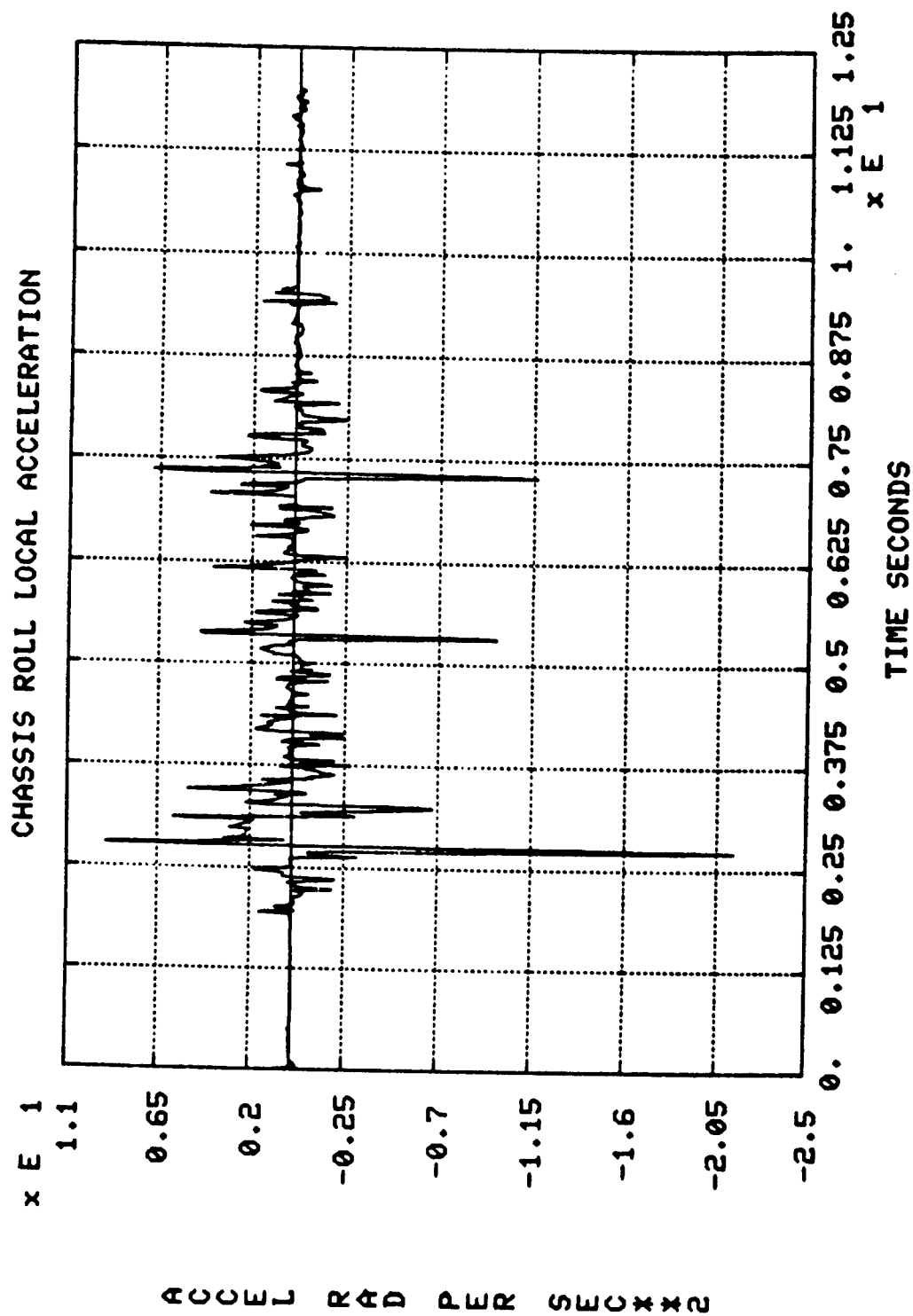


Figure 5-24. Chassis Roll Local Acceleration

Figures 5-25 through 5-27 show the chassis yaw angle, yaw velocity, and yaw acceleration. Positive yaw angle is equivalent to a left turn while a negative yaw angle represents a right turn. After the front wheels clear the first obstacle and are off the ground, and when the front wheels strike the ground upon their return, the forces on the vehicle cause the vehicle to turn towards the left. The maximum yaw angle is less than 3 degrees.

Figures 5-28 through 5-31 show the spring force for the front left, the front right, the rear left, and the rear right springs. Since the spring stiffness is a constant, the spring deflection curves have the same shape. The spring deflections, and likewise the spring forces, are limited by the travel limits of the shock absorbers.

Figures 5-32 through 5-35 show the length of each shock absorber. The shock length is limited by metal stops within the shock as explained in section 5.3.7. titled "Shock Absorbers." Metal-to-metal contact occurs at a compressed length of 12.76 inches and an extended length of 16.48 inches. Shock absorber lengths less than 12.76 inches are shown. This is a result of modeling the metal stops as a linear stiff spring element. Penetration into the metal stops represents the deflection and buckling of the internal shock absorber components.

Figures 5-36 through 5-39 show the impact forces generated when the shock makes metal-to-metal contact. The front left shock and the front right shock reach the metal-to-metal condition in compression only after clearing the first obstacle. The front shock reaches the metal-to-metal condition in extension seven times, once after clearing each of the seven obstacles. These events occur as the front wheels leave the ground. Compression of the spring causes the suspension unit to "open up." Metal stops within the shock limit the amount of travel. The rear left and rear right shocks reach the metal-to-metal condition in compression several times. The rear right shock experiences this condition more frequently and to a greater degree. Having the chassis CG located rearward and to the right of the vehicle is one of the factors causing these events to occur more frequently at the right rear suspension.

Figures 5-40 through 5-43 show the relative velocity of each shock absorber. Negative velocity represents compression and positive velocity represents extension.

Figures 5-44 through 5-47 give the total force generated by the shock absorber. The total force is the sum of the damping force, metal-to-metal contact impact force, and friction. Spikes within the curves are generally a result of the impact forces caused by the shock reaching the metal-to-metal condition.

Figures 5-48 through 5-51 show the tire deflection for the front left, the front right, the rear left, and the rear right tires. At zero tire

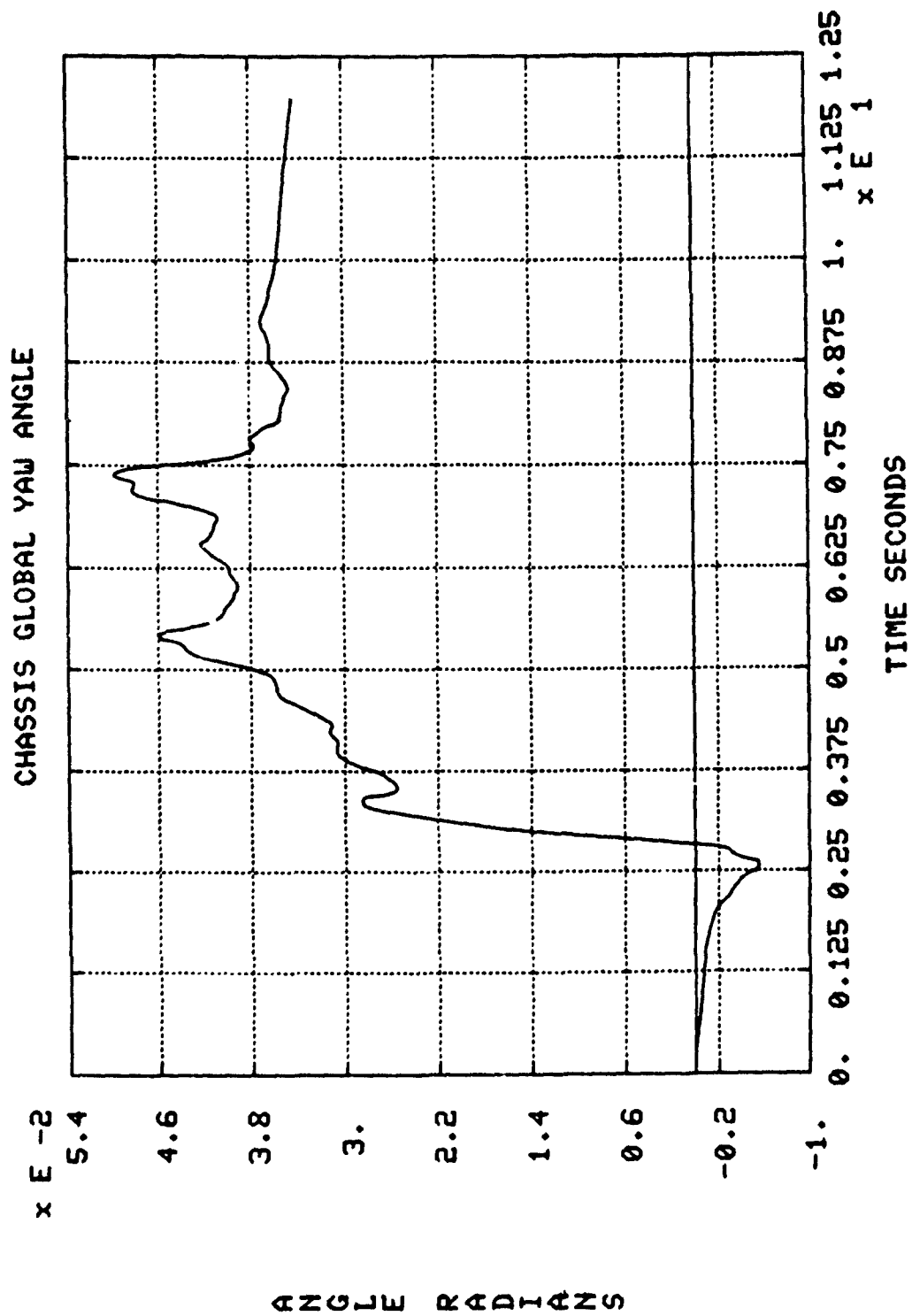


Figure 5-25. Chassis Global Yaw Angle

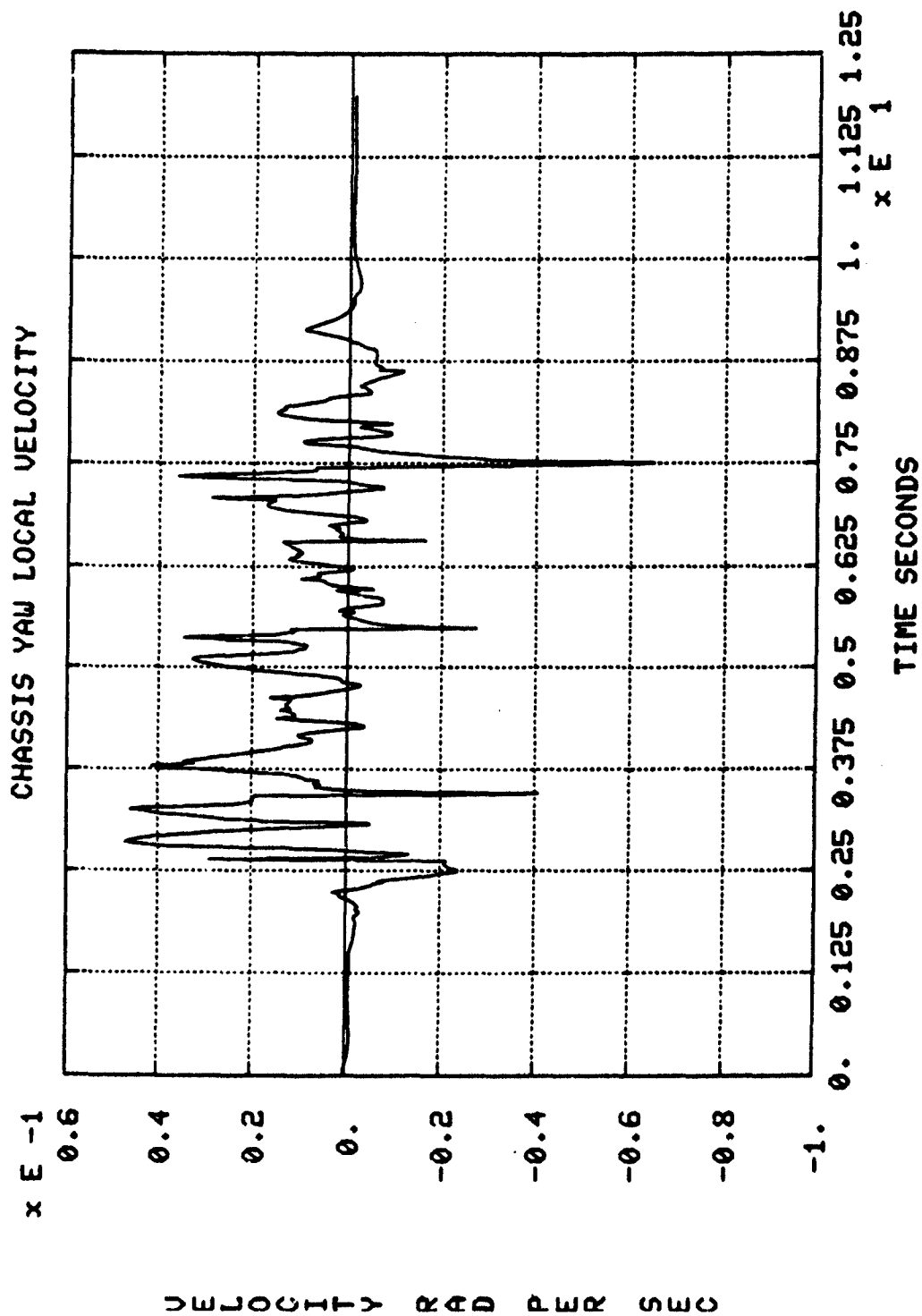


Figure 5-26. Chassis Yaw Local Velocity

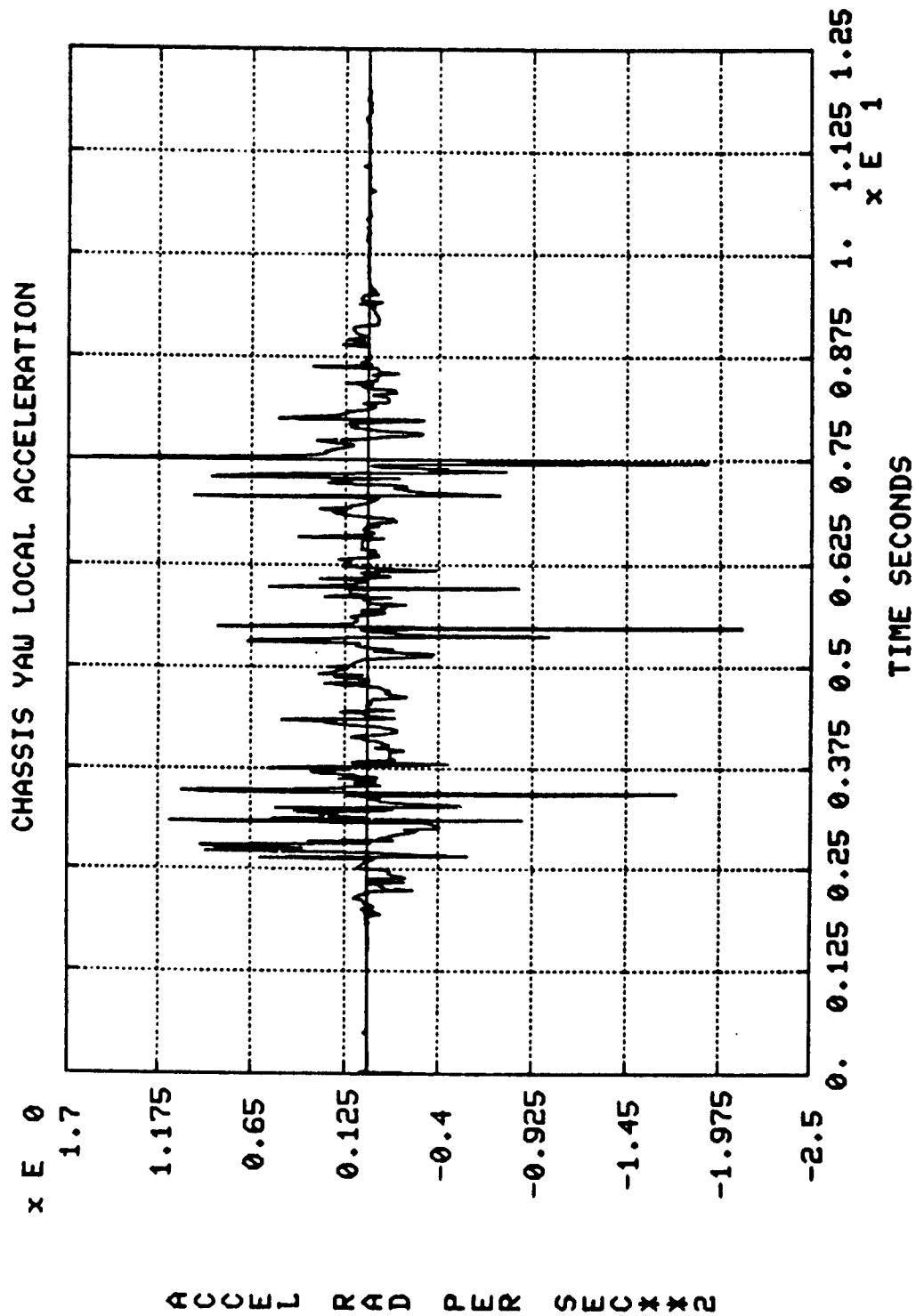


Figure 5-27. Chassis Yaw Local Acceleration.

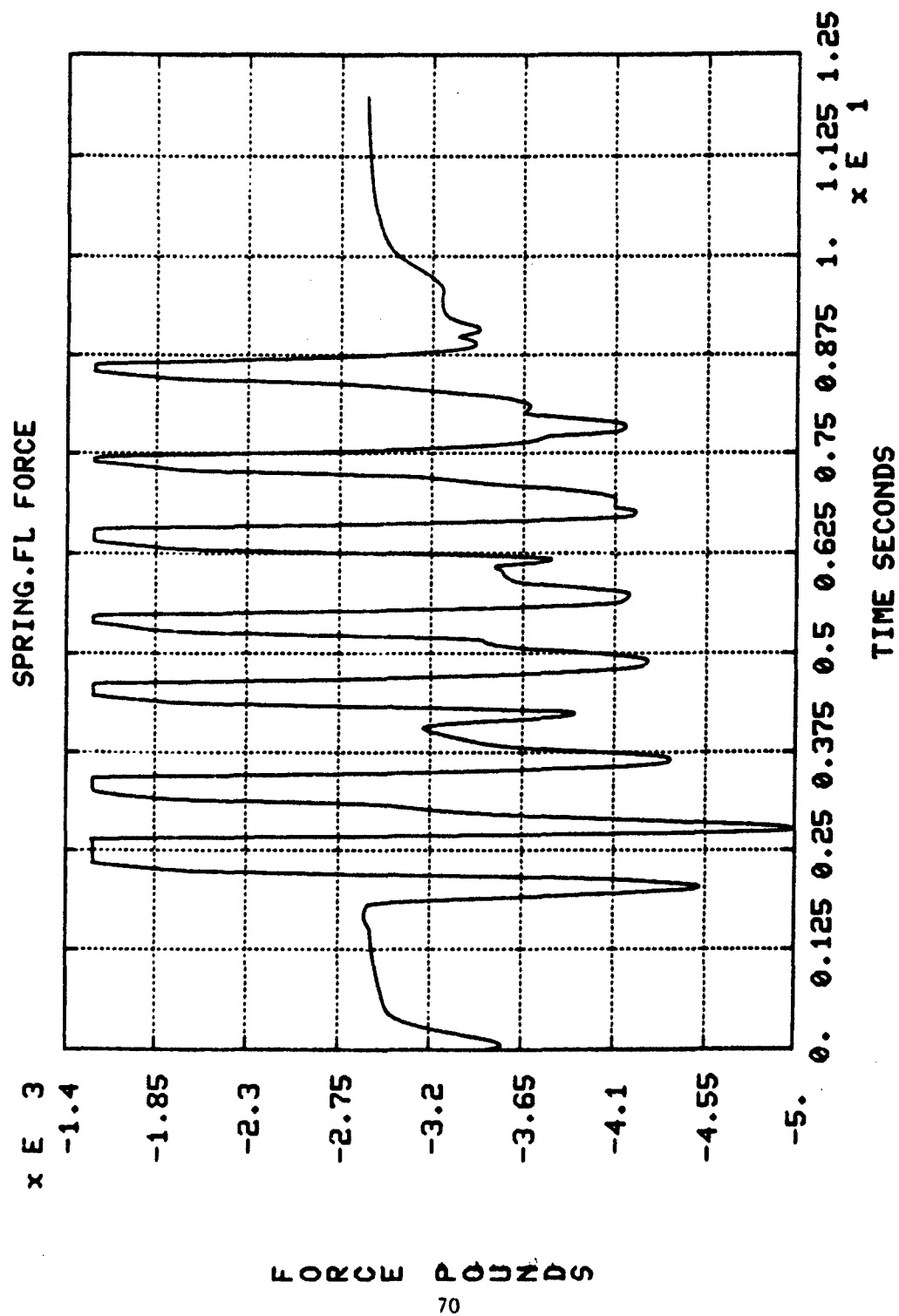
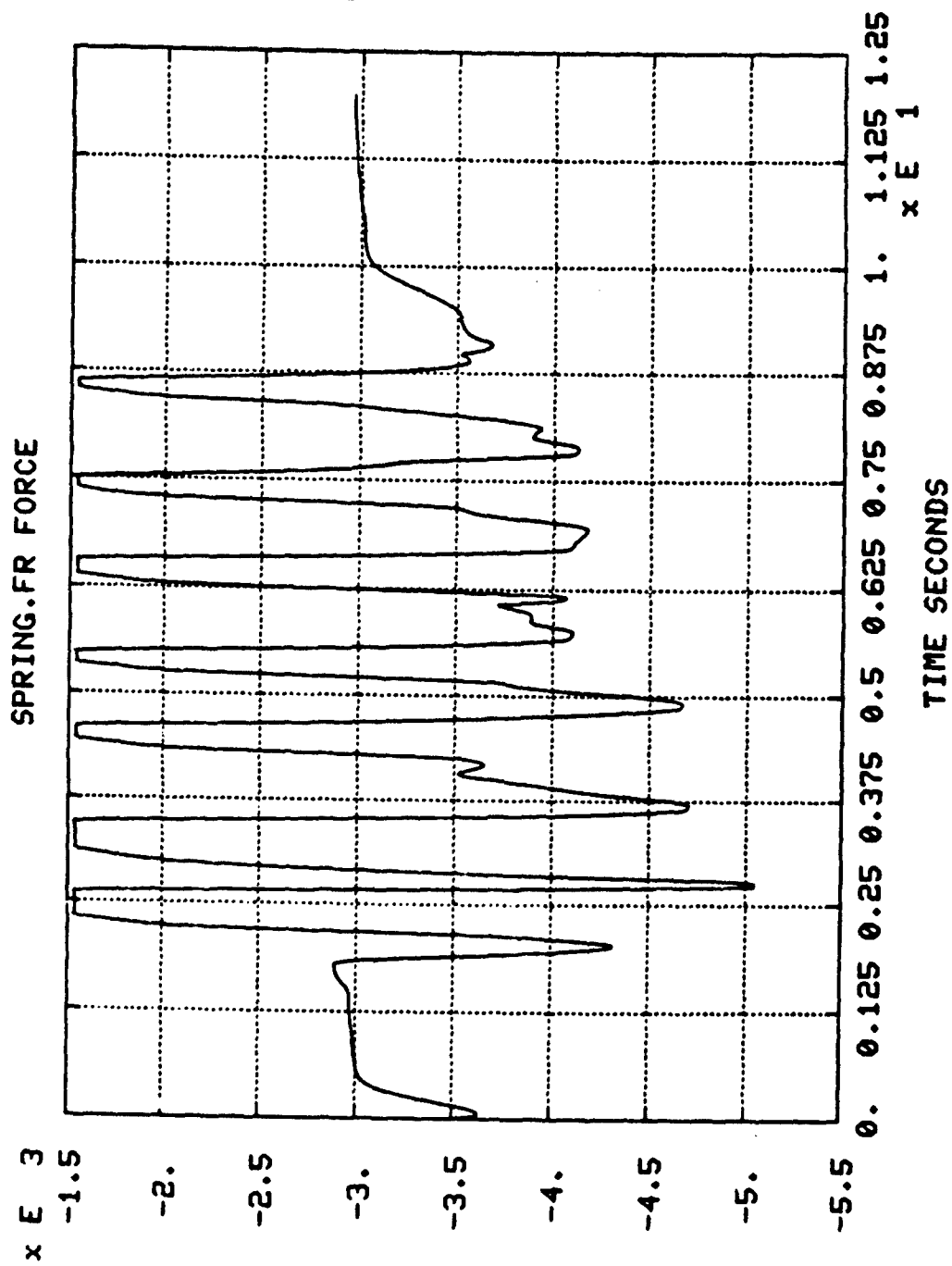
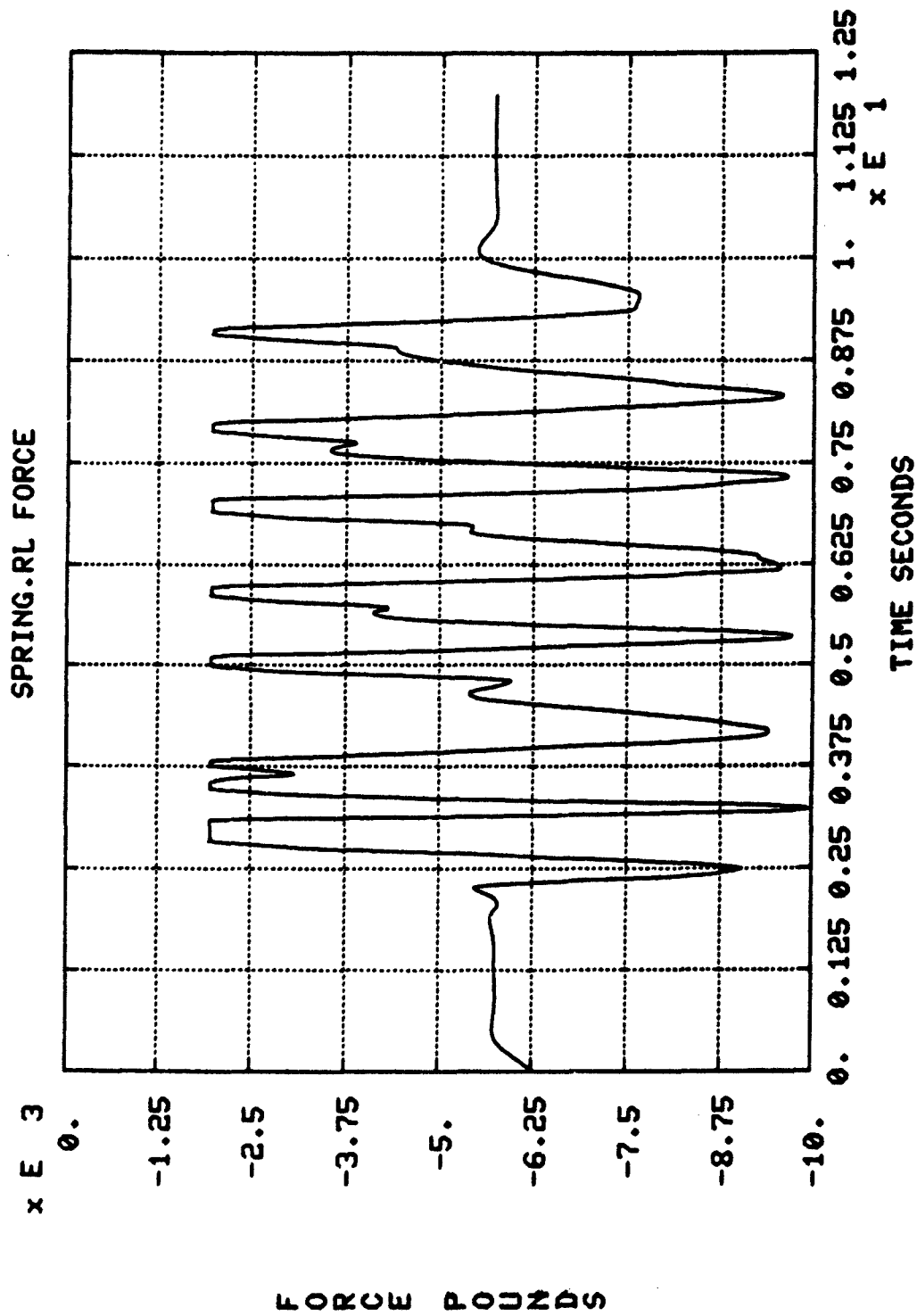


Figure 5-28. Front Left Spring Force



FORCE POUNDS

Figure 5-29. Front Right Spring Force



FORCE POUNDS

72

Figure 5-30. Rear Left Spring Force

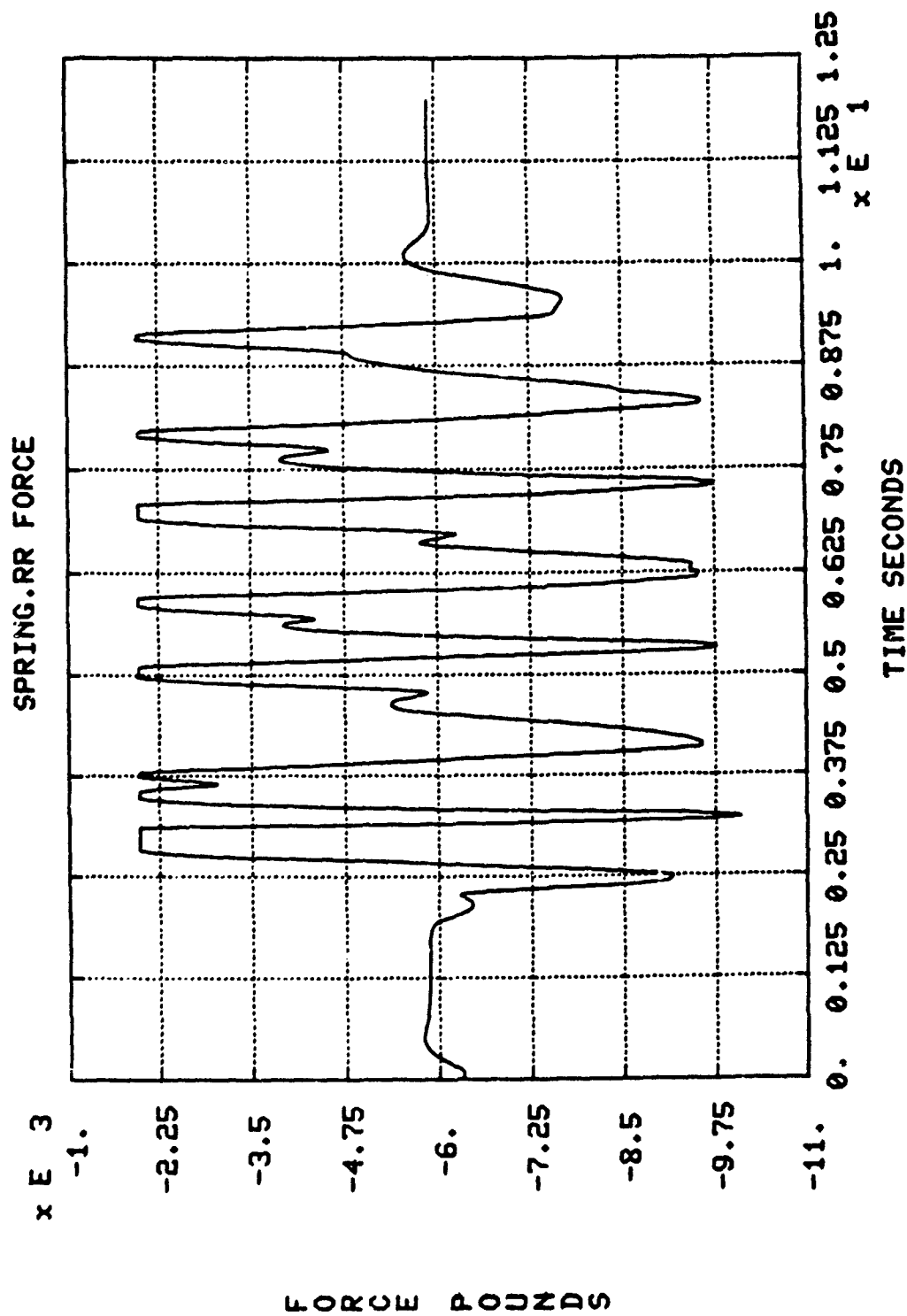
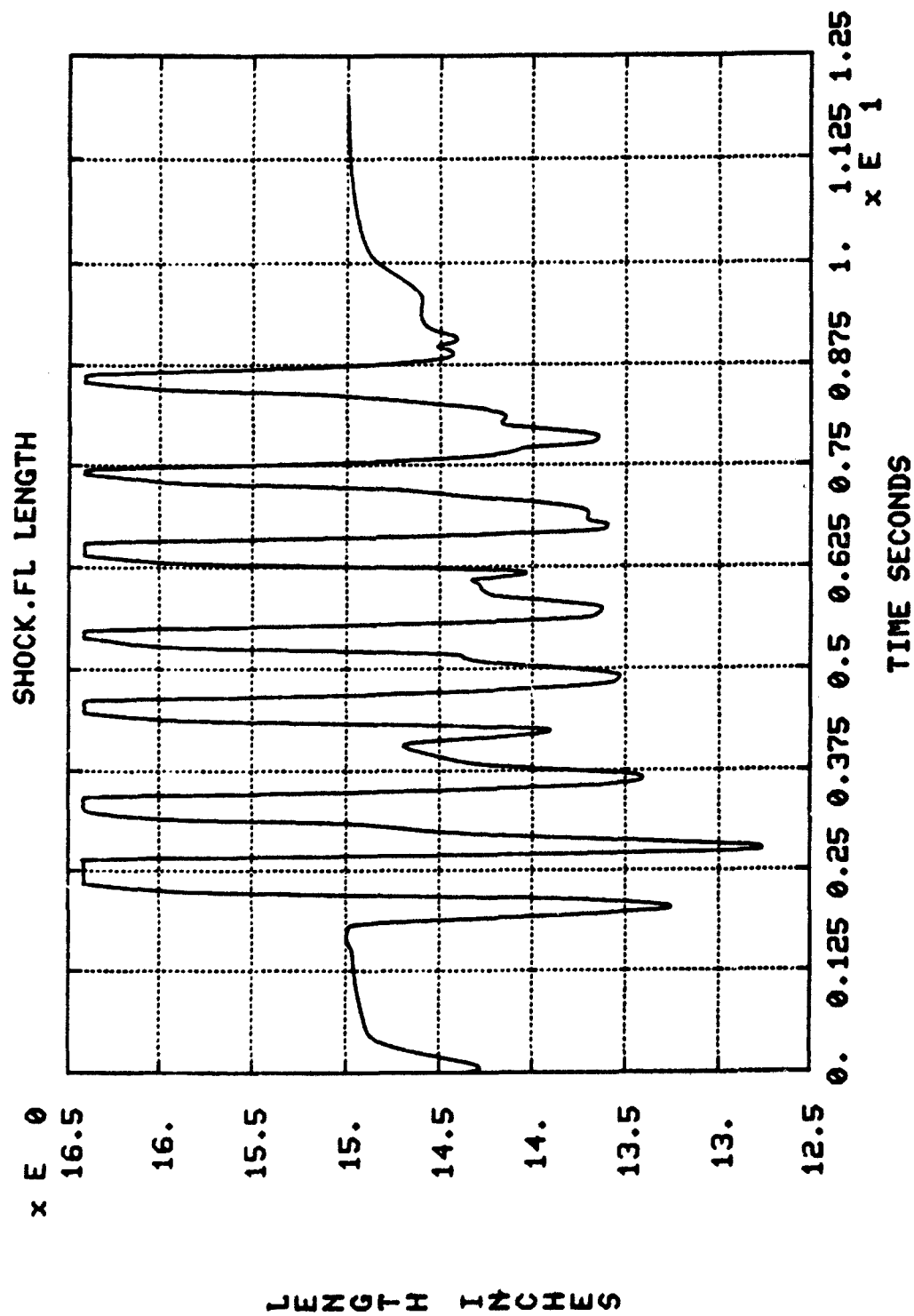


Figure 5-31. Rear Right Spring Force



LENGTH INCHES

Figure 5-32. Front Left Shock Length

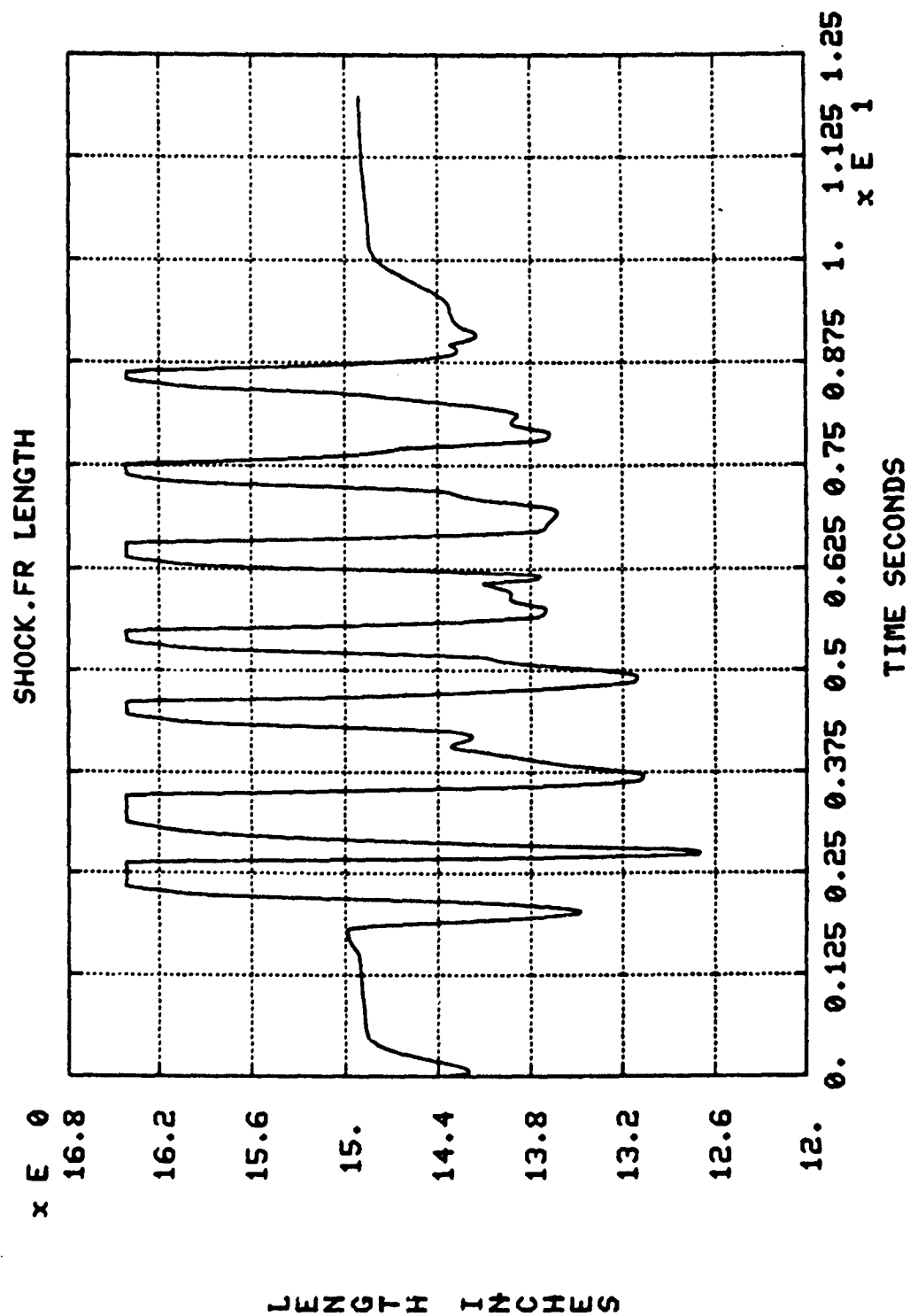


Figure 5-33. Front Right Shock Length

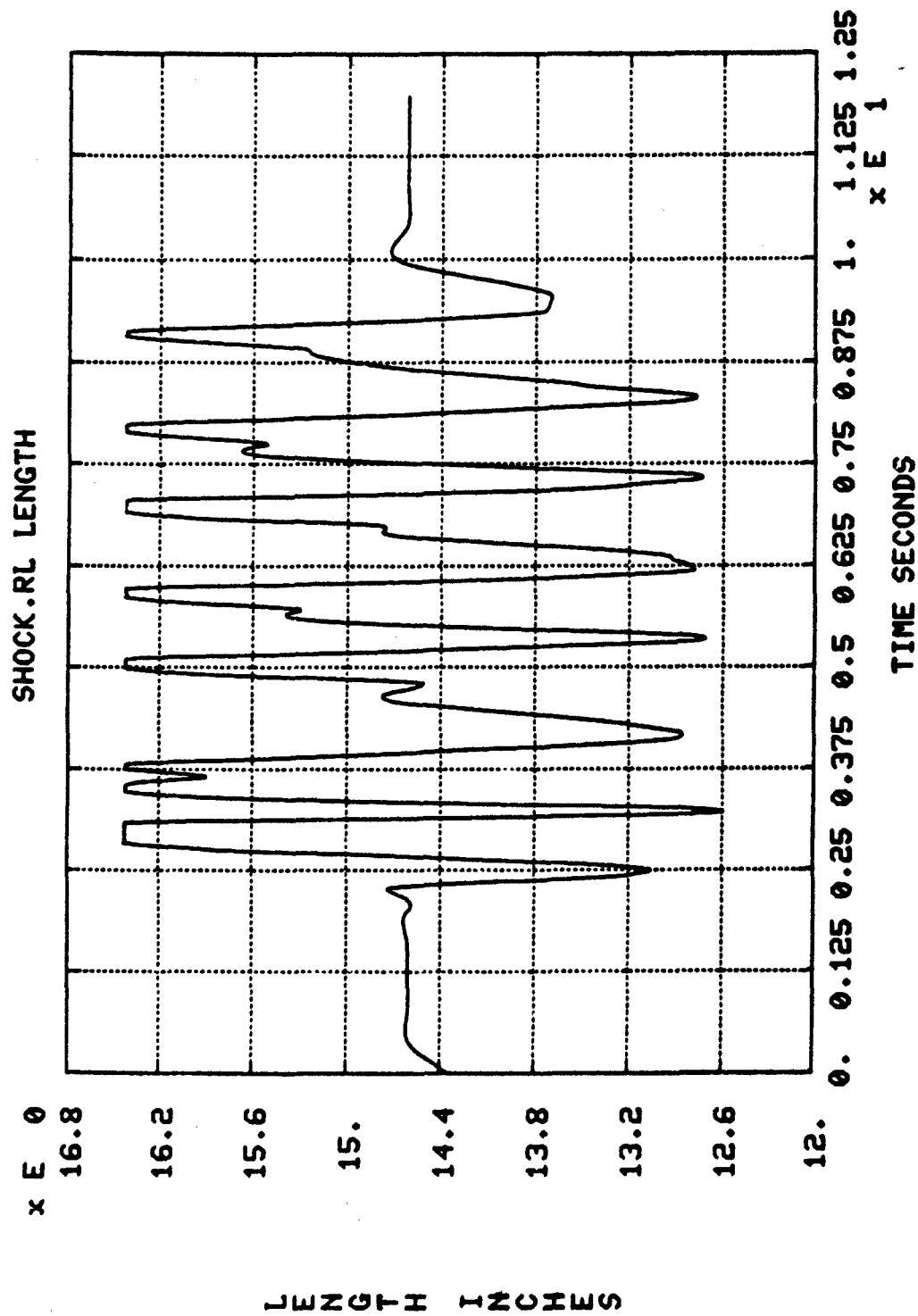


Figure 5-34. Rear Left Shock Length

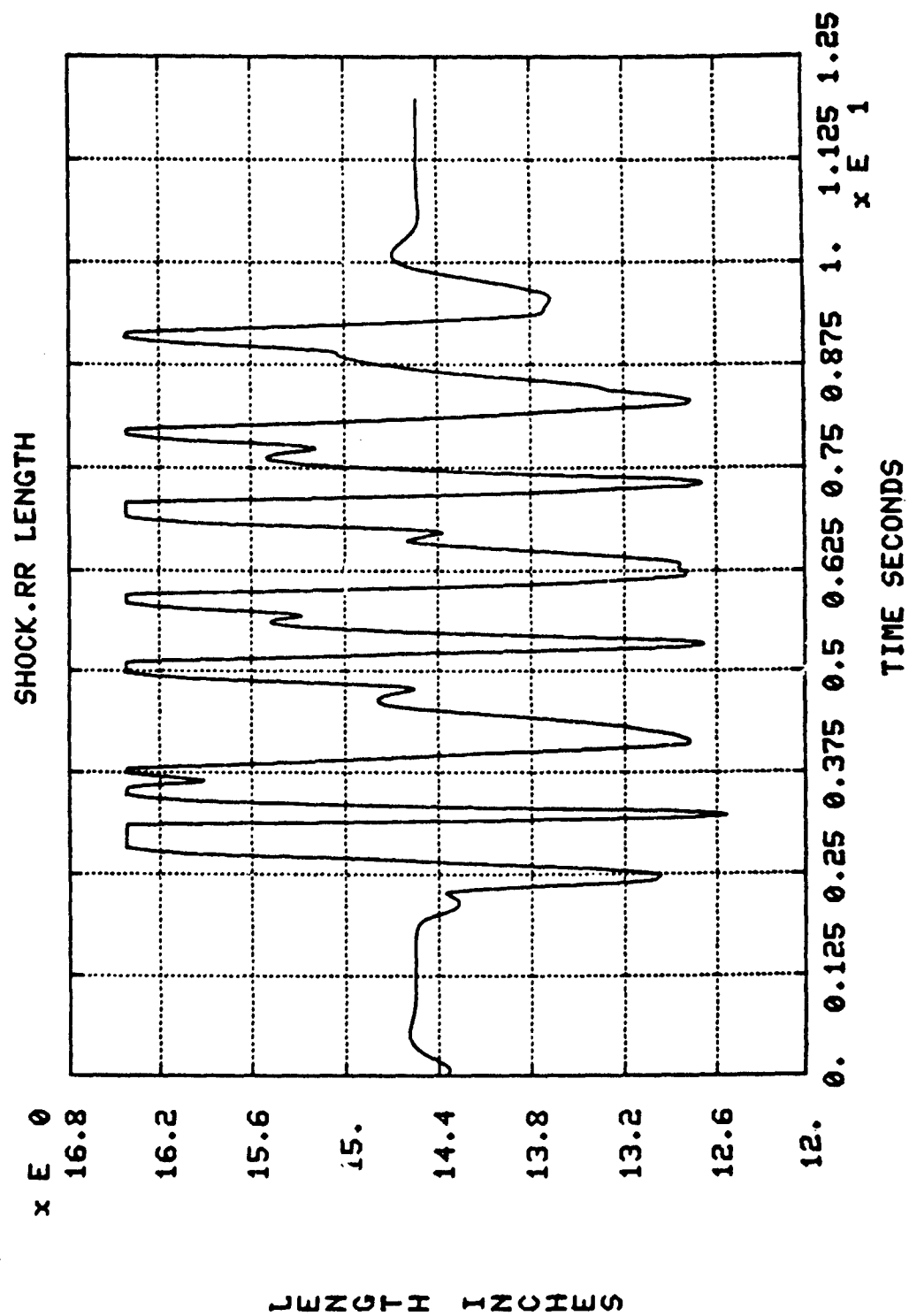


Figure 5-35. Rear Right Shock Length

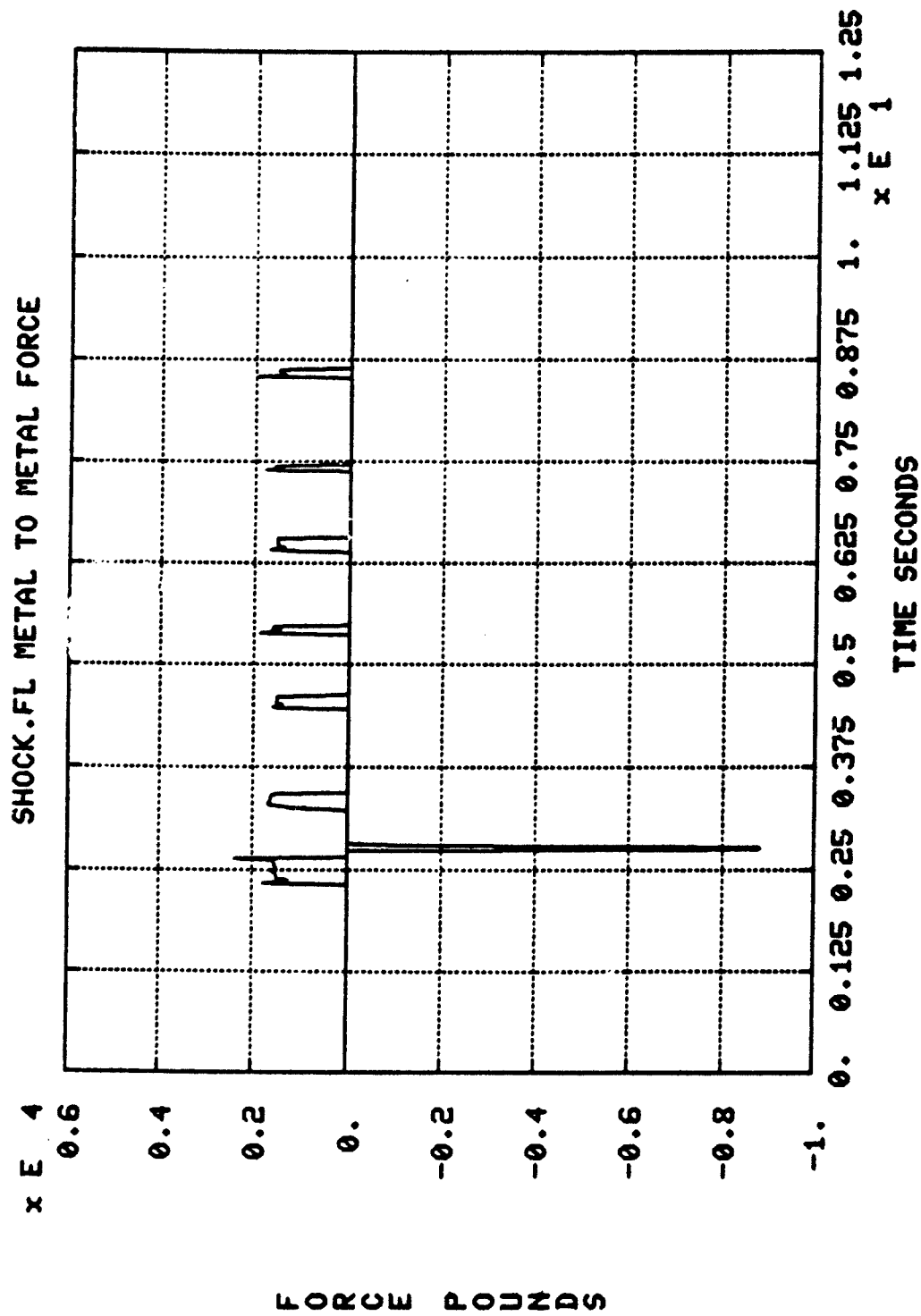
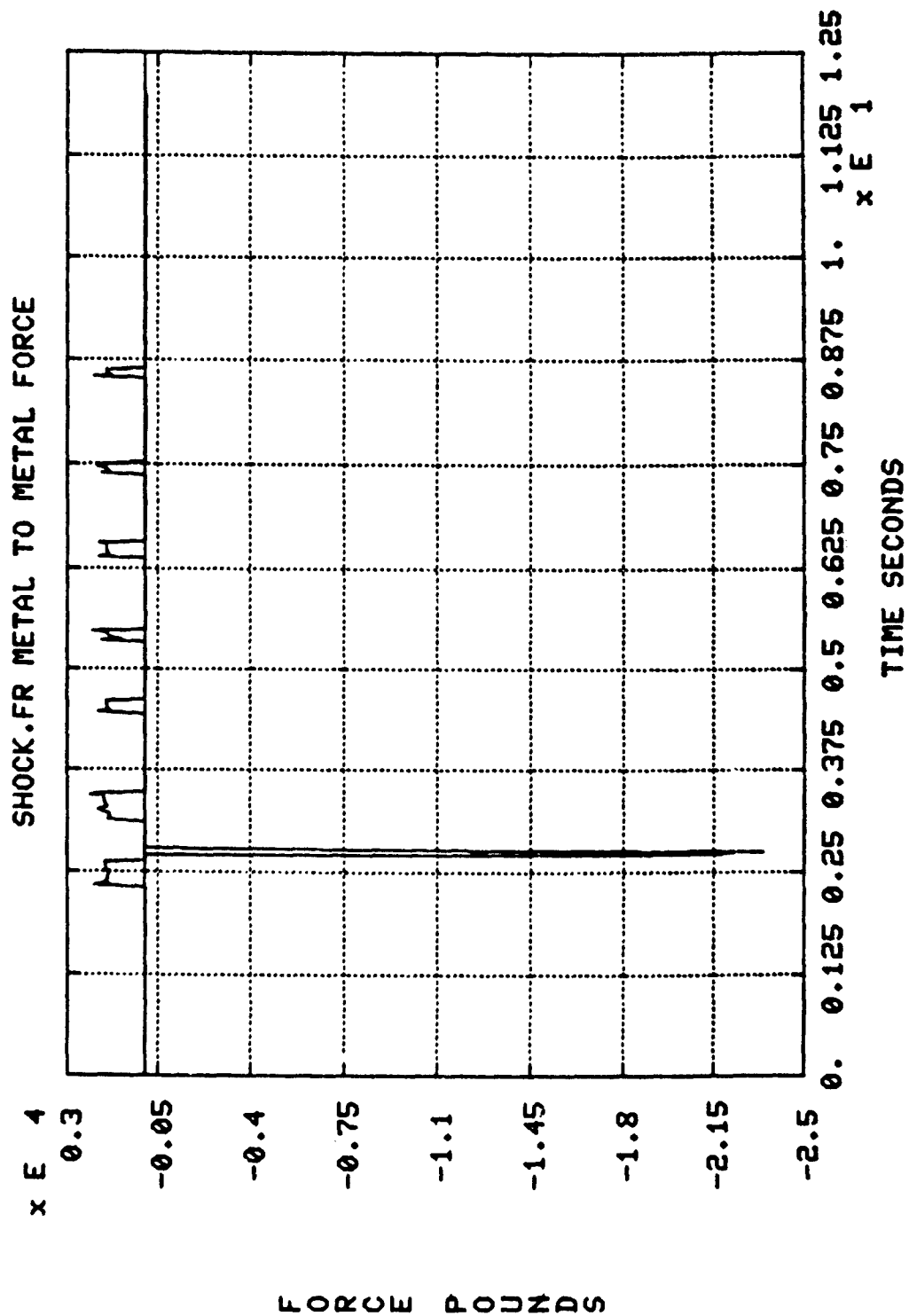
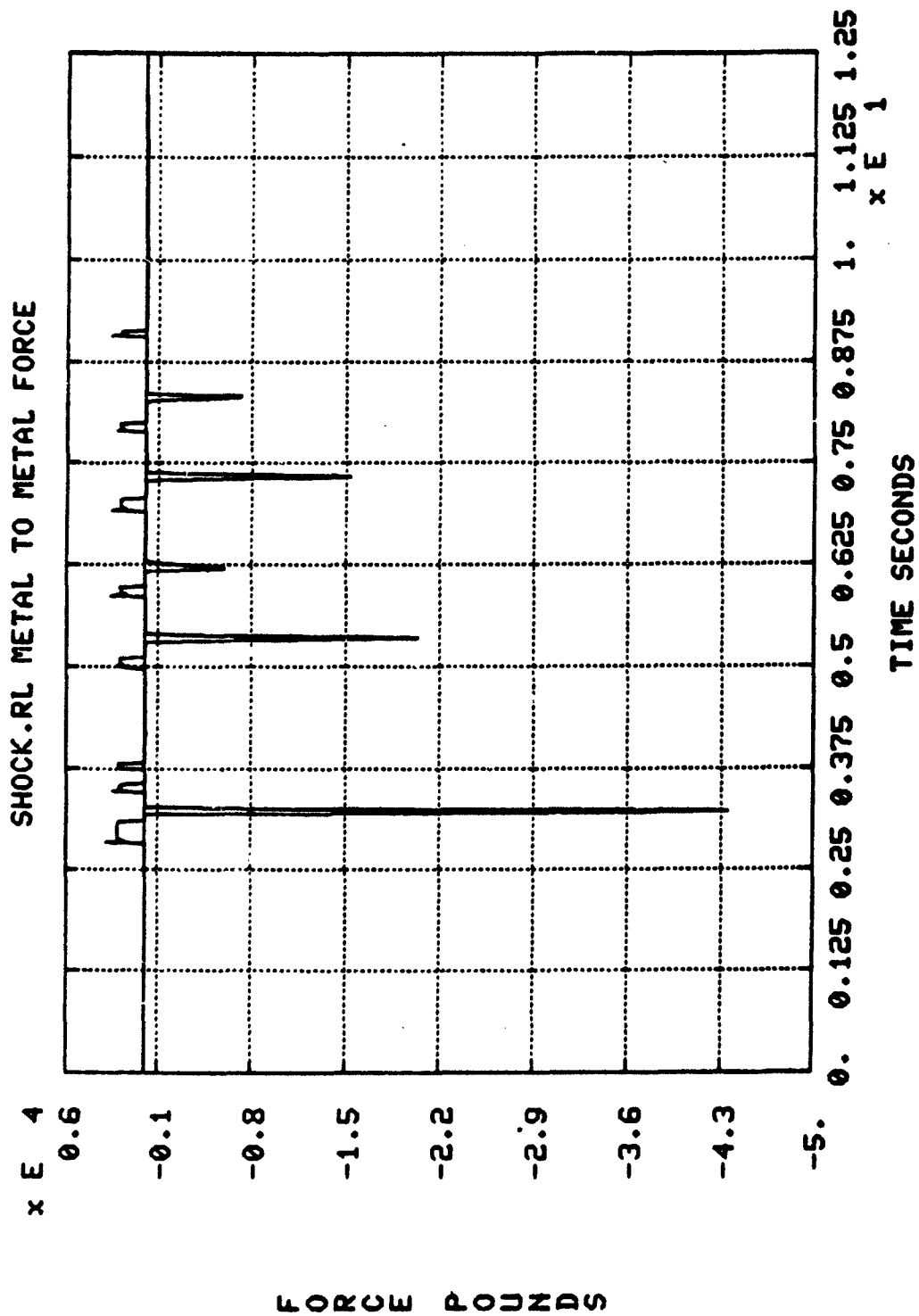


Figure 5-36. Front Left Shock Metal to Metal Force



FORCE POUNDS

Figure 5-37. Front Right Shock Metal to Metal Force



80

Figure 5-38. Rear Left Shock Metal to Metal Force

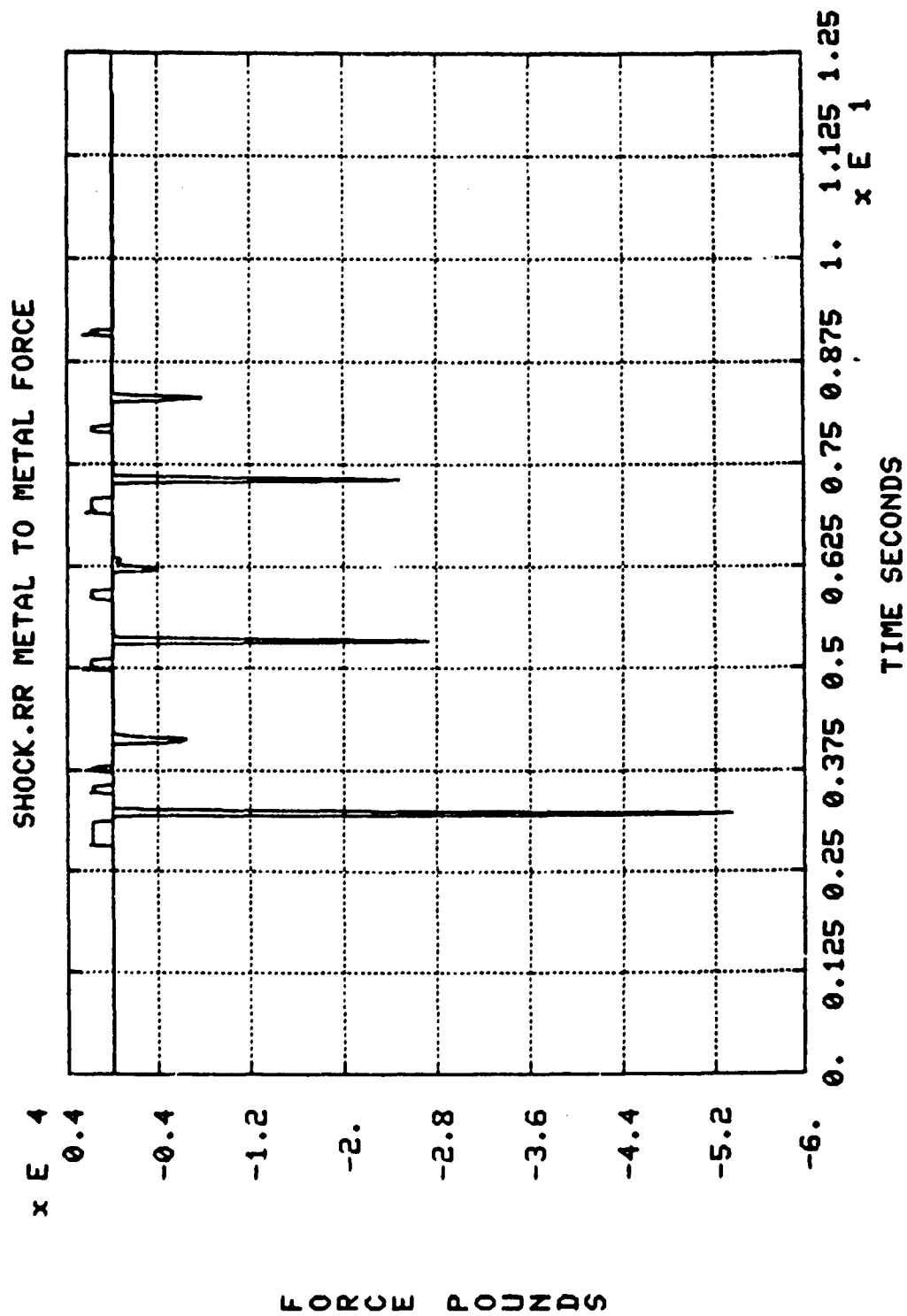
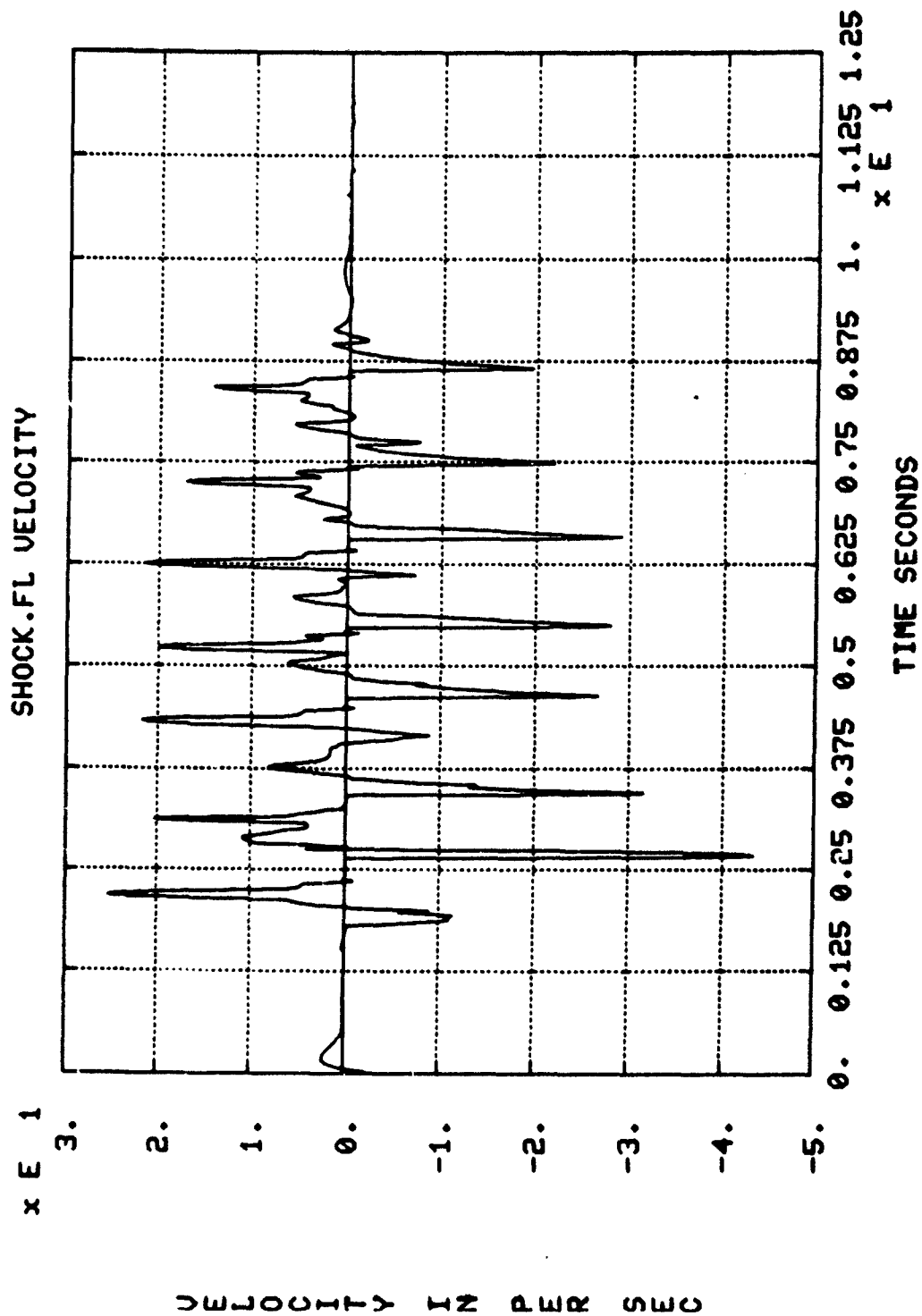
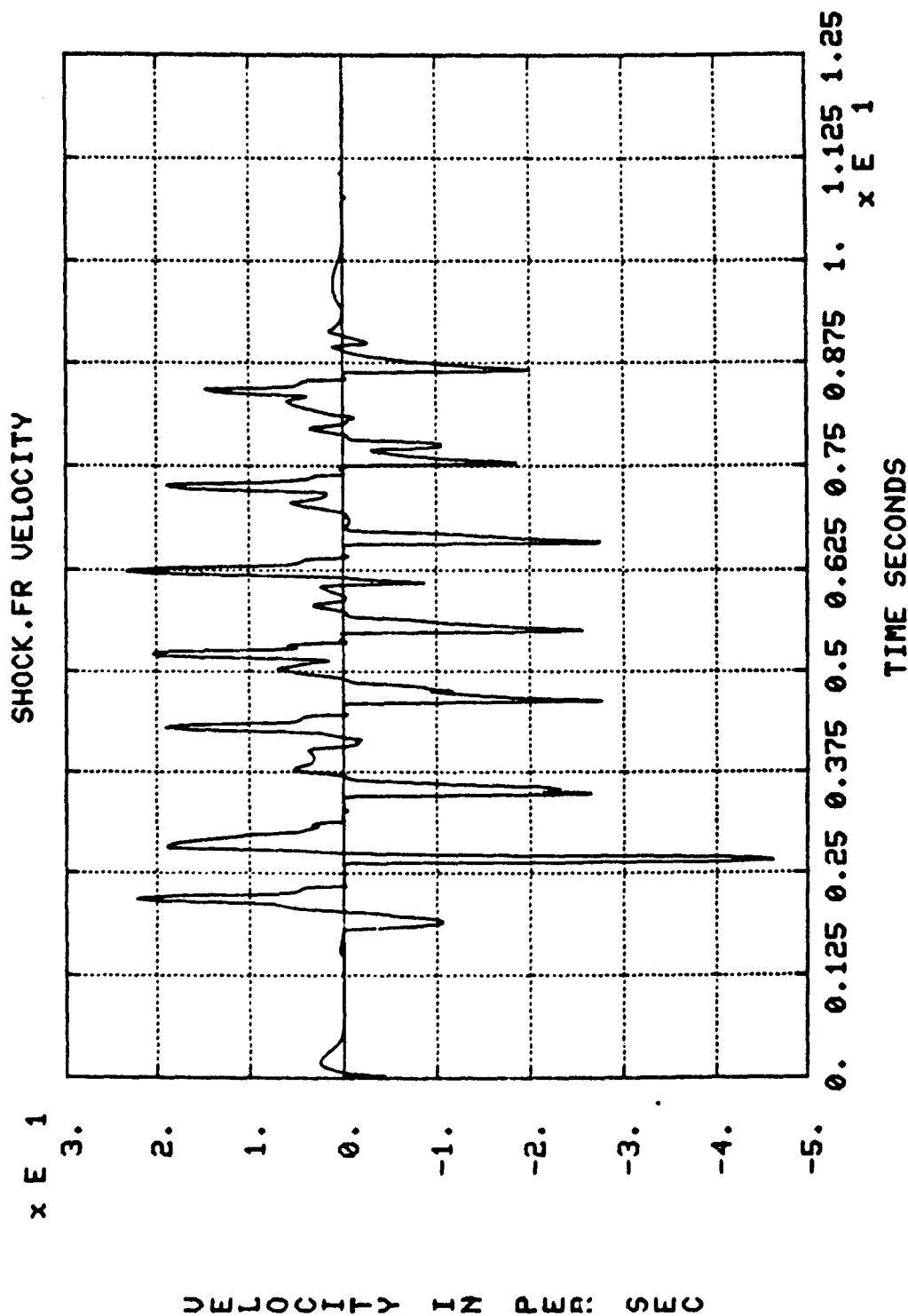


Figure 5-39. Rear Right Shock Metal To Metal Force



VELOCITY IN PER SEC

Figure 5-46. Front Left Shock Velocity



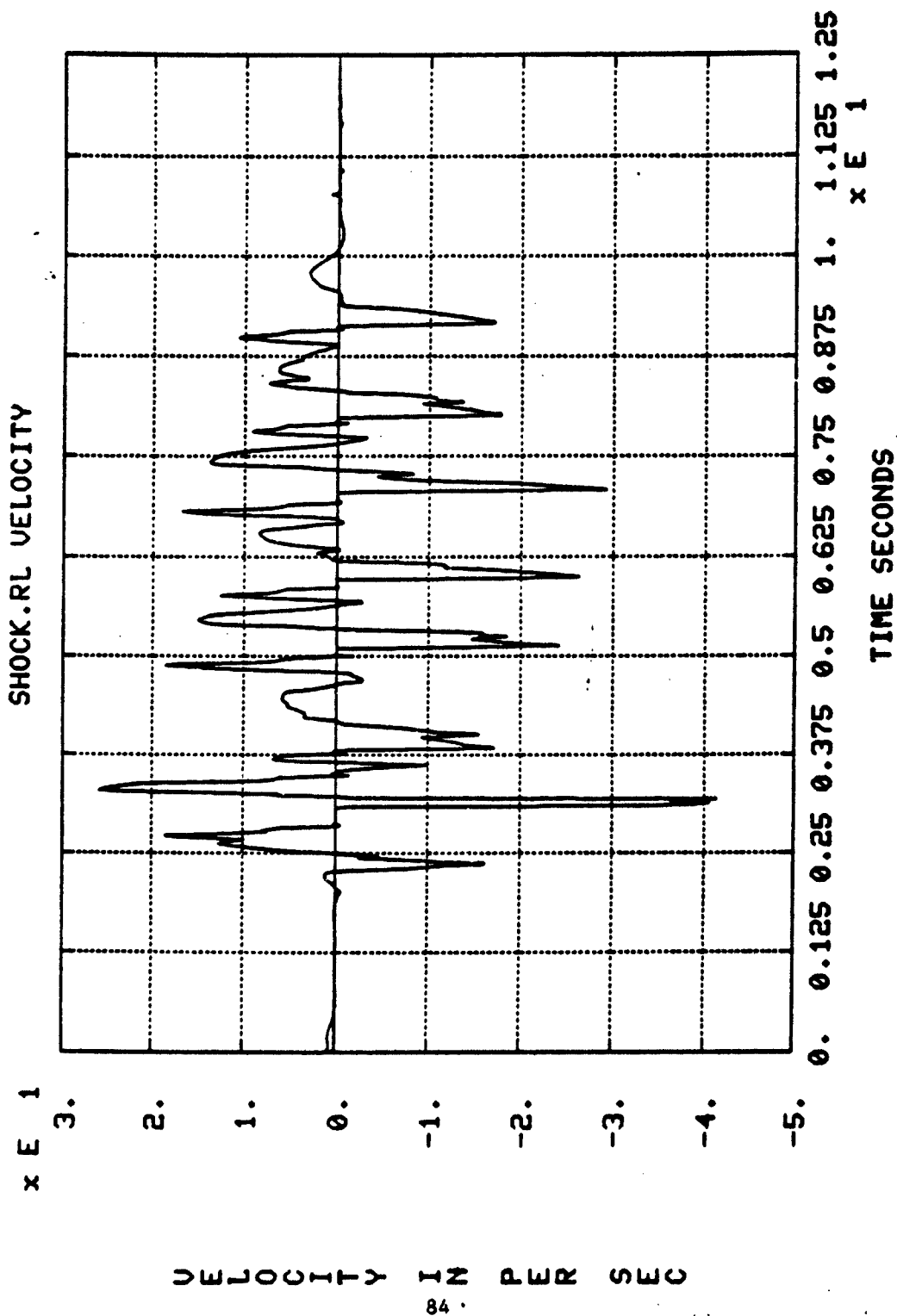


Figure 5-42. Rear Left Shock Velocity

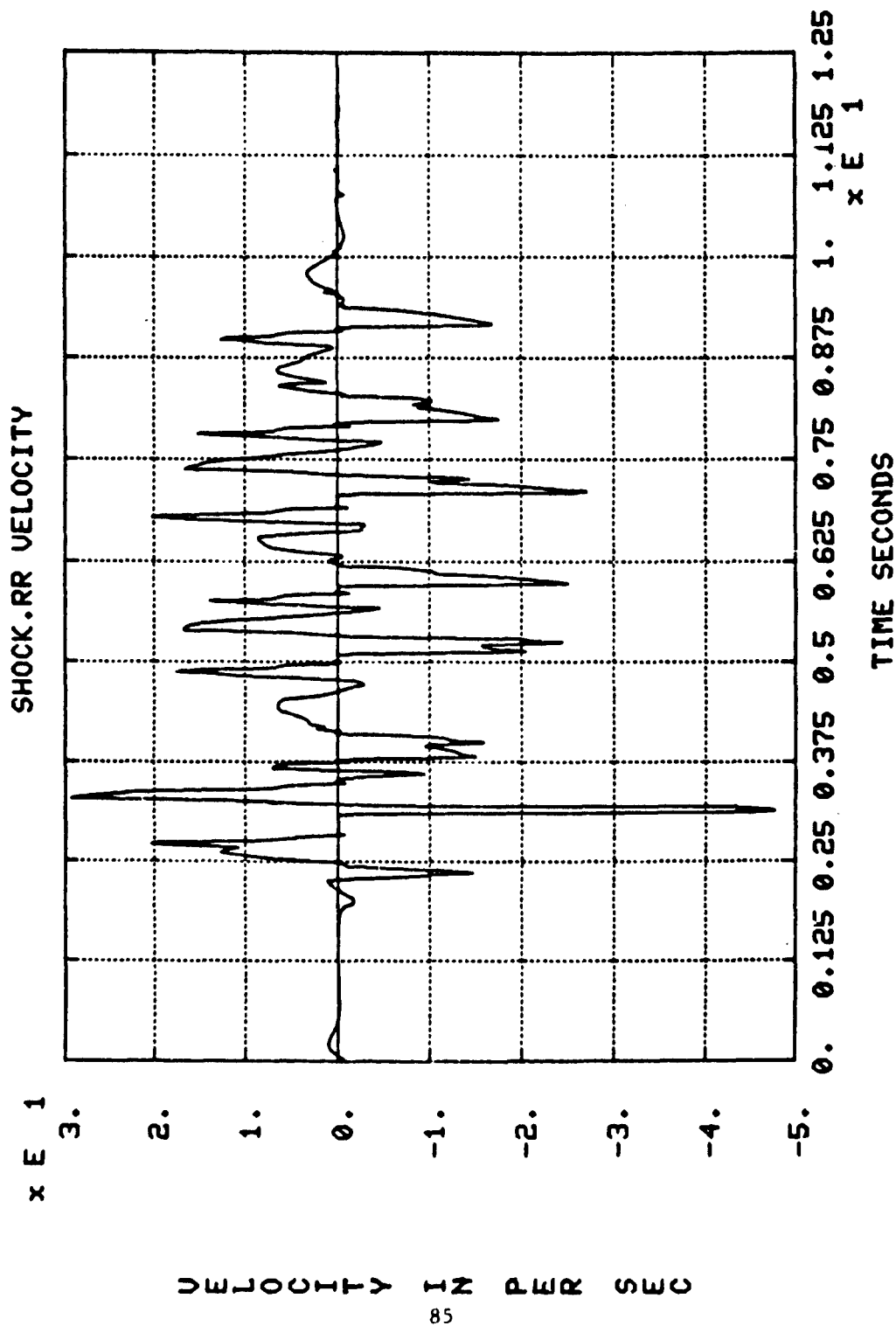
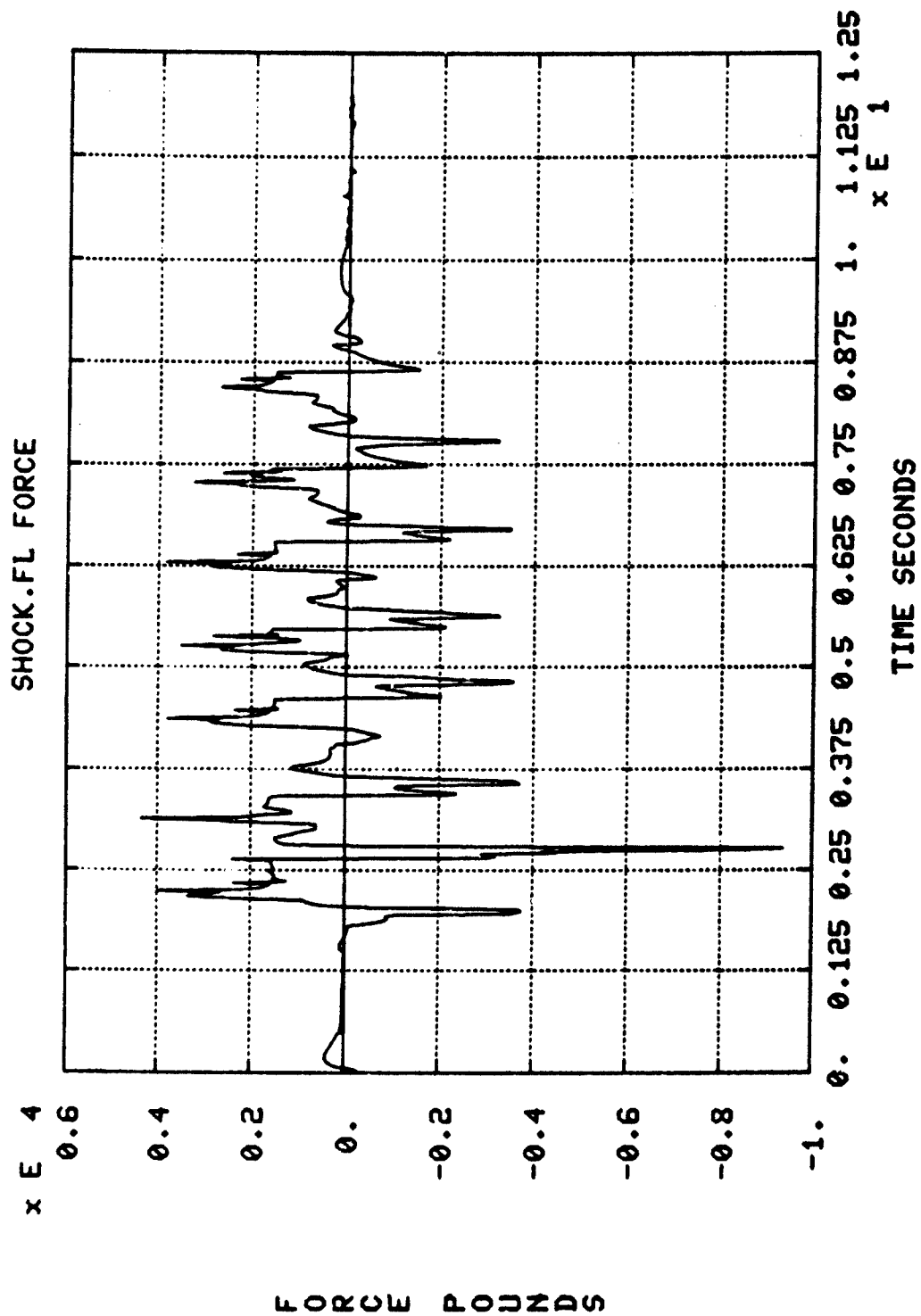


Figure 5-43. Rear Right Shock Velocity



FORCE POUNDS

Figure 5-44. Front Left Shock Force

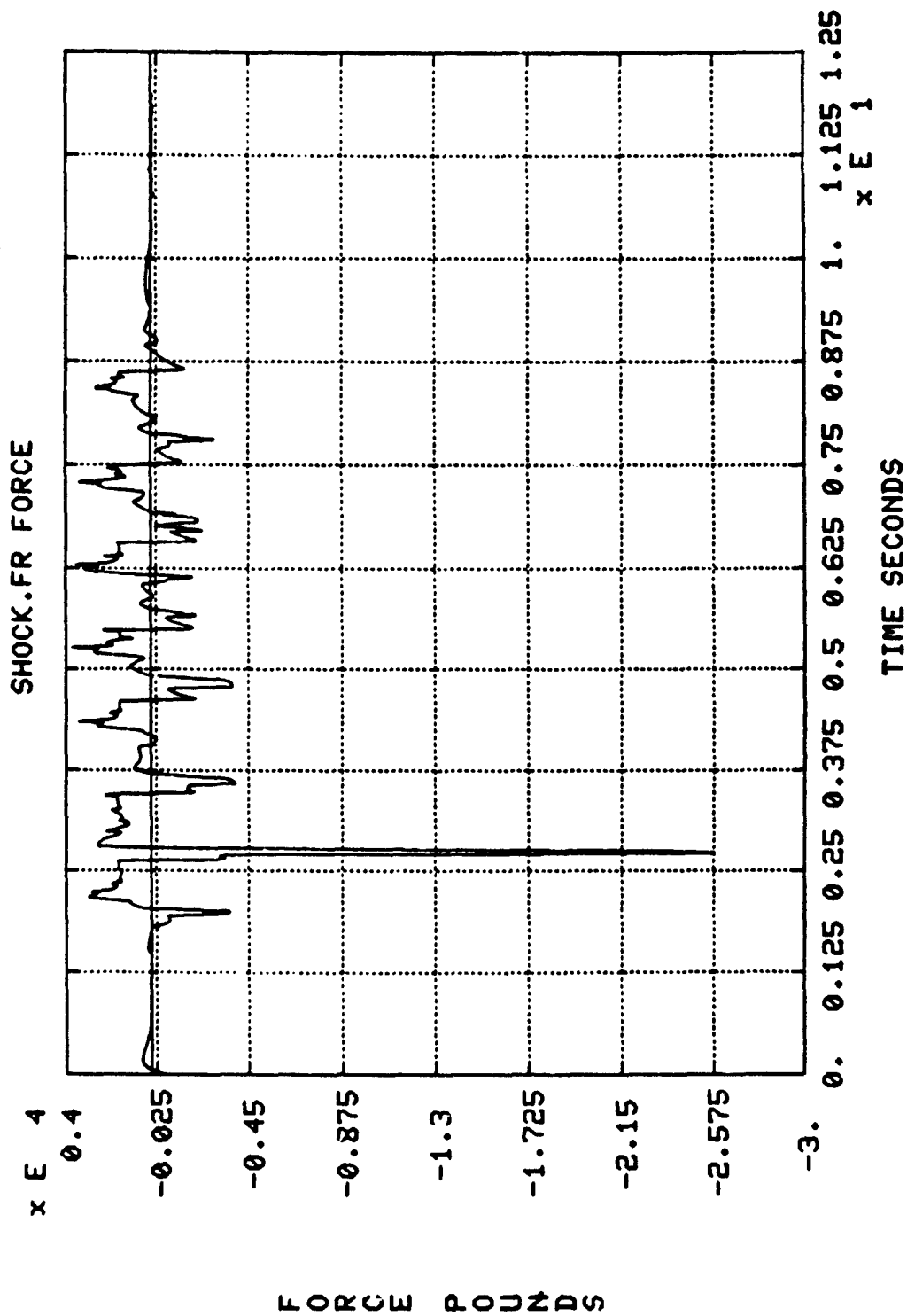


Figure 5-45. Front Right Shock Force

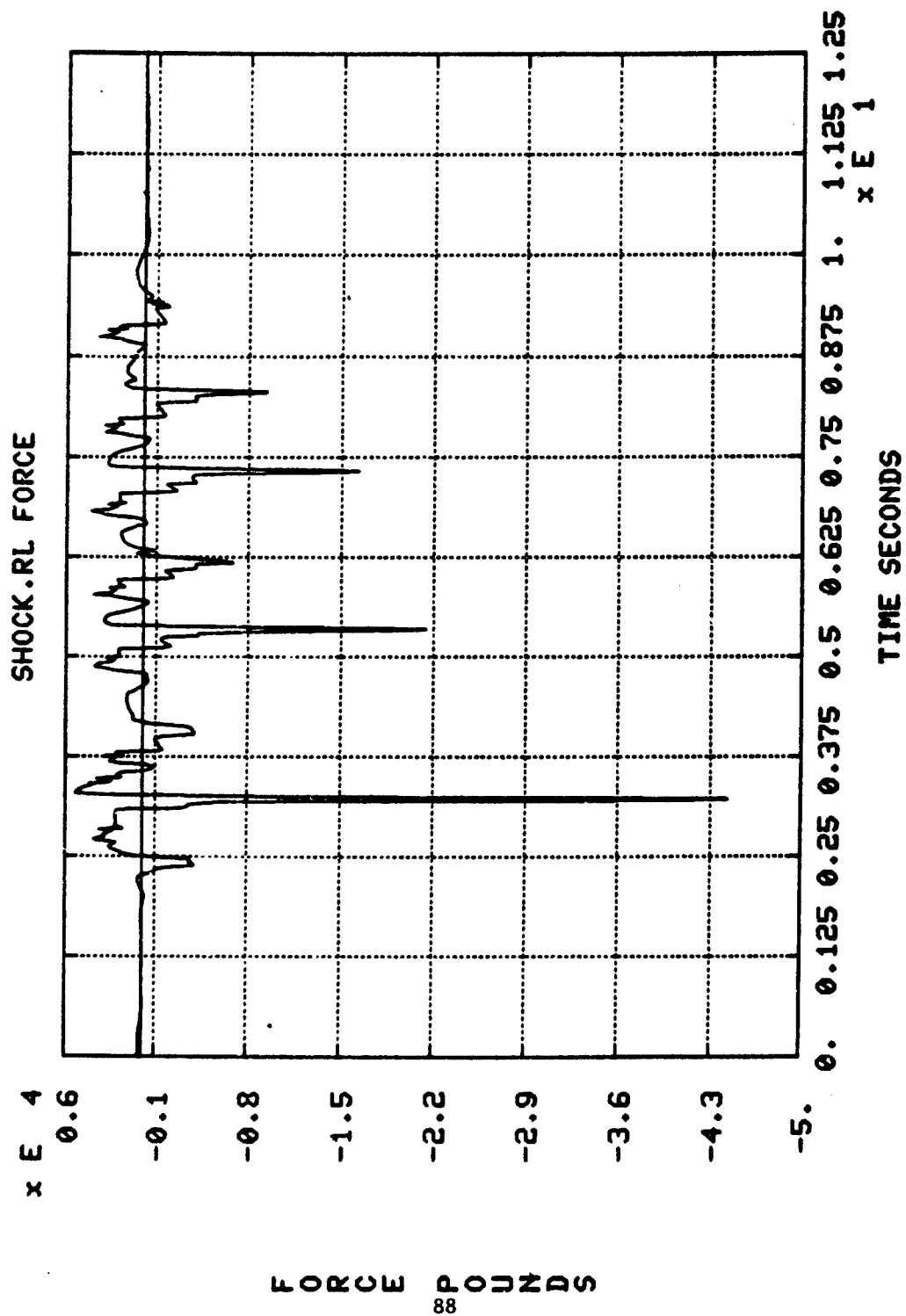


Figure 5-46. Rear Left Shock Force

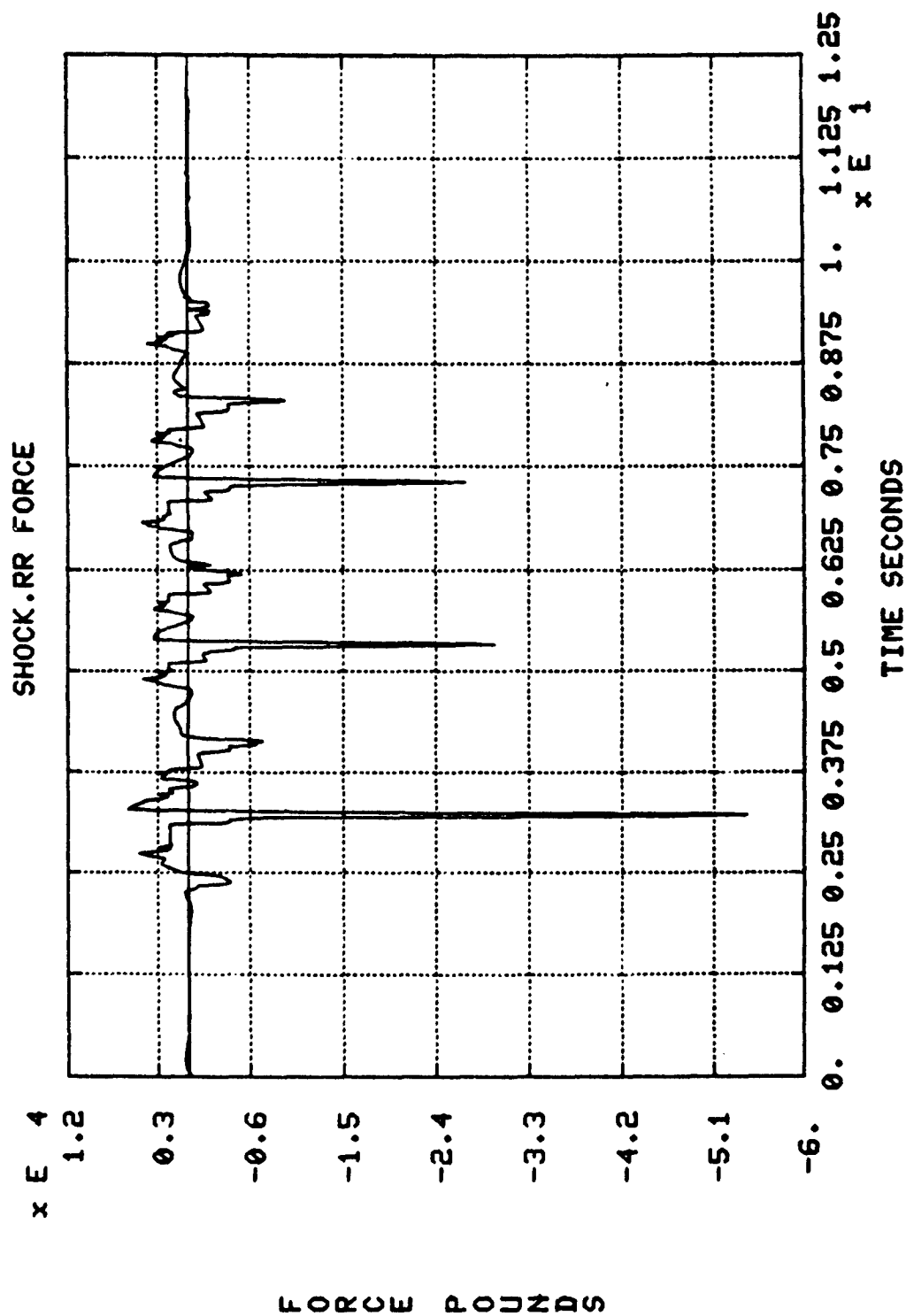


Figure 5-47. Rear Right Shock Force

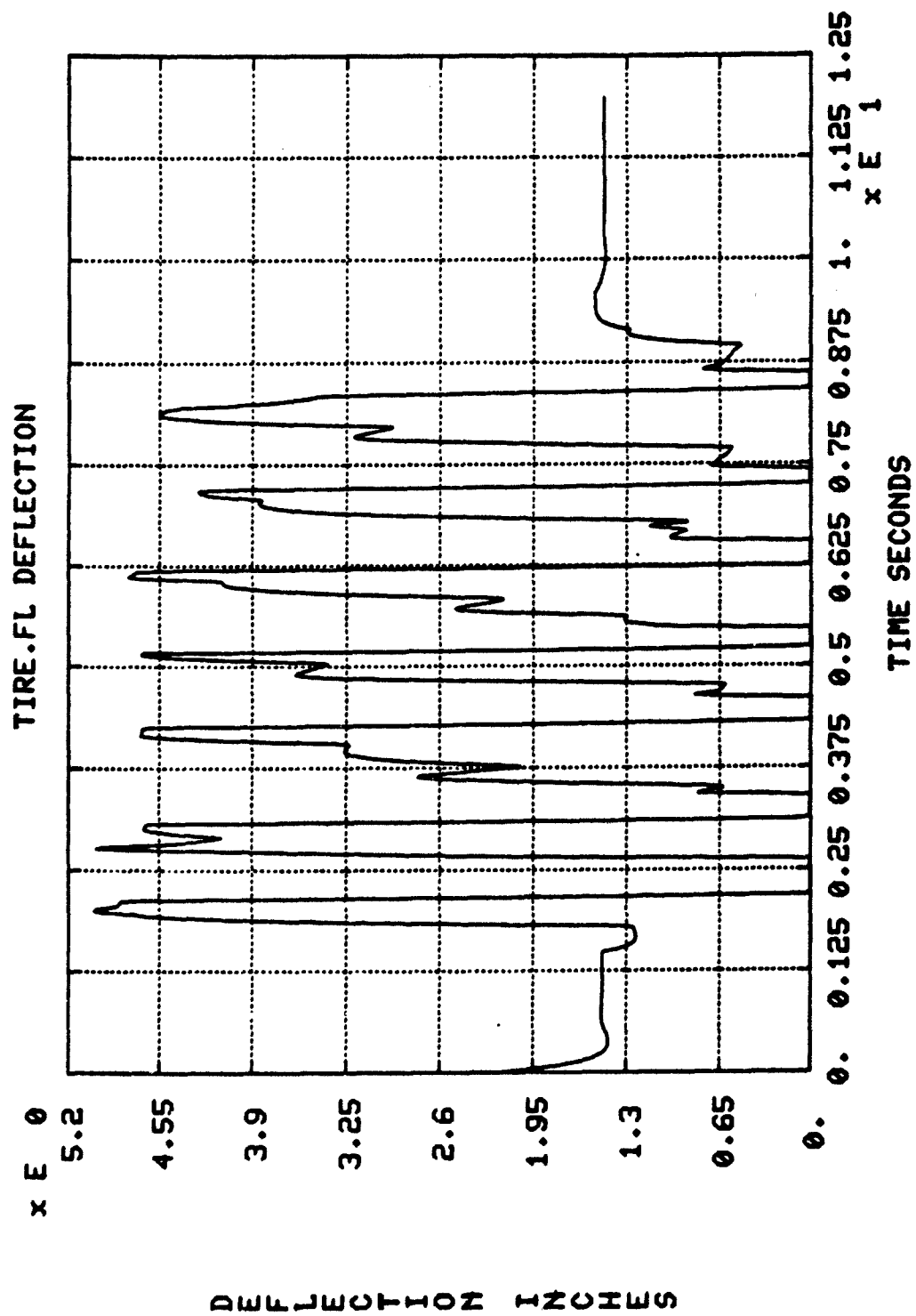


Figure 5-48. Front Left Tire Deflection

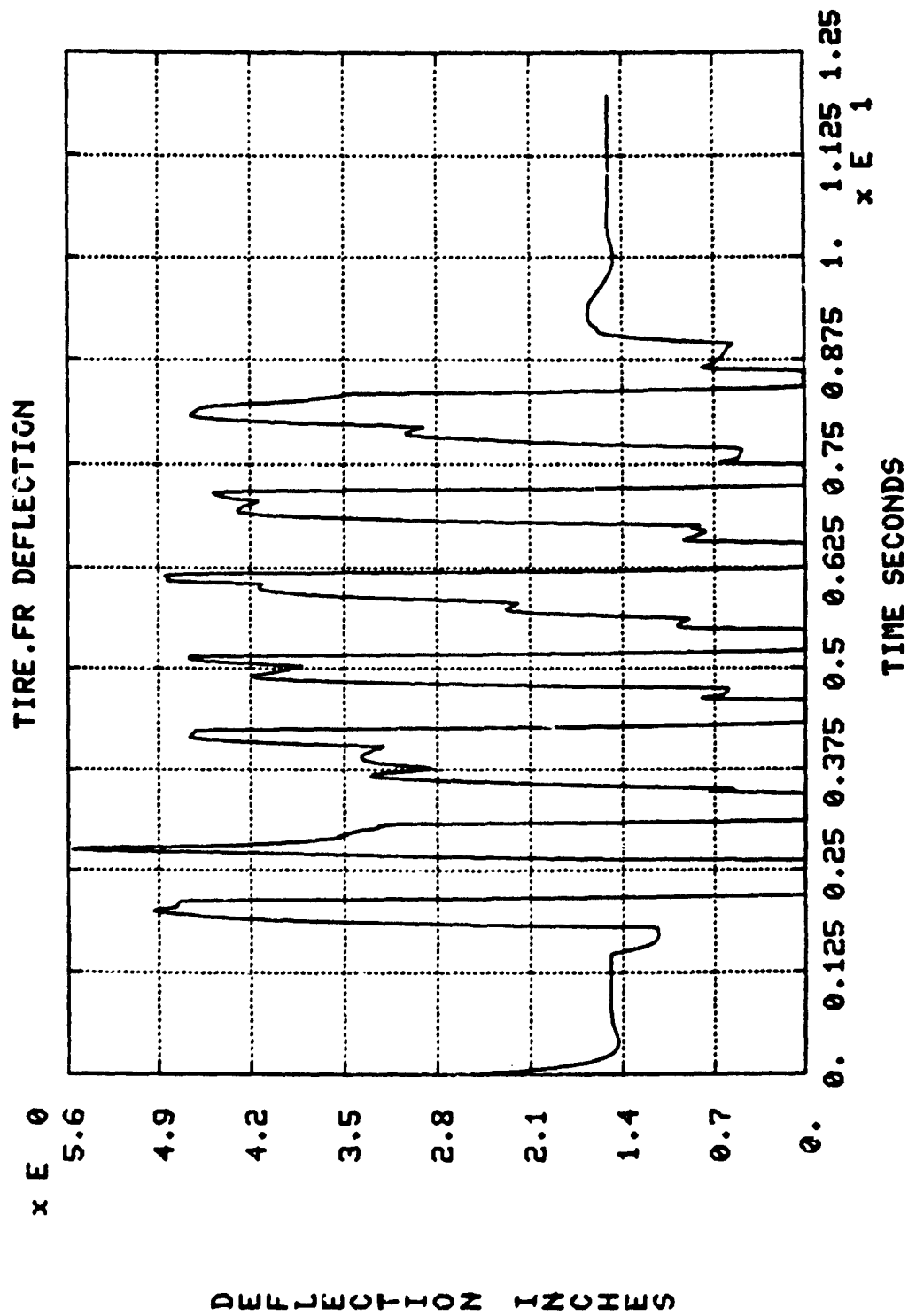


Figure 5-49. Front Right Tire Deflection

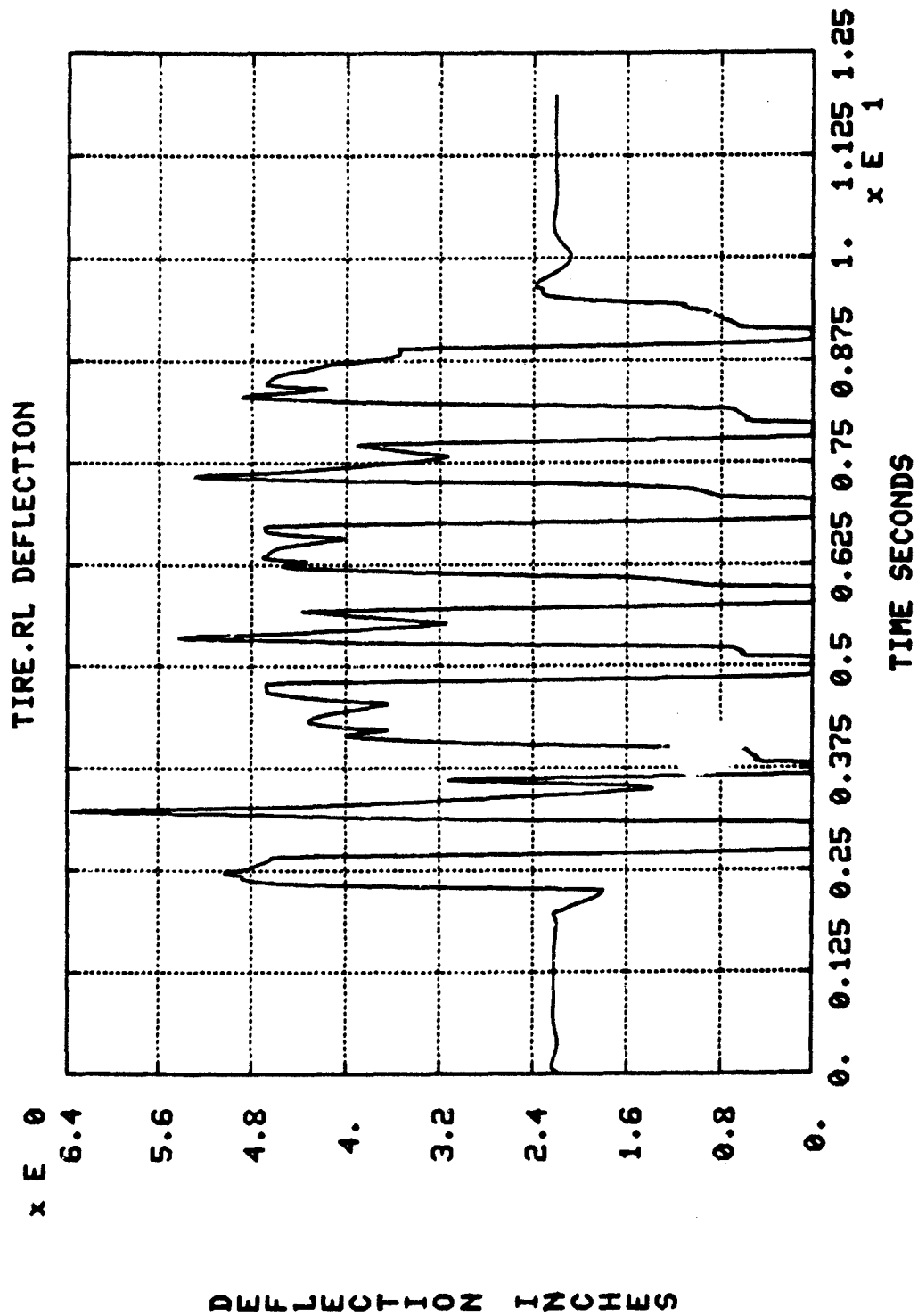


Figure 5-50. Rear Left Tire Deflection

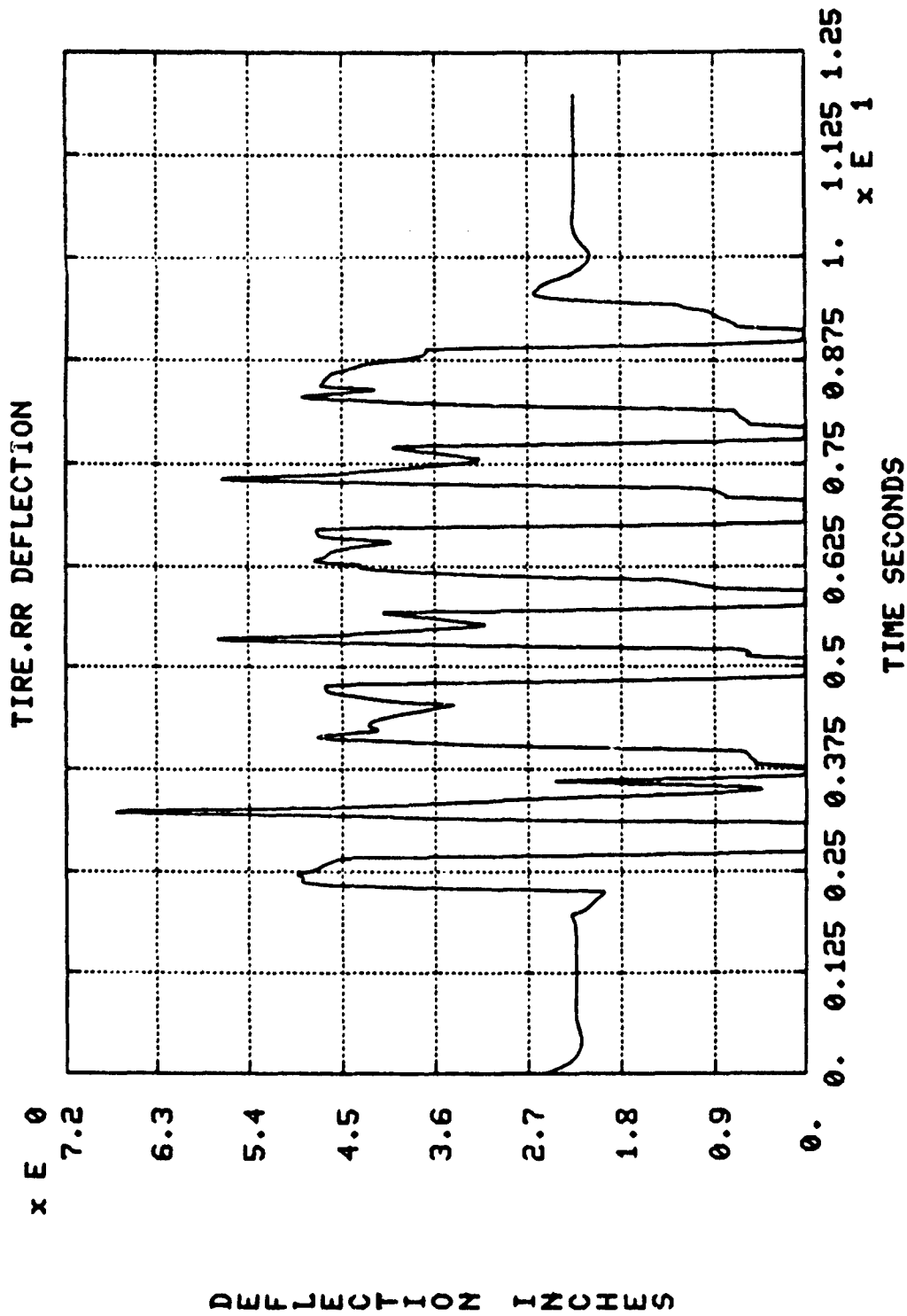


Figure 5-51. Rear Right Tire Deflection

deflection the wheel is off the ground. The front wheels and the rear wheels come off the ground after clearing each of the seven obstacles.

The radius of the run-flat device is 12.50 inches. The free radius of the tire is 18.15 inches. Assuming that the tire rubber thickness is 1.00 inches, if tire deflections exceed 4.65 inches then the inside of the tire has made contact with the run-flat device. The tolerance on the deflection is assumed to be plus or minus one-sixteenth of an inch. The run-flat device is modeled as a linear stiff spring element.

Figures 5-52 through 5-55 show the force generated when the tire makes contact with the run-flat device. The first and second occurrences of contacting the run-flat devices with the front and rear tires occur as the wheels strike the first obstacle and as the wheels return to the ground and strike the second obstacle.

Figures 5-56 through 5-59 show the total force generated by the tire. This includes tire stiffness, tire damping, and run-flat forces.

Figures 5-60 through 5-63 show the slip angles for the front left, the front right, the rear left, and the rear right tires.

Figures 5-64 through 5-67 show the lateral force on each tire. Lateral force is a function of slip angle and vertical tire force.

Figures 5-68 through 5-83 show the tensile and shear forces acting in each upper and lower ball joint. Tensile forces act along the kingpin axis. The kingpin axis is the line between the upper and lower ball joints. Shear force is the magnitude of the forces perpendicular to the kingpin axis acting at the center of the ball.

For a ductile material, such as steel, the maximum shear stress theory can be used to predict yielding. Joseph E. Shigley states in his book "Mechanical Engineering Design", "this theory predicts that the yield strength in shear is half the yield strength in tension. This theory is conservative and is always on the safe side of test results."¹²

The distortion energy theory can also be used to define the beginning of yield for ductile materials. This theory predicts that the ratio of yield strength in shear to the yield strength in tension is 0.577.¹³

Both theories clearly indicate that for a given ductile material shear forces are more dangerous than tensile forces.

The largest tensile and shear force occur within the lower rear right ball joint when the right rear wheel strikes the ground after clearing the first obstacle. At this time the right rear shock makes metal-to-metal contact in compression and the right rear tire makes contact with the run-flat device. These tire and shock absorber forces generate the large tensile and shear forces experienced by the ball joint.

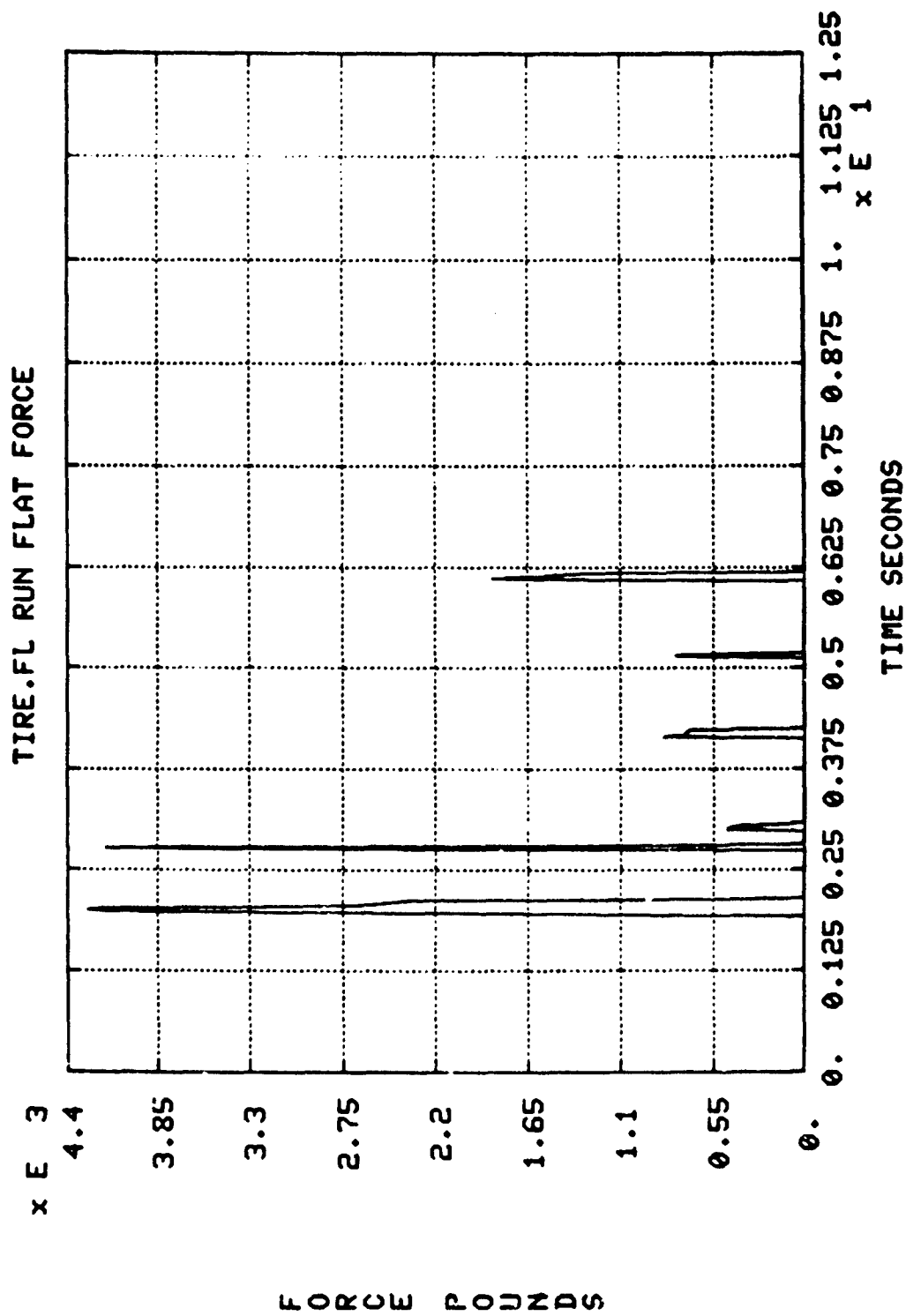


Figure 5-52. Front Left Tire Run Flat Force

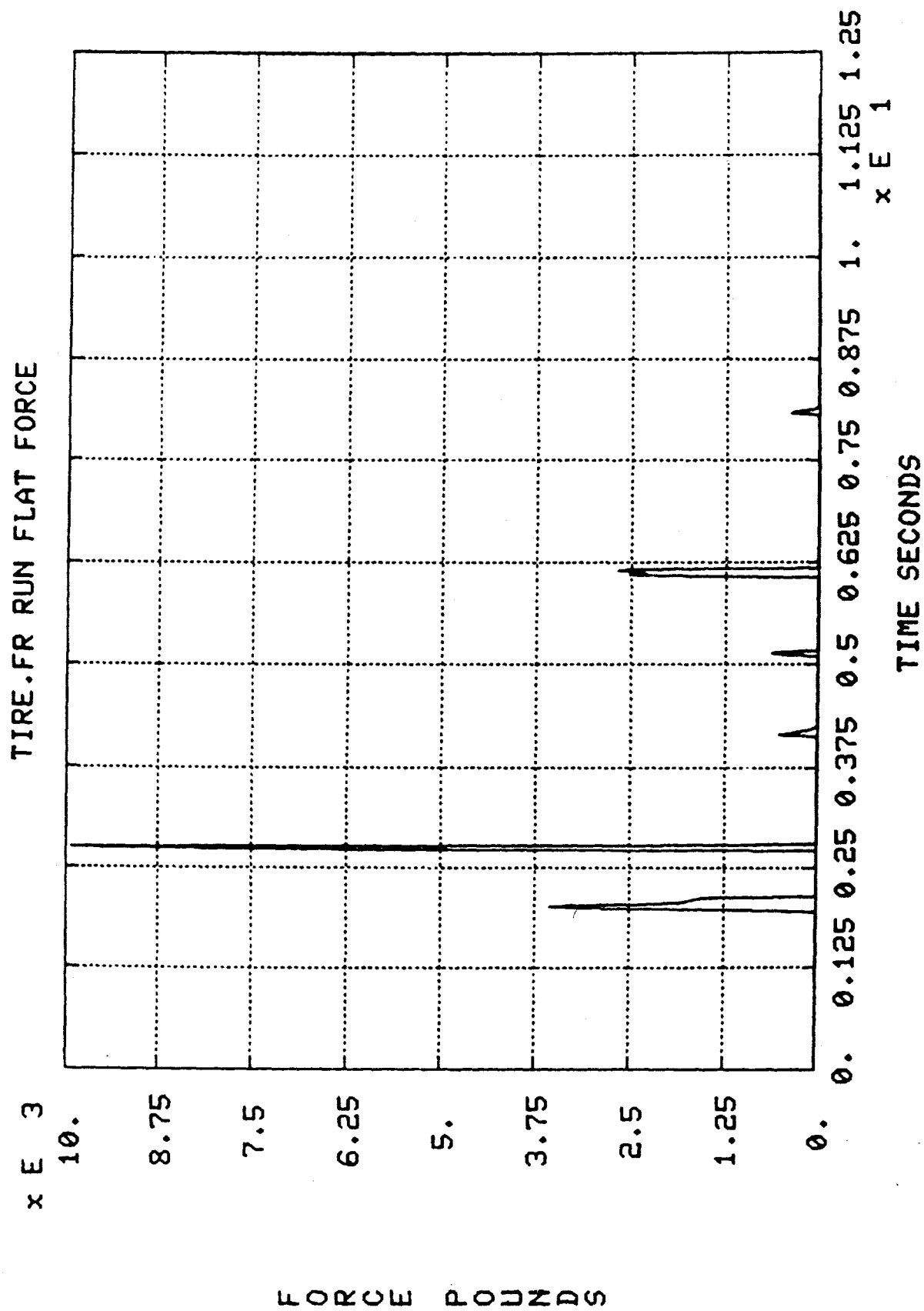


Figure 5-53. Front Right Tire Run Flat Force

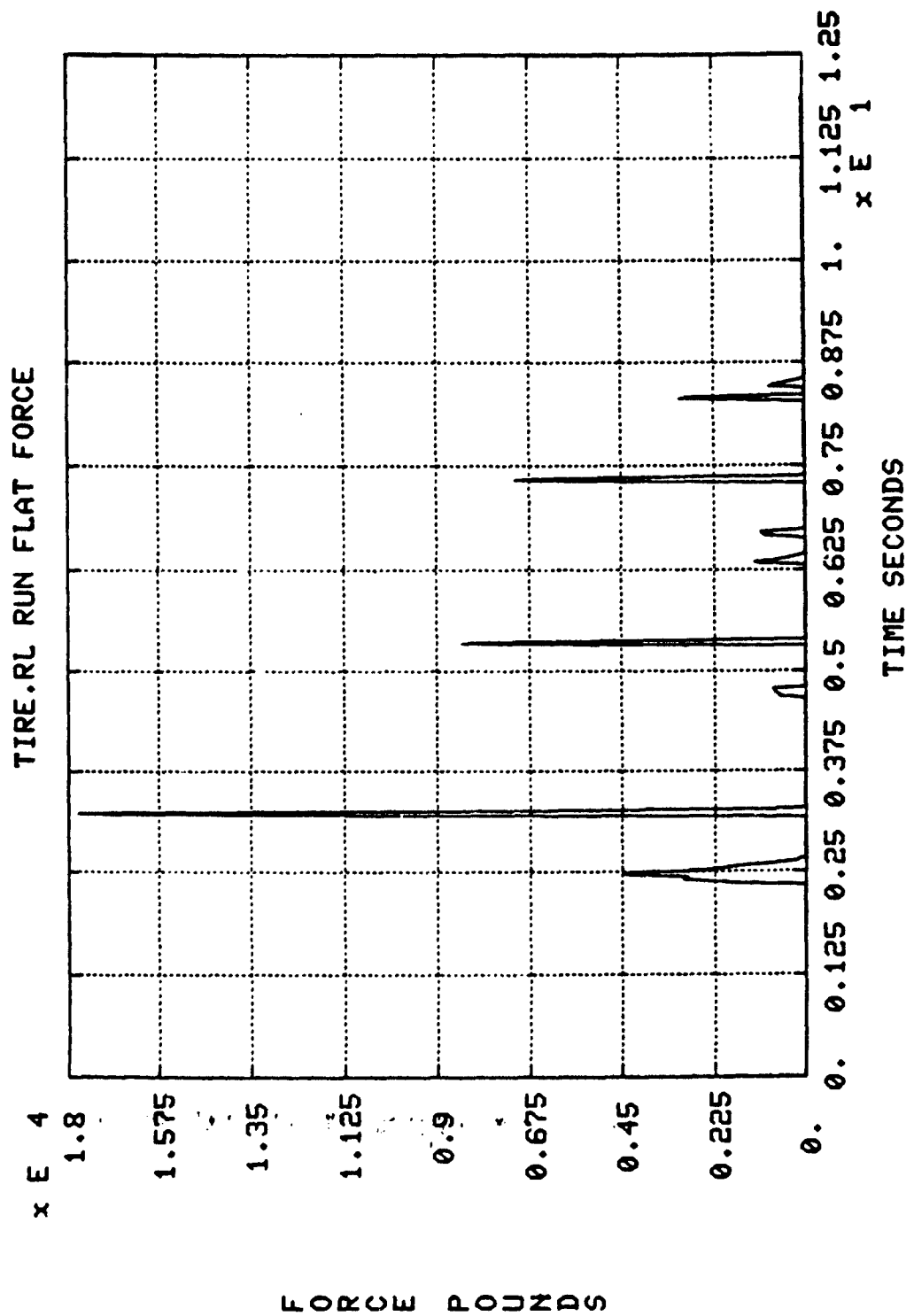


Figure 5-54. Rear Left Tire Run Flat Force

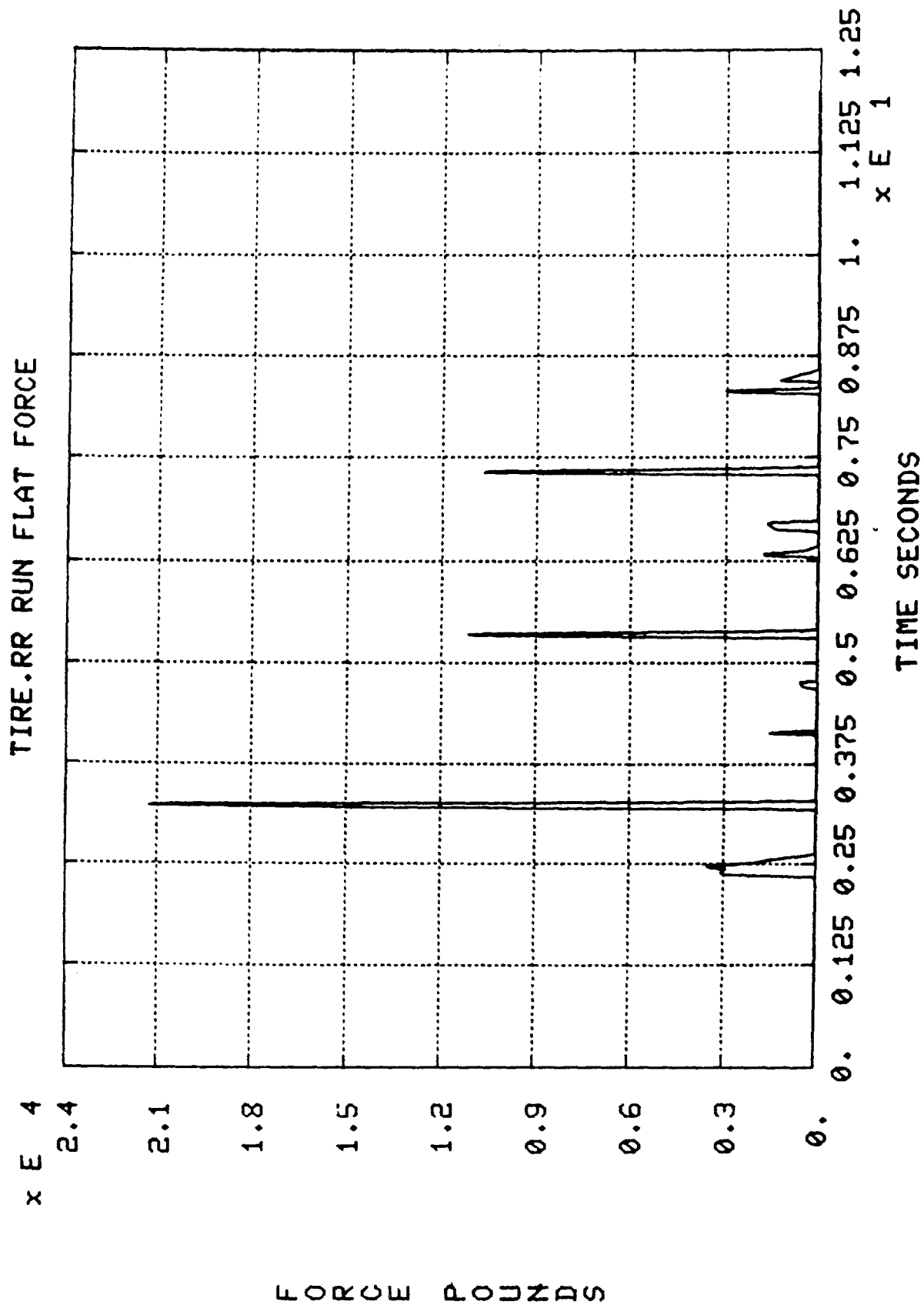


Figure 5-55. Rear Right Tire Run Flat Force

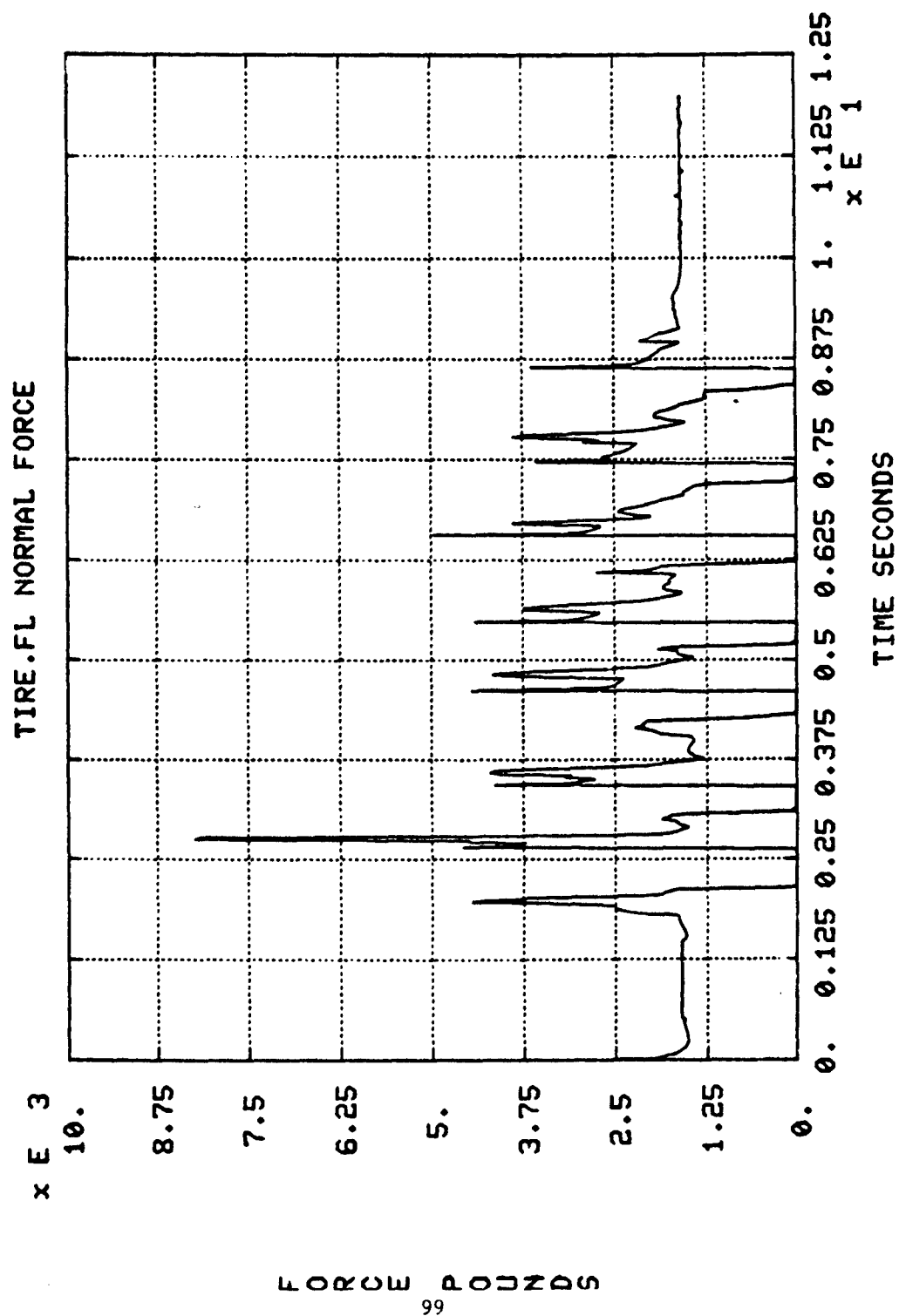
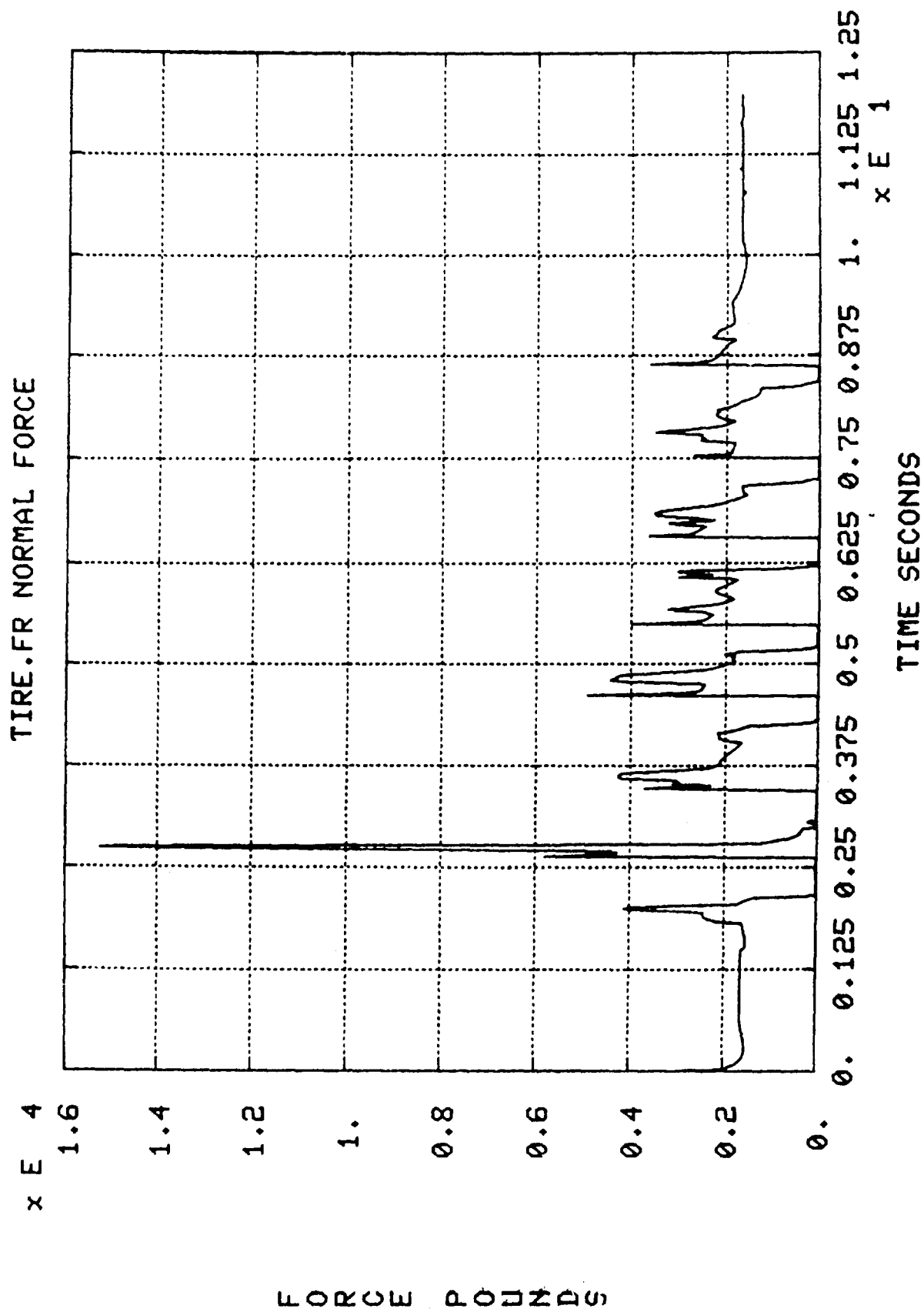
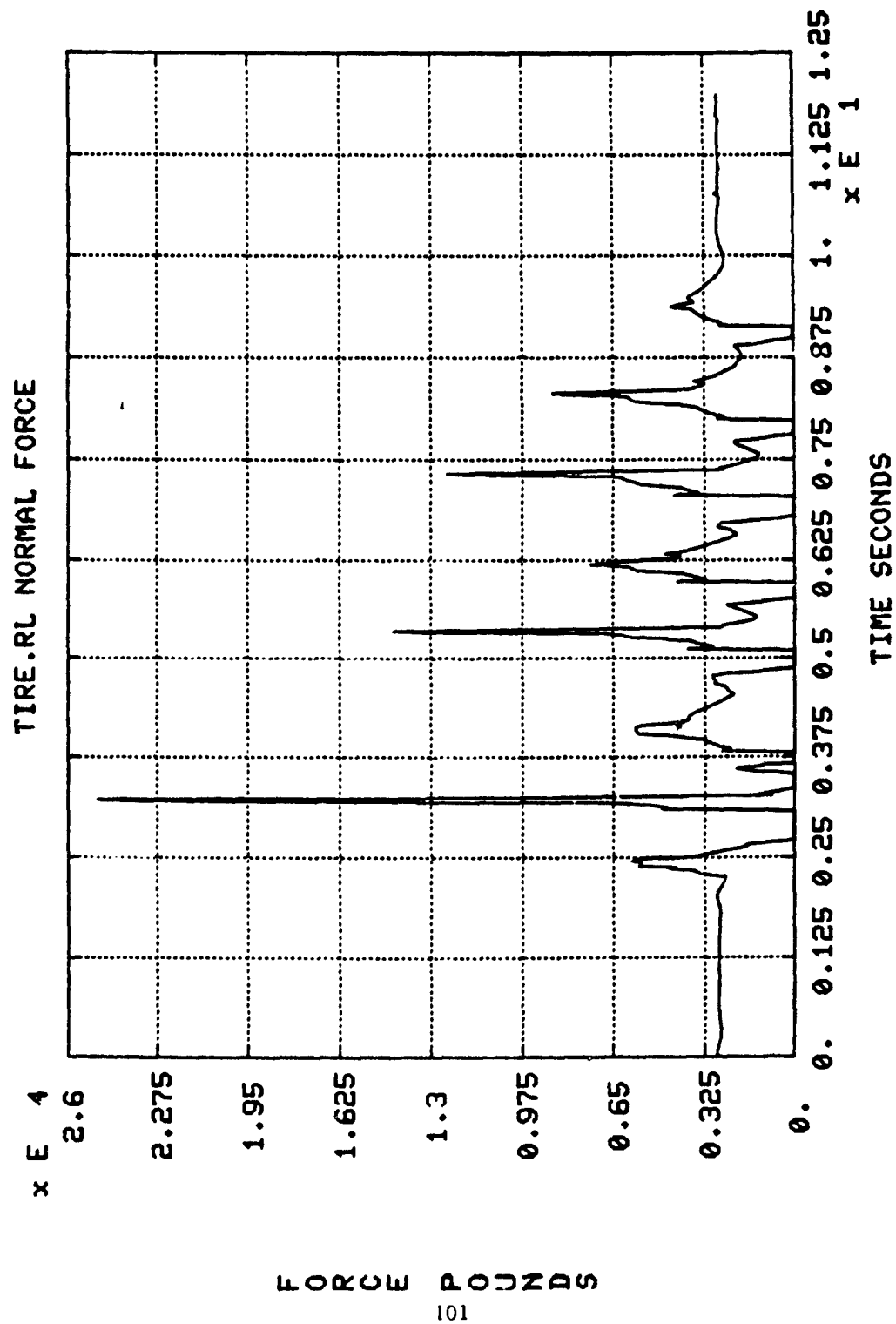


Figure 5-56. Front Left Tire Normal Force



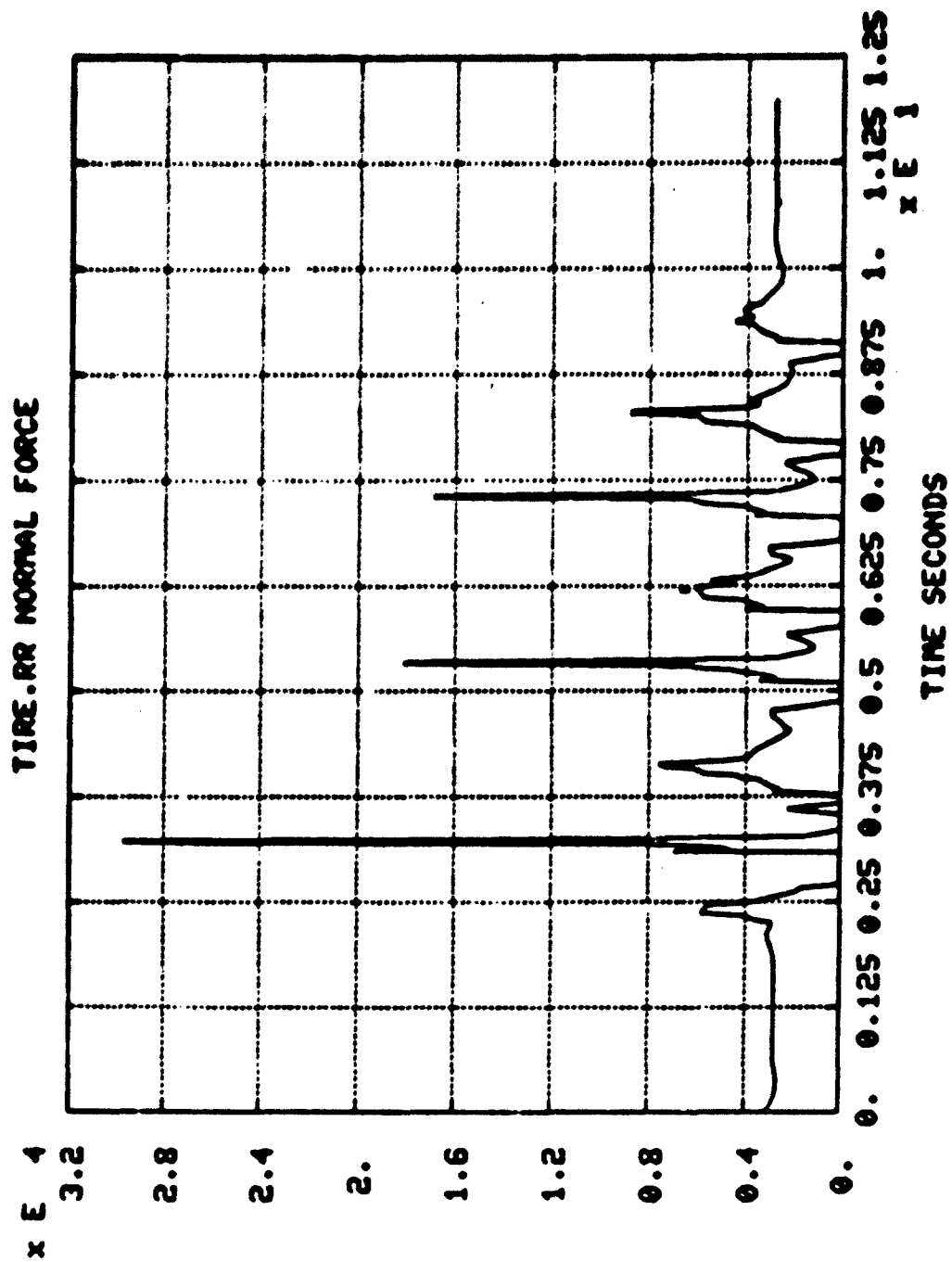
100

Figure 5-57. Front Right Tire Normal Force



101

Figure 5-58. Rear Left Tire Normal Force



FORCE POUNDS

102

Figure 5-59. Rear Right Tire Normal Force

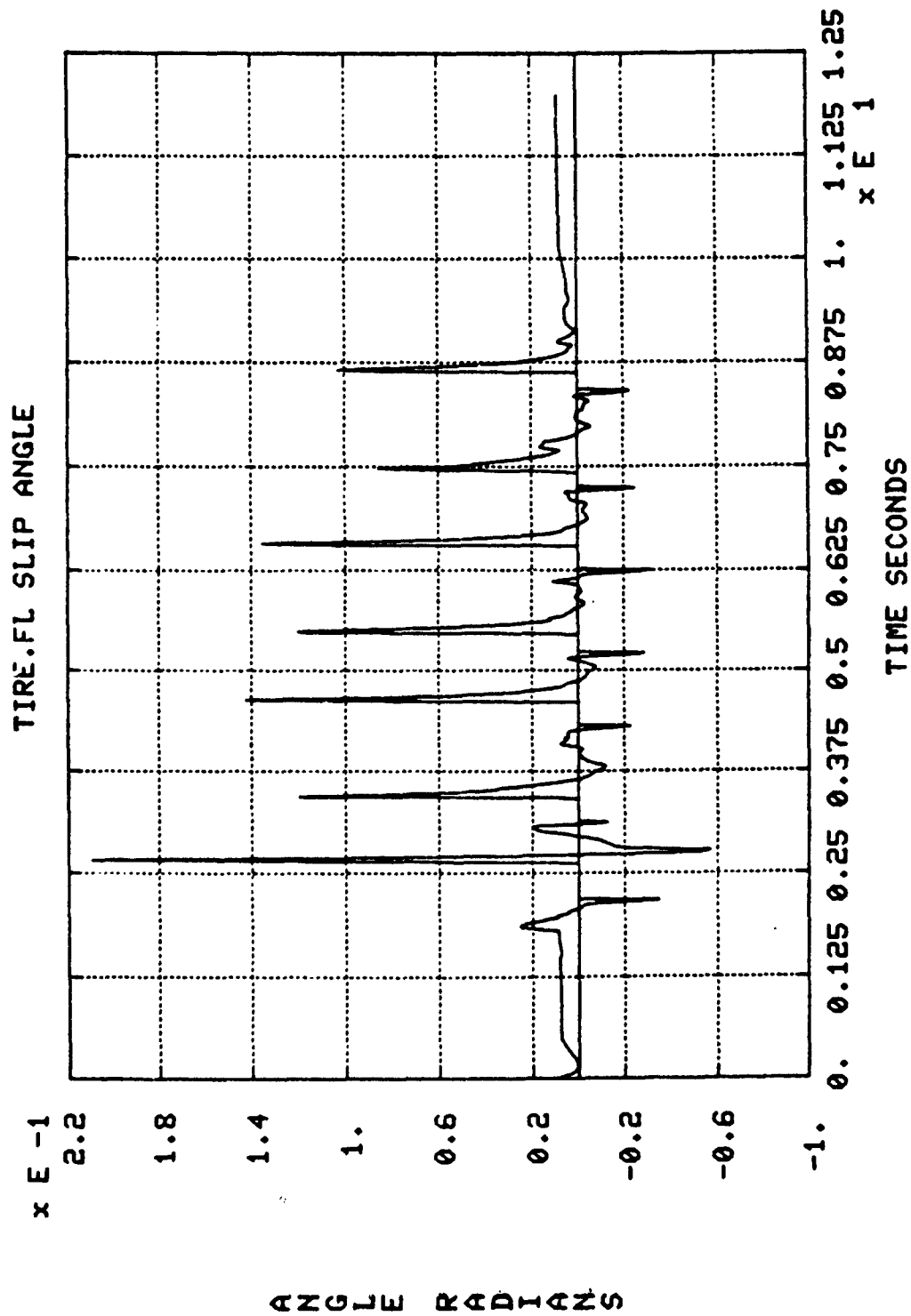


Figure 5-60. Front Left Tire Slip Angle

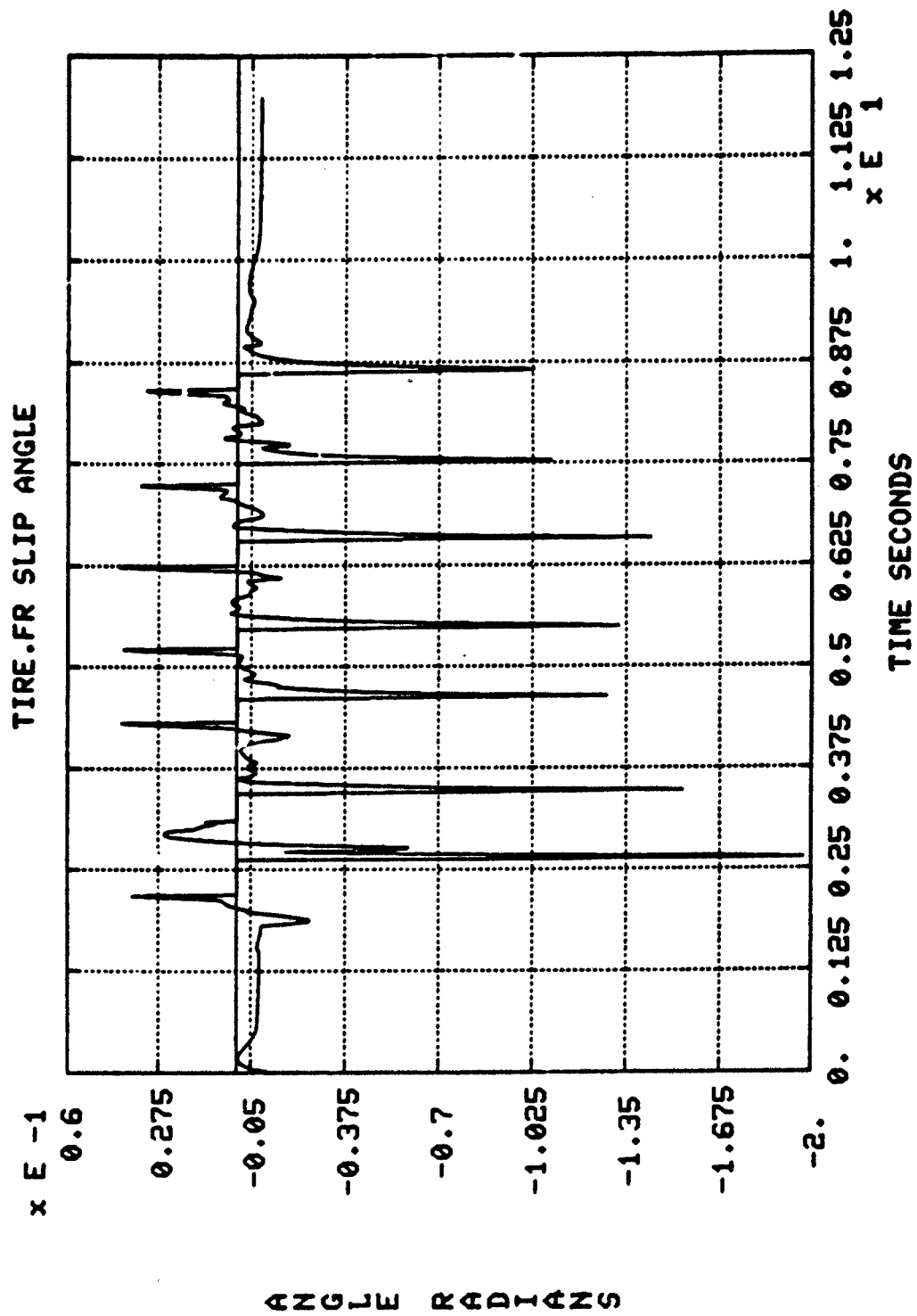


Figure 5-61. Front Right Tire Slip Angle

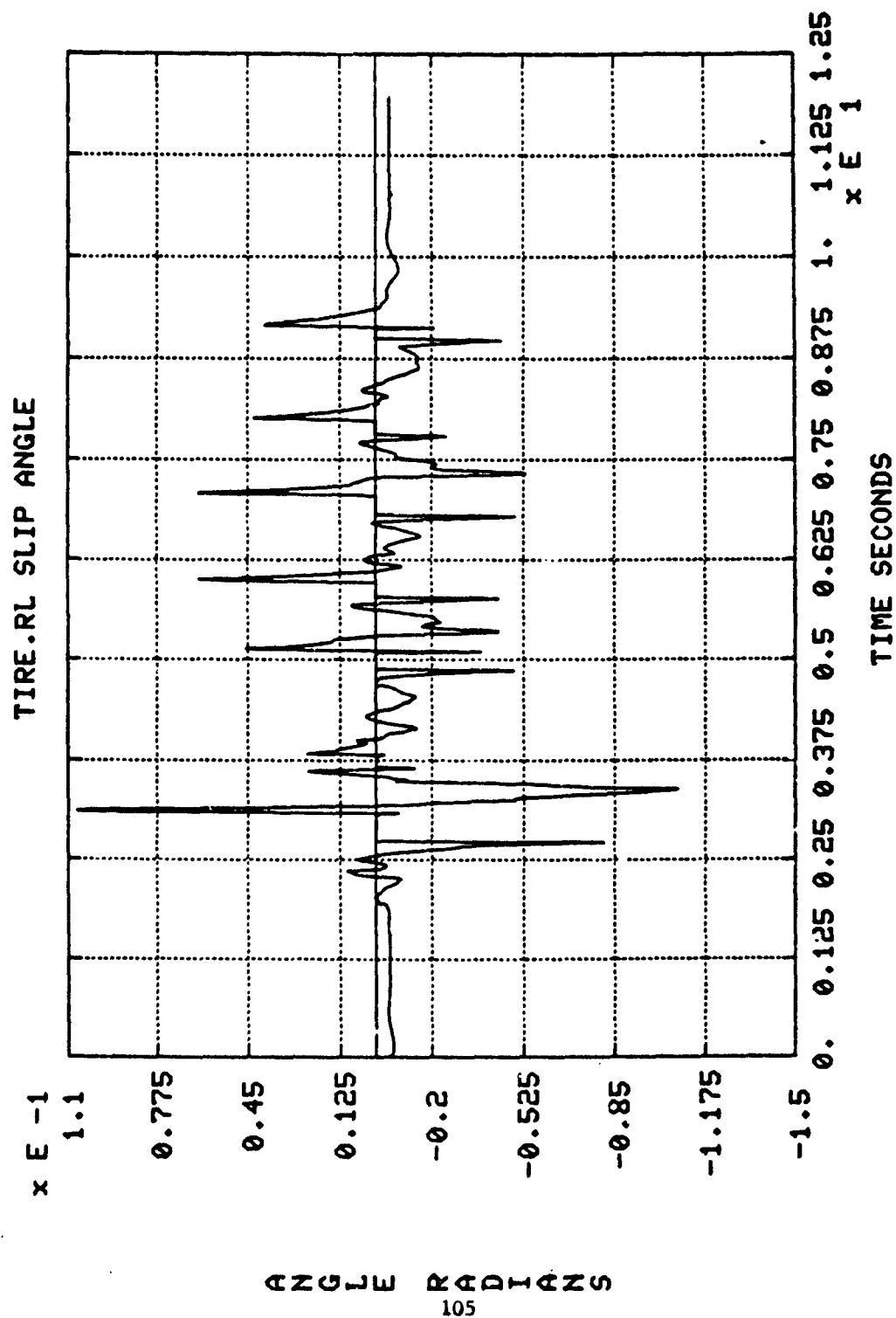


Figure 5-62. Rear Left Tire Slip Angle

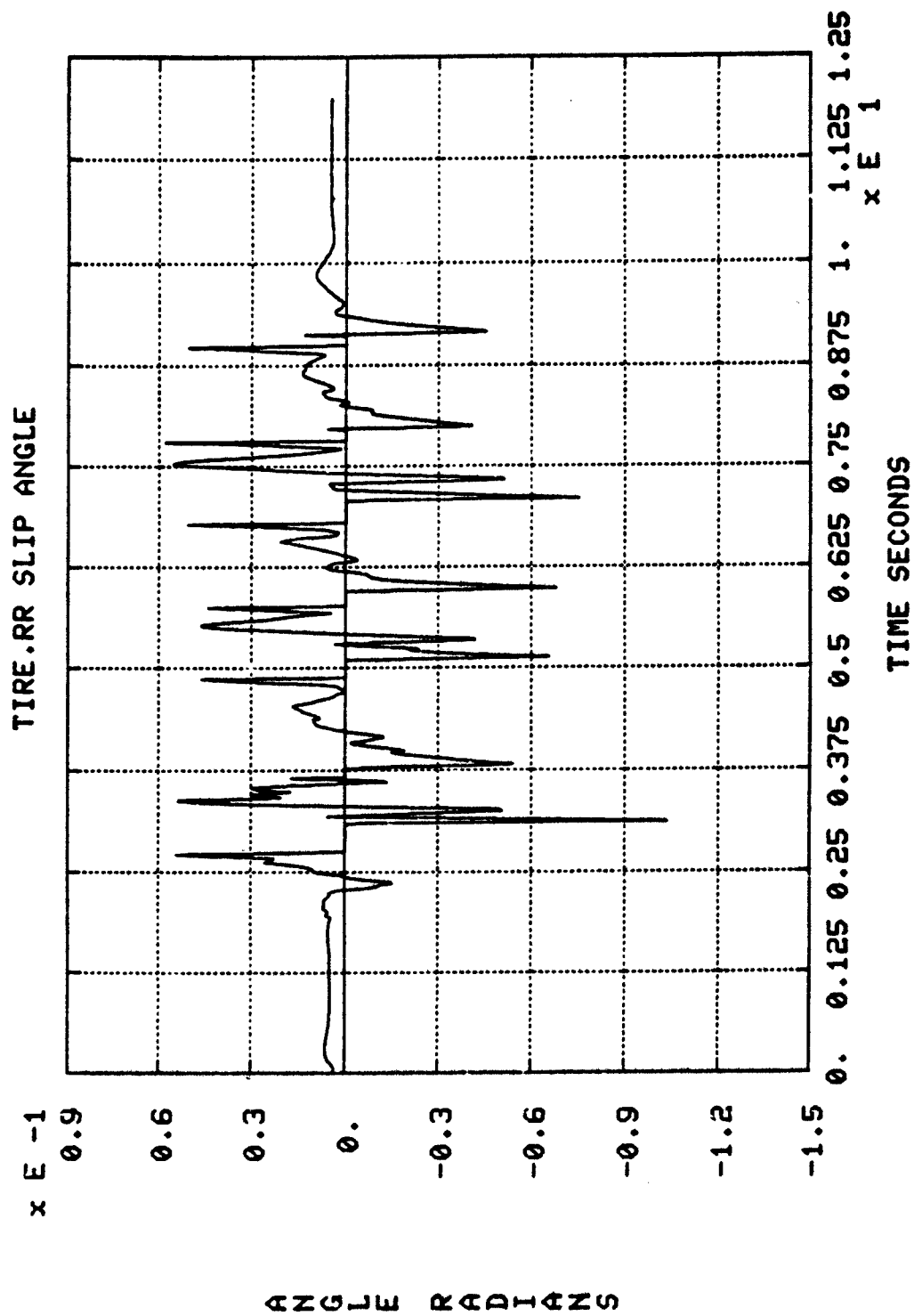


Figure 5-63. Rear Right Tire Slip Angle

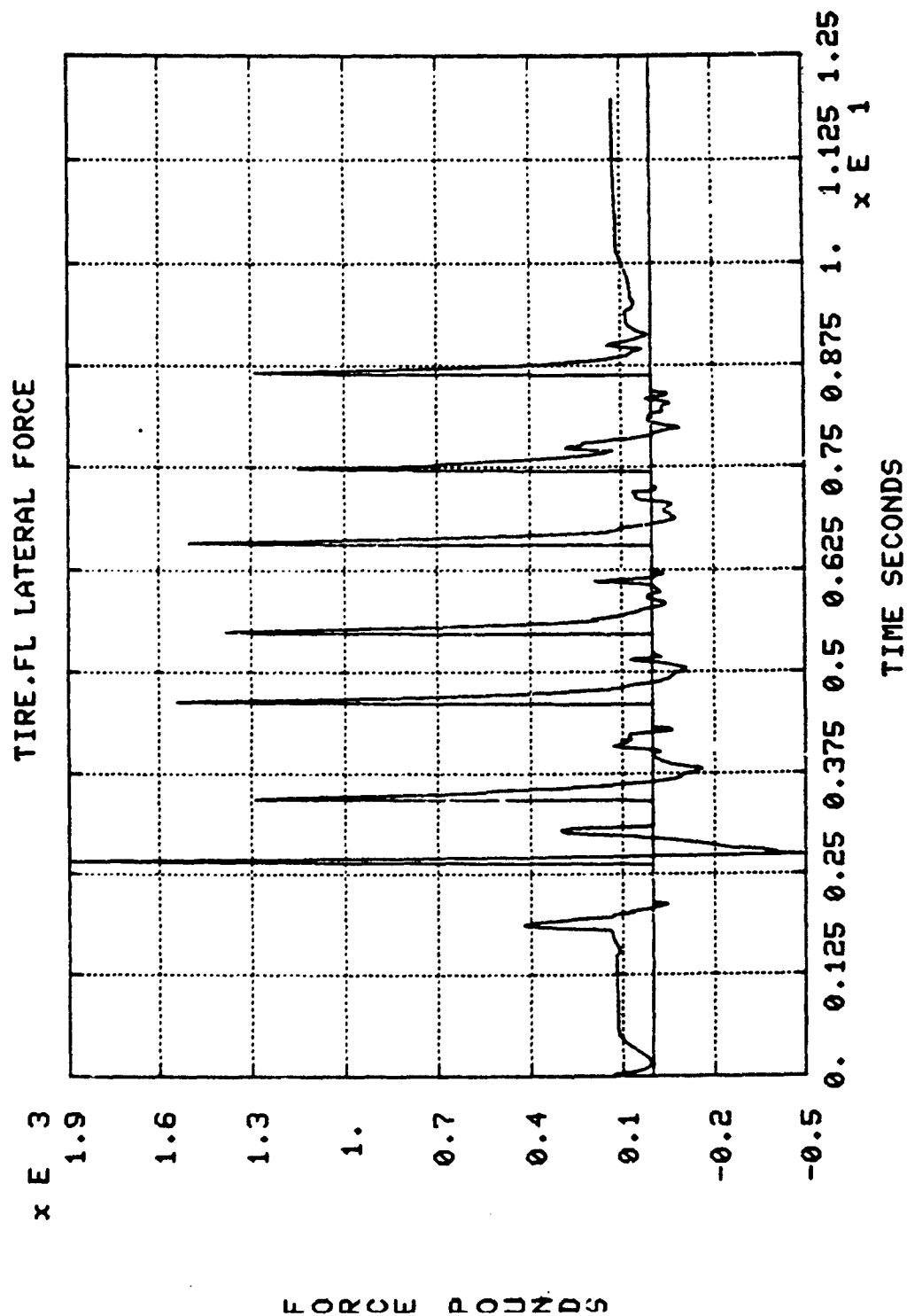
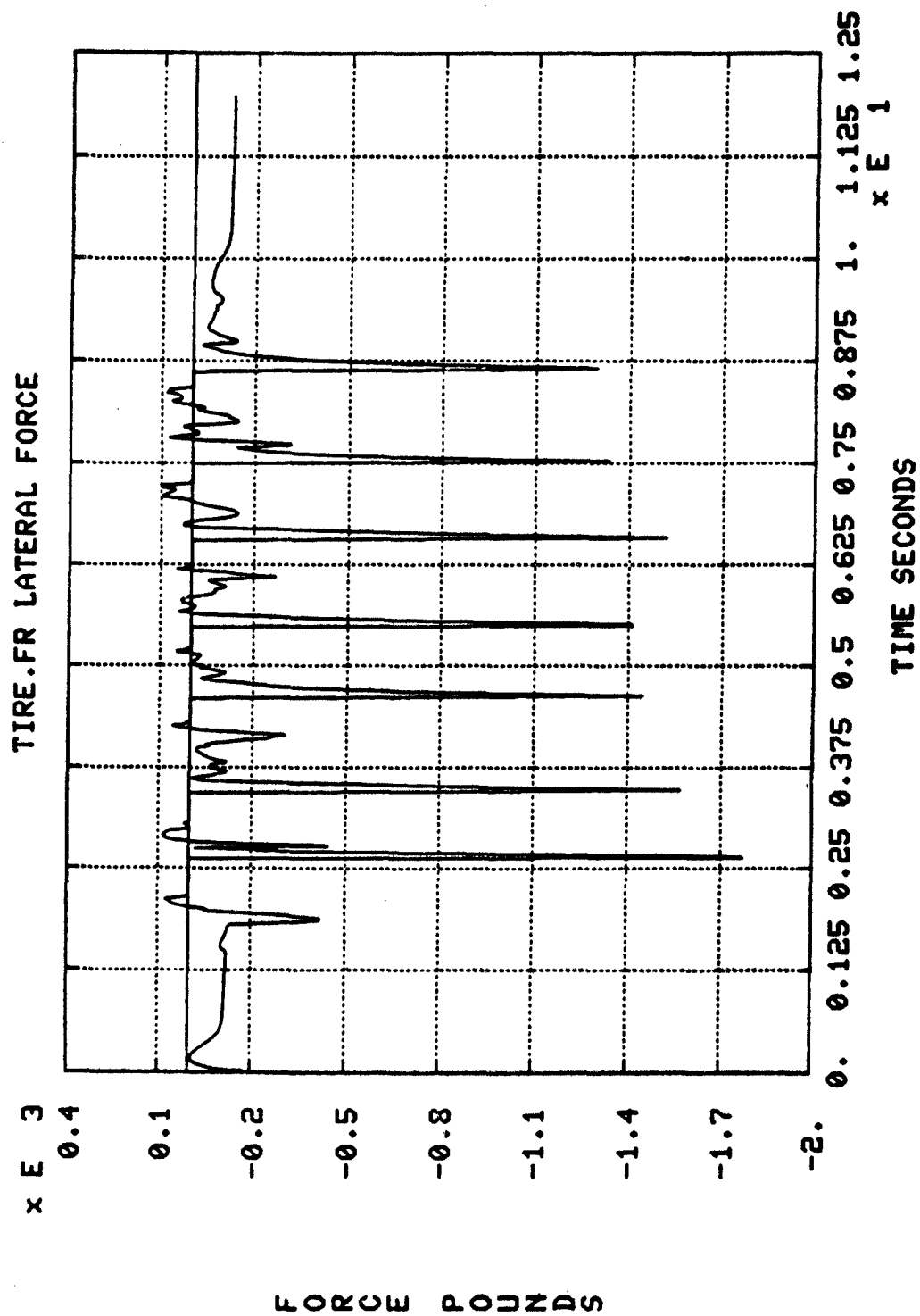


Figure 5-64. Front Left Tire Lateral Force



108

Figure 5-65 Front Right Tire Lateral Force

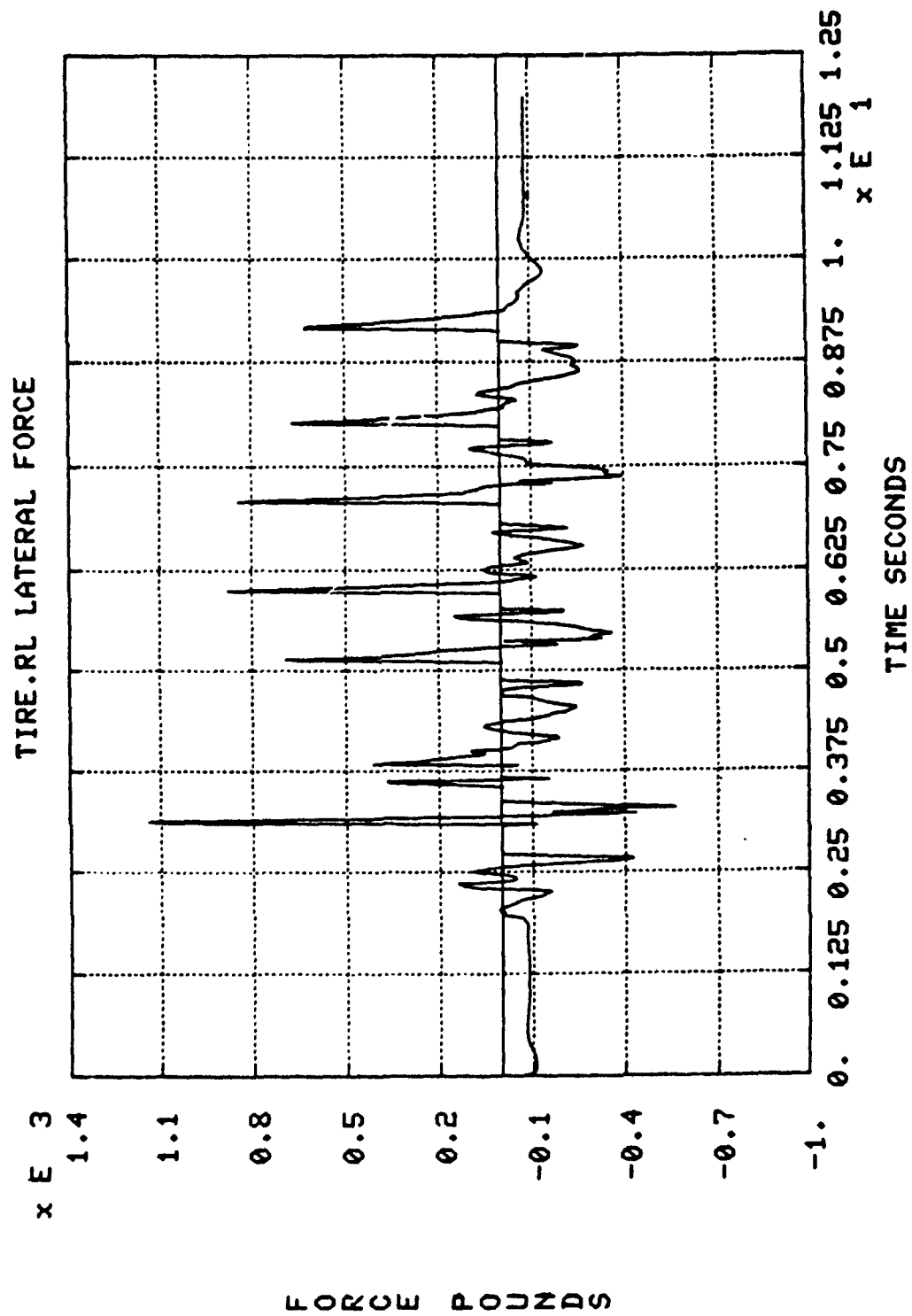


Figure 5-66. Rear Left Tire Lateral Force

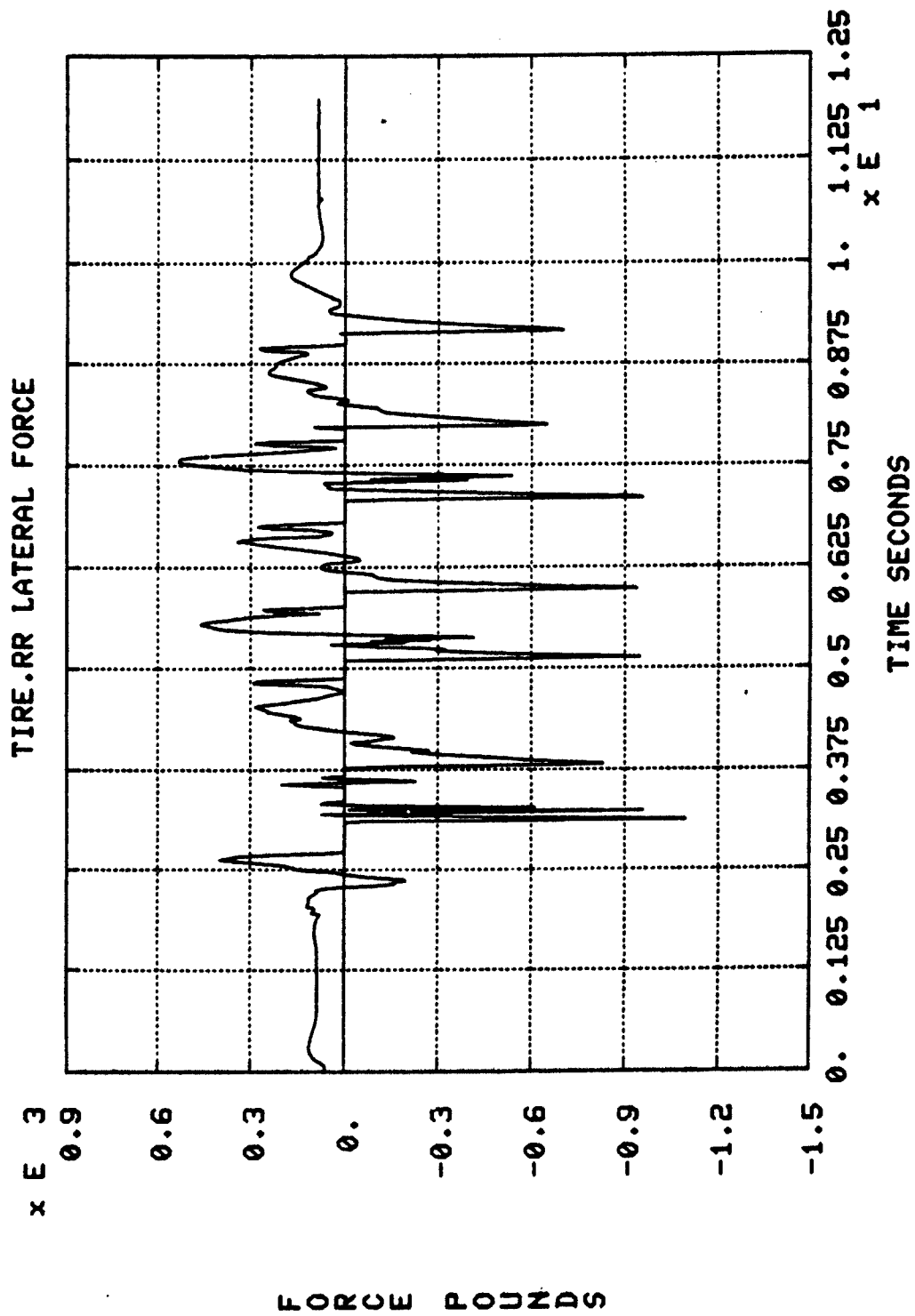


Figure 5-67. Rear Right Tire Lateral Force

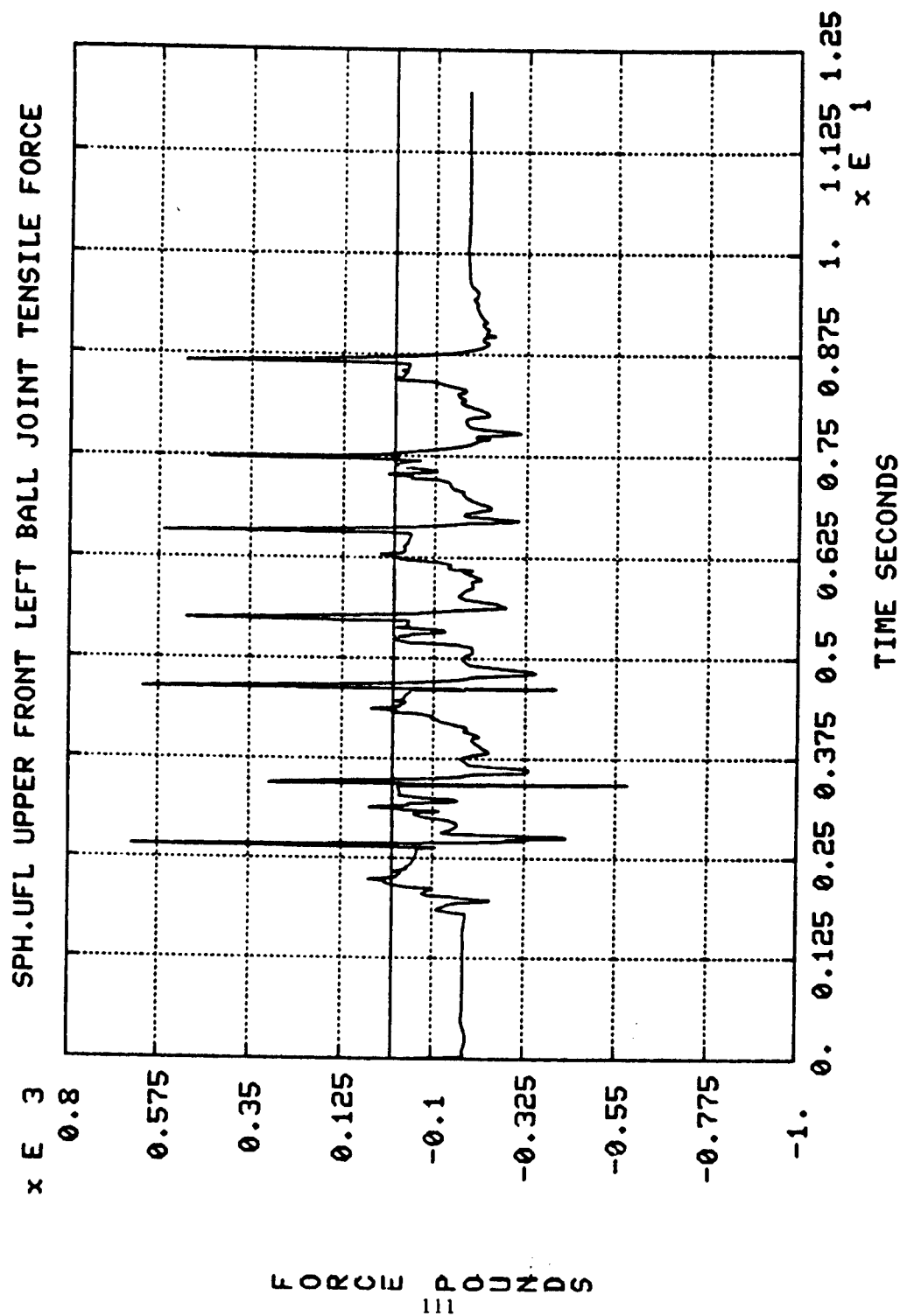


Figure 5-68. Upper Front Left Ball Joint Tensile Force

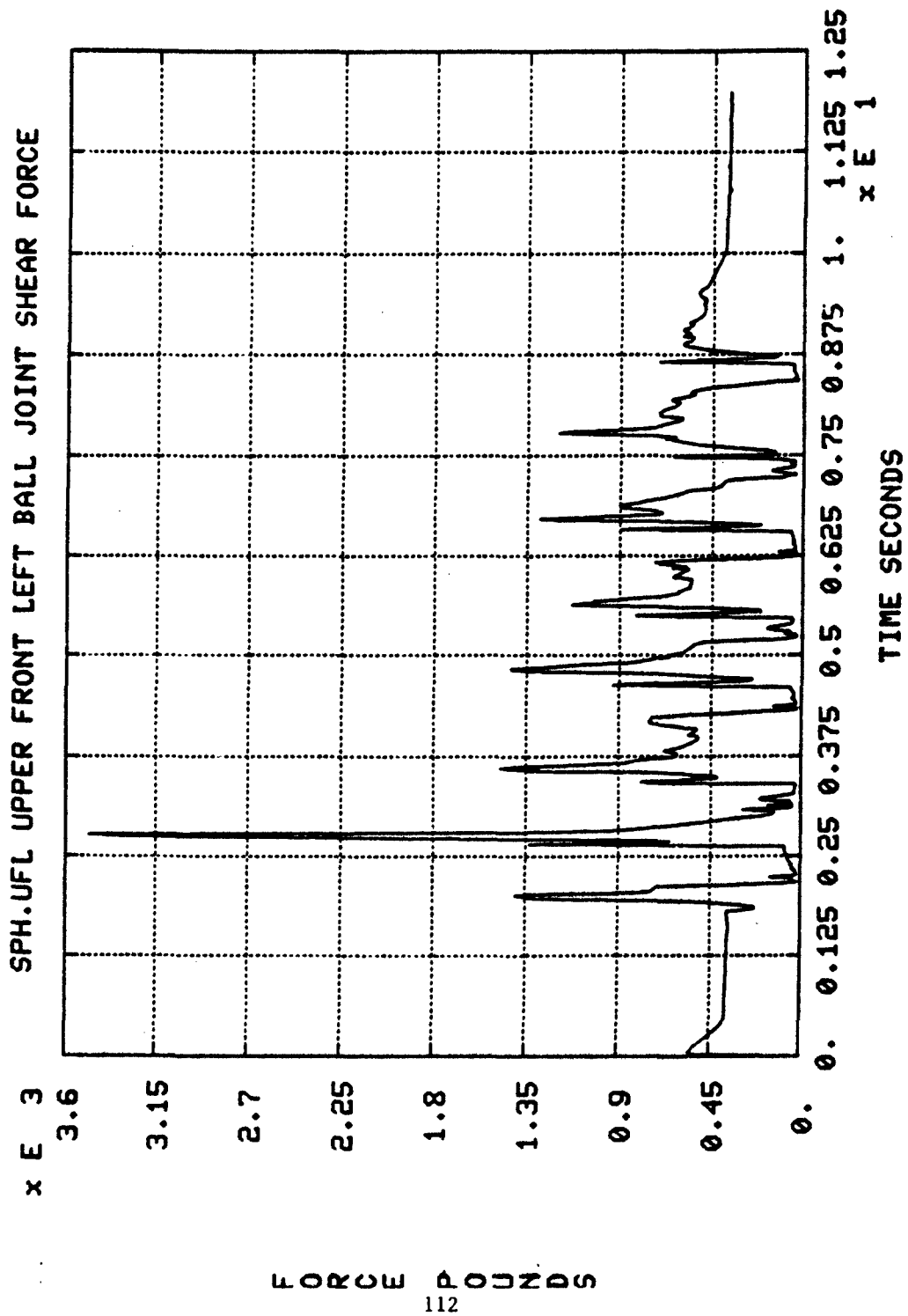
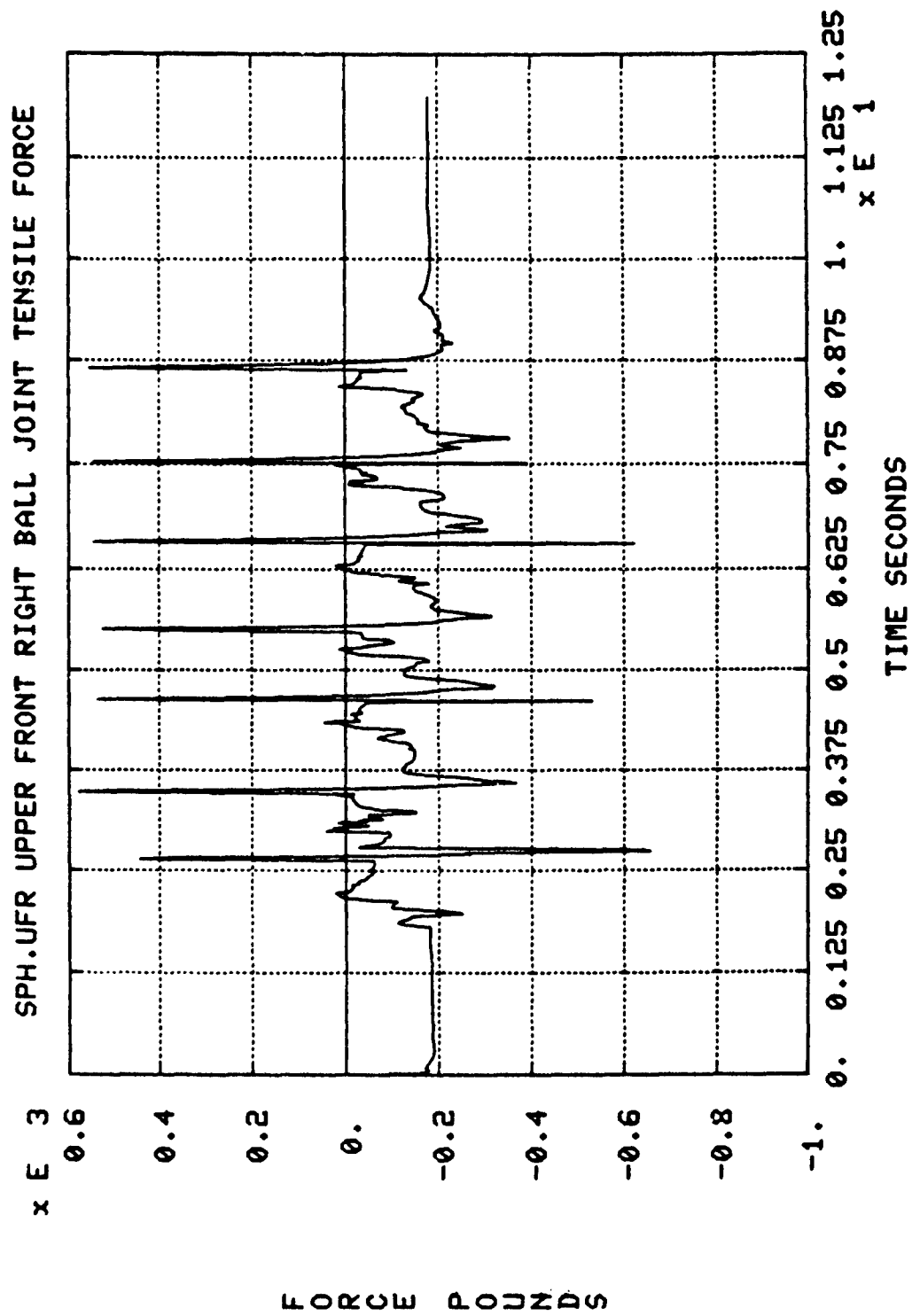


Figure 5-69. Upper Front Left Ball Joint Shear Force



113

Figure 5-70. Upper Front Right Ball Joint Tensile Force

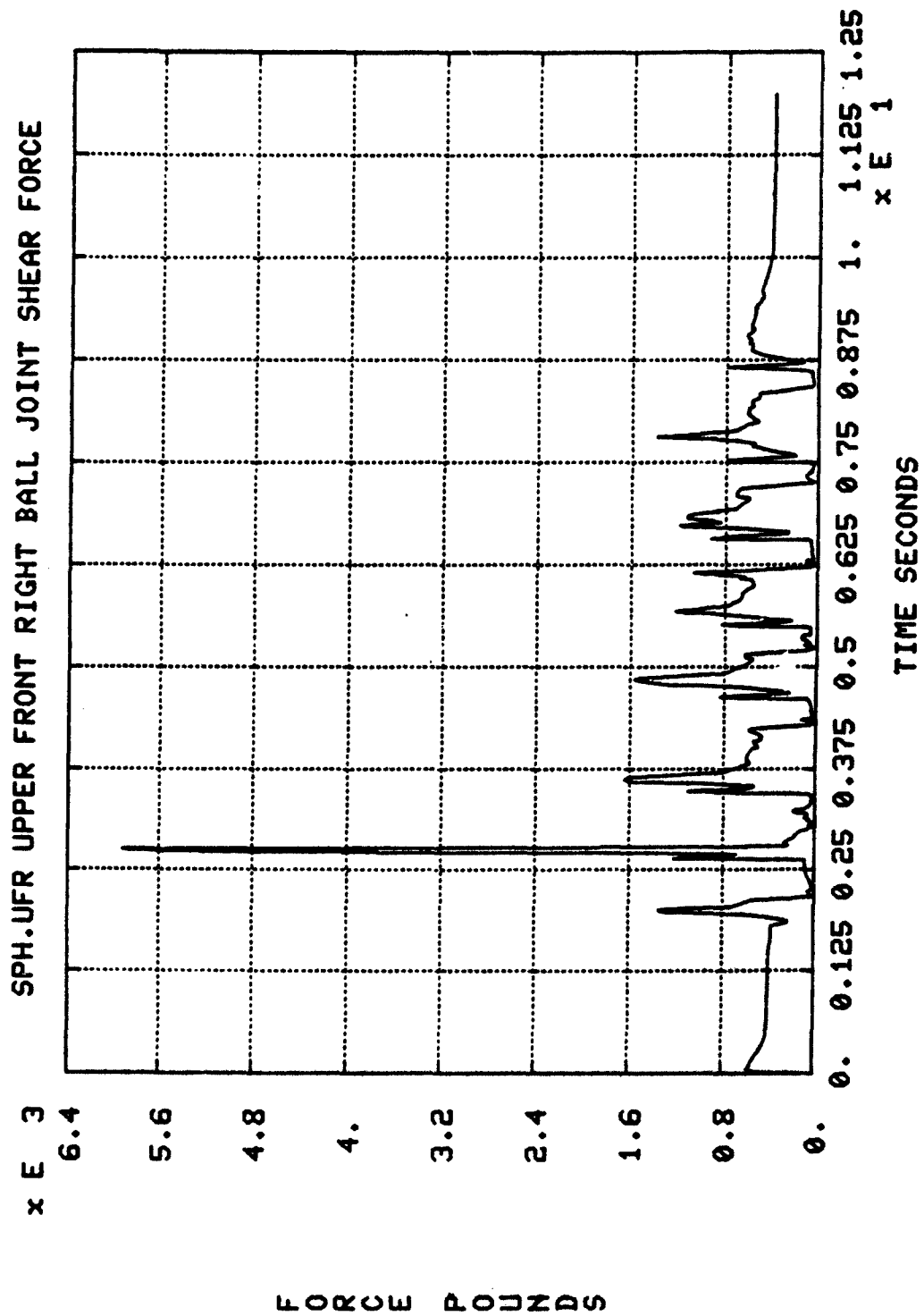


Figure 5-71. Upper Front Right Ball Joint Shear Force

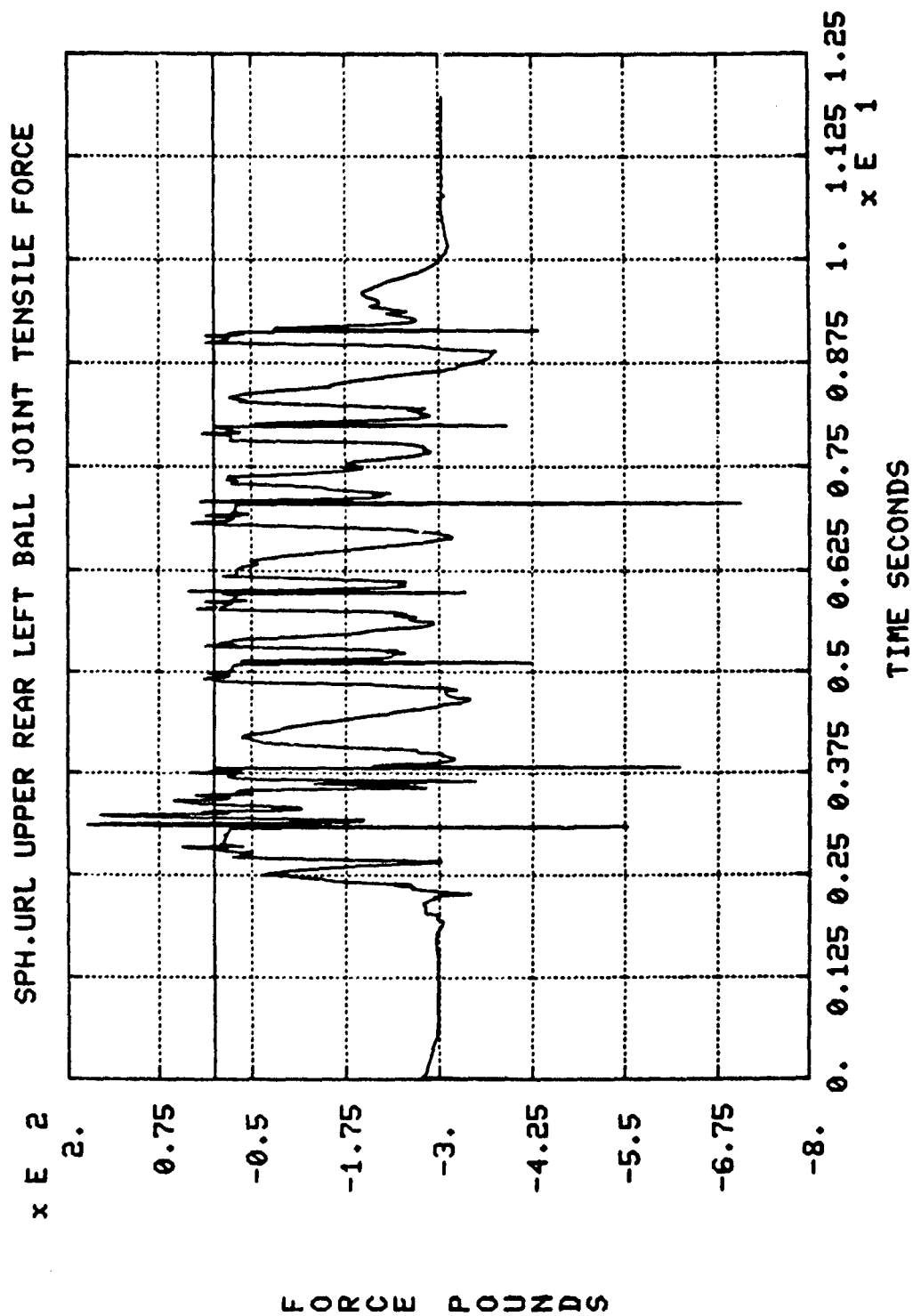
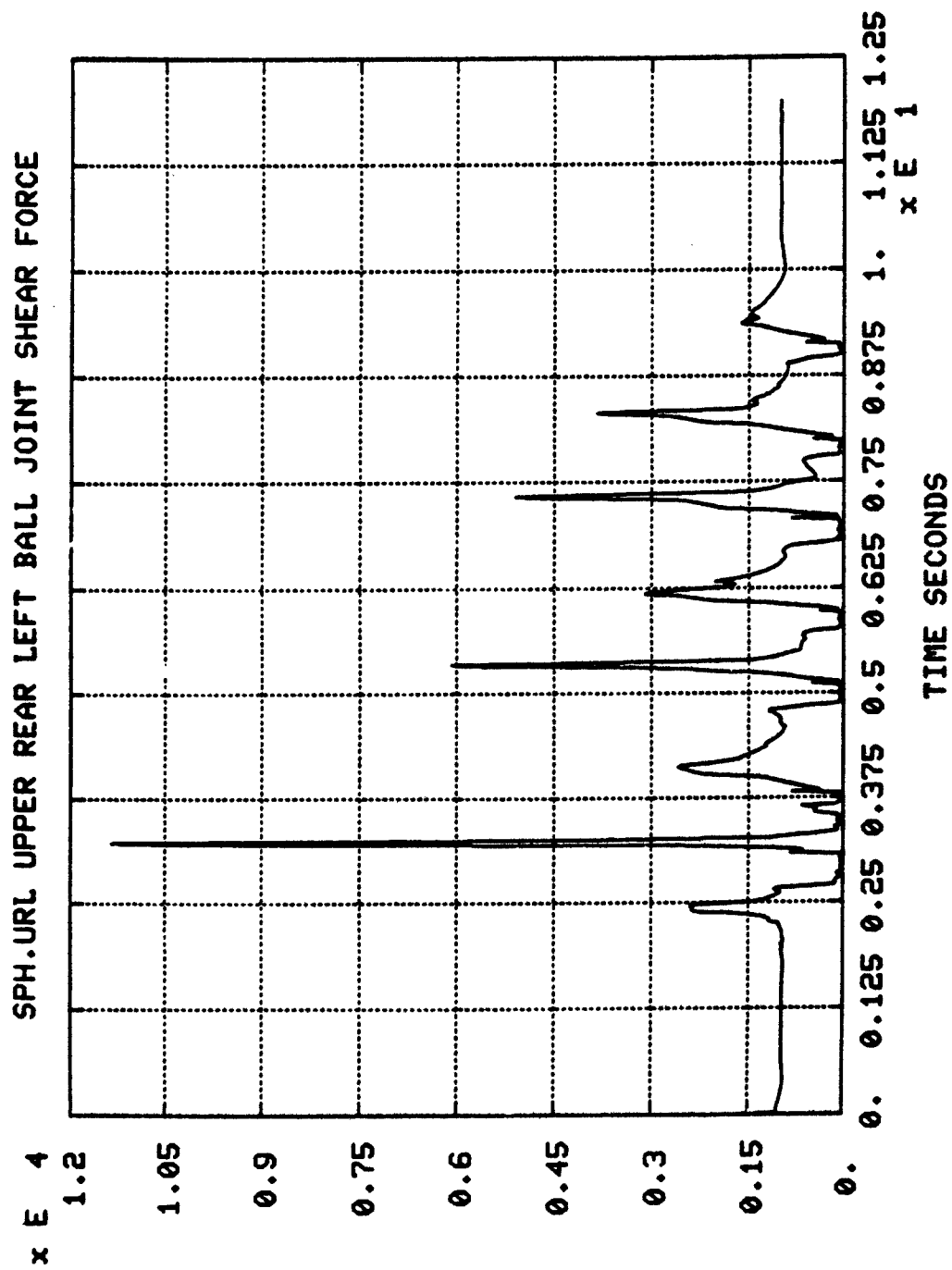
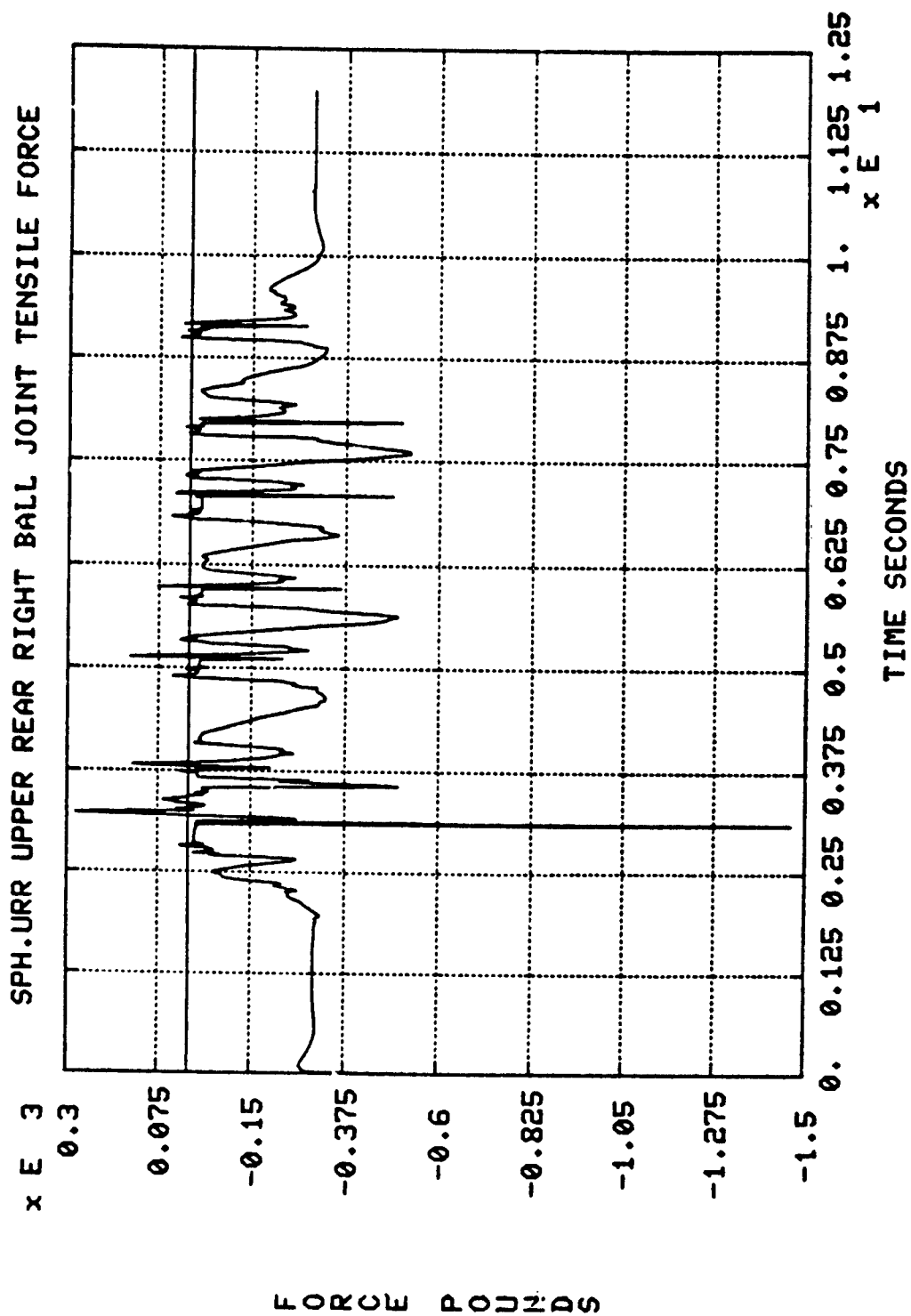


Figure 5-72. Upper Rear Left Ball Joint Tensile Force



FORCE POUNDS

Figure 5-73. Upper Rear Left Ball Joint Shear Force



117

Figure 5-74. Upper Rear Right Ball Joint Tensile Force

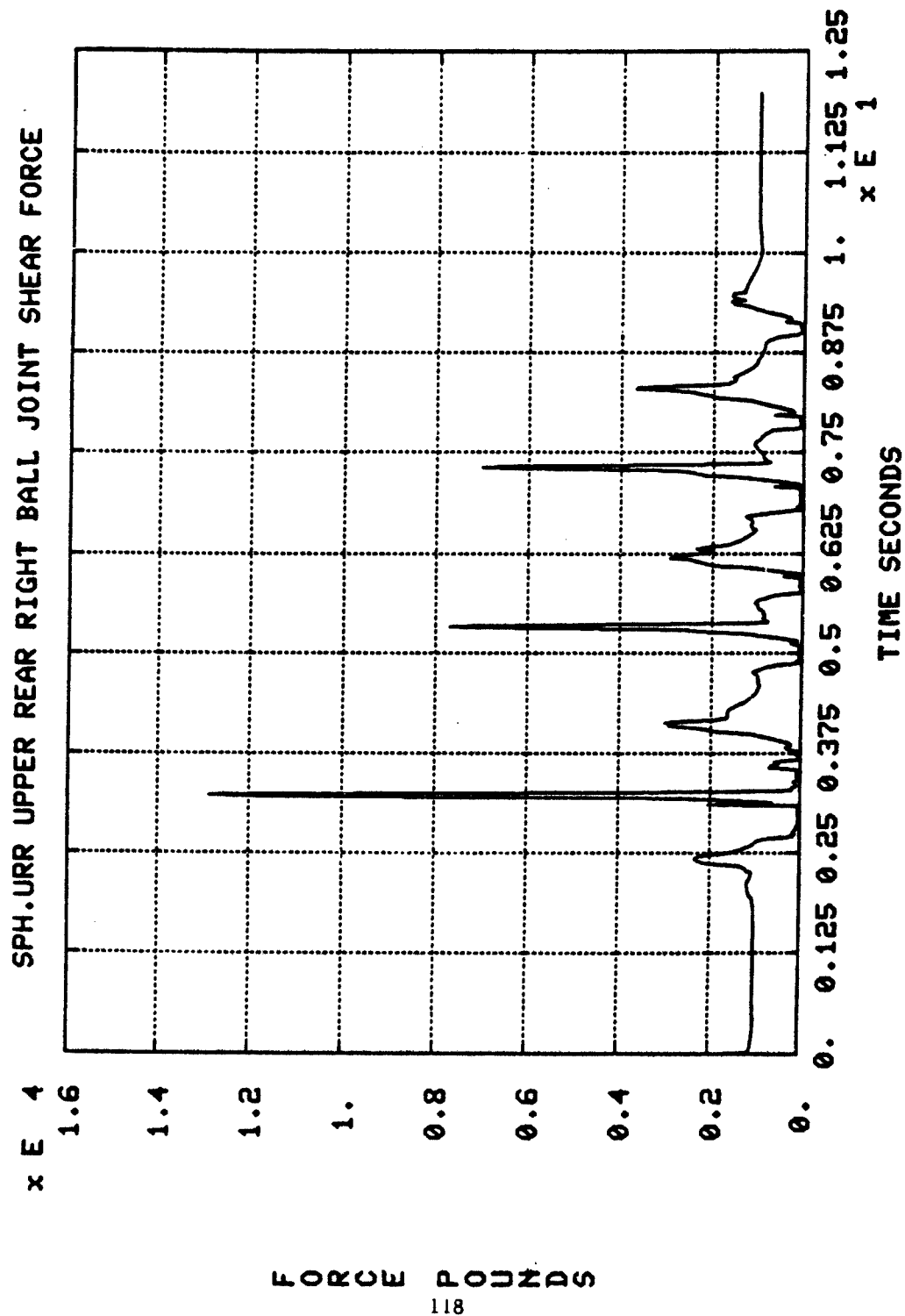


Figure 5-75. Upper Rear Right Ball Joint Shear Force

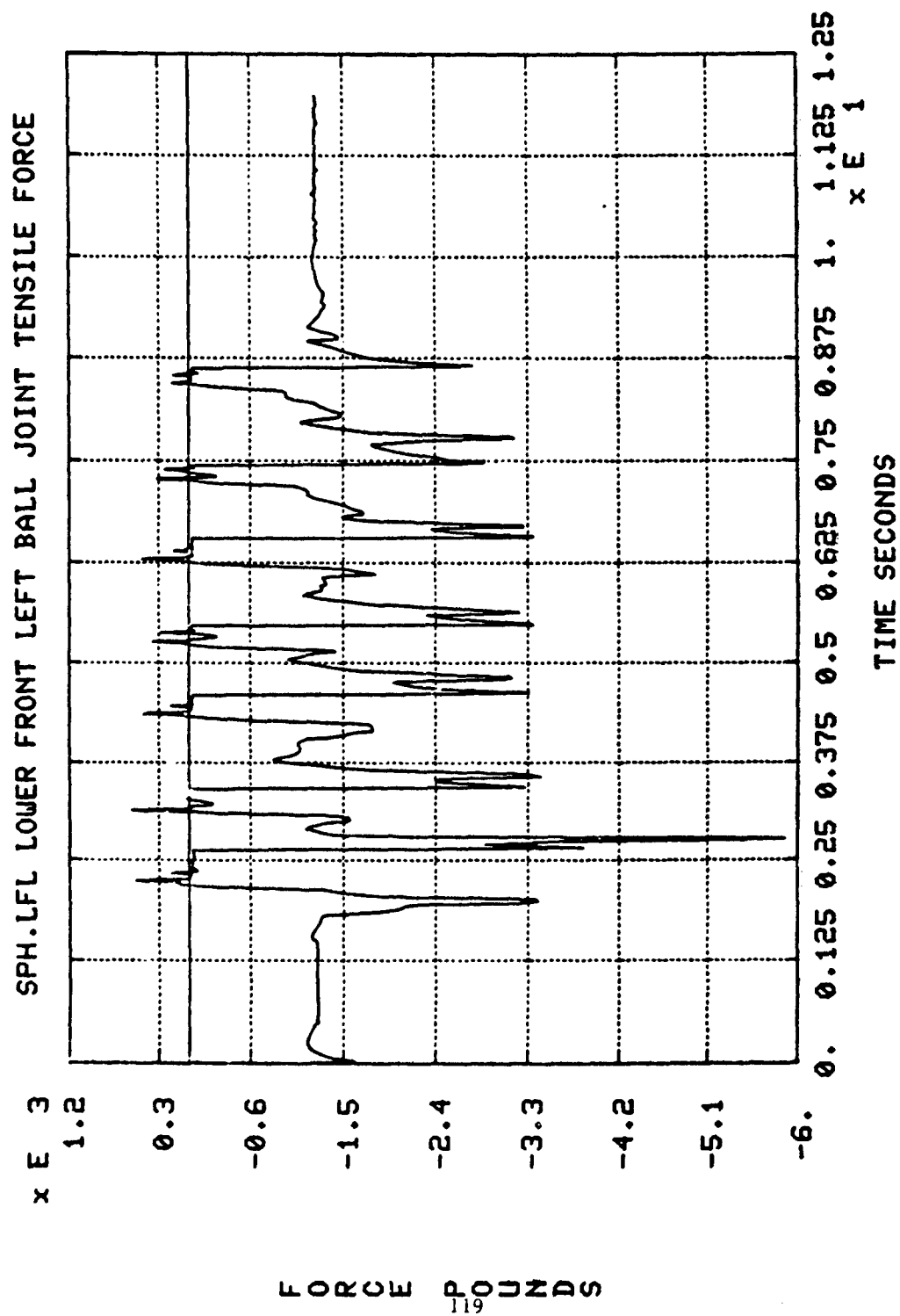


Figure 5-76. Lower Front Left Ball Joint Tensile Force

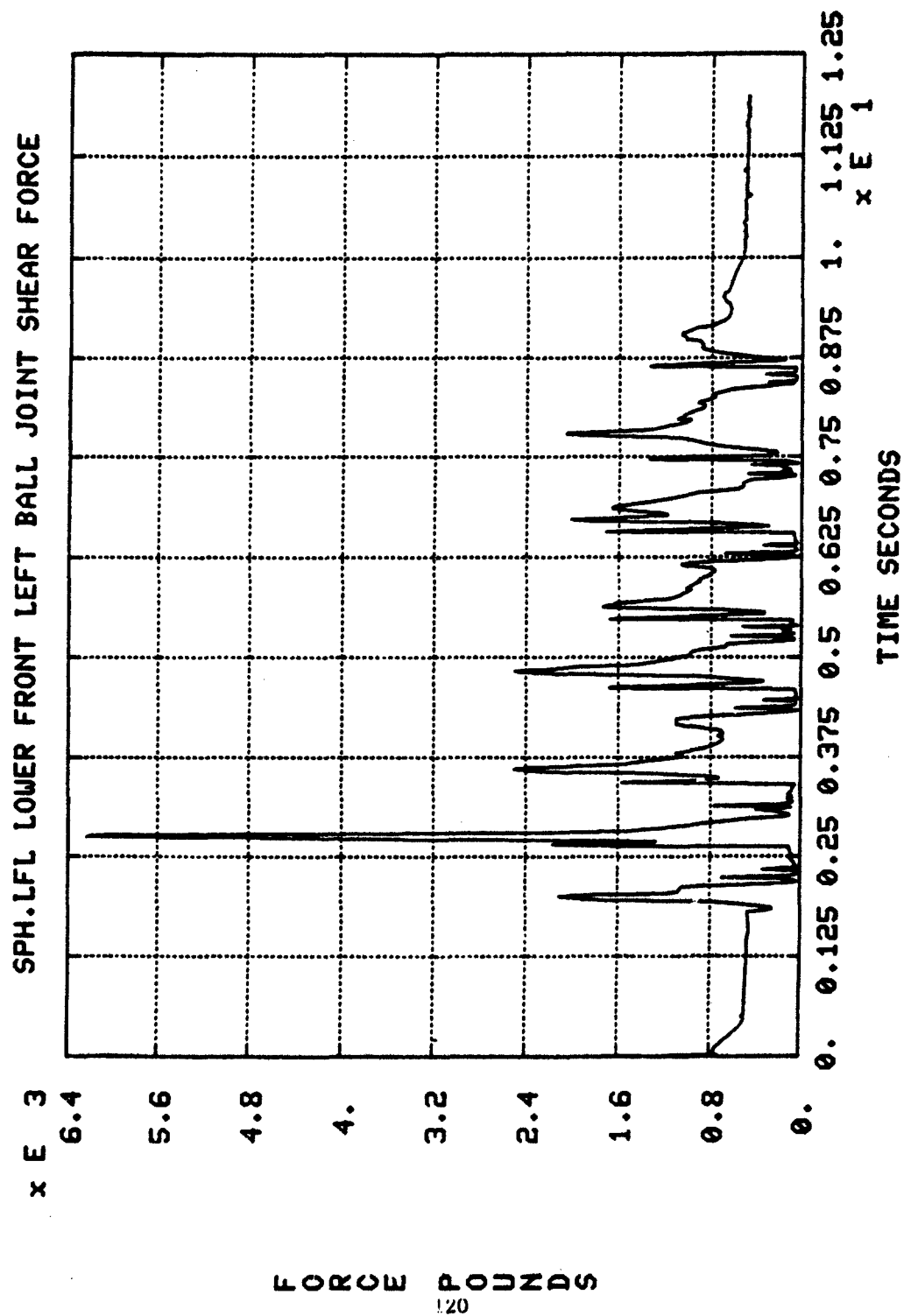
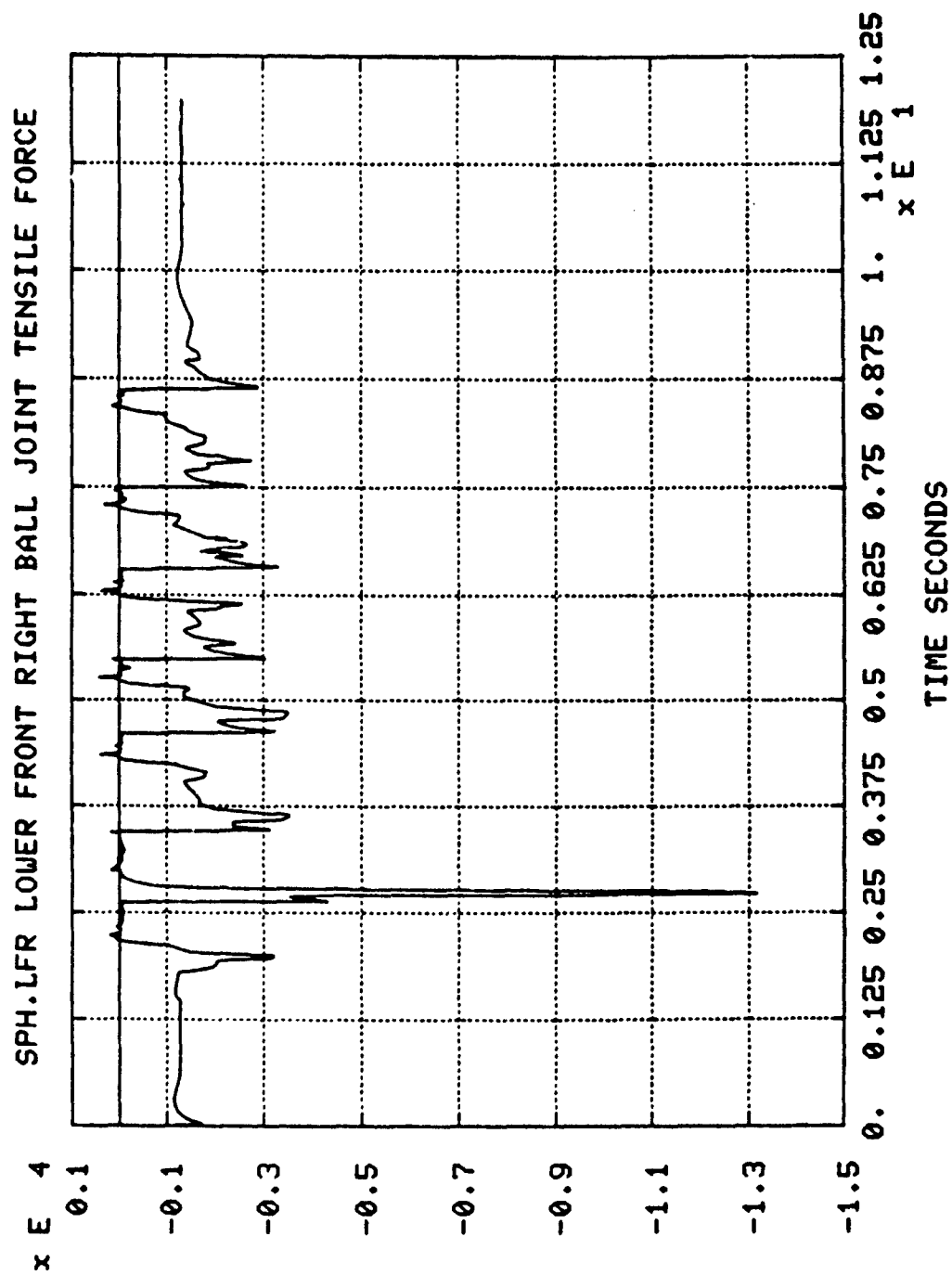


Figure 5-77. Lower Front Left Ball Joint Shear Force



FORCE POUNDS

121

Figure 5-78. Lower Front Right Ball Joint Tensile Force

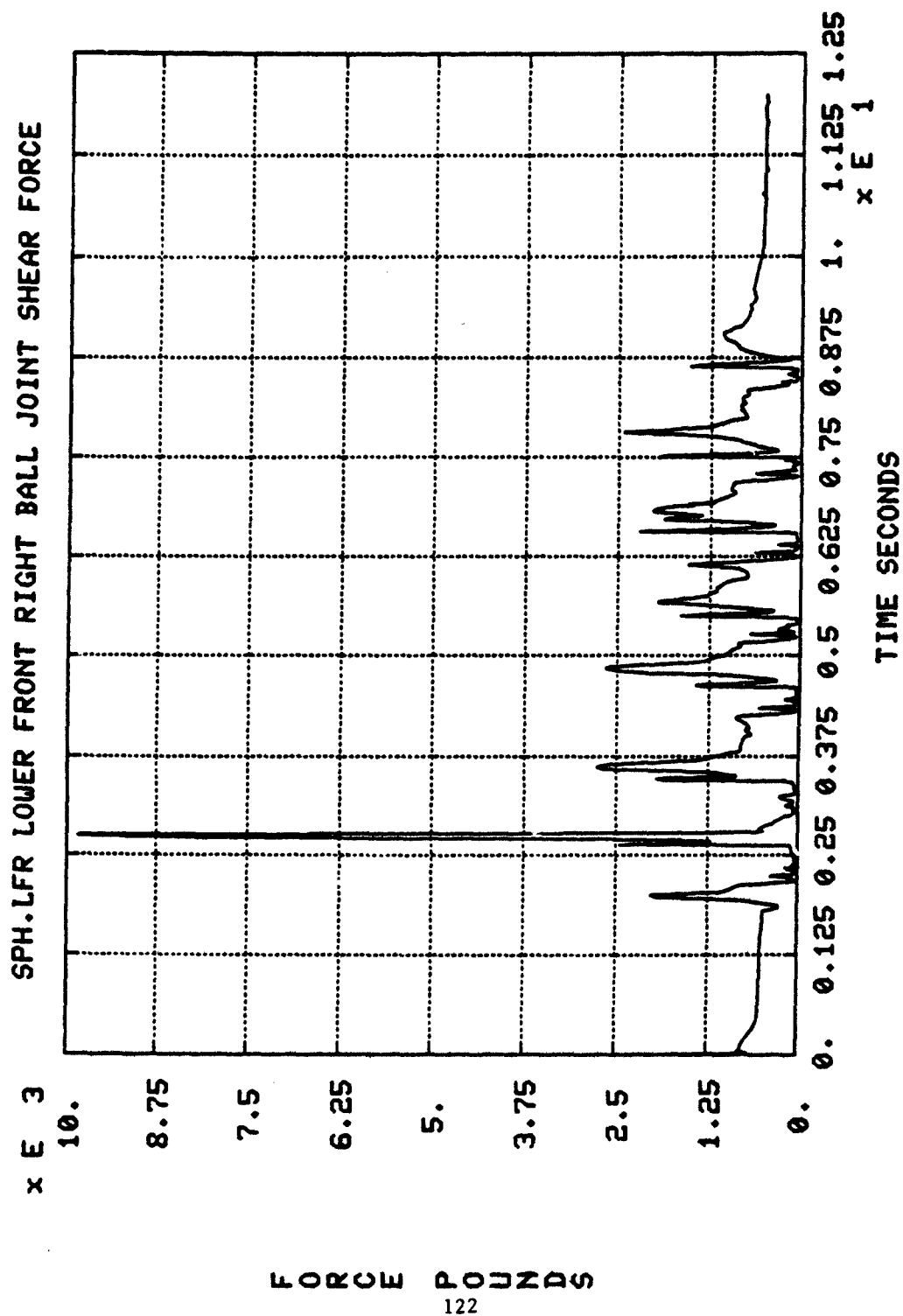


Figure 5-79. Lower Front Right Ball Joint Shear Force

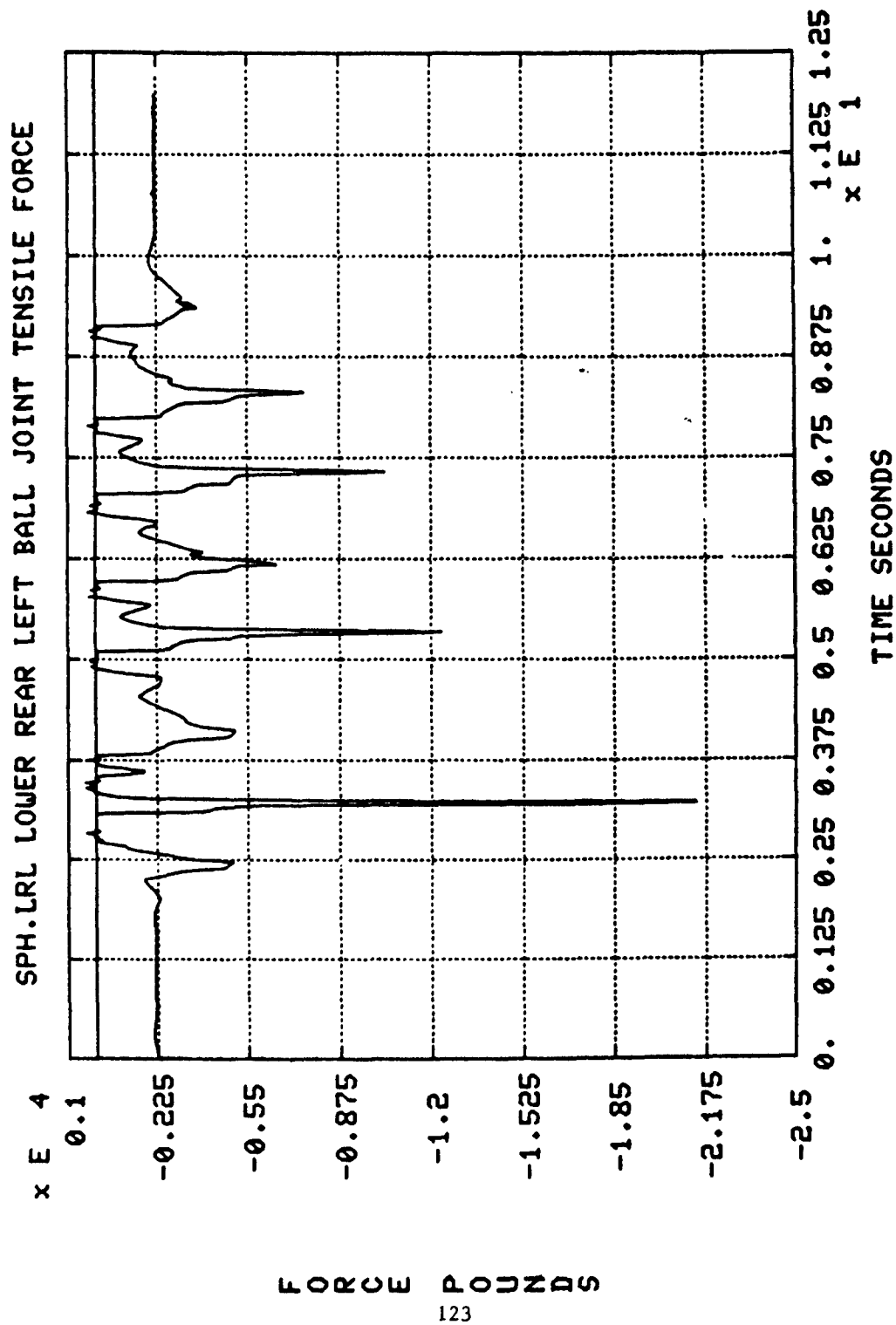


Figure 5-30. Lower Rear Left Ball Joint Tensile Force

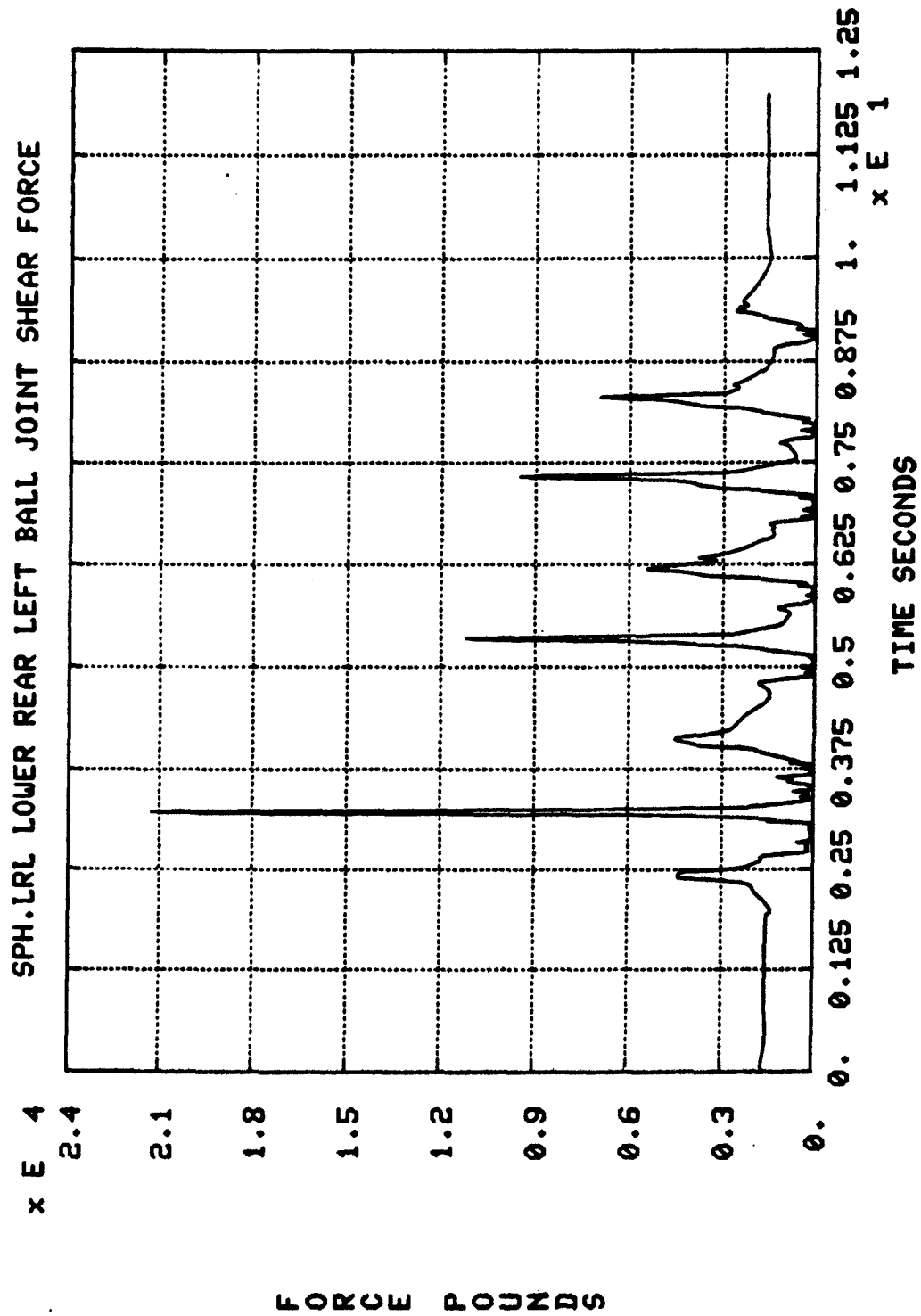


Figure 5-81. Lower Rear Left Ball Joint Shear Force

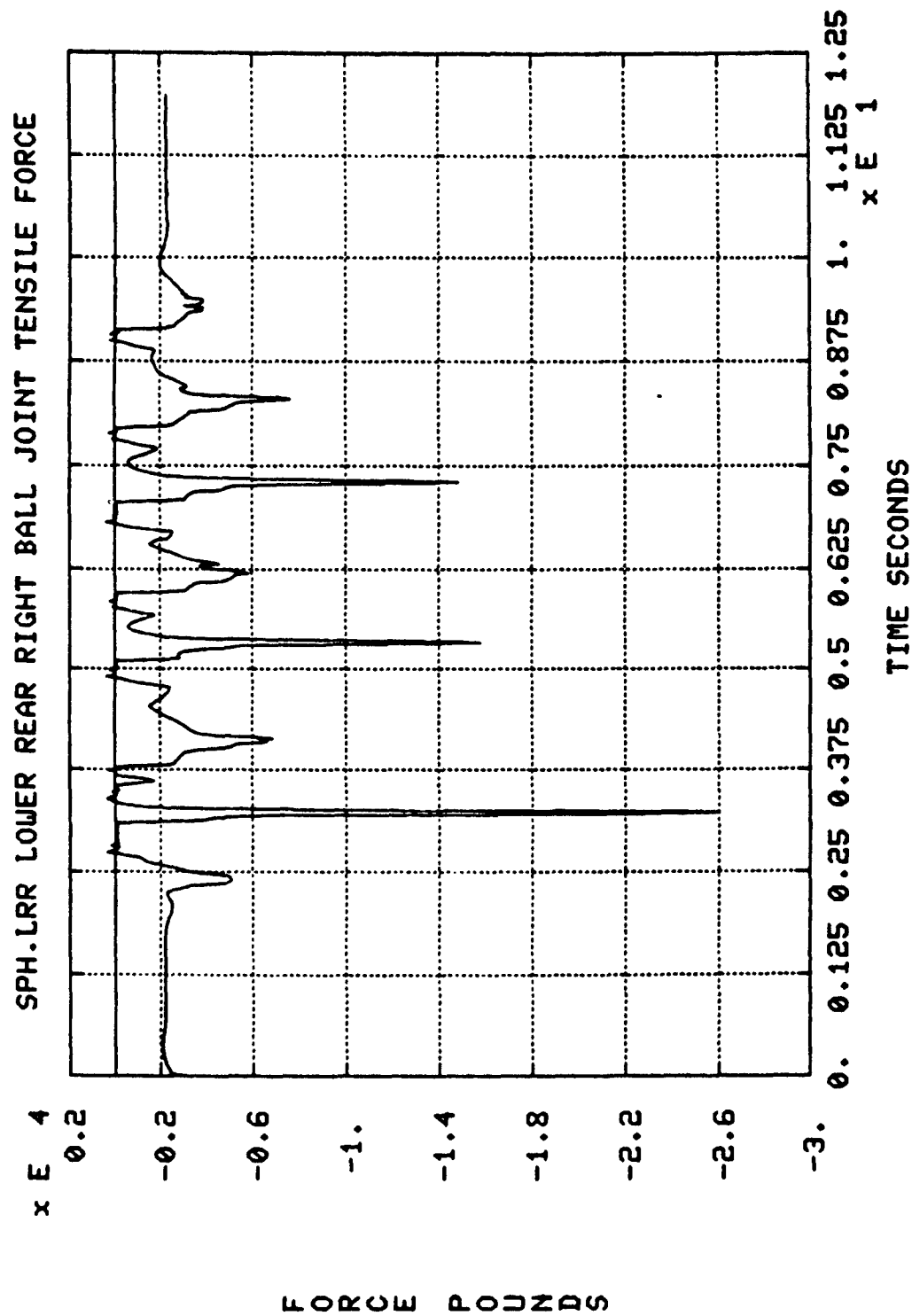


Figure 5-82. Lower Rear Right Ball Joint Tensile Force

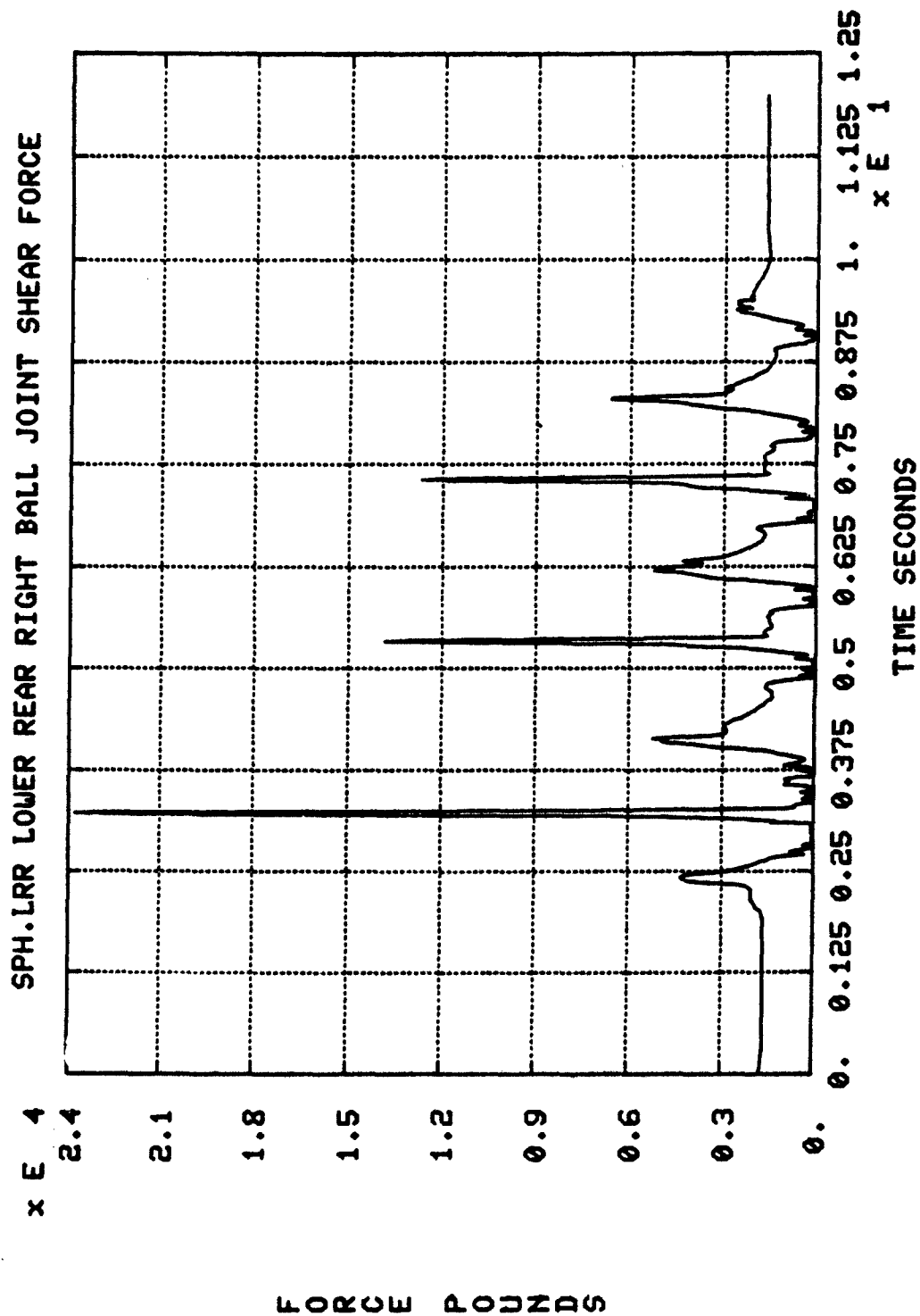


Figure 5-83. Lower Rear Right Ball Joint Shear Force

Figures 5-84 through 5-91 show the joint angle as defined in section 5.3.12. titled "Ball Joints" for each upper and lower ball joint. The calculations show that the ball joints do not exceed the recommended maximum allowable angle.

5.7. Static Analysis

5.7.1. Heavy Duty Right Rear Suspension Model. The purpose of this analysis was to determine the magnitude of the joint forces under given forces applied to the wheel body. The analysis results provide the design sensitivity of this suspension unit to externally applied forces.

The external forces applied to the wheel body included a combination of vertical, lateral, and longitudinal forces acting at the wheel and road interface. For this analysis tire dynamics were not considered and the tire radius was assumed to be constant at 16.355 inches. Also for this analysis the chassis body was fixed to ground to prevent any chassis motion.

This analysis was actually executed in dynamics mode because the shock absorber was modeled. If the combination of externally applied forces caused the shock to be compressed into the metal-to-metal region, then the shock acted as a very stiff element as explained in section 5.3.7. titled "Shock Absorber." The analysis was run for a sufficient time until static equilibrium of all elements was obtained.

The static analysis of the HMMWV heavy duty right rear suspension unit uses the same program described in section 5.6. titled "Dynamic Analysis". However, for this analysis the set of bodies, joints, and other constraint elements are limited only to the right rear suspension unit. The DADS elements listed in Table 5-19 were used to describe the HMMWV heavy duty right rear suspension unit. A sample of one *.VB3 verbatim file is given in Appendix F.

The coordinate reference frames used in this analysis are the same as those in the dynamic analysis.

Six combinations of externally applied vertical, lateral, and longitudinal forces were analyzed. For each combination the vertical force was increased by 2,500-pound increments. Based upon a coefficient of friction equal to 0.5 between the wheel and road, which is equivalent to a gravel road, the lateral and longitudinal forces were assumed to be one-half the magnitude of the vertical forces. No applied torques are generated by the vertical force because the line of action is through the wheel center. No applied torques generated by the fore-aft longitudinal forces were placed upon the wheel body because these torques are transmitted directly through the half drive shaft assembly. The six loading combinations which were analyzed and their directory location on the VAX8800 computer are given in Table 5-20.

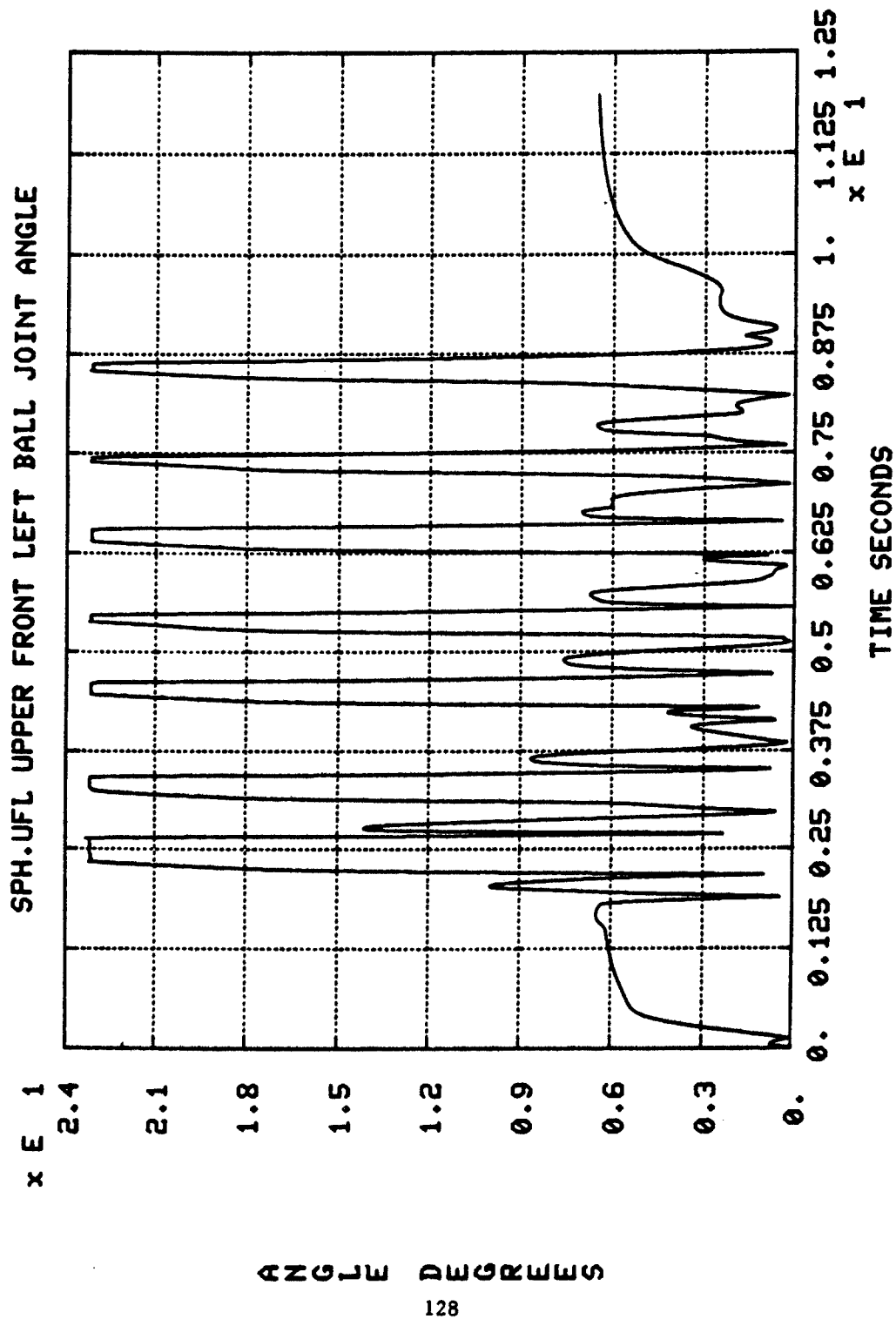


Figure 5-84. Upper Front Left Ball Joint Angle

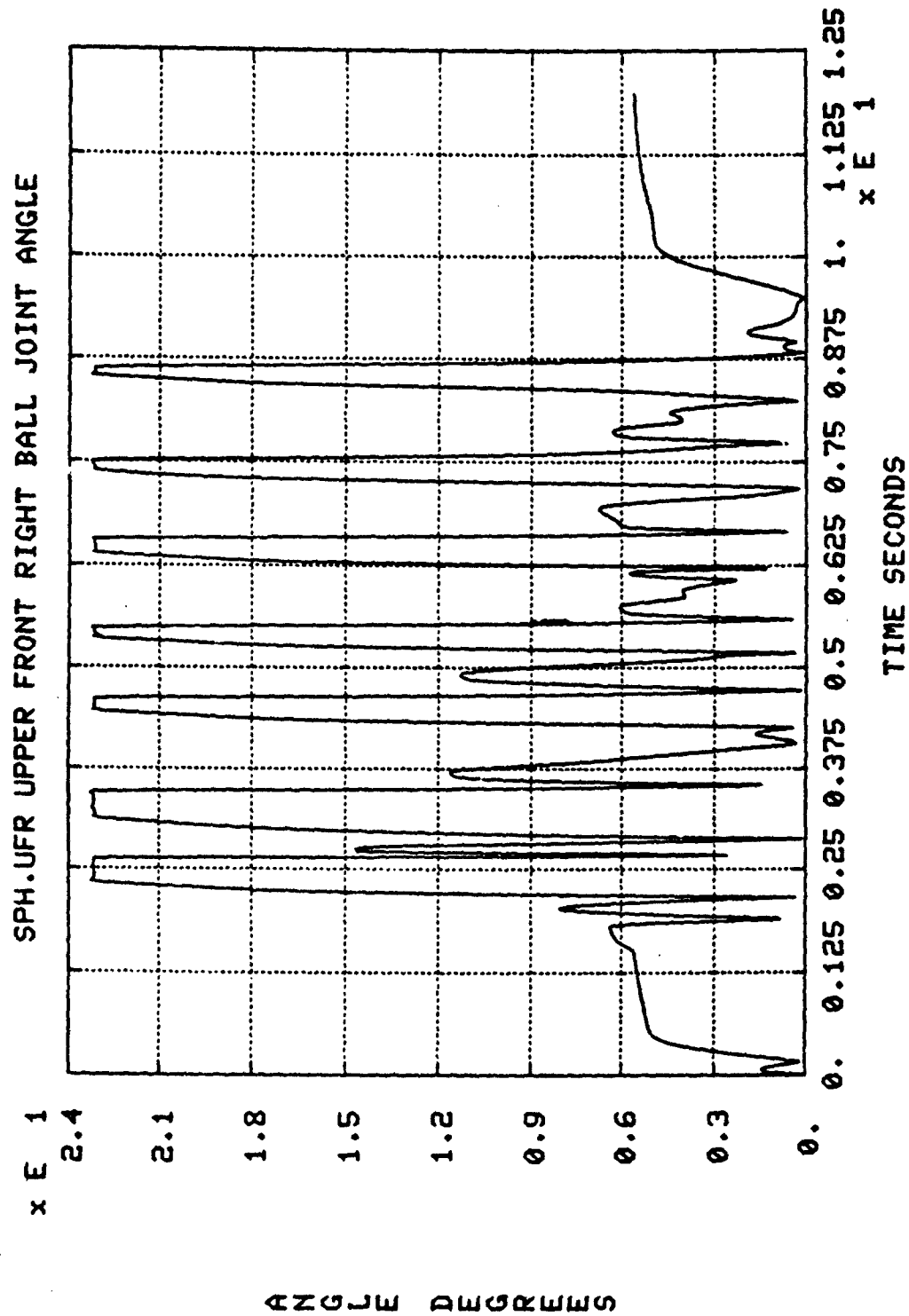
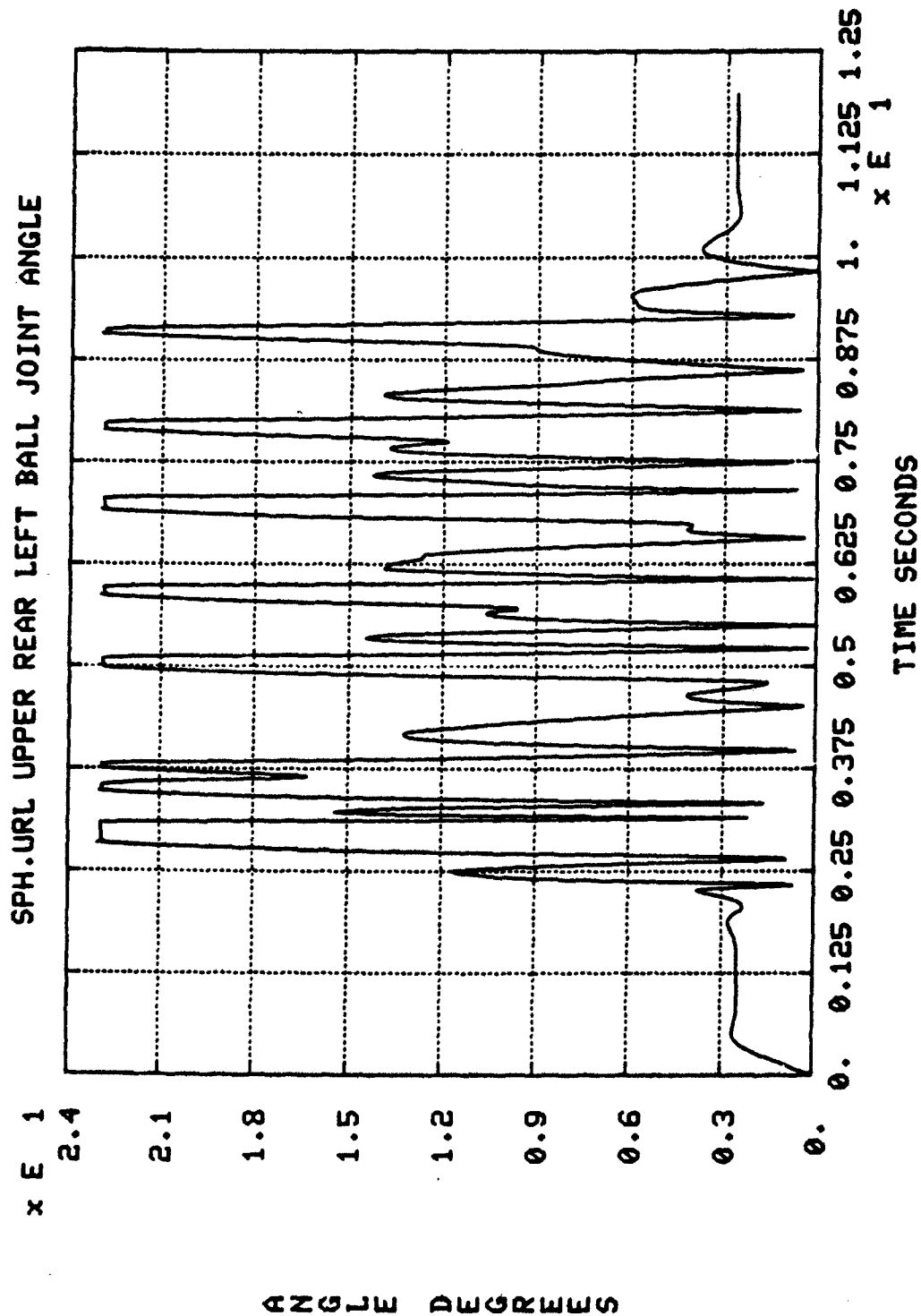


Figure 5-85. Upper Front Right Ball Joint Angle



130

Figure 5-86. Upper Rear Left Ball Joint Angle

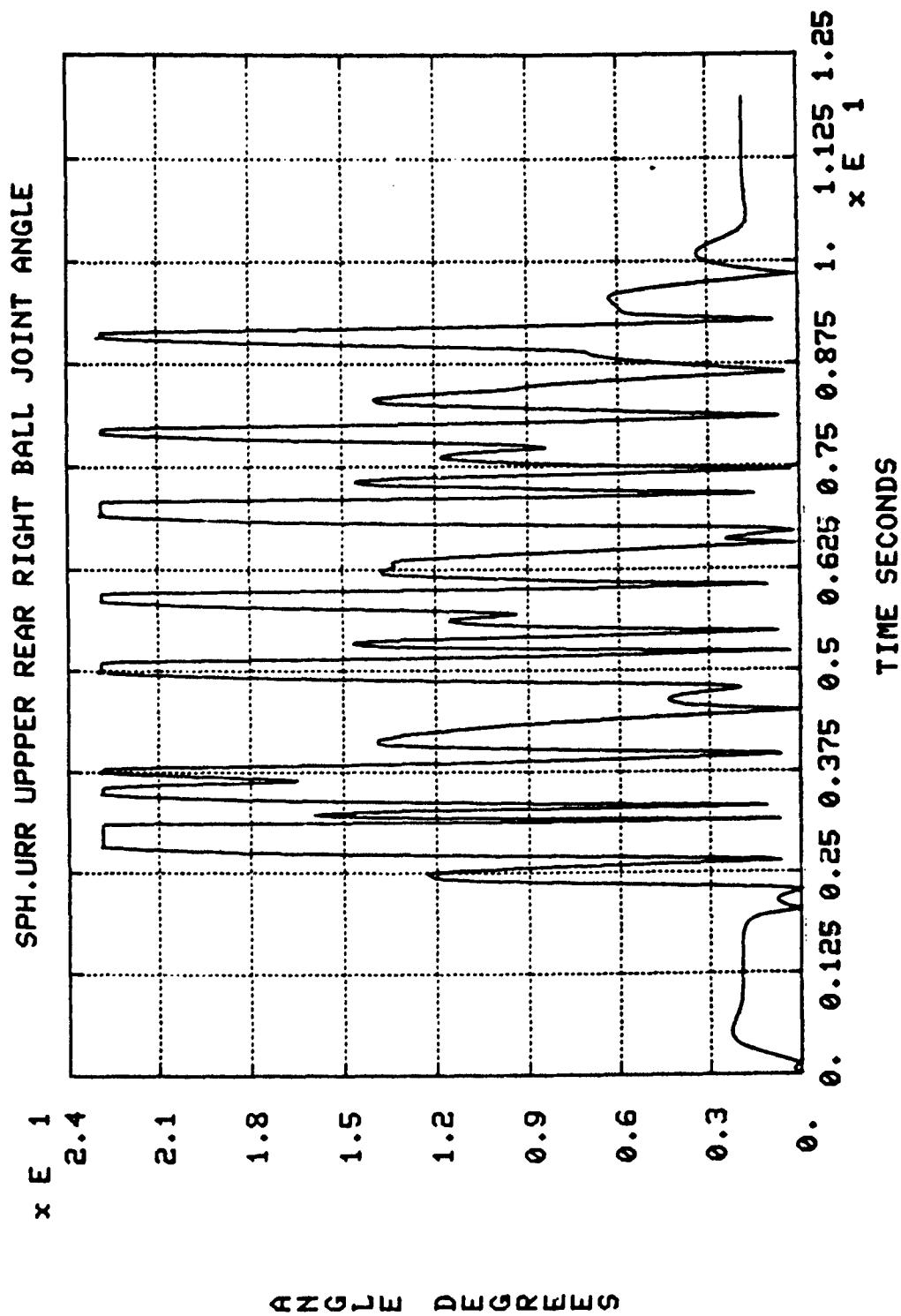
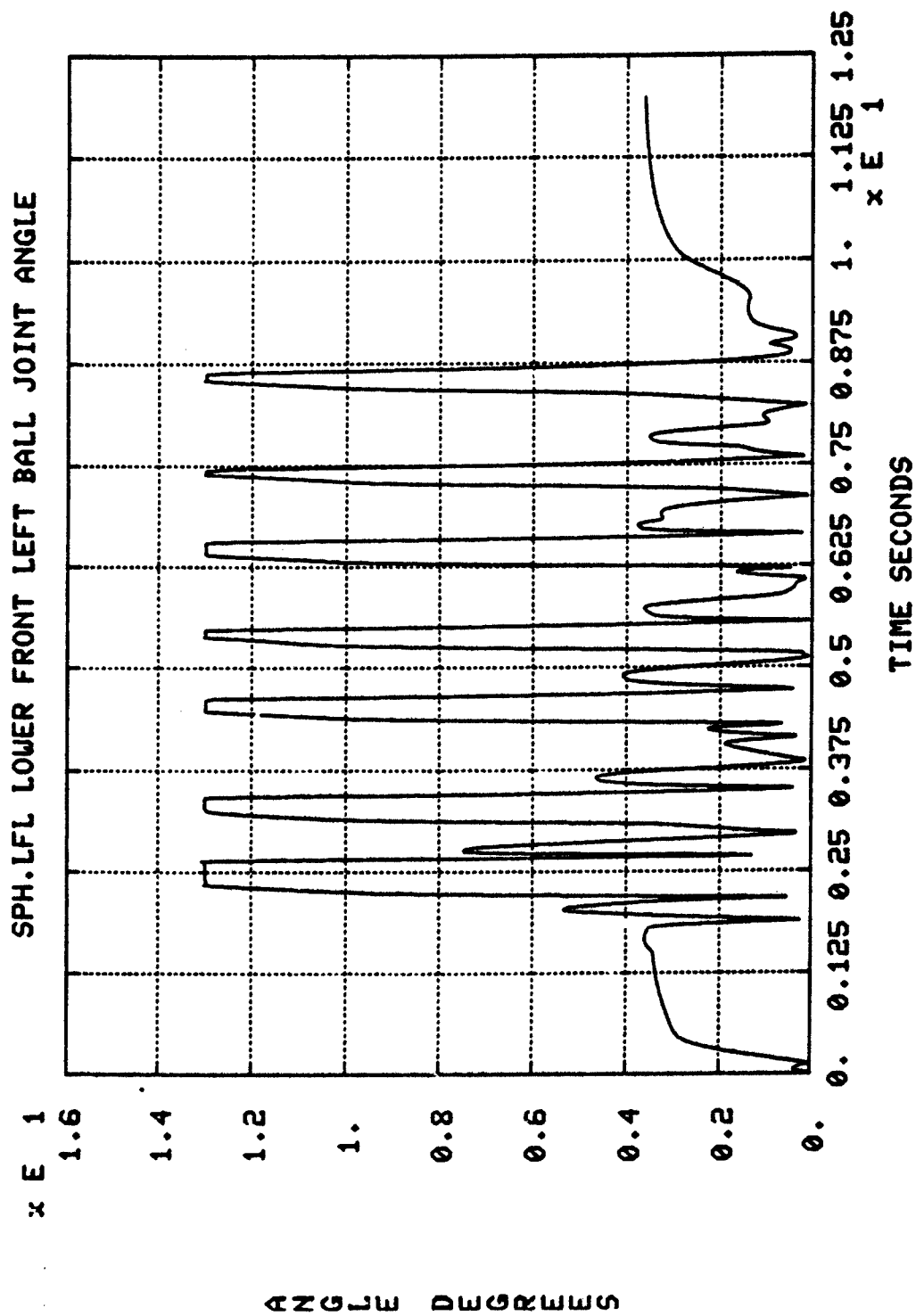


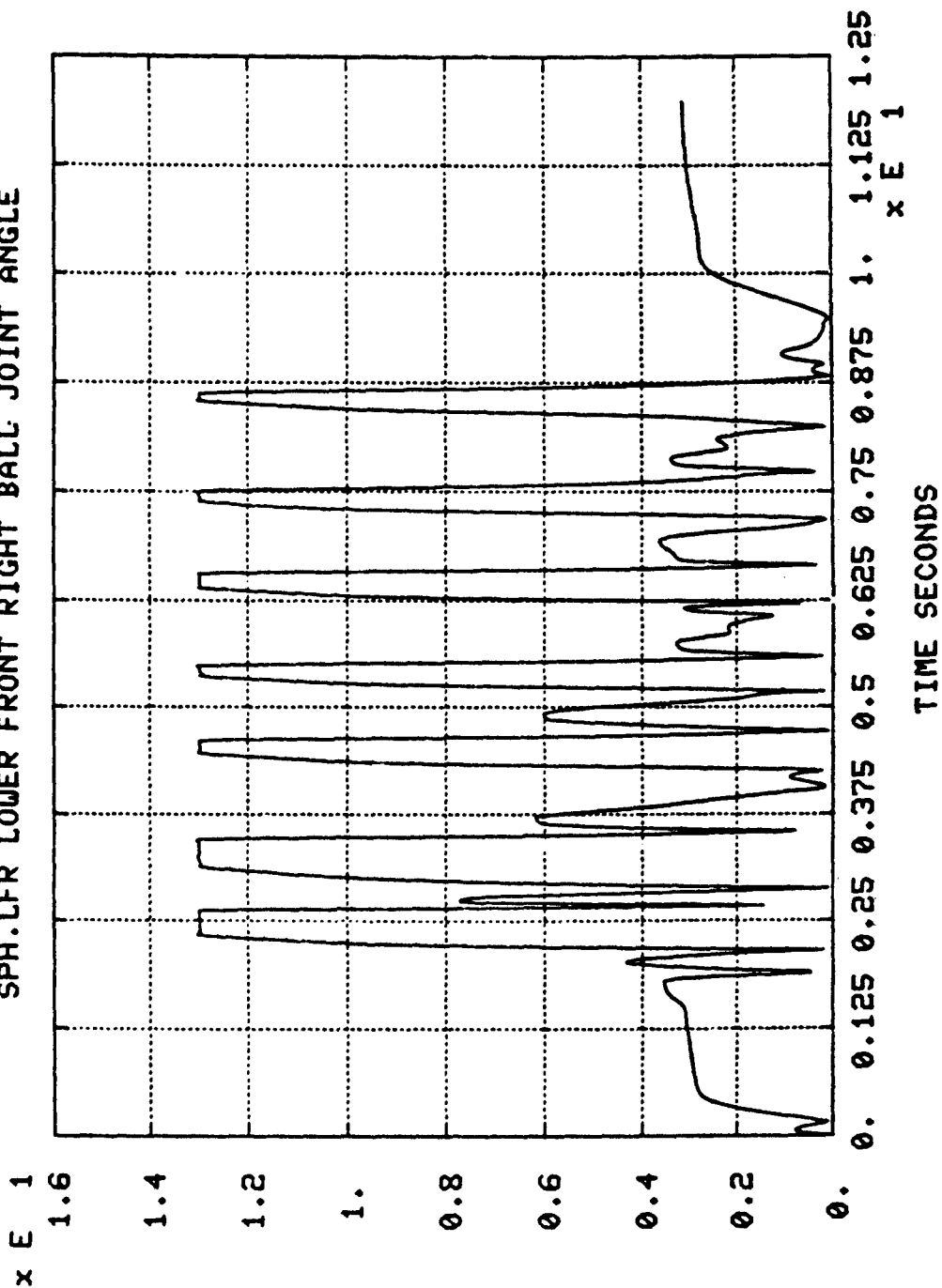
Figure 5-87. Upper Rear Right Ball Joint Angle



ANGLE DEGREES

Figure 5-88. Lower Front Left Ball Joint Angle

SPH.LFR LOWER FRONT RIGHT BALL JOINT ANGLE



ANGLE DEGREES

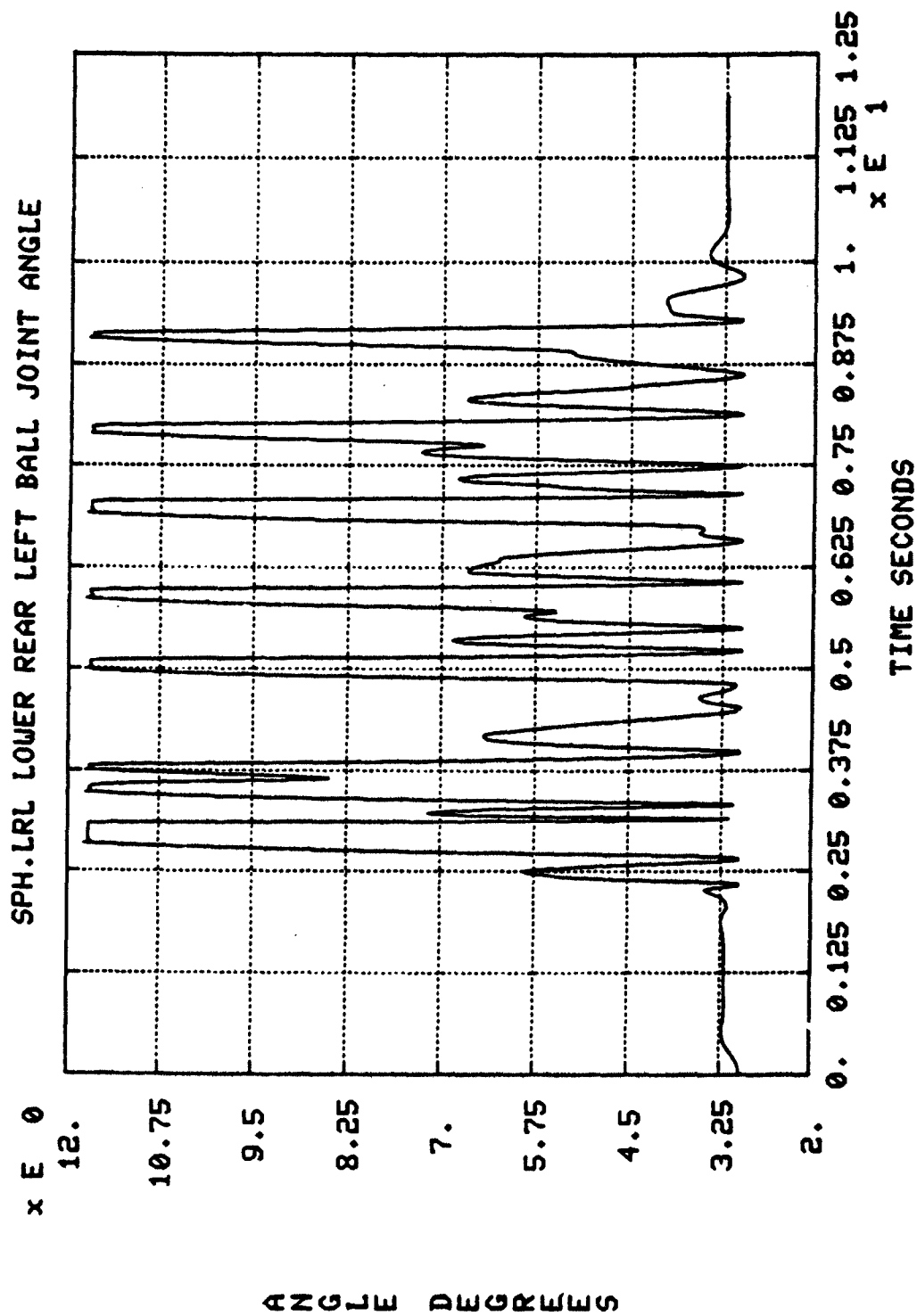


Figure 5-90. Lower Rear Left Ball Joint Angle

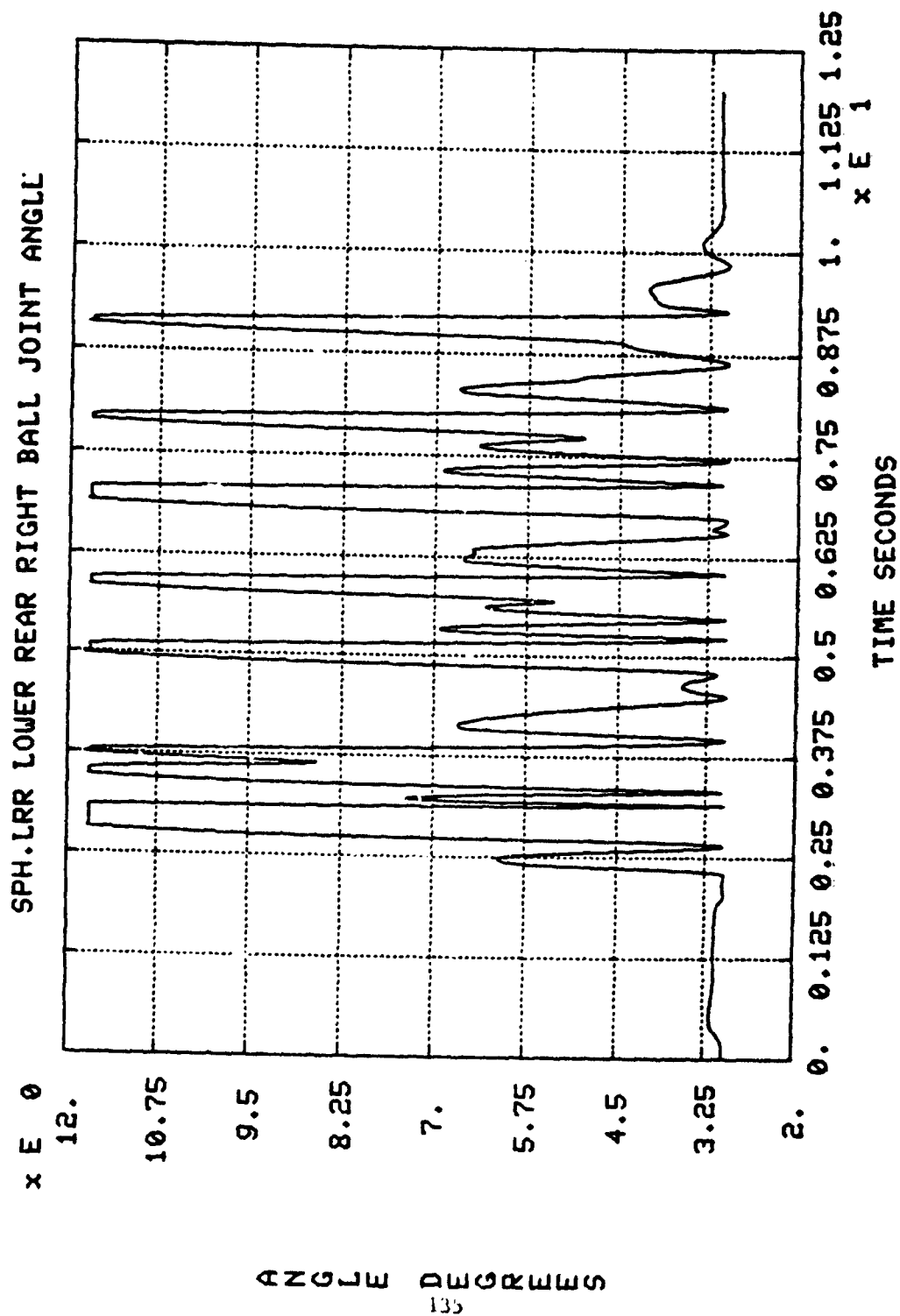


Figure 5-91. Lower Rear Right Ball Joint Angle

Table 5-19. DADS Elements

DADS ELEMENT	ELEMENT NAME	DESCRIPTION
HEADER	HEADER	Comments
SYSTEM	SYSTEM.DATA	Simulation Parameters
DYNAMIC	DYNAMIC.DATA	Simulation Parameters
DISTANCE.CONSTRAINT	RAD-ROD.RR	Rear right Rad Rod
TSDA	DUMMY_TSDA_1	Increment Counter
TSDA	DUMMY_TSDA_2	Increment Counter
TSDA	DUMMY_TSDA_3	Increment Counter
TSDA	SPRING.RR	Rear Right Spring
TSDA	SHOCK.RR	Rear Right Shock
REVOLUTE.JOINT	REV.LRR	Lower Rear Right
REVOLUTE.JOINT	REV.URR	Upper Rear Right
SPHERICAL	SPH.LRR	Lower Rear Right
SPHERICAL	SPH.URR	Upper Rear Right
BODY	CHASSIS	Fixed to Ground
BODY	ARM.LRR	Lower Rear Right
BODY	ARM.URR	Upper Rear Right
BODY	WHEEL.RR	Rear Right Wheel
INITIAL.CONDITION	INIT.WHEEL.RR	Rear Right Wheel 2

Table 5-20. Static Loading Combinations and Directory Locations

Loading	Directory
Vertical Forces	[AARDEMA.DADS3D.HMMWV.103/.REAR_SUSP.FORCE_Z]
Vertical and Forward Longitudinal Forces	[AARDEMA.DADS3D.HMMWV.103/.REAR_SUSP.FORCE_Y.POS_Y]
Vertical and Rearward Longitudinal Forces	[AARDEMA.DADS3D.HMMWV.1037.REAR_SUSP.FORCE_Y.NEG_Y]
Vertical and Outward Lateral Forces	[AARDEMA.DADS3D.HMMWV.1037.REAR_SUSP.FORCE_X.POS_X]
Vertical and Inward Lateral Forces	[AARDEMA.DADS3D.HMMWV.1037.REAR_SUSP.FORCE_X.NEG_X]
Vertical and Forward Longitudinal Outward Lateral Forces	[AARDEMA.DADS3D.HMMWV.1037.REAR_SUSP.FORCE_XYZ]

Forward longitudinal forces are generated during acceleration and rearward longitudinal forces are generated during braking. For the right rear suspension unit, outward lateral forces are generated during a right turn and inward lateral forces are generated during left turns. Vertical forces are generated to support the vehicle.

5.7.2. Results. Results for the six combinations of loading are plotted in Figures 5-92 through 5-97. Tensile forces act along the kingpin axis. The kingpin axis is the line between the two ball joints. Shear force is the magnitude of the forces perpendicular to the kingpin axis acting at the center of the ball.

Based upon the stress theories discussed in section 5.6.4. titled "Dynamic Results," the shear forces are more dangerous than tensile forces. Comparing Figures 5-93 and 5-94, the shear forces in the lower arm ball joint are greater when the fore-aft longitudinal forces are in the forward direction. Likewise, comparing Figures 5-95 and 5-96, shear forces in the lower ball joint are greater for outward lateral forces than for inward lateral forces. Thus, the worst case occurs when the combination of forces include both forward longitudinal forces and outward lateral forces and this case is shown in Figure 5-97. For this condition the shear forces in the lower arm ball joint increase greatly with only relatively small increases in the externally applied forces. This analysis shows that the rear lower ball joint is most sensitive to a combination of forward longitudinal forces and outward lateral forces along with the vertical support forces applied to the wheel.

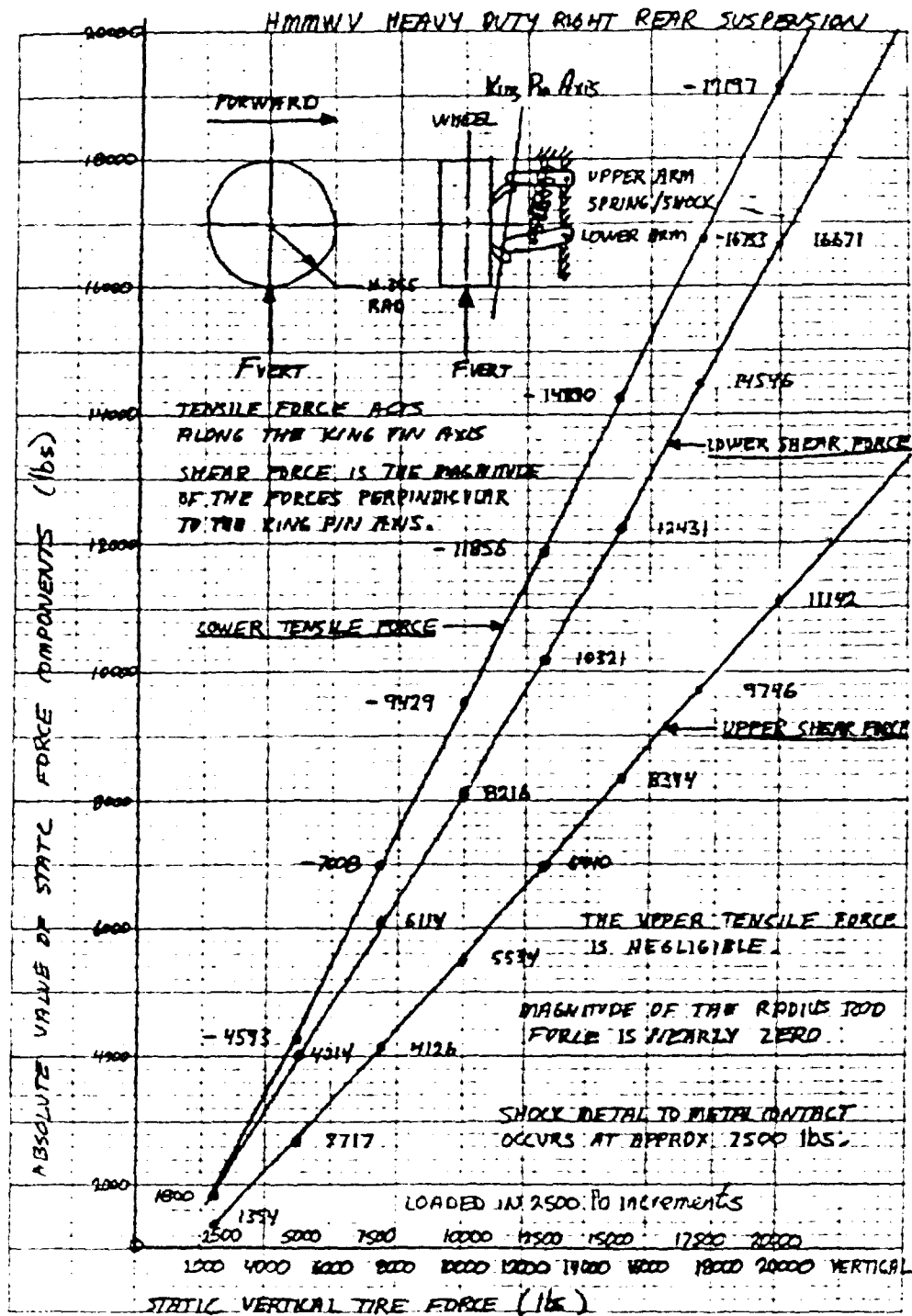


Figure 5-92. Static Vertical Tire Force

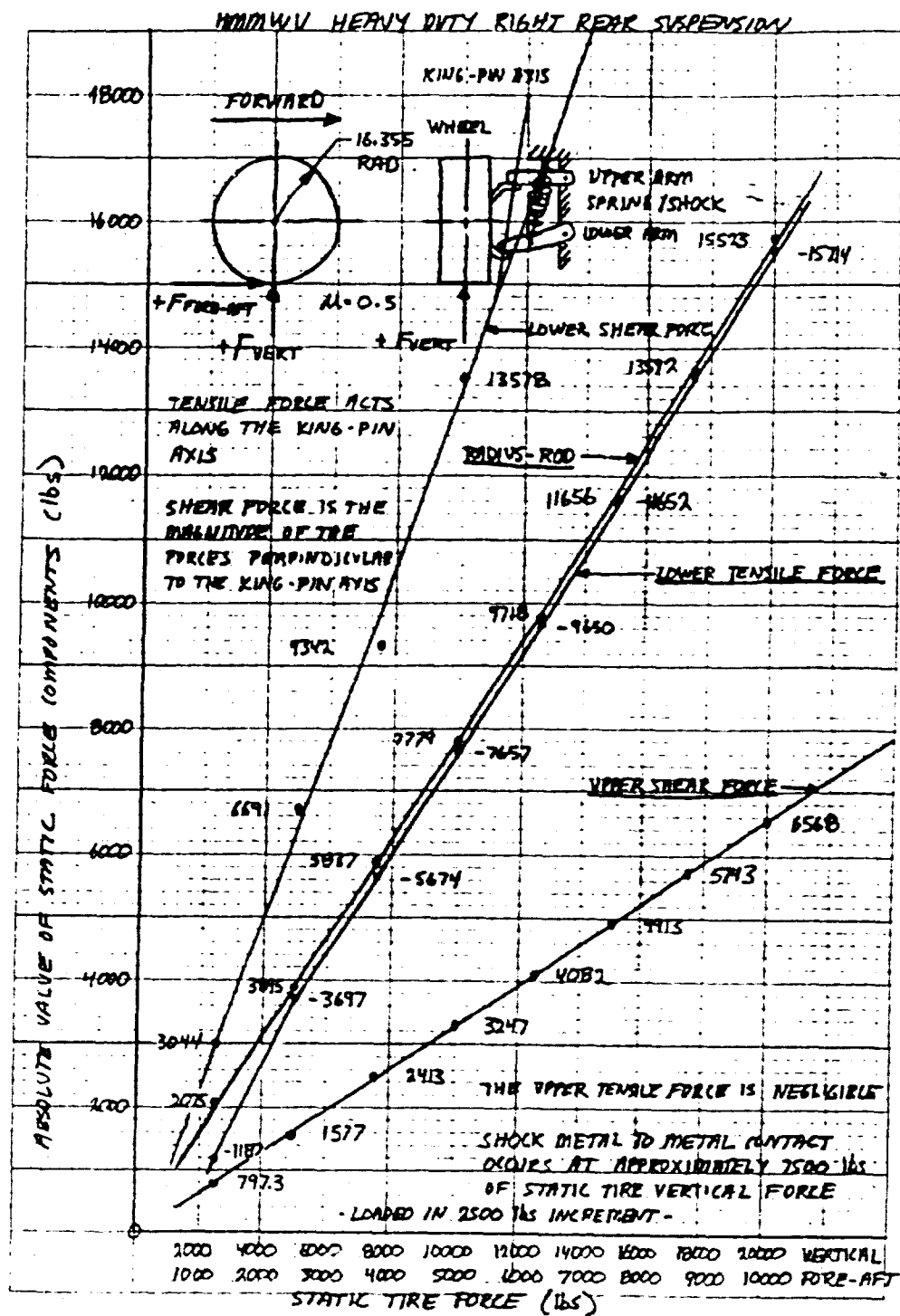


Figure 5-93. Static Vertical and Forward Longitudinal Forces

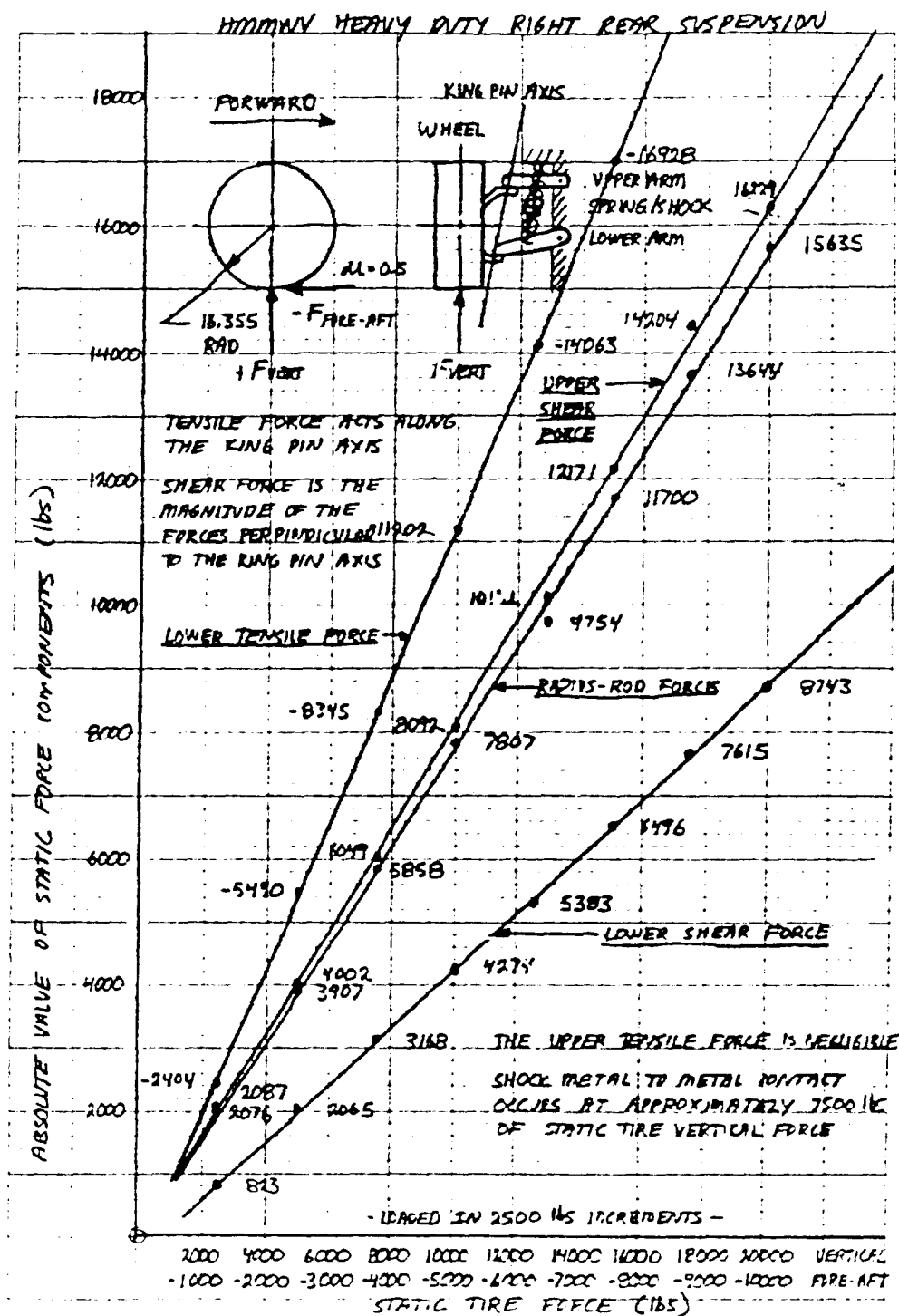


Figure 5-94. Static Vertical and Rearward Longitudinal Forces

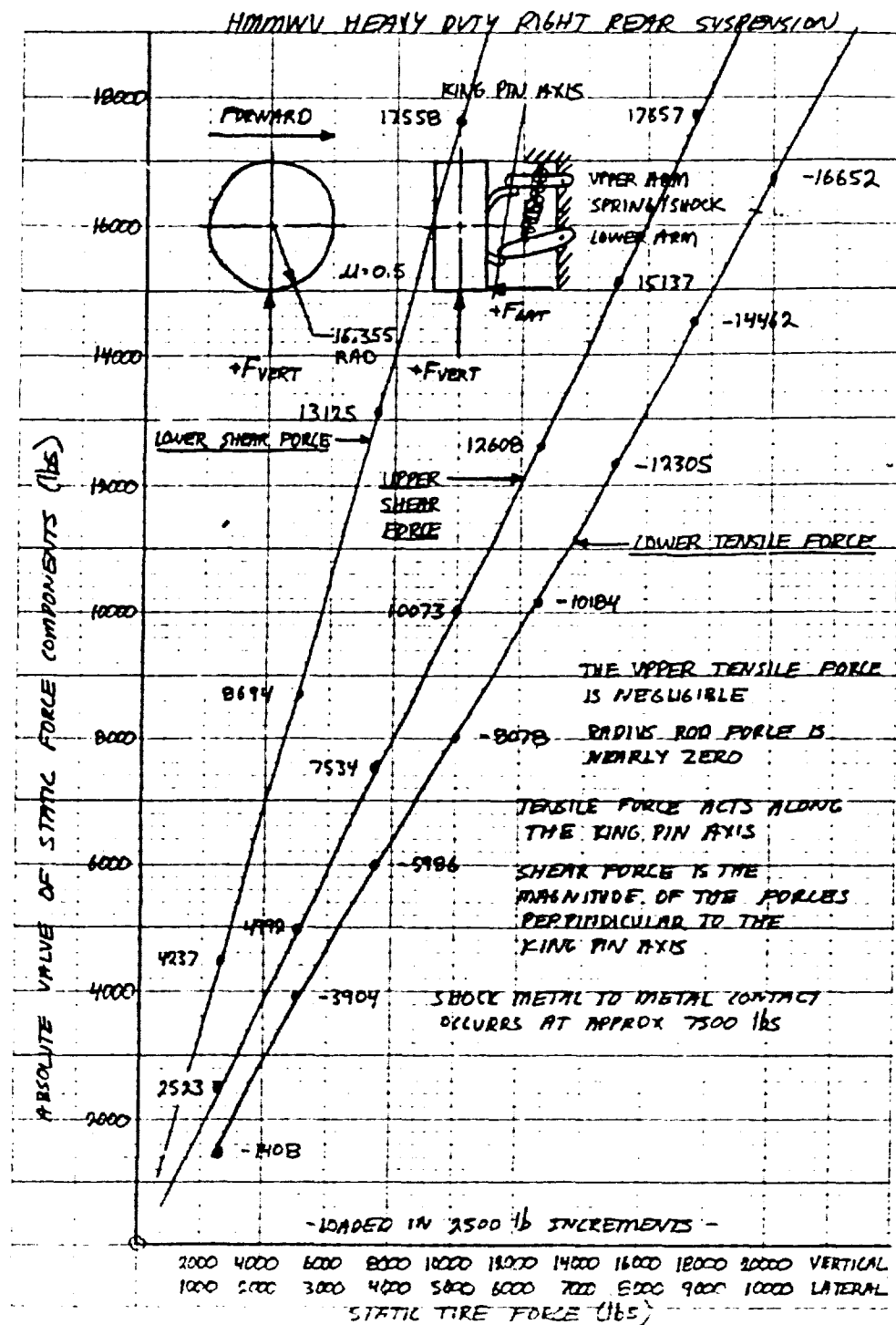
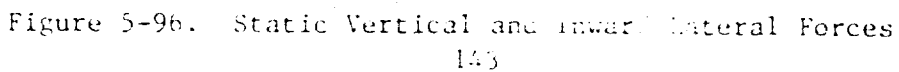


Figure 5-95. Static Vertical and Outward Lateral Forces



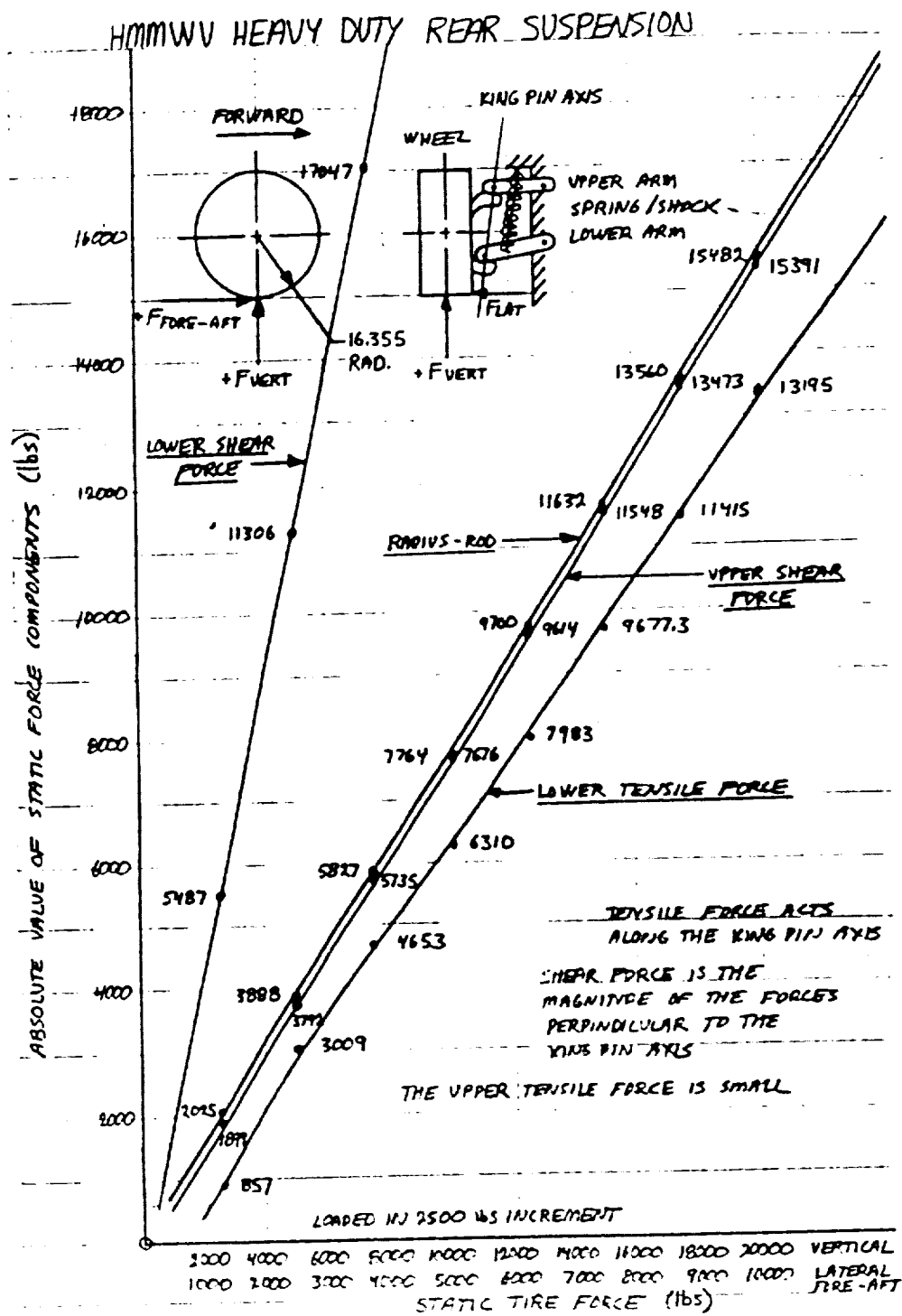


Figure 5-97. Static Vertical, Forward Longitudinal, and Outward Lateral Forces

LIST OF REFERENCES

- 1 SAE J670d, "Vehicle Dynamics Terminology," SAE Recommended Practice, Society of Automotive Engineers, Inc., Warrendale, PA, p. 7 (1975)
- 2 University of Michigan, "Mechanics of Heavy-Duty Trucks and Truck Combinations, "University of Michigan - College of Engineering, Ann Arbor, MI, p. 291 (1986)
- 3 Taborek, Jaroslav J., "Mechanics of Vehicles," Machine Design, p. 14 (1957)
- 4 SAE J670d, "Vehicles Dynamics Terminology," SAE Recommended Practice, Society of Automotive Engineers, Inc., Warrendale, PA, p. 7 (1975)
- 5 SAE J670d, "Vehicle Dynamics Terminology," SAE Recommended Practice, Society of Automotive Engineers, Inc., Warrendale, PA, p. 7 (1975)
- 6 University of Michigan, "Mechanics of Heavy-Duty Trucks and Truck Combinations, "University of Michigan - College of Engineering, Ann Arbor, MI, pp. 294-295 (1986)
- 7 SAE J670d, "Vehicle Dynamics Terminology," SAE Recommended Practice, Society of Automotive Engineers, Inc., Warrendale, PA, p. 8 (1975)
- 8 Taborek, Jaroslav J., "Mechanics of Vehicles," Machine Design, p. 12 (1957)
- 9 University of Michigan, "Mechanics of Heavy-Duty Trucks and Truck Combinations, "University of Michigan - College of Engineering, Ann Arbor, MI, p. 287 (1986)
- 10 SAE J670d, "Vehicle Dynamics Terminology," SAE Recommended Practice, Society of Automotive Engineers, Inc., Warrendale, PA, p. 8 (1975)
- 11 Taborek, Jaroslav J., "Mechanics of Vehicles," Machine Design, p. 13 (1957)
- 12 Shigley, Joseph E., "Mechanical Engineering Design," McGraw-Hill, New York, NY, p. 169 (1977)
- 13 Shigley, Joseph E., "Mechanical Engineering Design," Mc Graw-Hill, New York, NY, pp. 170-171 (1977)

SELECTED BIBLIOGRAPHY

SAE J670d, "Vehicle Dynamics Terminology," SAE Recommended Practice, Society of Automotive Engineers, Inc., Warrendale, PA, (1975)

University of Michigan, "Mechanics of Heavy-Duty Trucks and Truck Combinations," University of Michigan - College of Engineering, Ann Arbor, MI, (1986)

Taborek, Jaroslav J., "Mechanics of Vehicles," Machine Design, (1957)

Shigley, Joseph E., "Mechanical Engineering Design," McGraw-Hill, New York, NY. p. 169 (1977)

APPENDIX A

MONROE AUTO EQUIPMENT SHOCK ABSORBER TEST REPORT L013497

TABLE	STANDARD MTS SET-UP PROCEDURE	REPORT #:
	FOR A.M. GENERAL HUMWV	PROJECT #:
	SHOCK ABSORBERS	PAGE OF
		DATE:

HYDRAULIC RESISTANCE VALUES (MIDSTROKE)

LOAD THE S/A INTO THE MTS IN THE MIDSTROKE POSITION. USING A 1.50 IN. STROKE, CYCLE THE S/A AT 0.10 HZ WITH THE HAVERSINE SIGNAL INPUT. ADJUST THE MTS SPAN SETTING UNTIL NEITHER THE RECOIL LOCK (STOP) OR COMPRESSION STOP CAN BE DETECTED ON THE OSCILLOSCOPE WAVEFORM. THE 2500 LB LOAD RANGE SHOULD BE USED FOR THIS MEASUREMENT.

RECOIL LOCK (STOP)

LOAD THE S/A INTO THE MTS IN THE MIDSTROKE POSITION, AND ZERO THE DISPLACEMENT INDICATOR OF THE MTS. RAISE THE CROSSHEAD OF THE MTS SLOWLY UNTIL THE S/A IS FULLY EXTENDED (METAL TO METAL). THE ZERO POINT OF THE MTS NOW CORRESPONDS TO THE FULLY EXTENDED POSITION. ACTIVATE THE HAVERSINE INVERT SIGNAL INPUT FUNCTION. ADJUST THE MTS TO A 1.50" STROKE USING THE 5.0 INCH STROKE RANGE (30% FSD). USE THE 10,000 LB LOAD RANGE.

COMPRESSION STOP

LOAD THE S/A IN THE MTS IN THE MIDSTROKE POSITION, AND ZERO THE DISPLACEMENT INDICATOR OF THE MTS. AS DESCRIBED ABOVE, LOWER THE CROSSHEAD UNTIL THE S/A IS FULLY COMPRESSED (METAL TO METAL) TO SET THE ZERO POINT. ACTIVATE THE HAVERSINE SIGNAL INPUT FUNCTION, AND ADJUST THE MTS FOR A 1.50 INCH STROKE (SEE ABOVE). USE THE 10,000 LB LOAD RANGE.

A-3

DISTRIBUTION:	PREPARED BY:
	APPROVED BY:

TABLE				REPORT #:		
FRONT * J90327-D				I. JECT #:		
F-V DATA				PAGE OF		
THIRD SAMPLE SUBMISSION (MAR 15 '85)				DATE:		

RECOIL				COMPRESSION			HYDRAULIC RESISTANCE
CPM	30	85	170	30	85	170	
FRONT 3 #	270	1030	1790	170	695	1000	
FRONT 4 #	260	940	1620	153	625	920	
AVERAGE	263	990	1715	160	650	955	

RECOIL				COMPRESSION			RECOIL LOCK (CUT-OFF)
CPM	30	85	170	30	85	170	
FRONT 3 #	1520	3550	5260				
FRONT 4 #	900	2380	4090				
AVERAGE	895	2750	4580				

RECOIL				COMPRESSION			COMPRESSION LOCK (CUT-OFF)
CPM	30	85	170	30	85	170	
FRONT 3 #				2650	3065	3405	1013456
FRONT 4 #				3780	3995	4000	
AVERAGE				3430	3673	3800	

A-4					
DISTRIBUTION: * - THIS DENOTES THOSE SAMPLES FORWARDED TO A.M. GENERAL FOR TESTING. ALL OTHERS RETAINED IN LAB.				PREPARED BY:	
				APPROVED BY:	

TABLE REAR # 1 10597-D F-V DATA THIRD SAMPLE SUBMISSION (MAR 15 '85)	REPORT #:
	JECT #:
	PAGE OF
	DATE:

RECOIL			
CPM	30	85	170
REAR 3 #	385	1300	2725
REAR 4 #	380	1410	2965
AVERAGE	371	1340	2740

COMPRESSION		
30	85	170
250	815	1070
240	690	960
250	706	980

HYDRAULIC
RESISTANCE

CPM	30	85	170
REAR 3 #	620	2510	4500
REAR 4 #	1090	3500	5780
AVERAGE	770	2790	4875

30	85	170

RECOIL
LOCK
(CUT-OFF)

CPM	30	85	170
REAR 3 #			
REAR 4 #			
AVERAGE			

30	85	170
3700	3900	3990
3100	3390	3720
3455	3745	3920

COMPRESSION
LOCK
(CUT-OFF)

1013459

DISTRIBUTION: * THIS DENOTES THOSE SAMPLES FORWARDED TO A.M. GENERAL FOR TESTING. ALL OTHERS RETAINED IN LAB.	PREPARED BY:
	APPROVED BY:

FIGURE

FRONT J590327-D
MIDSTROKE (HYDRAULIC) VALVES

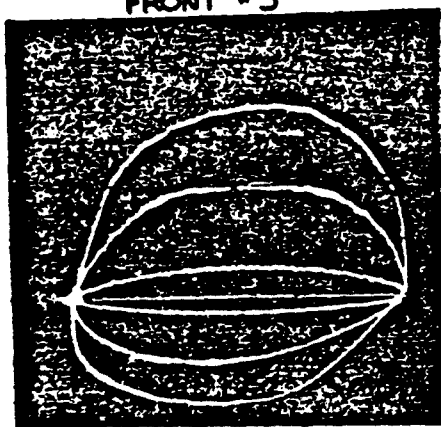
REPORT #:

PROJECT #:

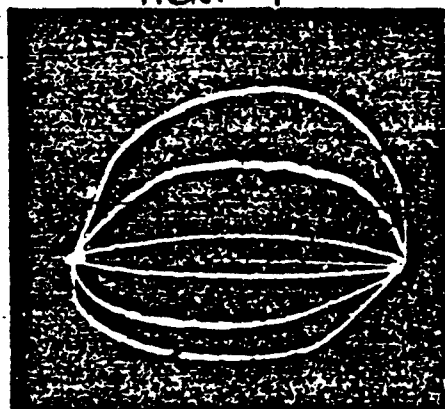
PAGE OF

DATE:

FRONT #3



FRONT #4



LOAD 500 lb/DIV, L
DISPLACEMENT 0.25 in/DIV, D

L013500

A-6

DISTRIBUTION: 30, 85, 170 CPM @ 1.5" STROKE
HAVERSINE SIGNAL INPUT

PREPARED BY:

APPROVED BY:

FIGURE

FRONT 5590327-D

RECOIL CUT-OFF VALUES

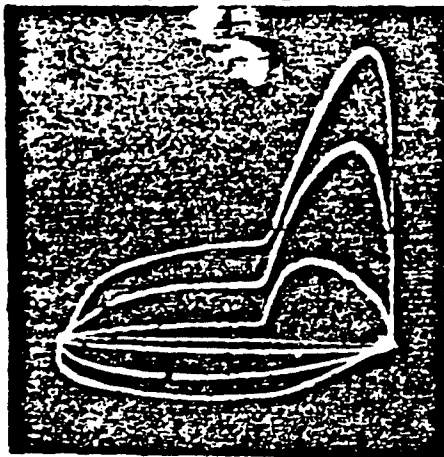
REPORT #:

PROJECT #:

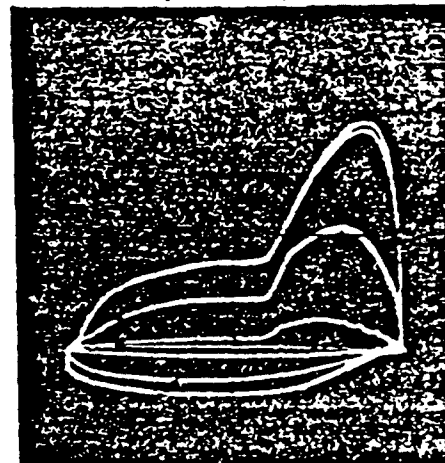
PAGE OF

DATE:

FRONT #3



FRONT #4



LOAD

1000 lb/DN

DISPLACEMENT

0.25 in/DN

L013501

A-7

DISTRIBUTION: 30, 85, 170 CPM @ 1.5" STROKE
HAVERSINE SIGNAL INPUT INVERTED

MTS ZERO POINT: S/A IN FULLY EXTENDED POSITION

PREPARED BY:

APPROVED BY:

FIGURE

FRONT 5590327-D

SAMPLE #3

COMPRESSION CUT-OFF VALUES

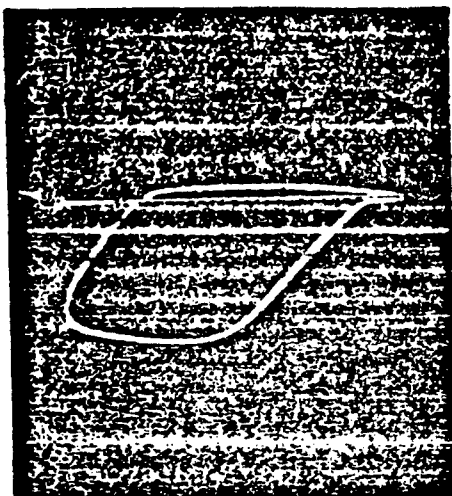
REPORT #:

PROJECT #:

PAGE OF

DATE:

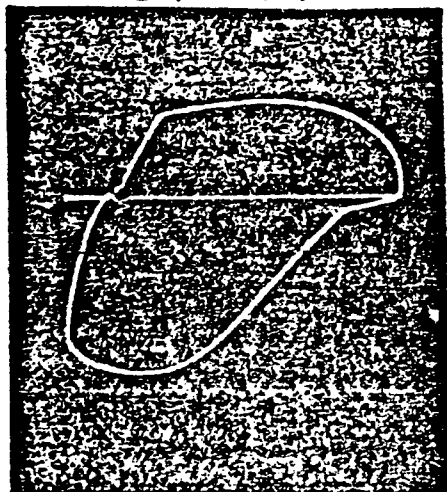
@ 30 CPM



@ 85 CPM



@ 170 CPM



LOAD

1000

lb/DIV

DISPLACEMENT

0.25

in/DIV

A-8

1013502

DISTRIBUTION: @ 1.5" STROKE
HAVERSINE SIGNAL INPUT

MTS ZERO POINT : S/A IN FULLY COLLAPSED POSITION

PREPARED BY:

APPROVED BY:

FIGURE

FRONT 0590327-D
SAMPLE #4

COMPRESSION CUT-OFF VALUES

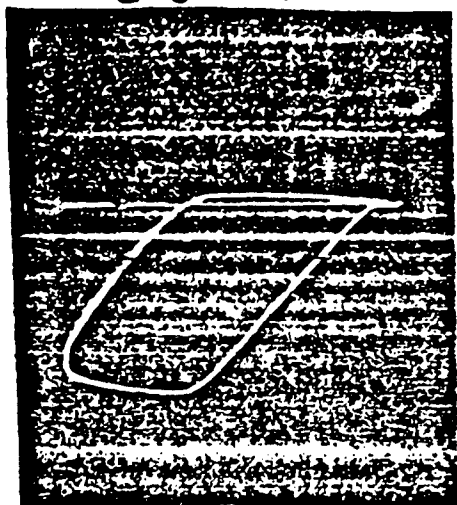
REPORT #:

PROJECT #:

PAGE OF

DATE:

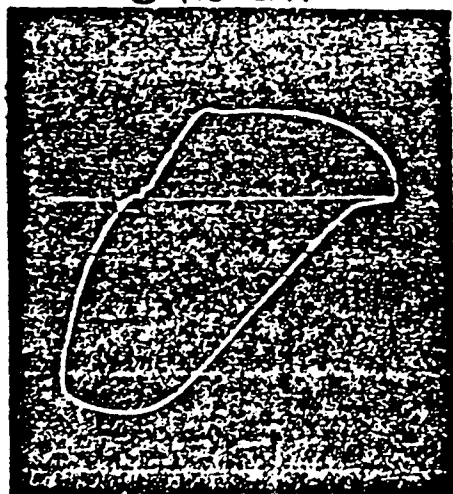
@ 30 CPM



@ 85 CPM



@ 170 CPM



LOAD 1000 lb/DIV
DISPLACEMENT 0.25 in/DIV

A-9

1073503

DISTRIBUTION: @ 1.5" STROKE
HAYERSINE SIGNAL INPUT

MTS ZERO POINT: 5/4 IN FULLY COLLAPSED POSITION

PREPARED BY:

APPROVED BY:

FIGURE

REAR 5590597-D
MIDSTROKE (HYDRAULIC) VALUES

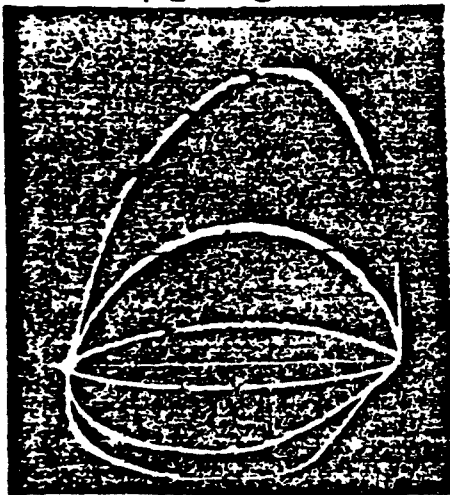
REPORT #:

PROJECT #:

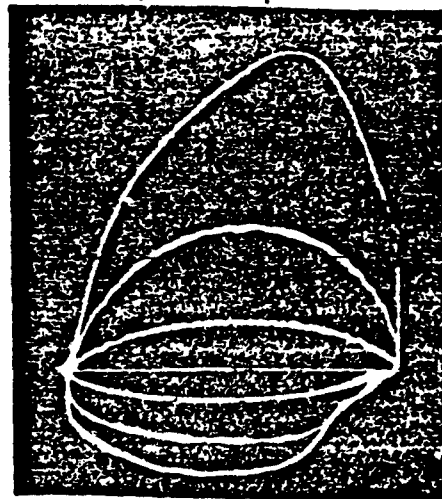
PAGE OF

DATE:

REAR #3



REAR #4



LOAD 500 L lb/DN

DISPLACEMENT 0.25 D in/DN

A-10

1013504

DISTRIBUTION: 30, 85, 170 CPM @ 1.5" STROKE
HAVERSINE SIGNAL INPUT

PREPARED BY:

APPROVED BY:

FIGURE

REAR 500597-D

RECOIL CUT-OFF VALUES

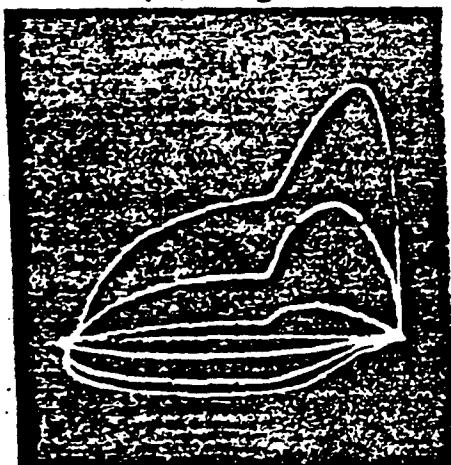
REPORT #:

PROJECT #:

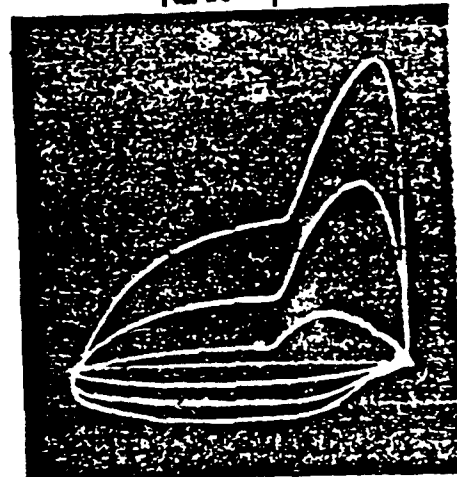
PAGE OF

DATE:

REAR #3



REAR #4



LOAD 1000 lb/DN

DISPLACEMENT 0.25 in/DN

A-11

1013505

DISTRIBUTION: 30, 85, 170 CPM @ 1.5" STROKE
HAVERSINE SIGNAL INPUT INVERTED

PREPARED BY:

MTS ZERO POINT : S/A FULLY EXTENDED POSITION

APPROVED BY:

FIGURE

REAR 5-10597-D

SAMPLE # 3

COMPRESSION CUT-OFF VALUES

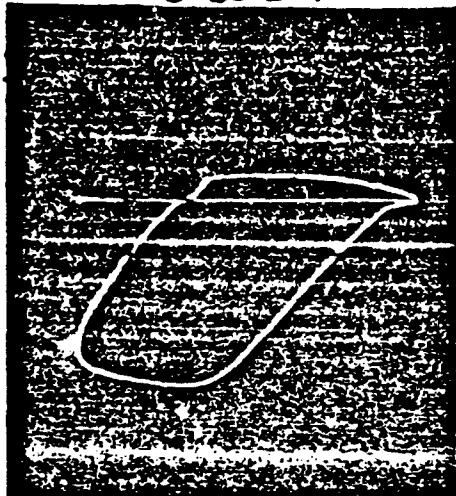
REPORT #:

PROJECT #:

PAGE OF

DATE:

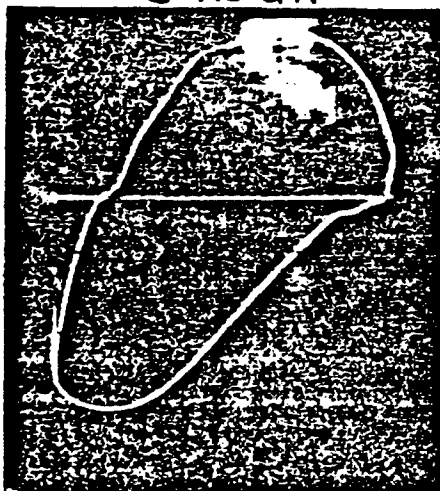
@ 30 cpm



@ 85²⁵ cpm



@ 170 cpm



LOAD 1000 lb/DIV

DISPLACEMENT 0.25 in/DIV

A-12

1013506

DISTRIBUTION: @ 1.5" STROKE
HAVERSINE SIGNAL INPUT

PREPARED BY:

MTS ZERO POINT : 3/A IN FULLY COLLAPSED POSITION

APPROVED BY:

FIGURE

REAR 5-10597-D

SAMPLE # 4

COMPRESSION CUT-OFF VALUES

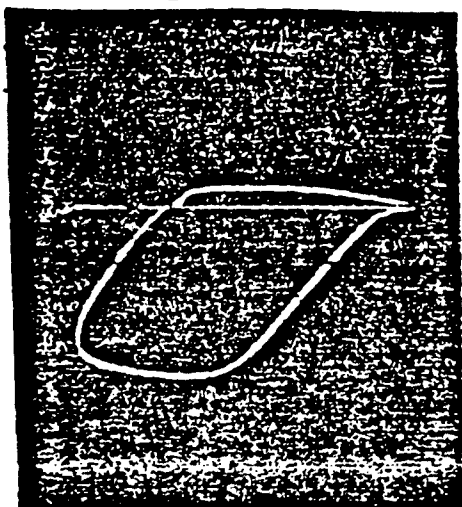
REPORT #:

PROJECT #:

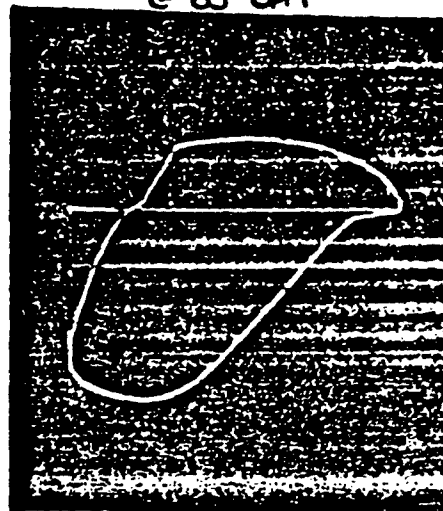
PAGE OF

DATE:

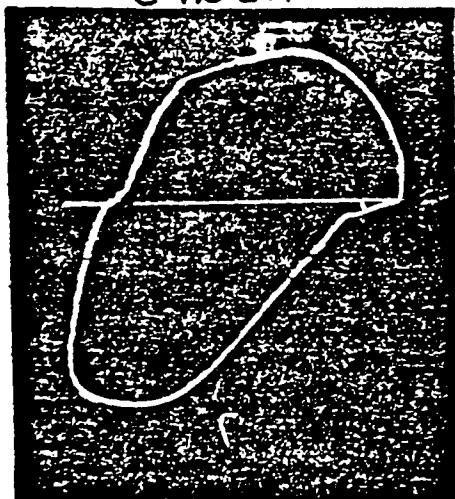
@ 30 CPM



@ 85 CPM



@ 170 CPM



LOAD

1000 lb/DN

DISPLACEMENT

0.25 in/DN

L013507

A-13

DISTRIBUTION: @ 1.5" STROKE
HAVERSINE SIGNAL INPUT

PREPARED BY:

MTS ZERO POINT : S/A IN FULLY COLLAPSED POSITION

APPROVED BY:

A-14

APPENDIX B

UNIVERSITY OF MICHIGAN TRANSPORTATION INSTITUTE LETTER DATED JULY 23, 1985

July 23, 1985

Mr. Roger Wehage

US ARMY TACOM
Warren, MI

Dear Roger:

The purpose of this letter is to present the results of a program of parameter measurements which UMTRI has recently conducted on the HMMWV 1-1/4 ton vehicle.

The program included the measurement of weight, center of gravity position and principle moments of inertia of the total vehicle. Vertical spring rate and Coulomb friction, roll steer and aligning moment steer were measured for the rear suspension. These, plus the influence of the auxiliary roll stiffness device, were measured for the front suspension. (The rear suspension has no "anti-sway bar".) Overall steering ratio was also measured.

Results of the inertia testing program are presented in tabular form on two enclosed sheets.

Suspension measurement results are presented graphically on eight enclosed sheets. Some comments on the suspension data follow.

1) Vertical spring rate and Coulomb friction.

At the nominal wheel load of 1500 lb, the front suspension shows a vertical spring rate of about 242 lb/in and Coulomb friction of about 106 lb. Front spring rate varies with load, however.

The rear suspension shows relatively constant spring rate of about 368 lb/in and Coulomb friction of about 112 lb.

For both front and rear, suspension travel is limited by shock absorber stroke in both rebound and compression. These limits are clearly apparent in the data.

2) Auxiliary roll stiffness.

Only the front suspension is equipped with an auxiliary roll stiffener. Vertical rate data with the device in play show a rate of 296 lb/in at 1500 lb wheel load. Comparing this with the base rate yields an auxiliary vertical rate of 54 lb/in. Given a 72 inch track width, this is equivalent to 2443 in-lb/deg of auxiliary roll stiffness.

$$\text{suspension roll} = \frac{1 \text{ in}}{\text{ArcTan}(\frac{1}{72})} = 1.2567 \text{ in/deg}$$

3) Steer properties, front suspension.

$$54 \frac{\text{lb}}{\text{in}} \times \frac{72 \text{ in}}{2} \times 1.2567 \frac{\text{in}}{\text{deg}} = 2443 \text{ in-lb/deg}$$

Overall steering system ratio was measured and is presented graphically. As per our telephone conversation, steer gear box ratio was not measured.

Front aligning moment compliance steer shows the typical "S" shape indicating a lash about zero moment and spring-like behavior at non-zero moments. This steering system shows about 1/2 deg lash and a rate of about 2200 in-lb/deg. This compliance steer would appear to be the strongest suspension steer influence on the vehicle.

Front roll steer data appears to indicate negligible roll steer on center. The response appears to be dominated by "wandering" within the steering system lash.

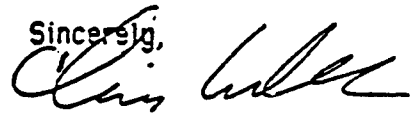
4) Steer properties, rear suspension.

Aligning moment steer at the rear is characterized by a rather consistent rate of about 14,300 in-lb/deg.

Unlike the front, roll steer at the rear is significant ranging from about -.05 deg/deg to about -.20 deg /deg depending on load and roll position. This variation reflects the non-linear quality of the suspension linkage. Roll steer measurements were made on the right rear wheel. Since the suspension is symmetric, the left wheel behavior will be similar with the polarity of both steer angle and roll angle axes reversed.

If I can be of further assistance, please call. (I will be on vacation
until Aug. 13.)

Sincerely,

A handwritten signature in cursive script, appearing to read "C.B. Winkler", written in dark ink.

C.B. Winkler

INERTIAL PROPERTIES TEST RESULTS*

Weight	5860 lbs
Center of Gravity Position	
Aft of Front Axle	61.8 inches
Above Ground	32.5 inches
Moments of Inertia	
Pitch	41,300 in-lb-sec**2
Yaw	52,300 in-lb-sec**2
Roll	13,900 in-lb-sec**2

***Vehicle tested with full fuel tanks, otherwise empty.**

UNITED: PITCH PLANE INERTIAL PROPERTIES TEST

TEST NO.:

DATE: 7-2-57 TIME: 8:00 OPERATOR: W. A. H.

I. VEHICLE ID

MANUFACTURER: Gen General WHEELBASE: 160

MODEL NO.: Hummer - T-1000 SERIAL NO.:

II. BODY ID

MANUFACTURER: DESCRIPTION:

MODEL NO.: SERIAL NO.:

III. VEHICLE CONDITION

GAS: Full LOADING: Empty

IV. RESULTS

	1	TEST 2	3	AUG
CG POSITION (INCHES)				
AFT OF FRONT AXLE	61.79	61.8	61.8	61.8
EXPECTED ERROR	.156	.155	.154	
STANDARD DEVIATION				SE-03
HEIGHT ABOVE VEHICLE				
REFERENCE POINT*	14.2	14.15	14.17	14.17
EXPECTED ERROR	.387	.393	.413	
STANDARD DEVIATION				.021
HEIGHT ABOVE GROUND				32.47
PITCH MOMENT OF INERTIA				
ABOUT CG (IN-LB-SEC ²)	40617	42577	40656	41293
EXPECTED ERROR	1333	1368	1333	
STANDARD DEVIATION				915
WEIGHT: 5360 LBS				

* REFERENCE POINT IS LOWER FACE OF FRAME AT CG

THOMAS / HANCOCK

Front Suspension

Vertical Spring Rate

(B3/4 side view together, see in assembly and for reference)

Left Wheel

Right Wheel

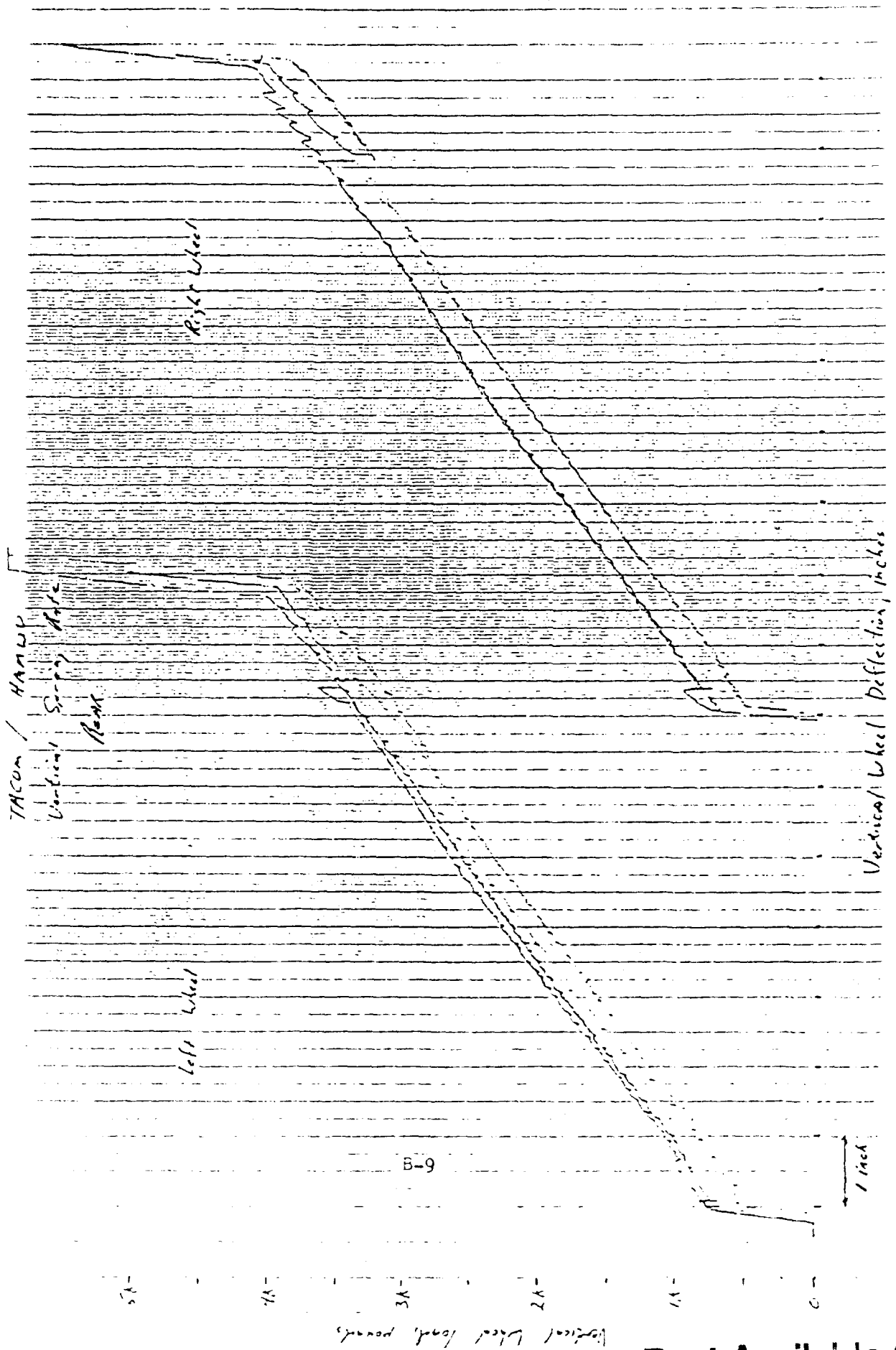
Vertical Wheel Deflection, inches

1 inch

B-8

Vertical Wheel Load, pounds

Best Available Co



TRUCK / HUMAN

FEAR SUSPENSION
VERTICAL SPRING RATE PLUS
SHOCKING TOP STIFFNESS

(Wheels do not feel operation times, i.e.
rate of spring rate + mass roll over influence)

Vertical Load (lb/ft)

5K

4K

3K

2K

1K

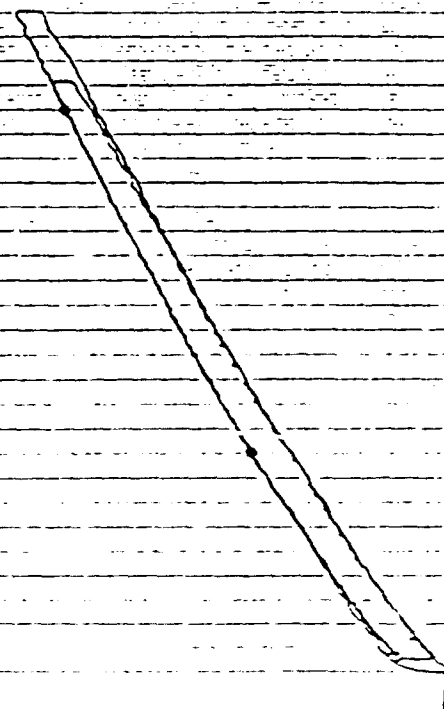
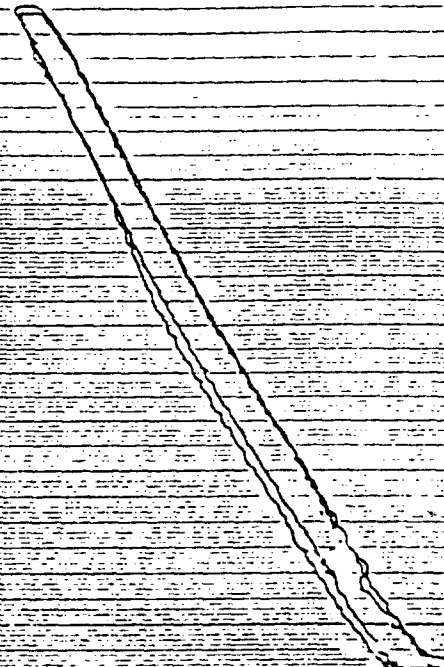
0

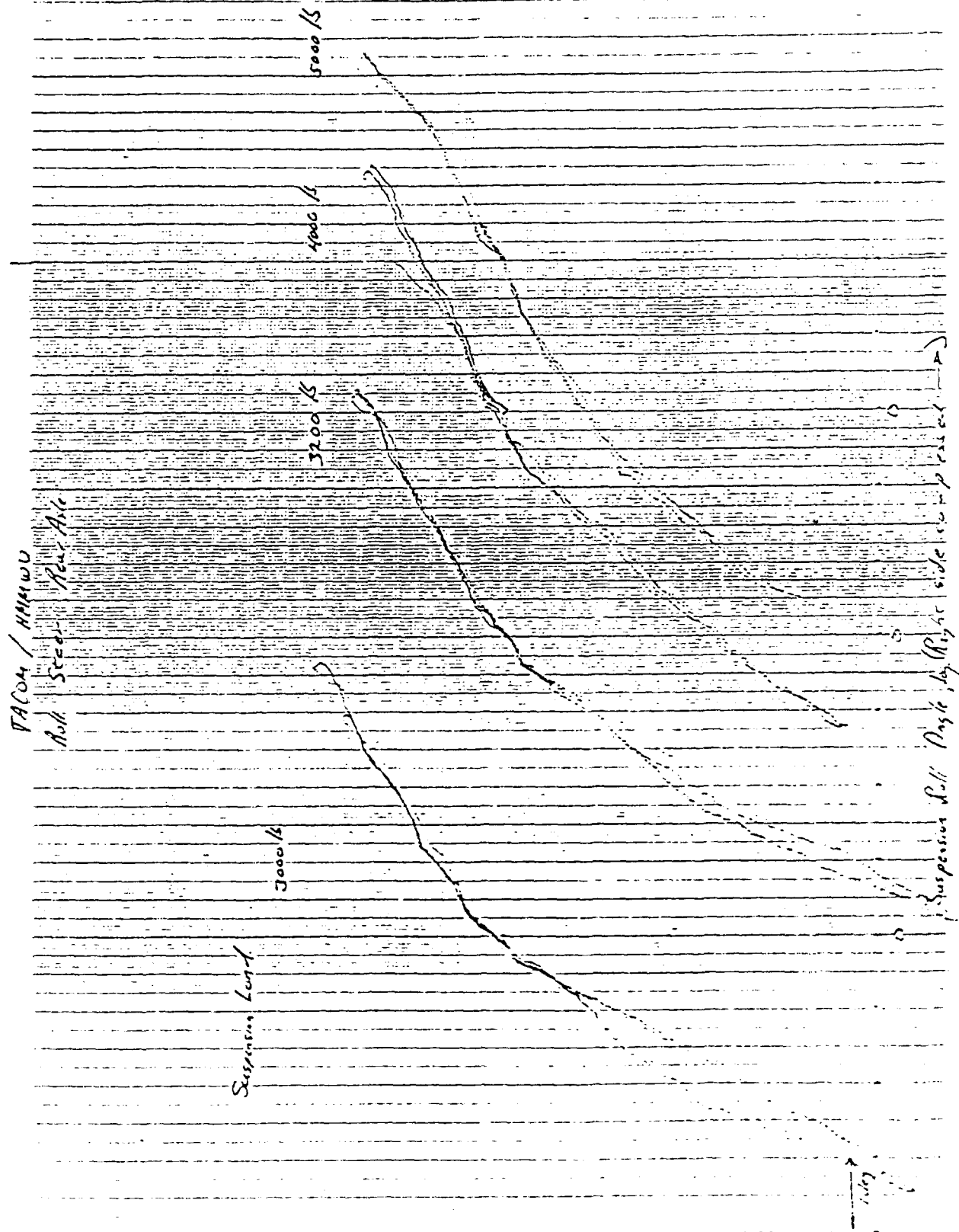
3-10

Best Available Cor

1 inch

Vertical Wheel Deflection, inches

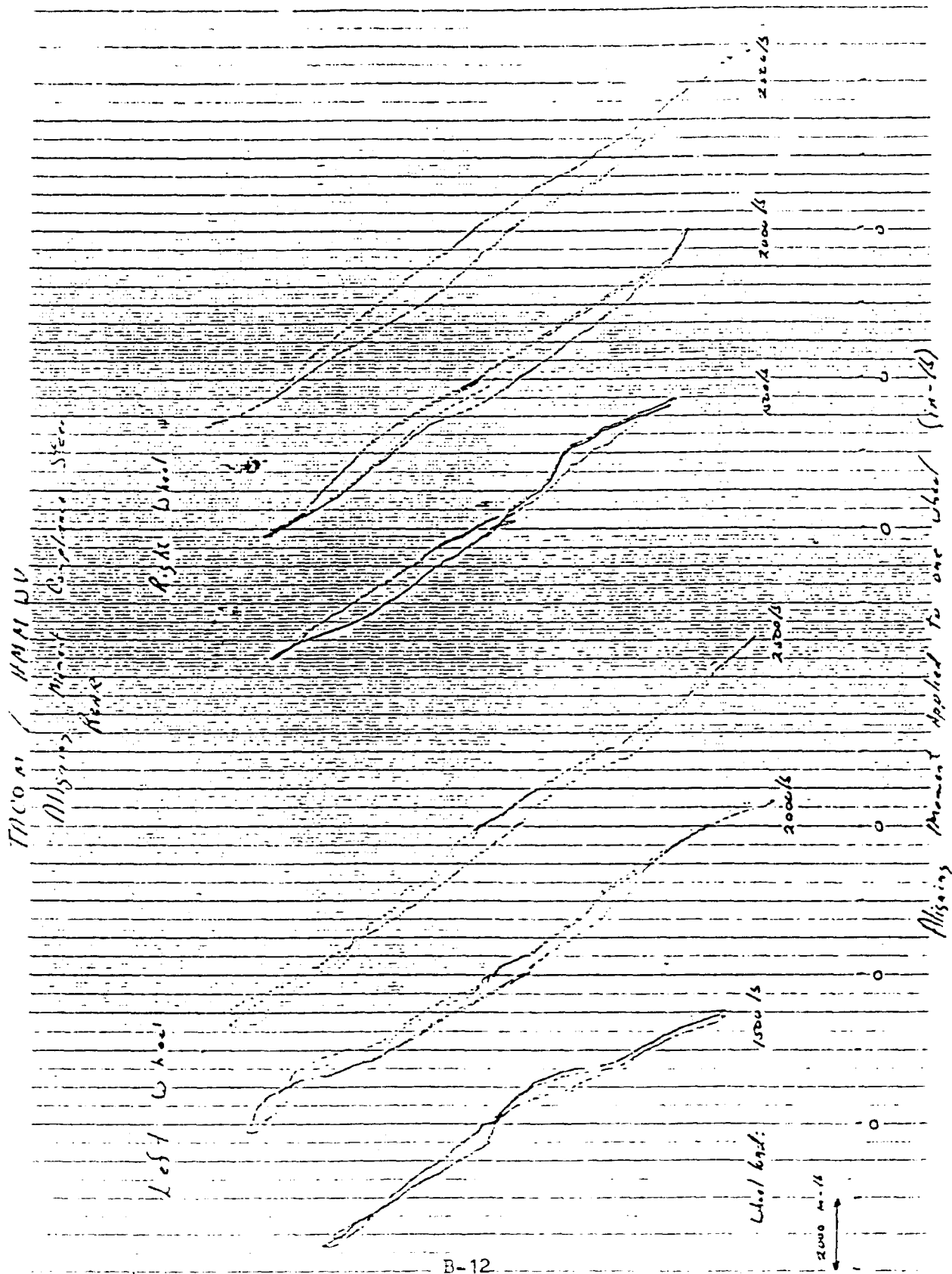




B-11

Figure 10: Roll Speed - New Age (when in right)

Best Available Copy



B-12

Wheel Speed (ft/sec to right)

Best Available Co

TACON / HANNU
Roll Steer, Fine

(Exposed from side, poor steering)

Suspension Load
3000 lb

1000 / 5

Suspension Roll Right side (Right side compressed)

1/16"

B-13

Best Available Copy

207
- 57
- 60
- 61
- 62
- 63
- 64
- 65

B-14

Suspension
hook

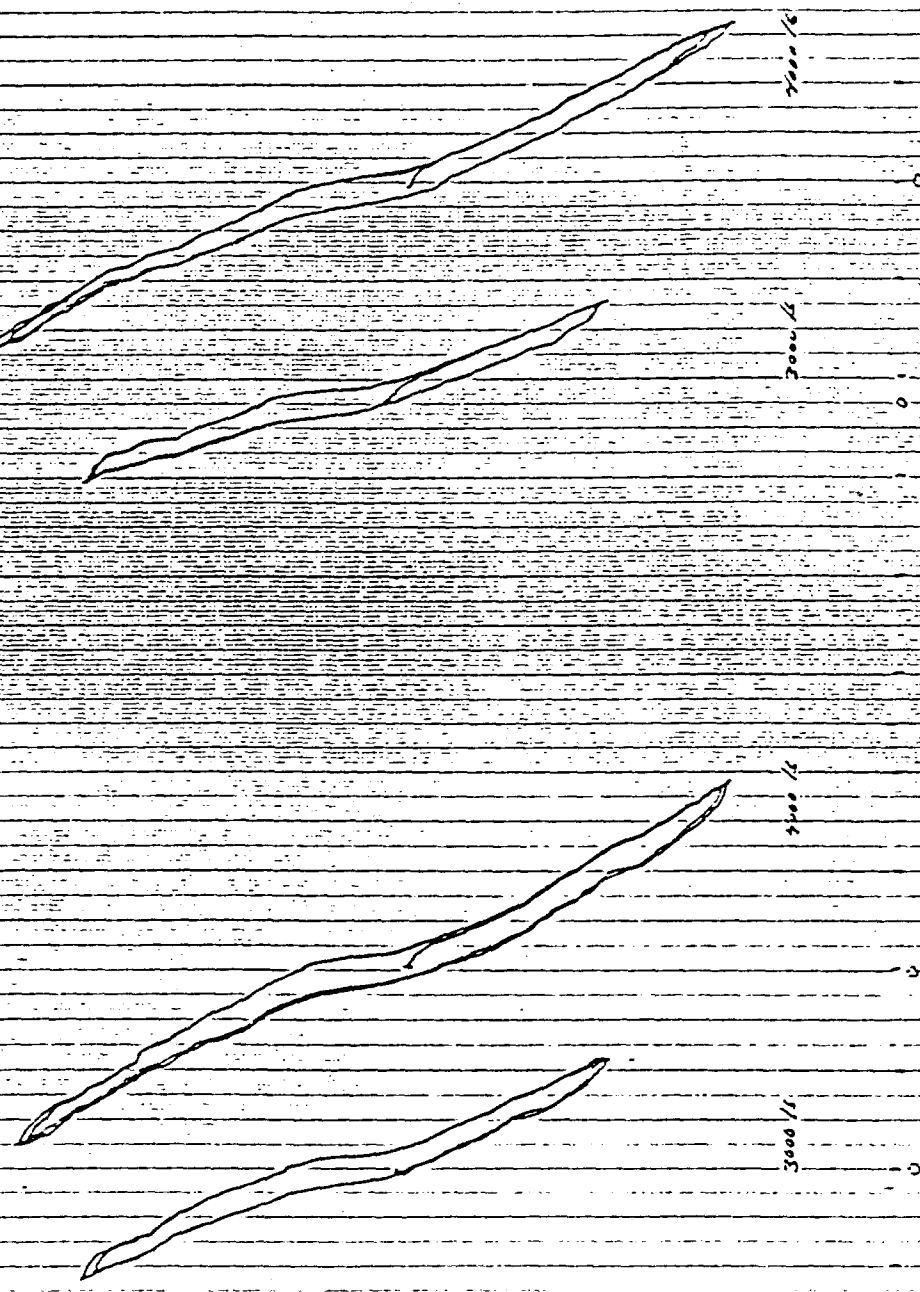
left wheel

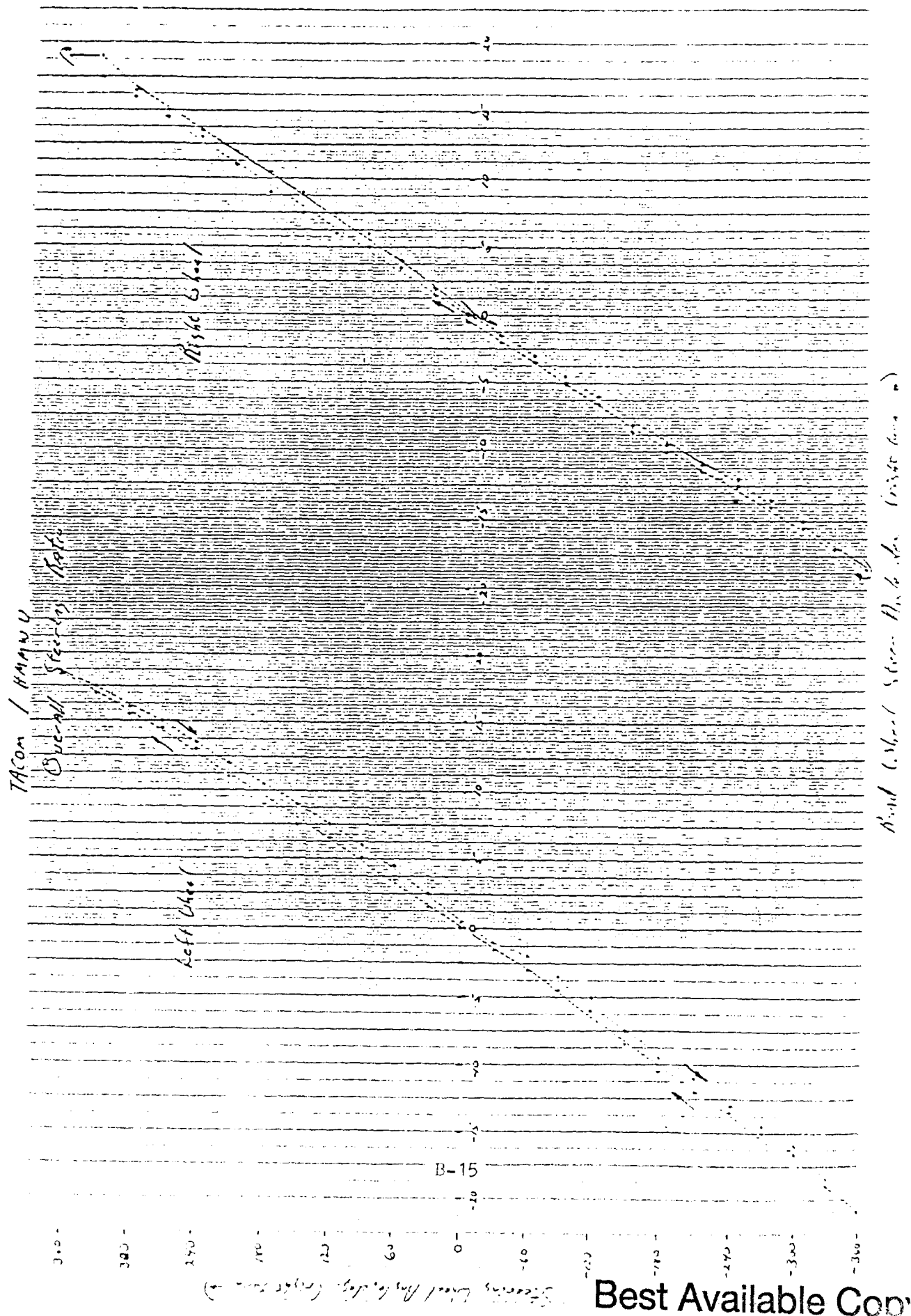
THCOM / HXHWV
Abstracts, Abstracts, Abstracts

Right Wheel

(Fog - running is power steering on)
Steering wheel locked on center

Aligning Moment. Per. Wheel, Applied to Two Wheels simultaneously





Best Available Copy

Coastal Wmpley R/S II
 7612.5-12.5 LT 481C

Side Force, lbs.

Camber Angle, deg	Slip Angle, deg						
	-1	0	1	2	4	8	16
-10		-53			-355	-435	-454
-5		-23			-299	-386	-437
-2		-5					
0	86 91	-5	-86	-163	-277	-378	-424
2		2	-83	-152	-265	-357	-409
5		8					
		24			-252	-343	-419
10		47			-247	-385	-454

B-16

Vertical load. 500 16

Inflation Press. 24 psi

Gauges by NIT II
30 x 12.5 x 16.5 LT USC

Side Force, lbs

Camber
Angle, deg

Slip Angle, deg

-1	0	1	2	4	8	16
-10	-122			-544	-672	-714
-5	-67			-500	-629	-686
-2	-18					
0	-2	-141	-262	-432	-587	-653
2	6	-137	-247	-417	-527	-632
5	23					
10	66			-409	-582	-671
	108			-352	-563	-685

B-17

Vertical load. 800 lb

Inflation Press. 2.4 psi

Side Force, lb.

Carlyon W-angle ATT II
36x12.5-16.5 LT LHC

Carlyon Angle, deg	-1	0	1	2	4	8	16
-10		-378			-1114	-1331	-1460
-5		-227			-1042	-1295	-1426
-2		-109					
0	280	3	-291	-522	-890	-1228	-1389
2	290	9	-274	-500	-871	-1203	-1367
5		88					
		212			-657	-1072	-1324
10		327			-502	-960	-1261

B-18

Vertical load. 1700 16

Inflation Press. 24 psc

Side Force, lb

Gauges Wraggle- R/T D
36V12.5-16.5 LT LHC

Carbide Angle, deg	-1	0	1	2	4	8	16
-10		-574			-1477	-1887	-2133
-5		-296			-1292	-1763	-2059
-2		-138					
0	311	-9	-315	-591	-1062	-1691	-1970
2	384	1	-311	-515	-1022	-1569	-1946
5		104					
10		271			-753	-1373	-1836
		507			-498	-1179	-1723

B-19

Vertical load 2600 lb

Inflation Press 2.4 psi

Gardner Wrangler RT II
3612.5-16.5 LT 24"

Side Force, lb.

Camber Angle, deg	-1	0	1	2	4	8	16
-10		-684	.		-1283	-1782	-2742
-5		-340			-1041	-1623	-2605
-2		-149					
0	167	-6	-198	-391	-754	-1403	-2476
2	212	-1	-251	-434	-748	-1392	-2418
5		129					
10		346			-447	-1166	-2286
		657			-151	-596	-2191

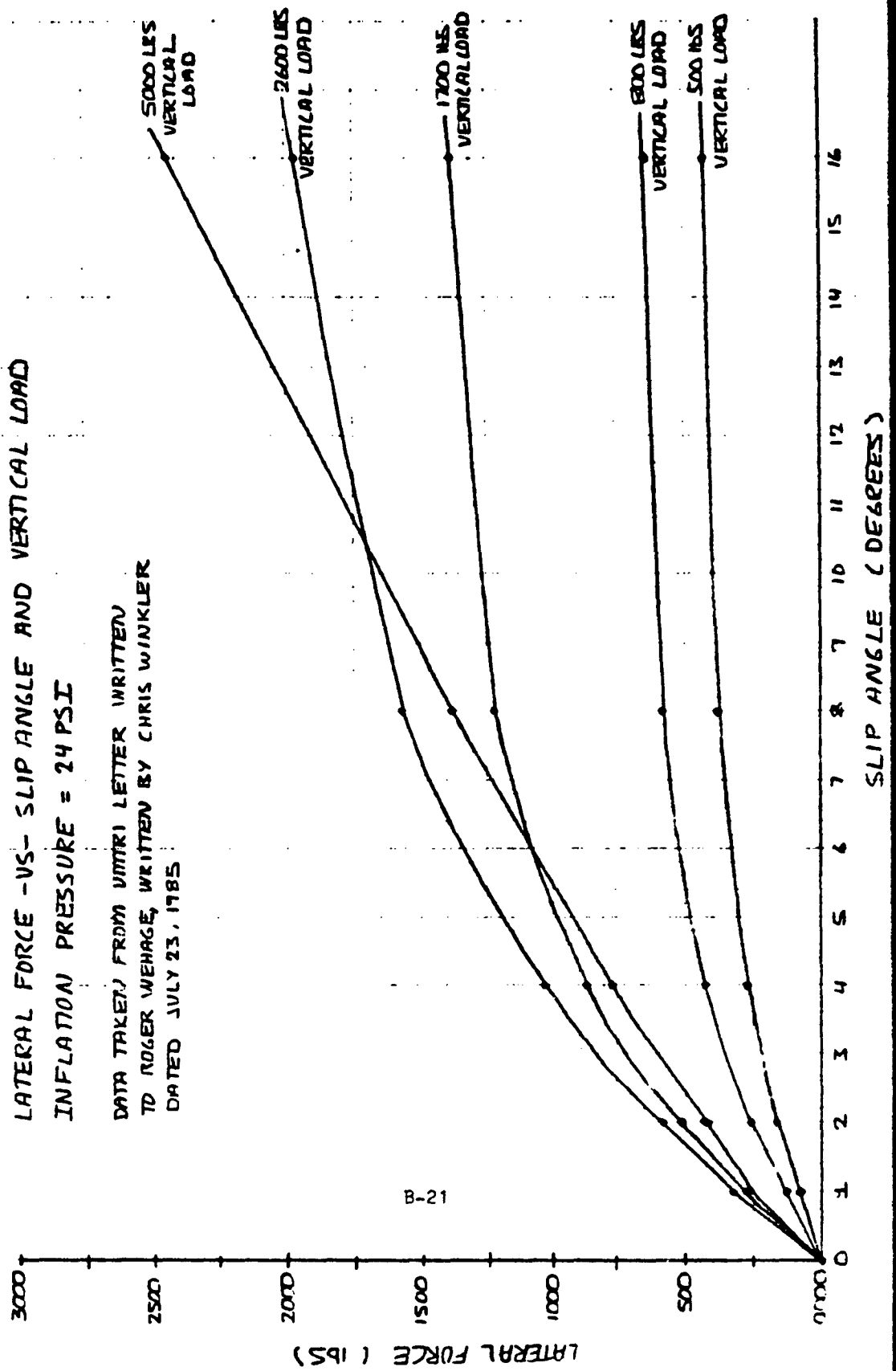
B-20

Vertical load. 5000 16

Inflation Press. 24 psc

GOODYEAR VIRANGLER 36x12.5-16.5 LT RT II TIRE
 LATERAL FORCE -VS- SLIP ANGLE AND VERTICAL LOAD
 INFLATION PRESSURE = 24 PSI

DATA TAKEN FROM UMTRI LETTER WRITTEN
 TO ROGER WEHAGE, WRITTEN BY CHRIS WINKLER
 DATED JULY 23, 1985



APPENDIX C
GOODYEAR TIRE DATA

GOODYEAR TECHNICAL CENTER



AKRON

AKRON, OHIO 44316-0001

July 21, 1987

AM General Division
LTV Aerospace & Defense Company
11900 Hubbard Drive
PO Box 3330
Livonia, MI 48151-3330

Attention: R J Fanco

Subject: 36X12.50-16.5 LT Data for TACOM

Dear Mr Fanco,

You requested through our Detroit office, the following technical data for the Bias HMMWV tire.

1. Tire Damping Coefficient

We do not have actual data for this tire but have included three statements from available publications that should be applicable.

"The tire acts as a linear spring to cushion shocks to the vehicle and to absorb impact loads. Unfortunately, the tire is not an effective damping device. Eliminating the adverse effects of bounce magnitude and frequency remains a function of the vehicle suspension system."

"While the exact nature of tire damping is speculative, it is measurable and has proven to be a very small value when determined for a rolling tire. Values ranging from 1 to 20 lb-sec/in have been noted."

"The damping coefficient (Zeta) for a bias truck tire (10.00-20) over the range of conditions tested ranged from 0.012 to 0.026."

July 21, 1987

-2-

2. Tire Coefficient of Friction

Concrete	dry	.7-.9
"	wet	.5-.7
Bituminous	dry	.6-.8
"	wet	.4-.7
Gravel, firm		.4-.7
Med. Soft Soil		.3-.5
Soft Loose Soil		.2-.4
Sand		.2-.3
Ice, Packed Snow		.05-.2
Mud		.1-.4
Steel	dry	.52
"	wet	.44

3. Tire Normal Force Displacement Curve

Load/Deflection Curve MD-319527 is attached.

4. Tire Tangential Force Displacement Curve

Both a tangential and lateral load/deflection curve of the 36X12.50-16.5 LT Wrangler R/T II are attached.

H R Vermie

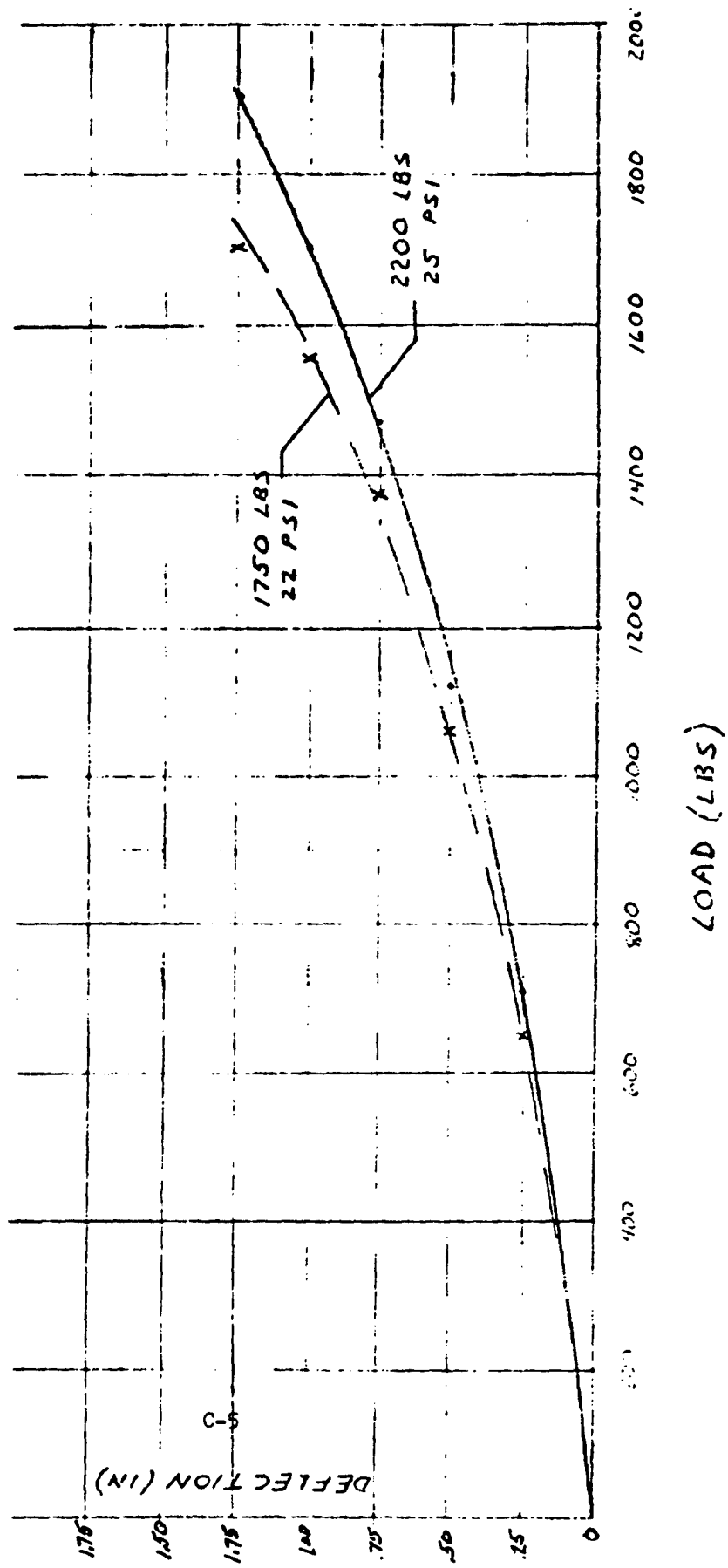
H R Vermie
Military Tire Applications

jfy

Attachments

36 X 12.50 - 16.5 LT WRANGLER R/T II

TANGENTIAL LOAD/DEFLECTION



36X12.50 - 16.5LT WRANGLER R/T II

LATERAL LOAD / DEFLECTION

SPRING RATE:

IF LATERAL LOAD IS KNOWN,

SPRING RATE IS SLOPE OF

CURVE AT THAT LATERAL LOAD.

IF LATERAL LOAD IS VARIABLE,

ASSUME STRAIGHT LINE BETWEEN

0 AND MAX ESTIMATED LATERAL

LOAD.

C-6

1.75

1.50

1.25

1.00

.75

.50

.25

0

100

200

300

400

500

600

700

800

900

1000

1750 LBS
22 PSI

2200 LBS
25 PSI

MD-319527

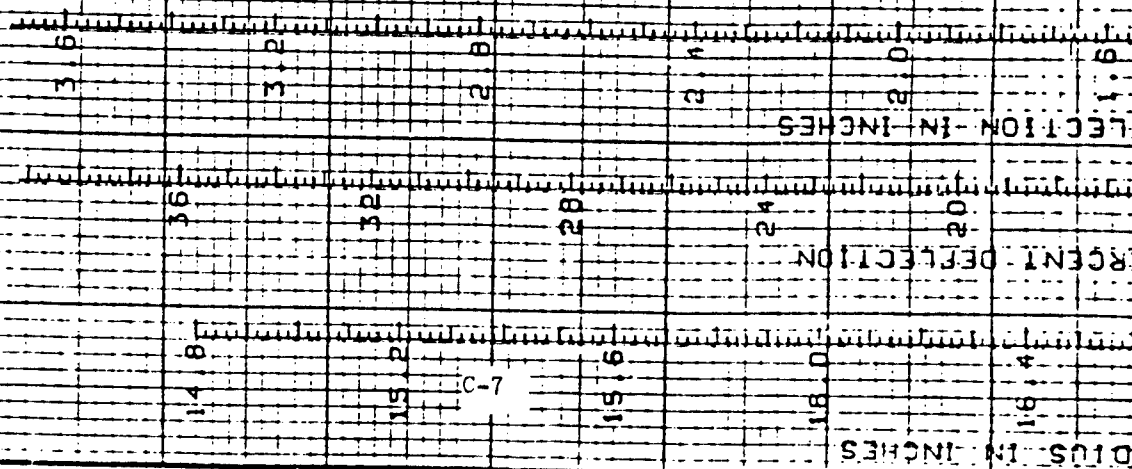
36X12-50-16.5 WRANGLER RT II

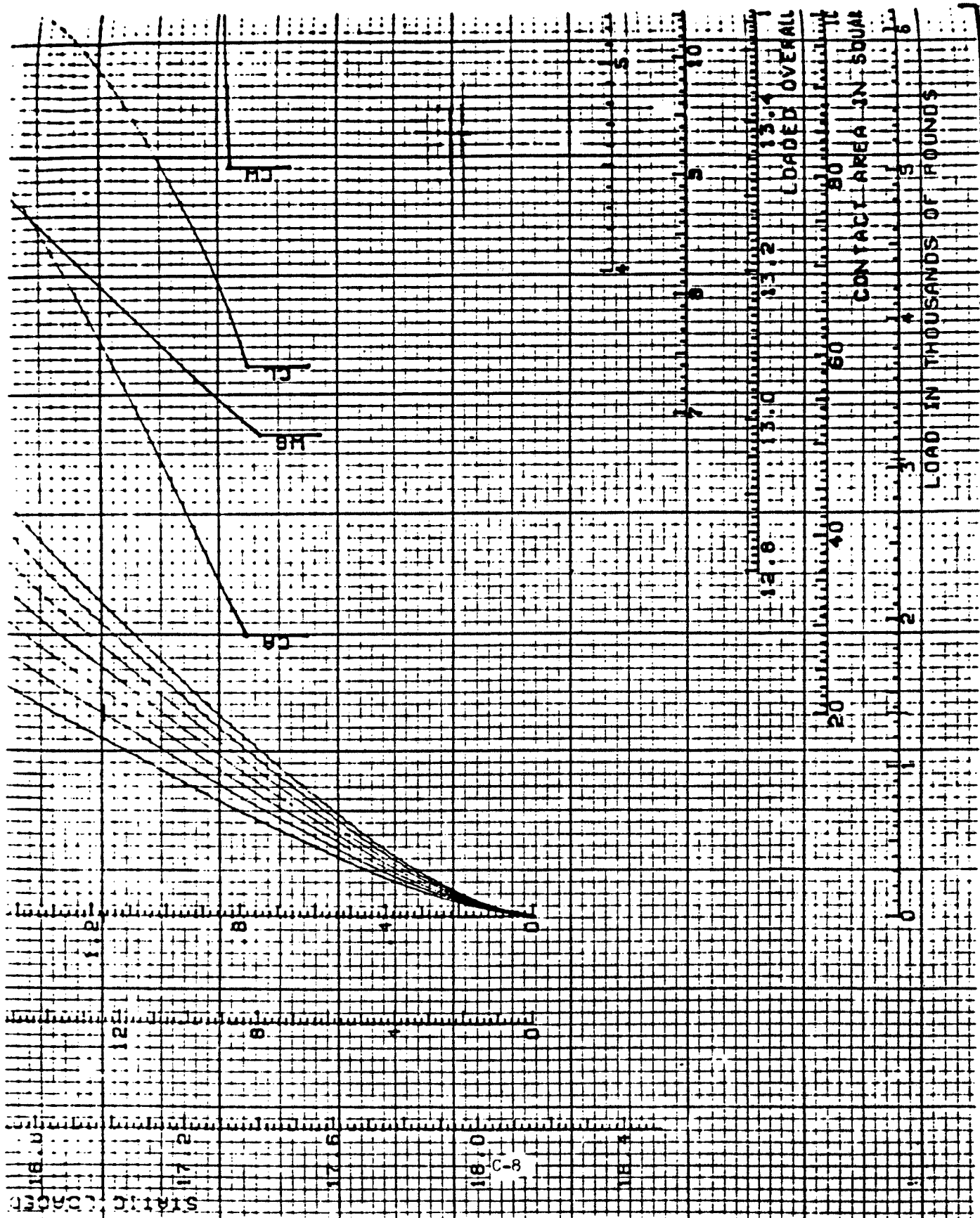
RIM 8.25

300165-6-11R-10

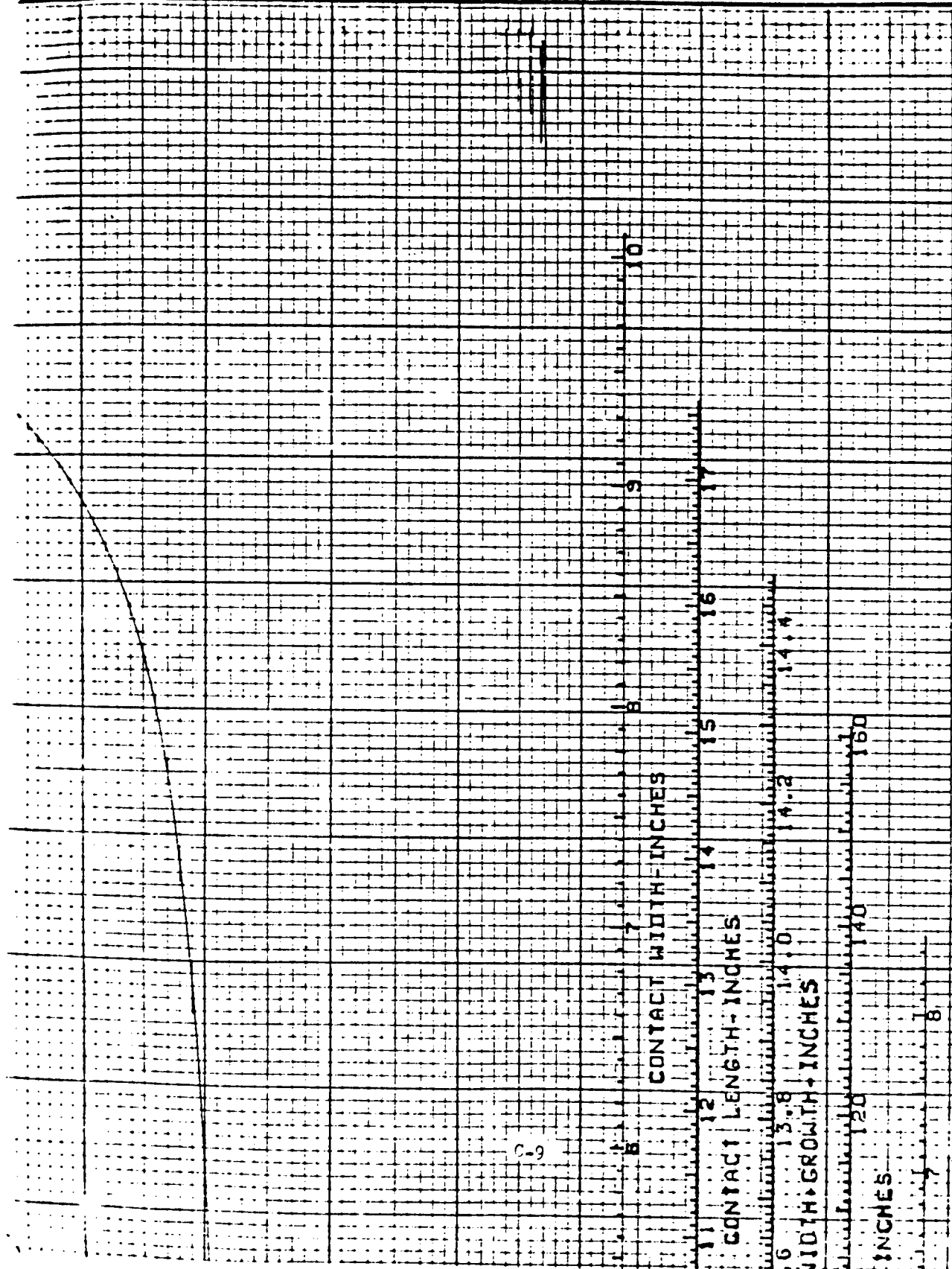
LAB DATA 3-17-84

20 PSI
25 PSI
30 PSI

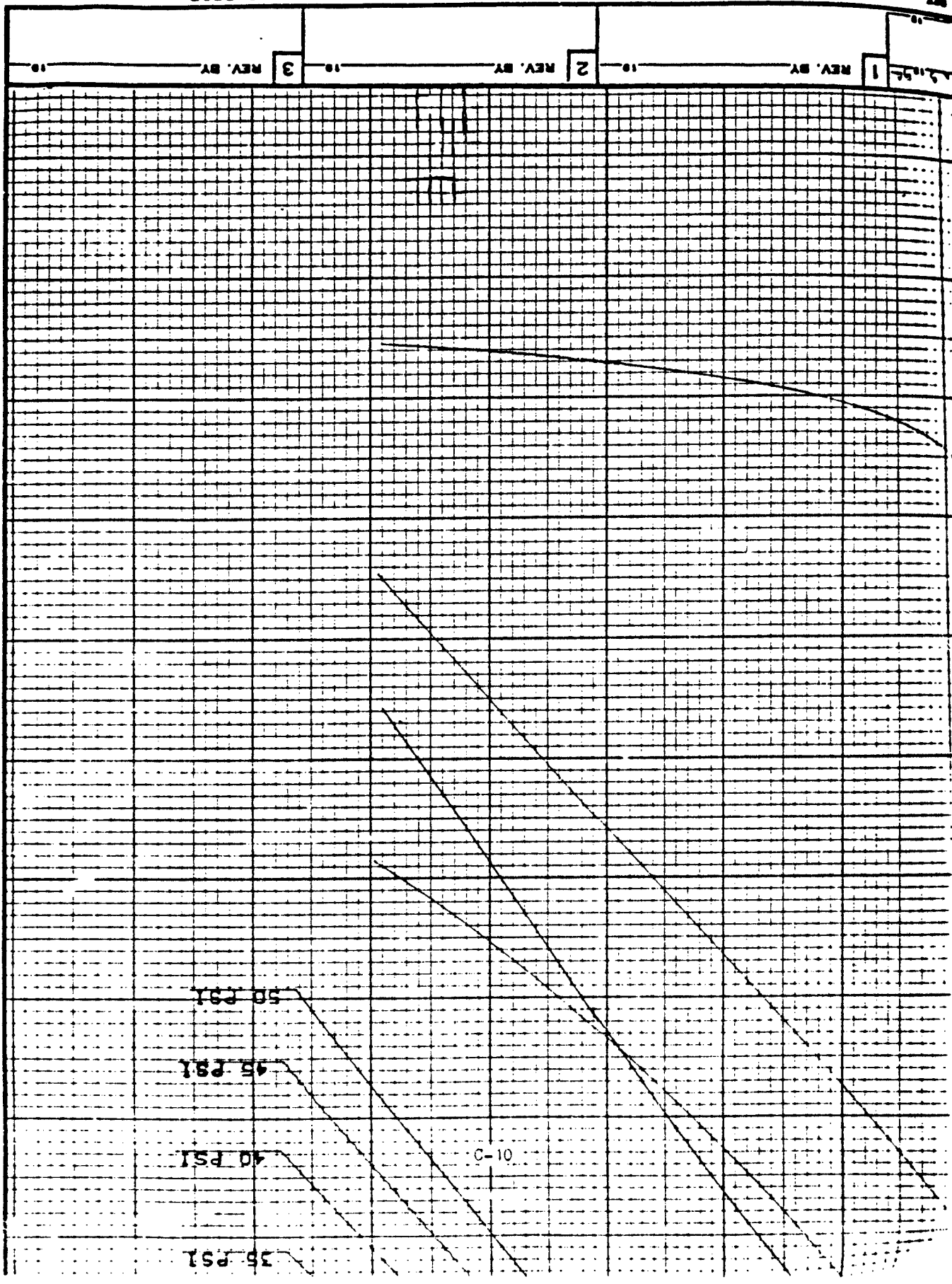




THE GOODYEAR TIRE & RUBBER COMPANY, AKRON, OHIO FILE 36X12-50-18.5 WRL PT 11 SELECTION CURVES	
SCALE DEPT. 4808	DRAWN BY DETHO JUN 4 1934 TRACED BY 19 APPRD BY



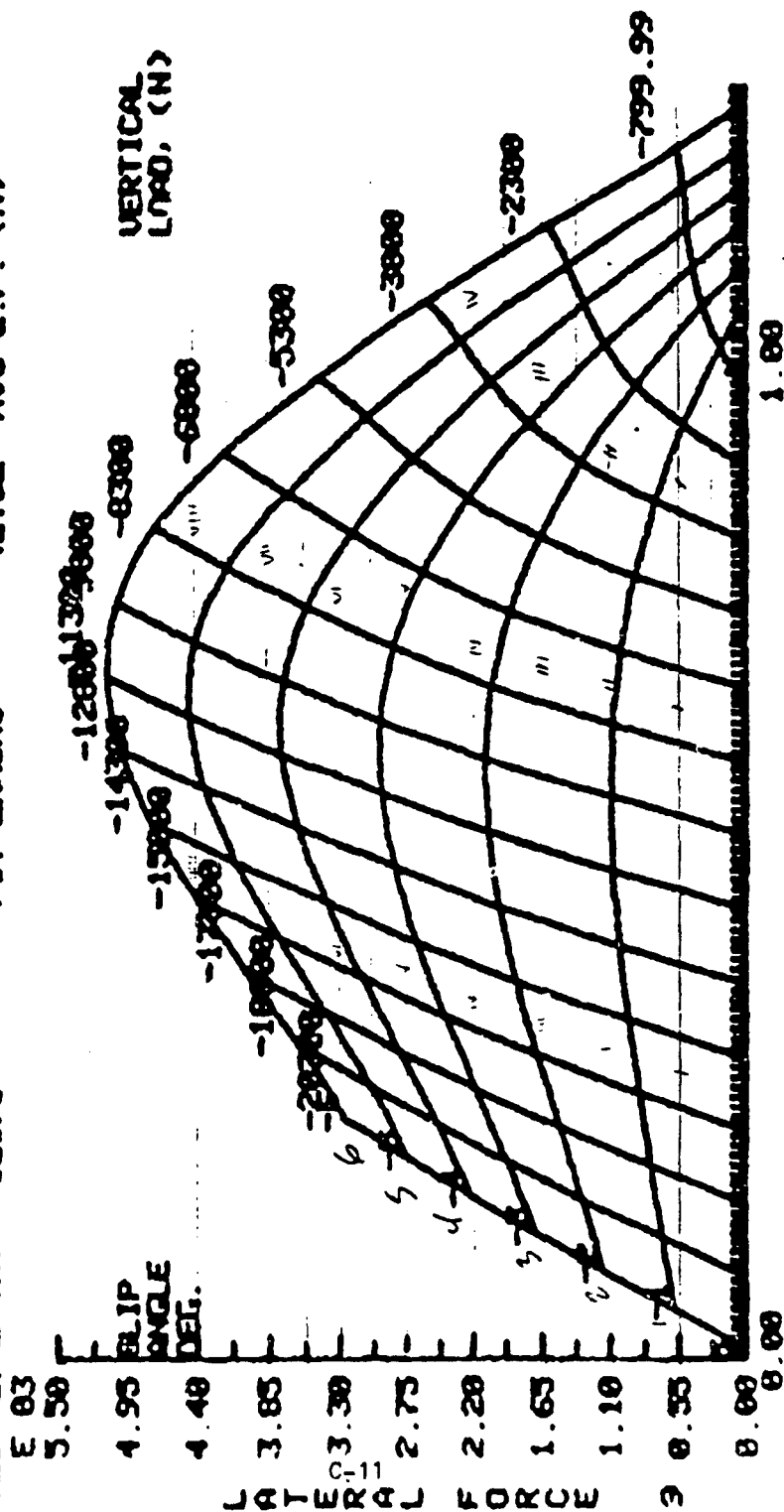
TOLERANCE ON FINISHED SURFACES
 ± 0.010 ON FRACTIONAL DIMENSIONS
 THE SUBJECT MATTER OF THIS DRAWING IS THE PROPERTY OF
 THE GOODYEAR TIRE AND RUBBER COMPANY OF AKRON, OHIO
 MD-319527



36X12.50-16.5LT WRANGLER R/T II - Bias Type

20 PSI

LATERAL FORCE VS SLIP ANGLE AND VERTICAL LOAD
 TEST DATA FILE# T9099 TEST DATE/TIME : 25-FEB-84/00:30
 TIRE SIZE : 36X12.5-16.5L MANUFACTURER : GTR
 INFLATION (KPA) : 138 RIM WIDTH (IN) : 8.25
 CONSTR. -DASH : 3C0163-7 AWB TEMP (C) : 26.2
 TEST NUMBER : 3C016T-L16A TIRE TYPE : WRANGLER R/T II
 MAX SLIP ANGLE : 6 ORIGINATOR (INIT) : LAWRENCE (REB)
 TEST LOAD (N) : 12673 FIT ERROR : 42.82 AUG L.F. (N)

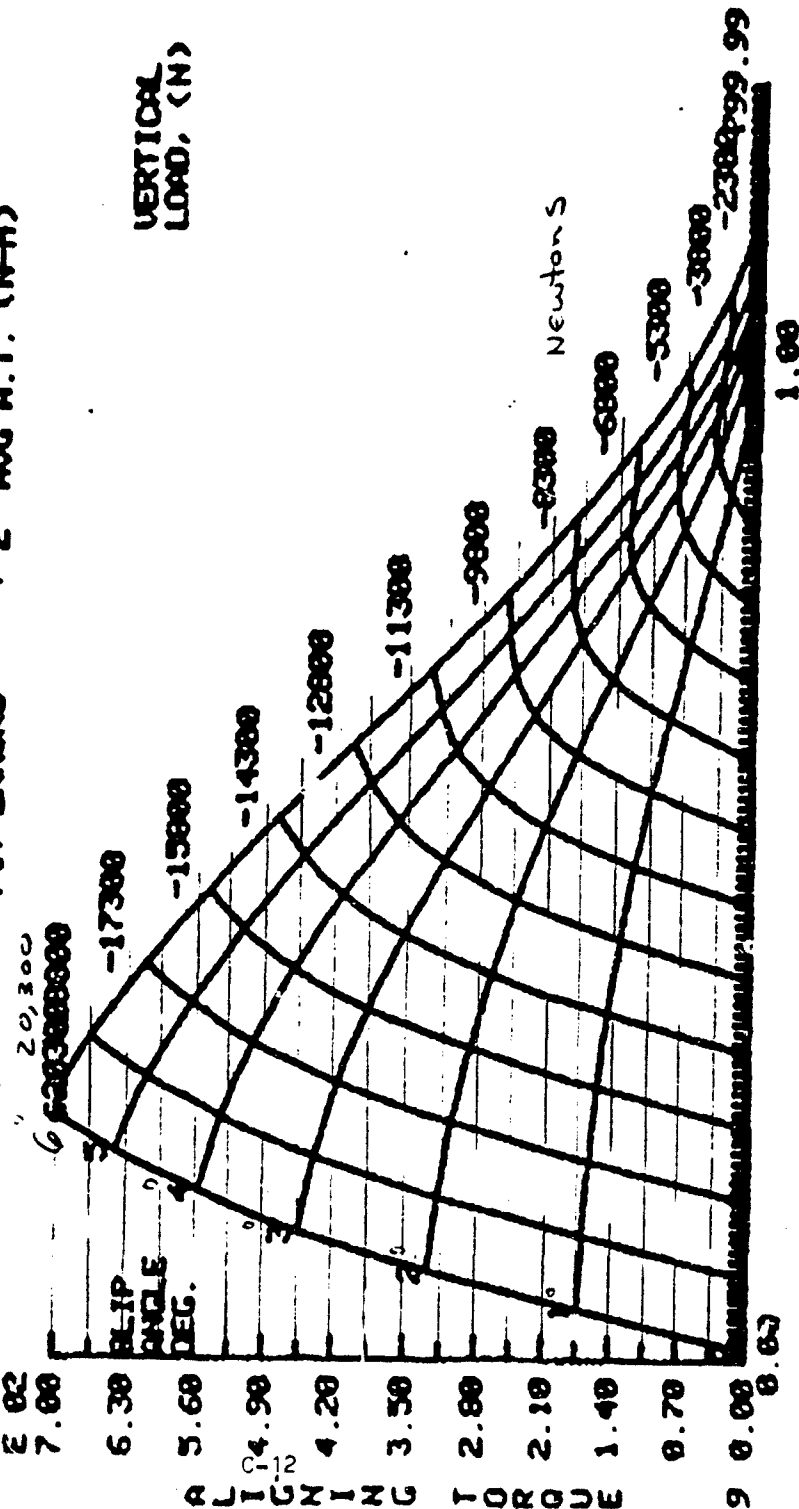


E 02

36X12.50-16.5LT WRANGLER R/T II - Bias Type

20 PSI

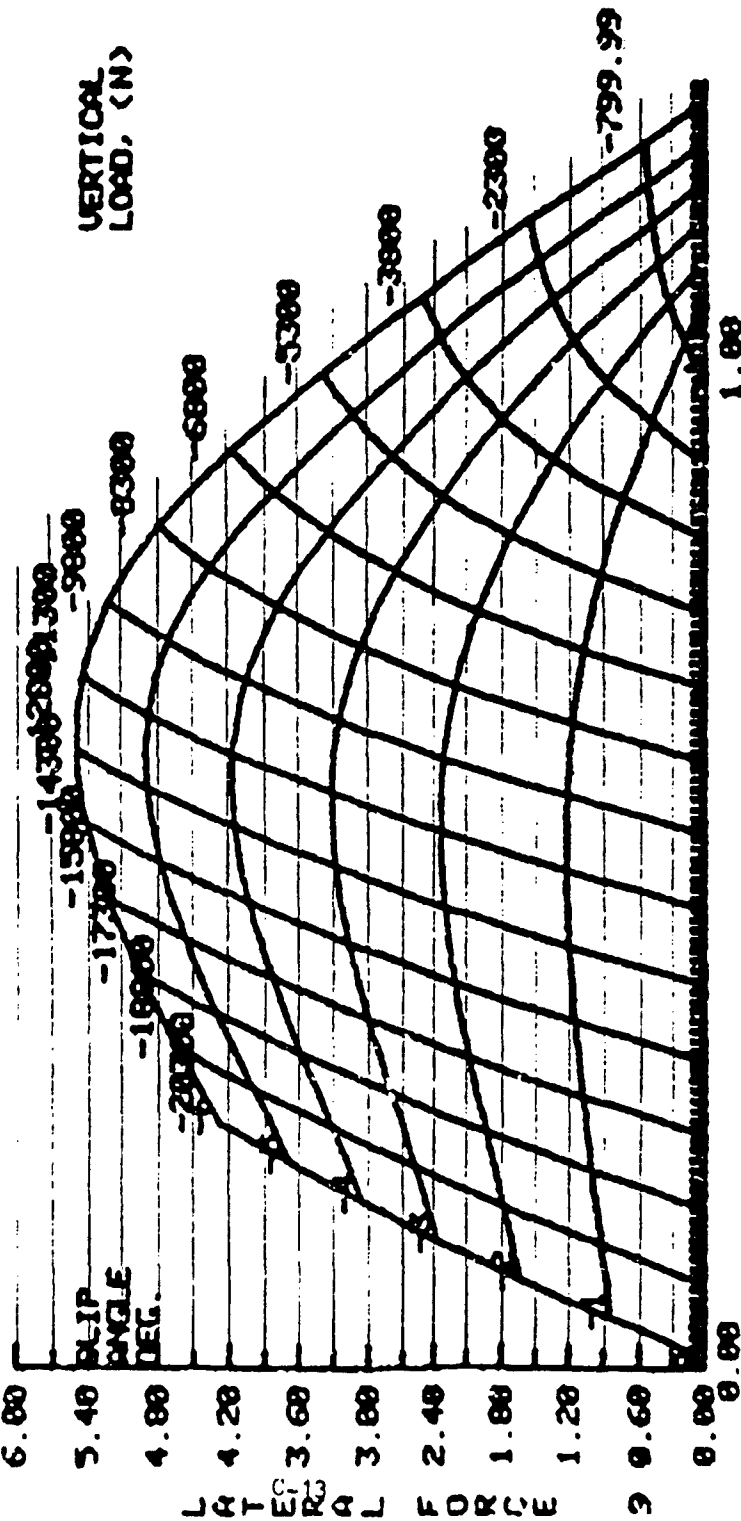
ALIGNING TORQUE US SLIP ANGLE AND VERTICAL LOAD
 TEST DATA FILE# T9099
 TIRE SIZE 36X12.5-16.5LT MANUFACTURER GTR
 INFLATION (KPA) 138 RIM WIDTH (IN) 8.25
 CONTR. -DASH 308163-7 AMB TEMP (C) 26.2
 TEST NUMBER 30816T-L16A TIRE TYPE WRANGLER R/T II
 MAX SLIP ANGLE .6 ORIGINATOR (INIT) LAWRENCE (REB)
 TEST LOAD (N) 12675 FIT ERRORS 2 AUG A.T. (N-M)



E 02

36 x 12.50 - 16.5LT WRANLER R/T II - Bias Type
22 PSI

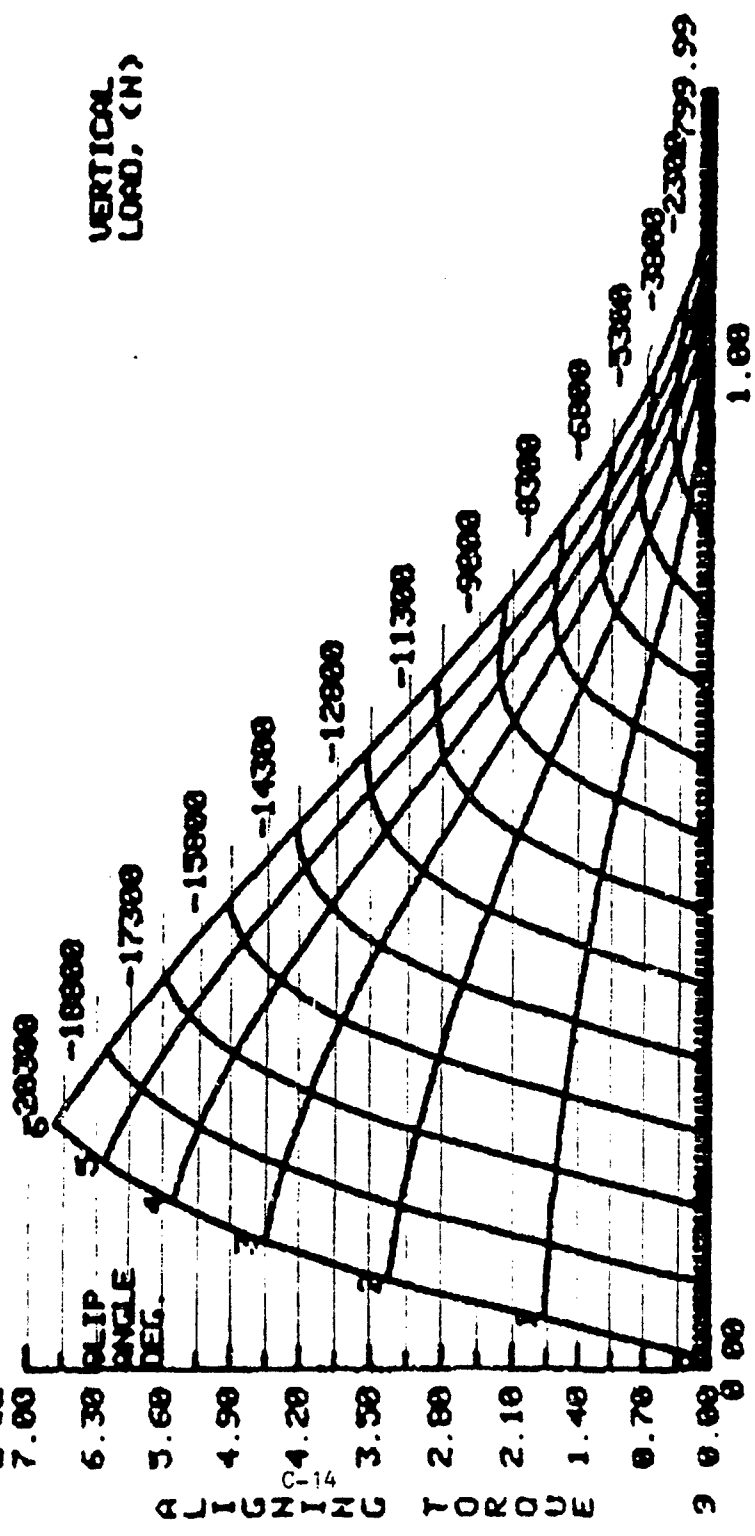
LATERAL FORCE VS SLIP ANGLE AND VERTICAL LOAD
TEST DATA FILE: 19898
TIRE SIZE: 36x12.50-16.5L
INFLATION (KPA): 152
CONST. - DASH: 308163-7
TEST NUMBER: 308167-L16A
MAX SLIP ANGLE: .6
TEST LOAD (N): 12675
E 83
TIRE DATE/TIME: 24-FEB-84/23.17
MANUFACTURER: GOYR
RIM WIDTH (IN): 8.25
AMB TEMP (C): 25.8
TIRE TYPE: WRANGLER R/T 2
ORIGINATOR (INIT): LAWRENCE (CH)
FIT ERRORS: 30.24 AUG L.F. (N)



E 82

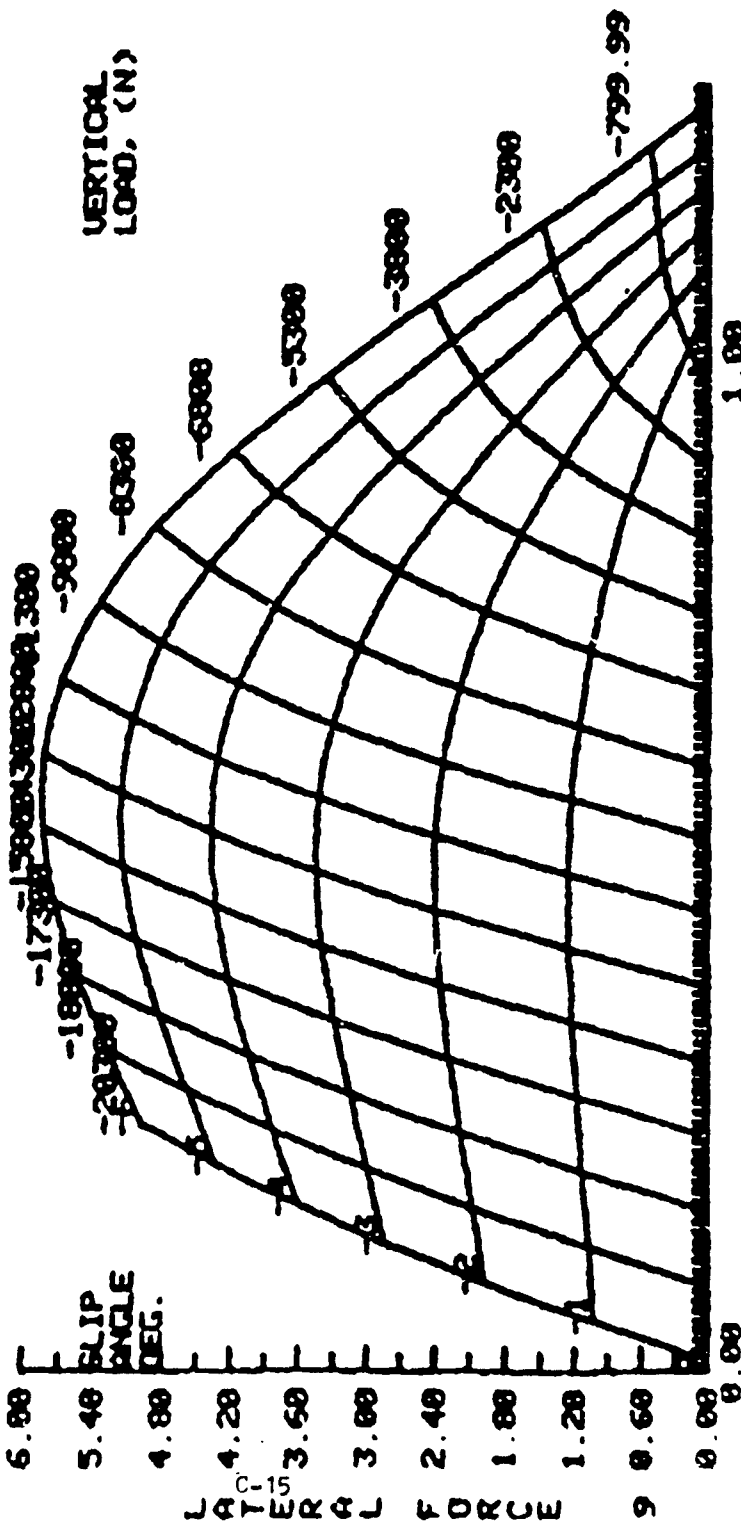
36 X 12.50-16.5LT WR VGLER R/T II Bias Type
 22 PSI

ALIGNING TORQUE VS SLIP ANGLE AND VERTICAL LOAD
 TEST DATA FILE: T9898 TEST DATE/TIME: 24-FEB-84/23:17
 TIRE SIZE: 36X12.50-16.5 MANUFACTURER: GOYR
 INFLATION (KPA): 152 RIM WIDTH (IN): 8.25
 CONSTR.: DASH 308165-7 AMB TEMP (C): 23.8
 TEST NUMBER: 30816T-L16A TIRE TYPE: WRANGLER R/T 2
 MAX SLIP ANGLE: 6 ORIGINAL (INIT): LAWRENCE (CH)
 TEST LOAD (N): 12675 FIT ERROR: 1.72 AUG A.T. (N-M)
 E 82



36X12.50 -16.5LT WRANGLER R/T II - Bias Type
25 PSI

LATERAL FORCE VS SLIP ANGLE AND VERTICAL LOAD
TEST DATA FILE# T9896 TEST DATE/TIME : 24-FEB-84/20:57
TIRE SIZE : 36X12.50-16.5 MANUFACTURER : COVR
INFLATION (KPA) : 172 RIM WIDTH (IN) : 8.25
CONSTR. - DASH : 308163-4 A/B TEMP (C) : 23.5
TEST NUMBER : 308167-L168 TIRE TYPE : WRANGLER R/T 2
MAX SLIP ANGLE : 6 ORIGINATOR (INIT) : LAWRENCE (CH)
TEST LOAD (N) : 12675 FIT ERRORS : 26.38 AUG L.F. (N)
E 83



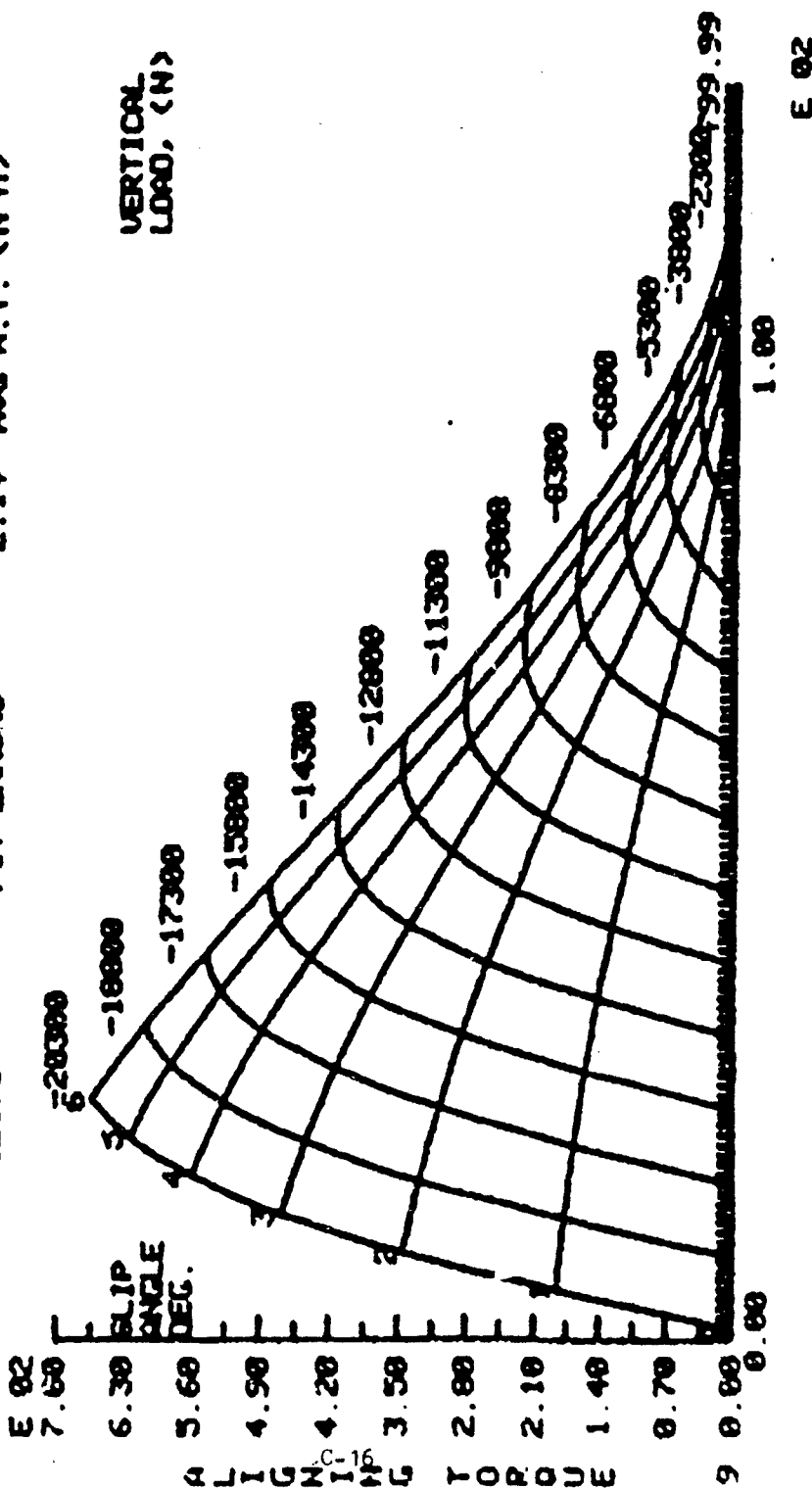
E 82

Copy available to DTIC does not
permit fully legible reproduction

36X12.50-16.5LT WRAN -ER R/T II -Bias Type
25 PSI

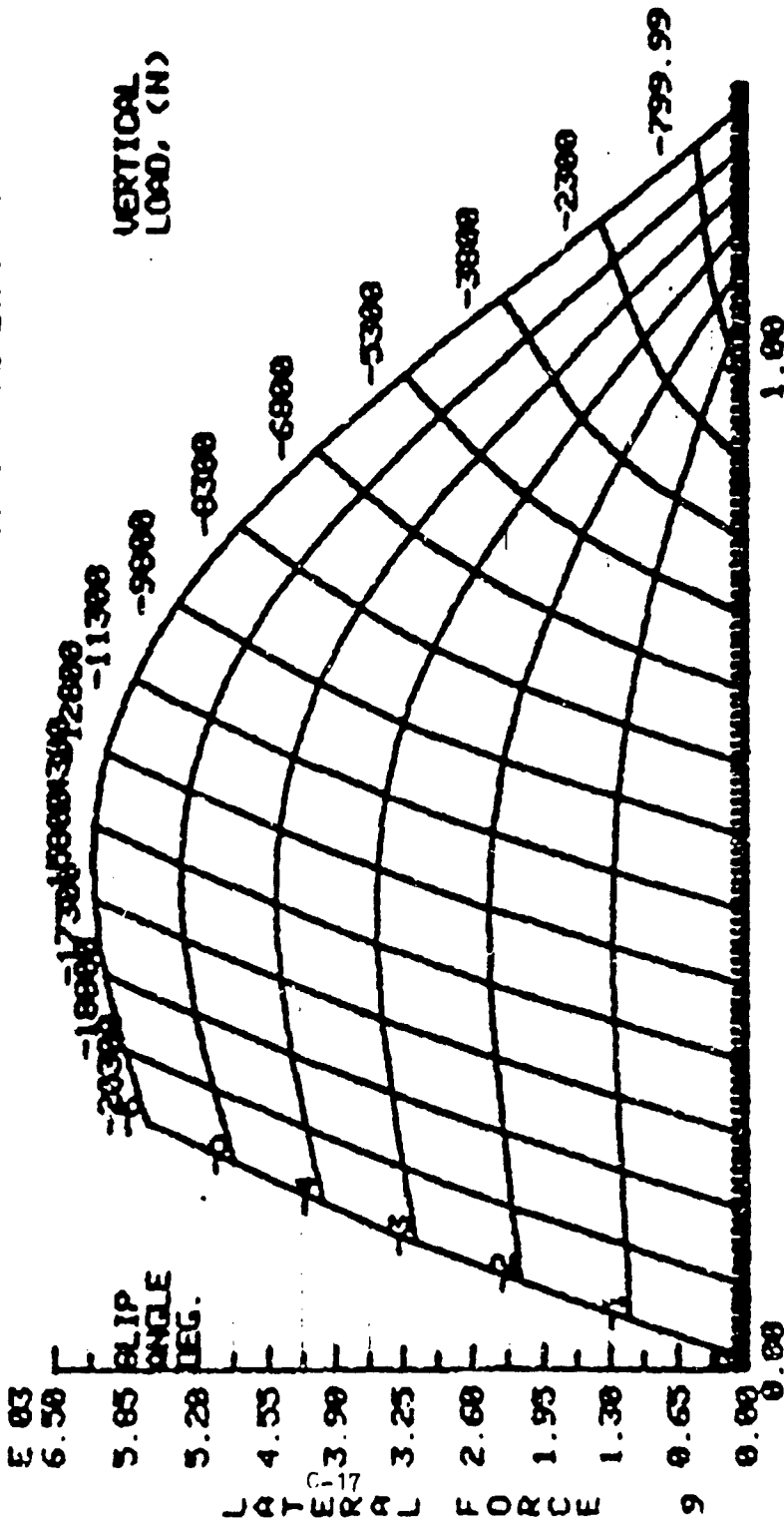
ALIGNING TORQUE VS SLIP ANGLE AND VERTICAL LOAD
TEST DATA FILE: 19896 TEST DATE/TIME: 24-FEB-84/20:57
TIRE SIZE: 36X12.50-16.5 MANUFACTURER: GOYR
INFLATION (KPA): 172 RIM WIDTH (IN): 8.25
CONSTR. -DASH: 308163-4 AMB TEMP (C): 23.5
TEST NUMBER: 30816T-L168 TIRE TYPE: WRANGLER R/T 2
MAX SLIP ANGLE: 16 ORIGINAL INIT.: LAURENCE (CH)
TEST LOAD (N): 12675 FIT ERRORS: 2.14 AUG A.T. (N-M)

Copy available to DTIC does not
permit fully legible reproduction



36 X 12.50 -16.5 LT WRA 3LER R/T II - Bins Type
28 PSI

LATERAL FORCE VS SLIP ANGLE AND VERTICAL LOAD
TEST DATA FILE: 19097 TEST DATE/TIME: 24-FEB-84/22:12
TIRE SIZE: 36X12.50-16.5 MANUFACTURER: GOYR
INFLATION (KPA): 193 RIM WIDTH (IN): 8.25
CONSTR.: DASH 3C0163-4 AIR TEMP (C): 24.4
TEST NUMBER: 3C016T-L168 TIRE TYPE: WRANGLER R/T 2
MAX SLIP ANGLE: 6 ORIGINATOR: LAURENCE <CH>
TEST LOAD (N): 12675 FIT ERRORS: 15.51 AVG L.F. (N)

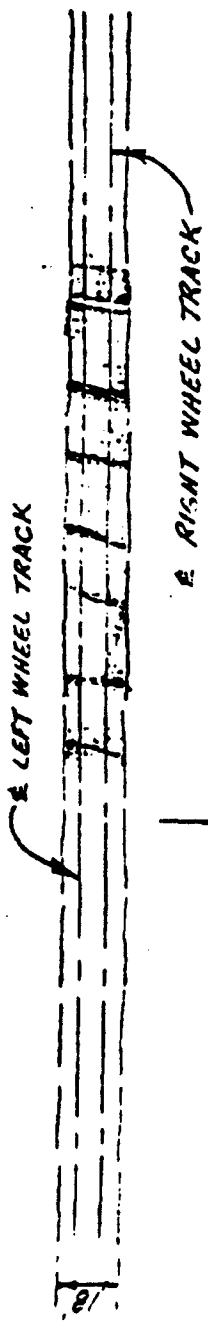


Copy available to DTIC does not
warrant fully legible reproduction

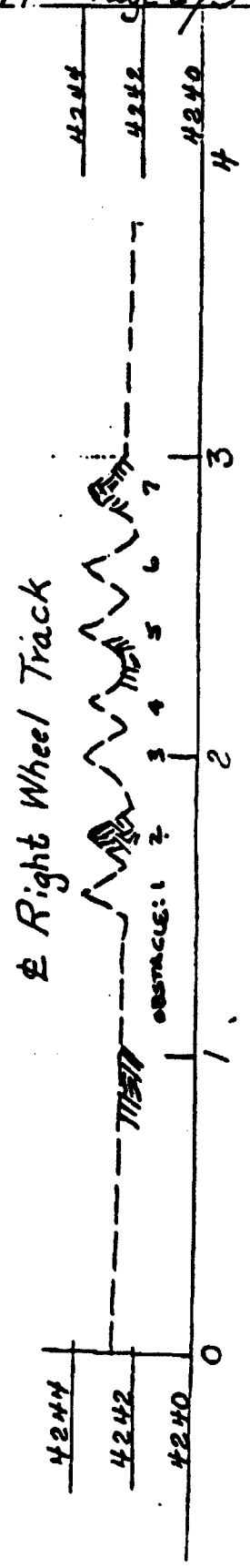
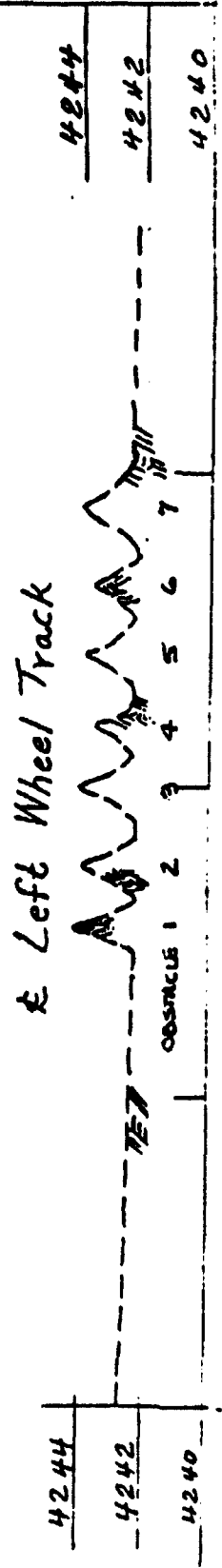
E 02

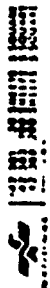
APPENDIX D
NATC TERRAIN DATA

13 12 11 10 9 8 7 6 5 4 3 2 1 0



PROFILE
HORIZ. = 1"=50'
VERT. = 1"=5'





LEFT WHEEL TRACK

2

OBSTACLE:

Sta. 1+38.97	El. 42+2.87
Sta. 1+45.58	El. 42+2.52
Sta. 1+49.06	El. 42+3.02
Sta. 1+53.10	El. 42+4.81
Sta. 1+56.67	El. 42+5.35
Sta. 1+63.05	El. 42+2.25
Sta. 1+67.07	El. 42+5.04
Sta. 1+73.37	El. 42+3.94
Sta. 1+76.82	El. 42+5.18
Sta. 1+82.35	El. 42+2.27

D-5

RIGHT WHEEL TRACK

2

OBSTACLE:

Sta. 1+58.58	El. 42+5.44
Sta. 1+65.38	El. 42+2.32
Sta. 1+69.45	El. 42+5.02
Sta. 1+72.94	El. 42+5.78
Sta. 1+76.69	El. 42+5.19
Sta. 1+82.80	El. 42+2.24
Sta. 1+88.21	El. 42+5.57
Sta. 1+92.48	El. 42+5.18
Sta. 1+98.00	El. 42+2.71

Horiz. Scale: 1"=5'
Vert. Scale: 1"=5'

APPENDIX E
DYNAMIC ANALYSIS VEHICLE INPUT DATA FILES

FILE: [AARDEMA.DADS3D.HMMWV.1037.HIGHCG.NATC]HMMWV_15MPH.VB3

CREATE HEADER

- *
1. This a model of the high C.G. HMMWV M1037 S-250 Shelter Carrier vehicle with bias tires.
 - *
 2. This model was used to determine the forces within the spherical Joints.
 - *
 3. The spherical Joint axis on the wheel are arranged such that the Z axis is along the King-Pin axis. If the forces are reported in the Joint coordinate system, then the forces acting on the wheel along the Joint Z axis would represent the tensile force in the spherical Joint. Likewise the forces acting on the wheel along the Joint X and Y axis are the shear forces in the spherical Joint.
 - *
 4. The spherical Joint axis on the arms are arranged to represent the mounting surface upon which the spherical Joint is bolted.
 - *
 5. By taking the dot product of the two Joint Z axis, the angular displacement of the spherical Joint can be calculated. This was done in the subroutine FRC15.FOR.
 - *
 6. See the user written subroutine USER_1SDA.FOR for the shock model. The subroutine will provide additional comments in more detail.
 - *
 7. A user written tire element data was written to calculate the tire forces. This was implemented in module 36 and is call TACOM-TIRE. See the source code for additional comments and methods used in implementing user force elements. The TACOM-TIRE module input data was design to be used with the preprocessor's tire data and supplemented with the data in the user input file. The user input file has a .INP extension. See the subroutines FRC36.FOR, TIREF.FOR, and USET.FOR for more detailed information.
 - *
 8. ***** IMPORTANT NOTE - PLEASE READ *****

If the preprocessor is used to create the tire force element, then the element name in the .FMS file must be changed from TIRE to TACOM-TIRE. This will then instruct the dads code to call the TACOM-TIRE model located in module number 36. If the name of the element name is not changed and remains TIRE, then the original CADSI tire model will be called. When changing the name, be careful to keep the original record format.
 - *
 9. The print interval is set to 1/60 second. This will allow greater accuracy when finding the maximum forces. If a larger time step was used the maximum force in a spike could be attenuated leading to a misrepresentation of the results. The animation can skip a frame and still maintain a 1/30 second time step per frame.
 - *
 10. The front tires are bias type at 20 psi
The rear tires are bias type at 30 psi -
Vertical force versus deflection curves for all tire are taken from the Goodgear Data. The lateral force versus slip angle curves was taken from the UMTRI data because the UMTRI data is valid upto 16 degrees of slip.
 - *

11. Assume the center of gravity of each wheel is at the wheel center. The angle of 0.247 degrees associated with each wheel represents the toe-in of the front wheels and the toe-out of the rear wheels. See the HMMWV Technical Manual TM 9-2320-280-20, sections 8-6 and 8-7.
*

ANALYSIS

CREATE SYSTEM.DATA

UNITS	:= 'ENG'
ANALYSIS.TYPE	:= 'DYNAMIC'
STARTING.TIME	:= '0.0'
ENDING.TIME	:= '12.0'
PRINT.INTERVAL	:= '0.016666666666666666'
GRAVITY.SEA.LEVEL	:= '386.400'
X.GRAVITY	:= '0.0'
Y.GRAVITY	:= '0.0'
Z.GRAVITY	:= '-1.0'
SCALE.GRAVITY.COEF	:= '1.0'
MATRIX.OPERATIONS	:= 'SPARSE'
REDUNDANCY.CHECK	:= 'TRUE'
LU.TOL	:= '1.0D-12'
ASSEMBLY.TOL	:= '1.0D-3'
BYPASS.ASSEMBLY	:= 'FALSE'
OUTPUT.FILE	:= 'BINARY'
REFERENCE.FRAME	:= 'GLOBAL'
DEBUG.FLAG	:= 'TRUE'

UP

CREATE DYNAMIC.DATA

REACTION.FORCES	:= 'TRUE'
FORCE.COORDINATES	:= 'JOINT'
PRINT.METHOD	:= 'INTERPOLATED'
MAX.INT.STEP	:= '0.05'
SOLUTION.TOL	:= '0.001'
INTEGRATION.TOL	:= '0.0001'

UP

UP

CONSTRAINTS

CREATE DISTANCE.CONSTRAINT

NAME	:= 'TIE-ROD.FL'
BODY.1.NAME	:= 'STEERING.LINK'
BODY.2.NAME	:= 'WHEEL.FL'
P.ON.BODY.1	:= (-17.655, -47.635, 32.905)
P.ON.BODY.2	:= (-32.327, -44.702, 30.127)
Q.ON.BODY.1	:= (-17.655, -47.635, 33.905)
Q.ON.BODY.2	:= (-32.327, -44.702, 31.127)
R.ON.BODY.1	:= (-16.655, -47.635, 32.905)
R.ON.BODY.2	:= (-31.327, -44.702, 30.127)
DISTANCE	:= '15.217994513076'
NODE.1	:= '0'
NODE.2	:= '0'

UP

CREATE DISTANCE.CONSTRAINT

E-4

NAME	:= 'TIE-ROD.FR'
BODY.1.NAME	:= 'STEERING.LINK'

BODY.2.NAME	:= 'WHEEL.FR'
P.ON.BODY.1	:= (17.655, -47.635, 32.905)
P.ON.BODY.2	:= (32.327, -44.702, 30.127)
Q.ON.BODY.1	:= (17.655, -47.635, 33.905)
Q.ON.BODY.2	:= (32.327, -44.702, 31.127)
R.ON.BODY.1	:= (18.655, -47.635, 32.905)
R.ON.BODY.2	:= (33.327, -44.702, 30.127)
DISTANCE	:= '15.217994513076'
NODE.1	:= '0'
NODE.2	:= '0'
UP	
CREATE DISTANCE.CONSTRAINT	
NAME	:= 'RAD-ROD.RL'
BODY.1.NAME	:= 'CHASSIS'
BODY.2.NAME	:= 'WHEEL.RL'
P.ON.BODY.1	:= (-16.380, -161.980, 33.080)
P.ON.BODY.2	:= (-32.327, -164.066, 30.405)
Q.ON.BODY.1	:= (-16.380, -161.980, 34.080)
Q.ON.BODY.2	:= (-32.327, -164.066, 31.405)
R.ON.BODY.1	:= (-15.380, -161.980, 33.080)
R.ON.BODY.2	:= (-31.327, -164.066, 30.405)
DISTANCE	:= '16.303798023773'
NODE.1	:= '0'
NODE.2	:= '0'
UP	
CREATE DISTANCE.CONSTRAINT	
NAME	:= 'RAD-ROD.RR'
BODY.1.NAME	:= 'CHASSIS'
BODY.2.NAME	:= 'WHEEL.RR'
P.ON.BODY.1	:= (16.380, -161.980, 33.080)
P.ON.BODY.2	:= (32.327, -164.066, 30.405)
Q.ON.BODY.1	:= (16.380, -161.980, 34.080)
Q.ON.BODY.2	:= (32.327, -164.066, 31.405)
R.ON.BODY.1	:= (17.380, -161.980, 33.080)
R.ON.BODY.2	:= (33.327, -164.066, 30.405)
DISTANCE	:= '16.303798023773'
NODE.1	:= '0'
NODE.2	:= '0'
UP	
UP	
FORCE	
CREATE TIRE	
NAME	:= 'TIRE.FL'
TIRE.BODY	:= 'WHEEL.FL'
CHASSIS.BODY	:= 'CHASSIS'
TYPE	:= 'BASIC'
P.ON.TIRE	:= (-35.815, -39.370, 29.735)
RADIUS	:= '18.150'
ROLLING.RESISTANCE	:= '0.0'
DAMPING.CONSTANT	:= '100.000'
VERTICAL.STIFF	:= '0.0'
LATERAL.STIFF	:= '0.0'
STEER.ANGLE	:= '0.0'
FRICITION.COEFF	:= '0.7'

CURVE.UTILITY	:= 'TIRE.COEF'
CURVE.VERTICAL	:= 'BIAS.TIRE.20PSI'
CURVE.TORQUE	:= 'NONE'
CURVE.STEER	:= 'TRAJECTORY'
ANGULAR.UNITS	:= 'DEGREES'
UP	
CREATE TIRE	
NAME	:= 'TIRE.FR'
TIRE.BODY	:= 'WHEEL.FR'
CHASSIS.BODY	:= 'CHASSIS'
TYPE	:= 'BASIC'
P.ON.TIRE	:= (35.815, -39.370, 29.735)
RADIUS	:= '18.150'
ROLLING.RESISTANCE	:= '0.0'
DAMPING.CONSTANT	:= '100.000'
VERTICAL.STIFF	:= '0.0'
LATERAL.STIFF	:= '0.0'
STEER.ANGLE	:= '0.0'
FRICTION.COEFF	:= '0.7'
CURVE.UTILITY	:= 'TIRE.COEF'
CURVE.VERTICAL	:= 'BIAS.TIRE.20PSI'
CURVE.TORQUE	:= 'NONE'
CURVE.STEER	:= 'NONE'
ANGULAR.UNITS	:= 'DEGREES'
UP	
CREATE TIRE	
NAME	:= 'TIRE.RL'
TIRE.BODY	:= 'WHEEL.RL'
CHASSIS.BODY	:= 'CHASSIS'
TYPE	:= 'BASIC'
P.ON.TIRE	:= (-35.815, -169.370, 29.735)
RADIUS	:= '18.150'
ROLLING.RESISTANCE	:= '0.0'
DAMPING.CONSTANT	:= '100.000'
VERTICAL.STIFF	:= '0.0'
LATERAL.STIFF	:= '0.0'
STEER.ANGLE	:= '0.0'
FRICTION.COEFF	:= '0.7'
CURVE.UTILITY	:= 'TIRE.COEF'
CURVE.VERTICAL	:= 'BIAS.TIRE.30PSI'
CURVE.TORQUE	:= 'NONE'
CURVE.STEER	:= 'NONE'
ANGULAR.UNITS	:= 'DEGREES'
UP	
CREATE TIRE	
NAME	:= 'TIRE.RR'
TIRE.BODY	:= 'WHEEL.RR'
CHASSIS.BODY	:= 'CHASSIS'
TYPE	:= 'BASIC'
P.ON.TIRE	:= (35.815, -169.370, 29.735)
RADIUS	:= '18.150'
ROLLING.RESISTANCE	:= '0.0'
DAMPING.CONSTANT	:= '100.000'
VERTICAL.STIFF	:= '0.0'

LATERAL STIFF	::= '0.0'
STEER.ANGLE	::= '0.0'
FRICTION.COEFF	::= '0.7'
CURVE.UTILITY	::= 'TIRE.COEFF'
CURVE.VERTICAL	::= 'BIAS.FIRE.30PSI'
CURVE.TORQUE	::= 'NONE'
CURVE.STEER	::= 'NONE'
ANGULAR.UNITS	::= 'DEGREES'
IF	
CREATE TSDA	
NAME	::= 'SPRING.FL'
BODY.1.NAME	::= 'CHASSIS'
BODY.2.NAME	::= 'ARM.LFL'
SPRING.CONSTANT	::= '954.000'
FREE.LENGTH.SPRING	::= '13.360'
DAMPING.COEFFICIENT	::= '0.0'
ACTUATOR.FORCE	::= '0.0'
P.ON.BODY.1	::= (-20.070, -33.685, 38.545)
P.ON.BODY.2	::= (-21.385, -33.953, 28.935)
Q.ON.BODY.1	::= (-20.070, -33.685, 39.545)
Q.ON.BODY.2	::= (-21.385, -33.953, 29.935)
R.ON.BODY.1	::= (-19.070, -33.685, 38.545)
R.ON.BODY.2	::= (-20.385, -33.953, 28.935)
CURVE.SPRING	::= 'NONE'
CURVE.DAMPER	::= 'NONE'
CURVE.ACTUATOR	::= 'NONE'
NODE.1	::= '0'
NODE.2	::= '0'
IF	
CREATE TSDA	
NAME	::= 'SPRING.FR'
BODY.1.NAME	::= 'CHASSIS'
BODY.2.NAME	::= 'ARM.LFR'
SPRING.CONSTANT	::= '954.000'
FREE.LENGTH.SPRING	::= '13.360'
DAMPING.COEFFICIENT	::= '0.0'
ACTUATOR.FORCE	::= '0.0'
P.ON.BODY.1	::= (20.070, -33.685, 38.545)
P.ON.BODY.2	::= (21.385, -33.953, 28.935)
Q.ON.BODY.1	::= (20.070, -33.685, 39.545)
Q.ON.BODY.2	::= (21.385, -33.953, 29.935)
R.ON.BODY.1	::= (21.070, -33.685, 38.545)
R.ON.BODY.2	::= (22.385, -33.953, 28.935)
CURVE.SPRING	::= 'NONE'
CURVE.DAMPER	::= 'NONE'
CURVE.ACTUATOR	::= 'NONE'
NODE.1	::= '0'
NODE.2	::= '0'
IF	
CREATE TSDA	
NAME	::= 'SPRING.RL'
BODY.1.NAME	::= 'CHASSIS'
BODY.2.NAME	::= 'ARM.LRL'
SPRING.CONSTANT	::= '2108.000'

FREE.LENGTH.SPRING	:= '15.030'
DAMPING.COEFFICIENT	:= '0.0'
ACTUATOR.FORCE	:= '0.0'
P.ON.BODY.1	:= (-19.747, -174.865, 40.868)
P.ON.BODY.2	:= (-21.385, -174.597, 28.935)
Q.ON.BODY.1	:= (-19.747, -174.865, 41.868)
Q.ON.BODY.2	:= (-21.385, -174.597, 29.935)
R.ON.BODY.1	:= (-18.747, -174.865, 40.868)
R.ON.BODY.2	:= (-20.385, -174.597, 28.935)
CURVE.SPRING	:= 'NONE'
CURVE.DAMPER	:= 'NONE'
CURVE.ACTUATOR	:= 'NONE'
NODE.1	:= '0'
NODE.2	:= '0'
UP	
CREATE TSDA	
NAME	:= 'SPRING.RR'
BODY.1.NAME	:= 'CHASSIS'
BODY.2.NAME	:= 'ARM.LRR'
SPRING.CONSTANT	:= '2108.00'
FREE.LENGTH.SPRING	:= '15.030'
DAMPING.COEFFICIENT	:= '0.0'
ACTUATOR.FORCE	:= '0.0'
P.ON.BODY.1	:= (19.747, -174.865, 40.868)
P.ON.BODY.2	:= (21.385, -174.597, 28.935)
Q.ON.BODY.1	:= (19.747, -174.865, 41.868)
Q.ON.BODY.2	:= (21.385, -174.597, 29.935)
R.ON.BODY.1	:= (20.747, -174.865, 40.868)
R.ON.BODY.2	:= (22.385, -174.597, 28.935)
CURVE.SPRING	:= 'NONE'
CURVE.DAMPER	:= 'NONE'
CURVE.ACTUATOR	:= 'NONE'
NODE.1	:= '0'
NODE.2	:= '0'
UP	
CREATE TSDA	
NAME	:= 'SHOCK.FL'
BODY.1.NAME	:= 'CHASSIS'
BODY.2.NAME	:= 'ARM.LFL'
SPRING.CONSTANT	:= '0.0'
FREE.LENGTH.SPRING	:= '0.0'
DAMPING.COEFFICIENT	:= '0.0'
ACTUATOR.FORCE	:= '0.0'
P.ON.BODY.1	:= (-19.598, -33.685, 43.492)
P.ON.BODY.2	:= (-21.415, -33.953, 29.259)
Q.ON.BODY.1	:= (-19.598, -33.685, 44.492)
Q.ON.BODY.2	:= (-21.415, -33.953, 30.259)
R.ON.BODY.1	:= (-18.598, -33.685, 43.492)
R.ON.BODY.2	:= (-20.415, -33.953, 29.259)
CURVE.SPRING	:= 'NONE'
CURVE.DAMPER	:= 'NONE'
CURVE.ACTUATOR	:= 'NONE'
NODE.1	:= '0'
NODE.2	:= '0'

UP

CREATE TSDA

NAME	:= 'SHOCK.FR'
BODY.1.NAME	:= 'CHASSIS'
BODY.2.NAME	:= 'ARM.LFR'
SPRING.CONSTANT	:= '0.0'
FREE.LENGTH.SPRING	:= '0.0'
DAMPING.COEFFICIENT	:= '0.0'
ACTUATOR.FORCE	:= '0.0'
P.ON.BODY.1	:= (19.598, -33.685, 43.492)
P.ON.BODY.2	:= (21.415, -33.953, 29.259)
Q.ON.BODY.1	:= (19.598, -33.685, 44.492)
Q.ON.BODY.2	:= (21.415, -33.953, 30.259)
R.ON.BODY.1	:= (20.598, -33.685, 43.492)
R.ON.BODY.2	:= (22.415, -33.953, 29.259)
CURVE.SPRING	:= 'NONE'
CURVE.DAMPER	:= 'NONE'
CURVE.ACTUATOR	:= 'NONE'
NODE.1	:= '0'
NODE.2	:= '0'

UP

CREATE TSDA

NAME	:= 'SHOCK.RL'
BODY.1.NAME	:= 'CHASSIS'
BODY.2.NAME	:= 'ARM.LRL'
SPRING.CONSTANT	:= '0.0'
FREE.LENGTH.SPRING	:= '0.0'
DAMPING.COEFFICIENT	:= '0.0'
ACTUATOR.FORCE	:= '0.0'
P.ON.BODY.1	:= (-19.598, -174.865, 43.492)
P.ON.BODY.2	:= (-21.415, -174.597, 29.259)
Q.ON.BODY.1	:= (-19.598, -174.865, 44.492)
Q.ON.BODY.2	:= (-21.415, -174.597, 30.259)
R.ON.BODY.1	:= (-18.598, -174.865, 43.492)
R.ON.BODY.2	:= (-20.415, -174.597, 29.259)
CURVE.SPRING	:= 'NONE'
CURVE.DAMPER	:= 'NONE'
CURVE.ACTUATOR	:= 'NONE'
NODE.1	:= '0'
NODE.2	:= '0'

UP

CREATE TSDA

NAME	:= 'SHOCK.RR'
BODY.1.NAME	:= 'CHASSIS'
BODY.2.NAME	:= 'ARM.LRR'
SPRING.CONSTANT	:= '0.0'
FREE.LENGTH.SPRING	:= '0.0'
DAMPING.COEFFICIENT	:= '0.0'
ACTUATOR.FORCE	:= '0.0'
P.ON.BODY.1	:= (19.598, -174.865, 43.492)
P.ON.BODY.2	:= (21.415, -174.597, 29.259)
Q.ON.BODY.1	:= (19.598, -174.865, 44.492)
Q.ON.BODY.2	:= (21.415, -174.597, 30.259)
R.ON.BODY.1	:= (20.598, -174.865, 43.492)

```

R.ON.BODY.2           := ( 22.415, -174.597, 29.259 )
CURVE.SPRING          := 'NONE'
CURVE.DAMPER          := 'NONE'
CURVE.ACTUATOR        := 'NONE'
NODE.1                := '0'
NODE.2                := '0'

UP
UP
JOINTS
CREATE REVOLUTE.JOINT
NAME                  := 'REV.LFL'
BODY.1.NAME           := 'CHASSIS'
BODY.2.NAME           := 'ARM.LFL'
P.ON.BODY.1           := ( -12.09, -37.78, 30.770 )
P.ON.BODY.2           := ( -12.09, -37.78, 30.770 )
Q.ON.BODY.1           := ( -12.09, -36.78, 30.770 )
Q.ON.BODY.2           := ( -12.09, -36.78, 30.770 )
R.ON.BODY.1           := ( -11.09, -37.78, 30.770 )
R.ON.BODY.2           := ( -11.09, -37.78, 30.770 )
NODE.1                := '0'
NODE.2                := '0'

UP
CREATE REVOLUTE.JOINT
NAME                  := 'REV.LFR'
BODY.1.NAME           := 'CHASSIS'
BODY.2.NAME           := 'ARM.LFR'
P.ON.BODY.1           := ( 12.09, -37.78, 30.770 )
P.ON.BODY.2           := ( 12.09, -37.78, 30.770 )
Q.ON.BODY.1           := ( 12.09, -36.78, 30.770 )
Q.ON.BODY.2           := ( 12.09, -36.78, 30.770 )
R.ON.BODY.1           := ( 13.09, -37.78, 30.770 )
R.ON.BODY.2           := ( 13.09, -37.78, 30.770 )
NODE.1                := '0'
NODE.2                := '0'

UP
CREATE REVOLUTE.JOINT
NAME                  := 'REV.LRL'
BODY.1.NAME           := 'CHASSIS'
BODY.2.NAME           := 'ARM.LRL'
P.ON.BODY.1           := ( -12.09, -170.77, 30.770 )
P.ON.BODY.2           := ( -12.09, -170.77, 30.770 )
Q.ON.BODY.1           := ( -12.09, -169.77, 30.770 )
Q.ON.BODY.2           := ( -12.09, -169.77, 30.770 )
R.ON.BODY.1           := ( -11.09, -170.77, 30.770 )
R.ON.BODY.2           := ( -11.09, -170.77, 30.770 )
NODE.1                := '0'
NODE.2                := '0'

UP
CREATE REVOLUTE.JOINT
NAME                  := 'REV.LRR'
BODY.1.NAME           := 'CHASSIS'
BODY.2.NAME           := 'ARM.LRR'
P.ON.BODY.1           := ( 12.09, -170.77, 30.770 )
ON.BODY.2             := ( 12.09, -170.77, 30.770 )

```


Q.ON.BODY.1	:= (12.09, -169.77, 30.770)
Q.ON.BODY.2	:= (12.09, -169.77, 30.770)
R.ON.BODY.1	:= (13.09, -170.77, 30.770)
R.ON.BODY.2	:= (13.09, -170.77, 30.770)
NODE.1	:= '0'
NODE.2	:= '0'
UP	
CREATE REVOLUTE.JOINT	
NAME	:= 'REV.UFL'
BODY.1.NAME	:= 'CHASSIS'
BODY.2.NAME	:= 'ARM.UFL'
P.ON.BODY.1	:= (-18.183, -44.003, 39.435)
P.ON.BODY.2	:= (-18.183, -44.003, 39.435)
Q.ON.BODY.1	:= (-17.558, -39.670, 40.400)
Q.ON.BODY.2	:= (-17.558, -39.670, 40.400)
R.ON.BODY.1	:= (-17.193, -44.146, 39.435)
R.ON.BODY.2	:= (-17.193, -44.146, 39.435)
NODE.1	:= '0'
NODE.2	:= '0'
UP	
CREATE REVOLUTE.JOINT	
NAME	:= 'REV.UFR'
BODY.1.NAME	:= 'CHASSIS'
BODY.2.NAME	:= 'ARM.UFR'
P.ON.BODY.1	:= (18.183, -44.003, 39.435)
P.ON.BODY.2	:= (18.183, -44.003, 39.435)
Q.ON.BODY.1	:= (17.558, -39.670, 40.400)
Q.ON.BODY.2	:= (17.558, -39.670, 40.400)
R.ON.BODY.1	:= (19.173, -43.860, 39.435)
R.ON.BODY.2	:= (19.173, -43.860, 39.435)
NODE.1	:= '0'
NODE.2	:= '0'
UP	
CREATE REVOLUTE.JOINT	
NAME	:= 'REV.URL'
BODY.1.NAME	:= 'CHASSIS'
BODY.2.NAME	:= 'ARM.URL'
P.ON.BODY.1	:= (-18.195, -162.380, 39.655)
P.ON.BODY.2	:= (-18.195, -162.380, 39.655)
Q.ON.BODY.1	:= (-18.195, -161.380, 39.655)
Q.ON.BODY.2	:= (-18.195, -161.380, 39.655)
R.ON.BODY.1	:= (-17.195, -162.380, 39.655)
R.ON.BODY.2	:= (-17.195, -162.380, 39.655)
NODE.1	:= '0'
NODE.2	:= '0'
UP	
CREATE REVOLUTE.JOINT	
NAME	:= 'REV.UKR'
BODY.1.NAME	:= 'CHASSIS'
BODY.2.NAME	:= 'ARM.UKR'
P.ON.BODY.1	:= (18.195, -162.380, 39.655)
P.ON.BODY.2	:= (18.195, -162.380, 39.655)
Q.ON.BODY.1	:= (18.195, -161.380, 39.655)
Q.ON.BODY.2	:= (18.195, -161.380, 39.655)

R.ON.BODY.1	:= (19.195, -162.380, 39.655)
R.ON.BODY.2	:= (19.195, -162.380, 39.655)
NODE.1	:= '0'
NODE.2	:= '0'
UP	
CREATE REVOLUTE.JOINT	
NAME	:= 'PITMAN.REV'
BODY.1.NAME	:= 'CHASSIS'
BODY.2.NAME	:= 'PITMAN.ARM'
P.ON.BODY.1	:= (-9.811, -55.355, 34.039)
P.ON.BODY.2	:= (-9.811, -55.355, 34.039)
Q.ON.BODY.1	:= (-9.811, -55.038, 34.987)
Q.ON.BODY.2	:= (-9.811, -55.038, 34.987)
R.ON.BODY.1	:= (-8.811, -55.355, 34.039)
R.ON.BODY.2	:= (-8.811, -55.355, 34.039)
NODE.1	:= '0'
NODE.2	:= '0'
UP	
CREATE REV-SPHR.JOINT	
NAME	:= 'IDLER.ARM'
REV.BODY.1.NAME	:= 'CHASSIS'
SPHR.BODY.2.NAME	:= 'STEERING.LINK'
P.ON.BODY.1	:= (12.803, -55.355, 34.039)
P.ON.BODY.2	:= (12.803, -50.556, 32.433)
Q.ON.BODY.1	:= (12.803, -55.038, 34.987)
Q.ON.BODY.2	:= (12.803, -50.239, 33.381)
R.ON.BODY.1	:= (13.803, -55.355, 34.039)
R.ON.BODY.2	:= (13.803, -50.556, 32.433)
DISTANCE	:= '5.06'
UP	
CREATE SPHERICAL.JOINT	
NAME	:= 'SPH.LFL'
BODY.1.NAME	:= 'ARM.LFL'
BODY.2.NAME	:= 'WHEEL.FL'
P.ON.BODY.1	:= (-30.965, -39.180, 26.120)
P.ON.BODY.2	:= (-30.965, -39.180, 26.120)
Q.ON.BODY.1	:= (-30.757, -39.232, 27.097)
Q.ON.BODY.2	:= (-28.170, -39.868, 39.254)
R.ON.BODY.1	:= (-31.943, -39.180, 26.328)
R.ON.BODY.2	:= (-44.099, -39.180, 28.915)
NODE.1	:= '0'
NODE.2	:= '0'
UP	
CREATE SPHERICAL.JOINT	
NAME	:= 'SPH.LFR'
BODY.1.NAME	:= 'ARM.LFR'
BODY.2.NAME	:= 'WHEEL.FR'
P.ON.BODY.1	:= (30.965, -39.180, 26.120)
P.ON.BODY.2	:= (30.965, -39.180, 26.120)
Q.ON.BODY.1	:= (30.757, -39.232, 27.097)
Q.ON.BODY.2	:= (28.170, -39.868, 39.254)
R.ON.BODY.1	:= (31.943, -39.180, 26.328)
R.ON.BODY.2	:= (44.099, -39.180, 28.915)
NODE.1	:= '0'

NODE.2
 UP
 CREATE SPHERICAL.JOINT
 NAME
 BODY.1.NAME
 BODY.2.NAME
 P.ON.BODY.1
 P.ON.BODY.2
 Q.ON.BODY.1
 Q.ON.BODY.2
 R.ON.BODY.1
 R.ON.BODY.2
 NODE.1
 NODE.2

:= '0'
 := 'SPH.LRL'
 := 'ARM.LRL'
 := 'WHEEL.RL'
 := (-30.965, -169.370, 26.120)
 := (-30.965, -169.370, 26.120)
 := (-30.757, -169.422, 27.097)
 := (-28.170, -169.370, 39.270)
 := (-31.943, -169.370, 26.328)
 := (-44.115, -169.370, 28.915)
 := '0'
 := '0'

UP
 CREATE SPHERICAL.JOINT
 NAME
 BODY.1.NAME
 BODY.2.NAME
 P.ON.BODY.1
 P.ON.BODY.2
 Q.ON.BODY.1
 Q.ON.BODY.2
 R.ON.BODY.1
 R.ON.BODY.2
 NODE.1
 NODE.2

:= 'SPH.LRR'
 := 'ARM.LRR'
 := 'WHEEL.RR'
 := (30.965, -169.370, 26.120)
 := (30.965, -169.370, 26.120)
 := (30.757, -169.422, 27.097)
 := (28.170, -169.370, 39.270)
 := (31.943, -169.370, 26.328)
 := (44.115, -169.370, 28.915)
 := '0'
 := '0'

UP
 CREATE SPHERICAL.JOINT
 NAME
 BODY.1.NAME
 BODY.2.NAME
 P.ON.BODY.1
 P.ON.BODY.2
 Q.ON.BODY.1
 Q.ON.BODY.2
 R.ON.BODY.1
 R.ON.BODY.2
 NODE.1
 NODE.2

:= 'SPH.UFL'
 := 'ARM.UFL'
 := 'WHEEL.FL'
 := (-28.170, -39.868, 39.254)
 := (-28.170, -39.868, 39.254)
 := (-27.962, -39.920, 40.231)
 := (-25.375, -40.556, 52.388)
 := (-29.148, -39.868, 39.462)
 := (-41.304, -39.868, 42.049)
 := '0'
 := '0'

UP
 CREATE SPHERICAL.JOINT
 NAME
 BODY.1.NAME
 BODY.2.NAME
 P.ON.BODY.1
 P.ON.BODY.2
 Q.ON.BODY.1
 Q.ON.BODY.2
 R.ON.BODY.1
 R.ON.BODY.2
 NODE.1
 NODE.2

:= 'SPH.UFR'
 := 'ARM.UFR'
 := 'WHEEL.FR'
 := (28.170, -39.868, 39.254)
 := (28.170, -39.868, 39.254)
 := (27.962, -39.920, 40.231)
 := (25.375, -40.556, 52.388)
 := (29.148, -39.868, 39.462)
 := (41.304, -39.868, 42.049)
 := '0'
 := '0'

UP

CREATE SPHERICAL.JOINT

NAME	:= 'SPH.URL'
BODY.1.NAME	:= 'ARM.URL'
BODY.2.NAME	:= 'WHEEL.RL'
P.ON.BODY.1	:= (-28.170, -169.370, 39.270)
P.ON.BODY.2	:= (-28.170, -169.370, 39.270)
Q.ON.BODY.1	:= (-25.375, -169.370, 52.420)
Q.ON.BODY.2	:= (-25.375, -169.370, 52.420)
R.ON.BODY.1	:= (-41.320, -169.370, 42.065)
R.ON.BODY.2	:= (-41.320, -169.370, 42.065)
NODE.1	:= '0'
NODE.2	:= '0'

UP

CREATE SPHERICAL.JOINT

NAME	:= 'SPH.URR'
BODY.1.NAME	:= 'ARM.URR'
BODY.2.NAME	:= 'WHEEL.RR'
P.ON.BODY.1	:= (28.170, -169.370, 39.270)
P.ON.BODY.2	:= (28.170, -169.370, 39.270)
Q.ON.BODY.1	:= (25.375, -169.370, 52.420)
Q.ON.BODY.2	:= (25.375, -169.370, 52.420)
R.ON.BODY.1	:= (41.320, -169.370, 42.065)
R.ON.BODY.2	:= (41.320, -169.370, 42.065)
NODE.1	:= '0'
NODE.2	:= '0'

UP

CREATE UNIVERSAL.JOINT

NAME	:= 'PITMAN.UNIV'
BODY.1.NAME	:= 'PITMAN.ARM'
BODY.2.NAME	:= 'STEERING.LINK'
P.ON.BODY.1	:= (-9.811, -50.556, 32.433)
P.ON.BODY.2	:= (-9.811, -50.556, 32.433)
Q.ON.BODY.1	:= (-9.811, -50.239, 33.381)
Q.ON.BODY.2	:= (-9.811, -49.608, 32.116)
R.ON.BODY.1	:= (-8.811, -50.556, 32.433)
R.ON.BODY.2	:= (-8.811, -50.556, 32.433)
NODE.1	:= '0'
NODE.2	:= '0'

UP

UP

CREATE BODY

NAME	:= 'CHASSIS'
CENTER.OF.GRAVITY	:= (0.585, -123.170, 63.064)
TYPE.ANGULAR.COORD	:= 'BRYANT'
ANGLE.1	:= '0.0'
ANGLE.2	:= '0.0'
ANGLE.3	:= '0.0'
FIXED.TO.GROUND	:= 'FALSE'
MASS	:= '20.049'
INERTIA.XXL	:= '52680.0'
INERTIA.YYL	:= '13320.0'
INERTIA.ZZL	:= '56280.0'
INERTIA.XYL	:= '0.0'
INERTIA.XZL	:= '0.0'

INERTIA.YZL	:	'0.0'
XG.FORCE	:	'0.0'
YG.FORCE	:	'0.0'
ZG.FORCE	:	'0.0'
XL.TORQUE	:	'0.0'
YL.TORQUE	:	'0.0'
ZL.TORQUE	:	'0.0'
CURVE.XGF	:	'NONE'
CURVE.YGF	:	'NONE'
CURVE.ZGF	:	'NONE'
CURVE.XLT	:	'NONE'
CURVE.YLT	:	'NONE'
CURVE.ZLT	:	'NONE'
SIGN.E0	:	'POSITIVE'
ANGULAR.UNITS	:	'DEGREES'
FLEXIBLE	:	'FALSE'
SUPERELEMENT	:	'FALSE'
UP		
CREATE BODY		
NAME	:	'ARM.LFL'
CENTER.OF.GRAVITY	:	(-21.5275, -37.78, 28.445)
TYPE.ANGULAR.COORD	:	'BRYANT'
ANGLE.1	:	'0.0'
ANGLE.2	:	'-13.84'
ANGLE.3	:	'0.0'
FIXED.TO.GROUND	:	'FALSE'
MASS	:	'0.0932'
INERTIA.XXL	:	'1.0'
INERTIA.YYL	:	'1.0'
INERTIA.ZZL	:	'1.0'
INERTIA.XYL	:	'0.0'
INERTIA.XZL	:	'0.0'
INERTIA.YZL	:	'0.0'
XG.FORCE	:	'0.0'
YG.FORCE	:	'0.0'
ZG.FORCE	:	'0.0'
XL.TORQUE	:	'0.0'
YL.TORQUE	:	'0.0'
ZL.TORQUE	:	'0.0'
CURVE.XGF	:	'NONE'
CURVE.YGF	:	'NONE'
CURVE.ZGF	:	'NONE'
CURVE.XLT	:	'NONE'
CURVE.YLT	:	'NONE'
CURVE.ZLT	:	'NONE'
SIGN.E0	:	'POSITIVE'
ANGULAR.UNITS	:	'DEGREES'
FLEXIBLE	:	'FALSE'
SUPERELEMENT	:	'FALSE'
UP		
CREATE BODY		
NAME	:	'ARM.LFR'
CENTER.OF.GRAVITY	:	(21.5275, -37.78, 28.445)
TYPE.ANGULAR.COORD	:	'BRYANT'

ANGLE.1	::= '0.0'
ANGLE.2	::= '13.84'
ANGLE.3	::= '0.0'
FIXED.TO.GROUND	::= 'FALSE'
MASS	::= '0.0932'
INERTIA.XXL	::= '1.0'
INERTIA.YYL	::= '1.0'
INERTIA.ZZL	::= '1.0'
INERTIA.XYL	::= '0.0'
INERTIA.XZL	::= '0.0'
INERTIA.YZL	::= '0.0'
XG.FORCE	::= '0.0'
YG.FORCE	::= '0.0'
ZG.FORCE	::= '0.0'
XL.TORQUE	::= '0.0'
YL.TORQUE	::= '0.0'
ZL.TORQUE	::= '0.0'
CURVE.XGF	::= 'NONE'
CURVE.YGF	::= 'NONE'
CURVE.ZGF	::= 'NONE'
CURVE.XLT	::= 'NONE'
CURVE.YLT	::= 'NONE'
CURVE.ZLT	::= 'NONE'
SIGN.E0	::= 'POSITIVE'
ANGULAR.UNITS	::= 'DEGREES'
FLEXIBLE	::= 'FALSE'
SUPERELEMENT	::= 'FALSE'
UP	
CREATE BODY	
NAME	::= 'ARM.LRL'
CENTER.OF.GRAVITY	::= (-21.5275, -170.77, 28.445)
TYPE.ANGULAR.COORD	::= 'BRYANT'
ANGLE.1	::= '0.0'
ANGLE.2	::= '-13.84'
ANGLE.3	::= '0.0'
FIXED.TO.GROUND	::= 'FALSE'
MASS	::= '0.0932'
INERTIA.XXL	::= '1.0'
INERTIA.YYL	::= '1.0'
INERTIA.ZZL	::= '1.0'
INERTIA.XYL	::= '0.0'
INERTIA.XZL	::= '0.0'
INERTIA.YZL	::= '0.0'
XG.FORCE	::= '0.0'
YG.FORCE	::= '0.0'
ZG.FORCE	::= '0.0'
XL.TORQUE	::= '0.0'
YL.TORQUE	::= '0.0'
ZL.TORQUE	::= '0.0'
CURVE.XGF	::= 'NONE'
CURVE.YGF	::= 'NONE'
CURVE.ZGF	::= 'NONE'
CURVE.XLT	::= 'NONE'
CURVE.YLT	::= 'NONE'

CURVE.ZLT	::= 'NONE'
SIGN.EO	::= 'POSITIVE'
ANGULAR.UNITS	::= 'DEGREES'
FLEXIBLE	::= 'FALSE'
SUPERELEMENT	::= 'FALSE'
UP	
CREATE BODY	
NAME	::= 'ARM.LKR'
CENTER.OF.GRAVITY	::= (21.5275, -170.77, 28.445)
TYPE.ANGULAR.COORD	::= 'BRYANT'
ANGLE.1	::= '0.0'
ANGLE.2	::= '13.84'
ANGLE.3	::= '0.0'
FIXED.TO.GROUND	::= 'FALSE'
MASS	::= '0.0932'
INERTIA.XXL	::= '1.0'
INERTIA.YYL	::= '1.0'
INERTIA.ZZL	::= '1.0'
INERTIA.XYL	::= '0.0'
INERTIA.XZL	::= '0.0'
INERTIA.YZL	::= '0.0'
XG.FORCE	::= '0.0'
YG.FORCE	::= '0.0'
ZG.FORCE	::= '0.0'
XL.TORQUE	::= '0.0'
YL.TORQUE	::= '0.0'
ZL.TORQUE	::= '0.0'
CURVE.XGF	::= 'NONE'
CURVE.YGF	::= 'NONE'
CURVE.ZGF	::= 'NONE'
CURVE.XLT	::= 'NONE'
CURVE.YLT	::= 'NONE'
CURVE.ZLT	::= 'NONE'
SIGN.EO	::= 'POSITIVE'
ANGULAR.UNITS	::= 'DEGREES'
FLEXIBLE	::= 'FALSE'
SUPERELEMENT	::= 'FALSE'
UP	
CREATE BODY	
NAME	::= 'ARM.UFL'
CENTER.OF.GRAVITY	::= (-23.1765, -41.935, 39.3145)
TYPE.ANGULAR.COORD	::= 'BRYANT'
ANGLE.1	::= '12.557'
ANGLE.2	::= '0.0'
ANGLE.3	::= '-8.209'
FIXED.TO.GROUND	::= 'FALSE'
MASS	::= '0.0311'
INERTIA.XXL	::= '1.0'
INERTIA.YYL	::= '1.0'
INERTIA.ZZL	::= '1.0'
INERTIA.XYL	::= '0.0'
INERTIA.XZL	::= '0.0'
INERTIA.YZL	::= '0.0'
XG.FORCE	::= '0.0'

YG.FORCE	::= '0.0'
ZG.FORCE	::= '0.0'
XL.TORQUE	::= '0.0'
YL.TORQUE	::= '0.0'
ZL.TORQUE	::= '0.0'
CURVE.XGF	::= 'NONE'
CURVE.YGF	::= 'NONE'
CURVE.ZGF	::= 'NONE'
CURVE.XLT	::= 'NONE'
CURVE.YLT	::= 'NONE'
CURVE.ZLT	::= 'NONE'
SIGN.E0	::= 'POSITIVE'
ANGULAR.UNITS	::= 'DEGREES'
FLEXIBLE	::= 'FALSE'
SUPERELEMENT	::= 'FALSE'

UP

CREATE BODY

NAME	::= 'ARM.UFR'
CENTER.OF.GRAVITY	::= (23.1765, -41.935, 39.3445)
TYPE.ANGULAR.COORD	::= 'BRYANT'
ANGLE.1	::= '12.557'
ANGLE.2	::= '0.0'
ANGLE.3	::= '8.209'
FIXED.TO.GROUND	::= 'FALSE'
MASS	::= '0.0311'
INERTIA.XXL	::= '1.0'
INERTIA.YYL	::= '1.0'
INERTIA.ZZL	::= '1.0'
INERTIA.XYL	::= '0.0'
INERTIA.XZL	::= '0.0'
INERTIA.YZL	::= '0.0'
XG.FORCE	::= '0.0'
YG.FORCE	::= '0.0'
ZG.FORCE	::= '0.0'
XL.TORQUE	::= '0.0'
YL.TORQUE	::= '0.0'
ZL.TORQUE	::= '0.0'
CURVE.XGF	::= 'NONE'
CURVE.YGF	::= 'NONE'
CURVE.ZGF	::= 'NONE'
CURVE.XLT	::= 'NONE'
CURVE.YLT	::= 'NONE'
CURVE.ZLT	::= 'NONE'
SIGN.E0	::= 'POSITIVE'
ANGULAR.UNITS	::= 'DEGREES'
FLEXIBLE	::= 'FALSE'
SUPERELEMENT	::= 'FALSE'

UP

CREATE BODY

NAME	::= 'ARM.URL'
CENTER.OF.GRAVITY	::= (-23.1825, -165.875, 39.4625)
TYPE.ANGULAR.COORD	::= 'BRYANT'
ANGLE.1	::= '0.0'
ANGLE.2	::= '-2.21'

E-18

ANGLE.3	: = '0.0'
FIXED.TO.GROUND	: = 'FALSE'
MASS	: = '0.0311'
INERTIA.XXL	: = '1.0'
INERTIA.YYL	: = '1.0'
INERTIA.ZZL	: = '1.0'
INERTIA.XYL	: = '0.0'
INERTIA.XZL	: = '0.0'
INERTIA.YZL	: = '0.0'
XG.FORCE	: = '0.0'
YG.FORCE	: = '0.0'
ZG.FORCE	: = '0.0'
XL.TORQUE	: = '0.0'
YL.TORQUE	: = '0.0'
ZL.TORQUE	: = '0.0'
CURVE.XGF	: = 'NONE'
CURVE.YGF	: = 'NONE'
CURVE.ZGF	: = 'NONE'
CURVE.XLT	: = 'NONE'
CURVE.YLT	: = 'NONE'
CURVE.ZLT	: = 'NONE'
SIGN.E0	: = 'POSITIVE'
ANGULAR.UNITS	: = 'DEGREES'
FLEXIBLE	: = 'FALSE'
SUPERELEMENT	: = 'FALSE'
UP	
CREATE BODY	
NAME	: = 'ARM.URR'
CENTER.OF.GRAVITY	: = (23.1825, -165.875, 39.4625)
TYPE.ANGULAR.COORD	: = 'BRYANT'
ANGLE.1	: = '0.0'
ANGLE.2	: = '2.21'
ANGLE.3	: = '0.0'
FIXED.TO.GROUND	: = 'FALSE'
MASS	: = '0.0311'
INERTIA.XXL	: = '1.0'
INERTIA.YYL	: = '1.0'
INERTIA.ZZL	: = '1.0'
INERTIA.XYL	: = '0.0'
INERTIA.XZL	: = '0.0'
INERTIA.YZL	: = '0.0'
XG.FORCE	: = '0.0'
YG.FORCE	: = '0.0'
ZG.FORCE	: = '0.0'
XL.TORQUE	: = '0.0'
YL.TORQUE	: = '0.0'
ZL.TORQUE	: = '0.0'
CURVE.XGF	: = 'NONE'
CURVE.YGF	: = 'NONE'
CURVE.ZGF	: = 'NONE'
CURVE.XLT	: = 'NONE'
CURVE.YLT	: = 'NONE'
CURVE.ZLT	: = 'NONE'
SIGN.E0	: = 'POSITIVE'

ANGULAR.UNITS	:= 'DEGREES'
FLEXIBLE	:= 'FALSE'
SUPERELEMENT	:= 'FALSE'
UP	
CREATE BODY	
NAME	:= 'WHEEL.FL'
CENTER.OF.GRAVITY	:= (-35.815, -39.37, 29.735)
TYPE.ANGULAR.COORD	:= 'BRYANT'
ANGLE.1	:= '0.0'
ANGLE.2	:= '0.0'
ANGLE.3	:= '-0.246'
FIXED.TO.GROUND	:= 'FALSE'
MASS	:= '0.5047'
INERTIA.XXL	:= '1.0'
INERTIA.YYL	:= '1.0'
INERTIA.ZZL	:= '1.0'
INERTIA.XYL	:= '0.0'
INERTIA.XZL	:= '0.0'
INERTIA.YZL	:= '0.0'
XG.FORCE	:= '0.0'
YG.FORCE	:= '0.0'
ZG.FORCE	:= '0.0'
XL.TORQUE	:= '0.0'
YL.TORQUE	:= '0.0'
ZL.TORQUE	:= '0.0'
CURVE.XGF	:= 'NONE'
CURVE.YGF	:= 'NONE'
CURVE.ZGF	:= 'NONE'
CURVE.XLT	:= 'NONE'
CURVE.YLT	:= 'NONE'
CURVE.ZLT	:= 'NONE'
SIGN.EO	:= 'POSITIVE'
ANGULAR.UNITS	:= 'DEGREES'
FLEXIBLE	:= 'FALSE'
SUPERELEMENT	:= 'FALSE'
UP	
CREATE BODY	
NAME	:= 'WHEEL.FR'
CENTER.OF.GRAVITY	:= (35.815, -39.37, 29.735)
TYPE.ANGULAR.COORD	:= 'BRYANT'
ANGLE.1	:= '0.0'
ANGLE.2	:= '0.0'
ANGLE.3	:= '0.246'
FIXED.TO.GROUND	:= 'FALSE'
MASS	:= '0.5047'
INERTIA.XXL	:= '1.0'
INERTIA.YYL	:= '1.0'
INERTIA.ZZL	:= '1.0'
INERTIA.XYL	:= '0.0'
INERTIA.XZL	:= '0.0'
INERTIA.YZL	:= '0.0'
XG.FORCE	:= '0.0'
YG.FORCE	:= '0.0'
ZG.FORCE	:= '0.0'

XL.TORQUE	::= '0.0'
YL.TORQUE	::= '0.0'
ZL.TORQUE	::= '0.0'
CURVE.XGF	::= 'NONE'
CURVE.YGF	::= 'NONE'
CURVE.ZGF	::= 'NONE'
CURVE.XLT	::= 'NONE'
CURVE.YLT	::= 'NONE'
CURVE.ZLT	::= 'NONE'
SIGN.E0	::= 'POSITIVE'
ANGULAR.UNITS	::= 'DEGREES'
FLEXIBLE	::= 'FALSE'
SUPERELEMENT	::= 'FALSE'
UP	
CREATE BODY	
NAME	::= 'WHEEL.RL'
CENTER.OF.GRAVITY	::= (-35.815, -169.37, 29.735)
TYPE.ANGULAR.COORD	::= 'BRYANT'
ANGLE.1	::= '0.0'
ANGLE.2	::= '0.0'
ANGLE.3	::= '0.246'
FIXED.TO.GROUND	::= 'FALSE'
MASS	::= '0.5046'
INERTIA.XXL	::= '1.0'
INERTIA.YYL	::= '1.0'
INERTIA.ZZL	::= '1.0'
INERTIA.XYL	::= '0.0'
INERTIA.XZL	::= '0.0'
INERTIA.YZL	::= '0.0'
XG.FORCE	::= '0.0'
YG.FORCE	::= '0.0'
ZG.FORCE	::= '0.0'
XL.TORQUE	::= '0.0'
YL.TORQUE	::= '0.0'
ZL.TORQUE	::= '0.0'
CURVE.XGF	::= 'NONE'
CURVE.YGF	::= 'NONE'
CURVE.ZGF	::= 'NONE'
CURVE.XLT	::= 'NONE'
CURVE.YLT	::= 'NONE'
CURVE.ZLT	::= 'NONE'
SIGN.E0	::= 'POSITIVE'
ANGULAR.UNITS	::= 'DEGREES'
FLEXIBLE	::= 'FALSE'
SUPERELEMENT	::= 'FALSE'
UP	
CREATE BODY	
NAME	::= 'WHEEL.RR'
CENTER.OF.GRAVITY	::= (35.815, -169.37, 29.735)
TYPE.ANGULAR.COORD	::= 'BRYANT'
ANGLE.1	::= '0.0'
ANGLE.2	::= '0.0'
ANGLE.3	::= '-0.246'
FIXED.TO.GROUND	::= 'FALSE'

MASS
 INERTIA.XXL
 INERTIA.YYL
 INERTIA.ZZL
 INERTIA.XYL
 INERTIA.XZL
 INERTIA.YZL
 XG.FORCE
 YG.FORCE
 ZG.FORCE
 XL.TORQUE
 YL.TORQUE
 ZL.TORQUE
 CURVE.XGF
 CURVE.YGF
 CURVE.ZGF
 CURVE.XLT
 CURVE.YLT
 CURVE.ZLT
 SIGN.EO
 ANGULAR.UNITS
 FLEXIBLE
 SUPERELEMENT

:=" 0.5046'
 :=" 1.0'
 :=" 1.0'
 :=" 1.0'
 :=" 0.0'
 :=" 0.0'
 :=" 0.0'
 :=" 0.0'
 :=" 0.0'
 :=" 0.0'
 :=" 0.0'
 :=" 0.0'
 :=" 0.0'
 :=" NONE'
 :=" NONE'
 :=" NONE'
 :=" NONE'
 :=" NONE'
 :=" NONE'
 :=" POSITIVE'
 :=" DEGREES'
 :=" FALSE'
 :=" FALSE'

IJP

CREATE BODY

NAME
 CENTER.OF.GRAVITY
 TYPE.ANGULAR.COORD
 ANGLE.1
 ANGLE.2
 ANGLE.3
 FIXED.TO.GROUND
 MASS
 INERTIA.XXL
 INERTIA.YYL
 INERTIA.ZZL
 INERTIA.XYL
 INERTIA.XZL
 INERTIA.YZL
 XG.FORCE
 YG.FORCE
 ZG.FORCE
 XL.TORQUE
 YL.TORQUE
 ZL.TORQUE
 CURVE.XGF
 CURVE.YGF
 CURVE.ZGF
 CURVE.XLT
 CURVE.YLT
 CURVE.ZLT
 SIGN.EO
 ANGULAR.UNITS
 FLEXIBLE

:=" PITHAN.ARM'
 :=" (-9.811, -52.936, 33.236)
 :=" BRYANT'
 :=" -18.3'
 :=" 0.0'
 :=" 0.0'
 :=" FALSE'
 :=" 0.0129'
 :=" 1.0'
 :=" 1.0'
 :=" 1.0'
 :=" 0.0'
 :=" 0.0'
 :=" 0.0'
 :=" 0.0'
 :=" 0.0'
 :=" 0.0'
 :=" 0.0'
 :=" 0.0'
 :=" 0.0'
 :=" 0.0'
 :=" 0.0'
 :=" 0.0'
 :=" NONE'
 :=" NONE'
 :=" NONE'
 :=" NONE'
 :=" NONE'
 :=" NONE'
 :=" NONE'
 :=" POSITIVE'
 :=" DEGREES'
 :=" FALSE'

SUPERELEMENT	:= 'FALSE'
UP	
CREATE BODY	
NAME	:= 'STEERING.LINK'
CENTER.OF.GRAVITY	:= (0.000, -50.556, 32.433)
TYPE.ANGULAR.COORD	:= 'BRYANT'
ANGLE.1	:= '-18.5'
ANGLE.2	:= '0.0'
ANGLE.3	:= '0.0'
FIXED.TO.GROUND	:= 'FALSE'
MASS	:= '.0518'
INERTIA.XXL	:= '1.0'
INERTIA.YYL	:= '1.0'
INERTIA.ZZL	:= '1.0'
INERTIA.XYL	:= '0.0'
INERTIA.XZL	:= '0.0'
INERTIA.YZL	:= '0.0'
XG.FORCE	:= '0.0'
YG.FORCE	:= '0.0'
ZG.FORCE	:= '0.0'
XL.TORQUE	:= '0.0'
YL.TORQUE	:= '0.0'
ZL.TORQUE	:= '0.0'
CURVE.XGF	:= 'NONE'
CURVE.YGF	:= 'NONE'
CURVE.ZGF	:= 'NONE'
CURVE.XLT	:= 'NONE'
CURVE.YLT	:= 'NONE'
CURVE.ZLT	:= 'NONE'
SIGN.E0	:= 'POSITIVE'
ANGULAR.UNITS	:= 'DEGREES'
FLEXIBLE	:= 'FALSE'
SUPERELEMENT	:= 'FALSE'
UP	
CREATE INITIAL.CONDITION	
NAME	:= 'INIT.CHASSIS.ORIEN'
BODY.1.NAME	:= 'CHASSIS'
BODY.2.NAME	:= 'NONE'
ELEMENT.NAME	:= 'NONE'
TYPE.INITIAL.COND	:= 'ORIENTATION'
INITIAL.VALUE	:= '0.0'
TIME.DERIVATIVE	:= '0.0'
OMEGA.Y	:= '0.0'
OMEGA.Z	:= '0.0'
P.ON.BODY.1	:= (0.0, 0.0, 0.0)
P.ON.BODY.2	:= (0.0, 0.0, 0.0)
EXTRA.COORD	:= '0'
ANGULAR.UNITS	:= 'DEGREES'
UP	
CREATE INITIAL.CONDITION	
NAME	:= 'INIT.CHASSIS.X'
BODY.1.NAME	:= 'CHASSIS'
BODY.2.NAME	:= 'NONE'
ELEMENT.NAME	:= 'NONE'

TYPE.INITIAL.COND	:= 'X'
INITIAL.VALUE	:= '0.0'
TIME.DERIVATIVE	:= '0.0'
OMEGA.Y	:= '0.0'
OMEGA.Z	:= '0.0'
P.ON.BODY.1	:= (0.0, 0.0, 0.0)
P.ON.BODY.2	:= (0.0, 0.0, 0.0)
EXTRA.COORD	:= '0'
ANGULAR.UNITS	:= 'DEGREES'
UP	
CREATE INITIAL.CONDITION	
NAME	:= 'INIT.CHASSIS.Y'
BODY.1.NAME	:= 'CHASSIS'
BODY.2.NAME	:= 'NONE'
ELEMENT.NAME	:= 'NONE'
TYPE.INITIAL.COND	:= 'Y'
INITIAL.VALUE	:= '0.0'
TIME.DERIVATIVE	:= '264.000'
OMEGA.Y	:= '0.0'
OMEGA.Z	:= '0.0'
P.ON.BODY.1	:= (0.0, 0.0, 0.0)
P.ON.BODY.2	:= (0.0, 0.0, 0.0)
EXTRA.COORD	:= '0'
ANGULAR.UNITS	:= 'DEGREES'
UP	
CREATE INITIAL.CONDITION	
NAME	:= 'INIT.CHASSIS.Z'
BODY.1.NAME	:= 'CHASSIS'
BODY.2.NAME	:= 'NONE'
ELEMENT.NAME	:= 'NONE'
TYPE.INITIAL.COND	:= 'Z'
INITIAL.VALUE	:= '0.0'
TIME.DERIVATIVE	:= '0.0'
OMEGA.Y	:= '0.0'
OMEGA.Z	:= '0.0'
P.ON.BODY.1	:= (0.0, 0.0, 0.0)
P.ON.BODY.2	:= (0.0, 0.0, 0.0)
EXTRA.COORD	:= '0'
ANGULAR.UNITS	:= 'DEGREES'
UP	
CREATE INITIAL.CONDITION	
NAME	:= 'INIT.WHEEL.FL'
BODY.1.NAME	:= 'WHEEL.FL'
BODY.2.NAME	:= 'NONE'
ELEMENT.NAME	:= 'NONE'
TYPE.INITIAL.COND	:= 'Z'
INITIAL.VALUE	:= '0.0'
TIME.DERIVATIVE	:= '0.0'
OMEGA.Y	:= '0.0'
OMEGA.Z	:= '0.0'
P.ON.BODY.1	:= (0.0, 0.0, 0.0)
P.ON.BODY.2	:= (0.0, 0.0, 0.0)
EXTRA.COORD	:= '0'
ANGULAR.UNITS	:= 'DEGREES'

UP	
CREATE INITIAL.CONDITION	
NAME	:= 'INIT.WHEEL.FR'
BODY.1.NAME	:= 'WHEEL.FR'
BODY.2.NAME	:= 'NONE'
ELEMENT.NAME	:= 'NONE'
TYPE.INITIAL.COND	:= 'Z'
INITIAL.VALUE	:= '0.0'
TIME.DERIVATIVE	:= '0.0'
OMEGA.Y	:= '0.0'
OMEGA.Z	:= '0.0'
P.ON.BODY.1	:= (0.0, 0.0, 0.0)
P.ON.BODY.2	:= (0.0, 0.0, 0.0)
EXTRA.COORD	:= '0'
ANGULAR.UNITS	:= 'DEGREES'
UP	
CREATE INITIAL.CONDITION	
NAME	:= 'INIT.WHEEL.RL'
BODY.1.NAME	:= 'WHEEL.RL'
BODY.2.NAME	:= 'NONE'
ELEMENT.NAME	:= 'NONE'
TYPE.INITIAL.COND	:= 'Z'
INITIAL.VALUE	:= '0.0'
TIME.DERIVATIVE	:= '0.0'
OMEGA.Y	:= '0.0'
OMEGA.Z	:= '0.0'
P.ON.BODY.1	:= (0.0, 0.0, 0.0)
P.ON.BODY.2	:= (0.0, 0.0, 0.0)
EXTRA.COORD	:= '0'
ANGULAR.UNITS	:= 'DEGREES'
UP	
CREATE INITIAL.CONDITION	
NAME	:= 'INIT.WHEEL.RR'
BODY.1.NAME	:= 'WHEEL.RR'
BODY.2.NAME	:= 'NONE'
ELEMENT.NAME	:= 'NONE'
TYPE.INITIAL.COND	:= 'Z'
INITIAL.VALUE	:= '0.0'
TIME.DERIVATIVE	:= '0.0'
OMEGA.Y	:= '0.0'
OMEGA.Z	:= '0.0'
P.ON.BODY.1	:= (0.0, 0.0, 0.0)
P.ON.BODY.2	:= (0.0, 0.0, 0.0)
EXTRA.COORD	:= '0'
ANGULAR.UNITS	:= 'DEGREES'
UP	
CREATE DRIVER	
NAME	:= 'DRIVER'
BODY.1.NAME	:= 'NONE'
BODY.2.NAME	:= 'NONE'
TYPE.DRIVER	:= 'REL.ANGLE'
DRIVING.FUNCTION	:= 'GENERAL'
FUNCTION.PARAMETERS	:= (0.0, 0.0, 0.0, 0.0)
P.ON.BODY.1	:= (0.0, 0.0, 0.0)

```

P.ON.BODY.2      := ( 0.0, 0.0, 0.0 )
Q.ON.BODY.1      := ( 0.0, 0.0, 1.0 )
Q.ON.BODY.2      := ( 0.0, 0.0, 1.0 )
R.ON.BODY.1      := ( 1.0, 0.0, 0.0 )
R.ON.BODY.2      := ( 1.0, 0.0, 0.0 )
CURVE.DRIVER     := 'TRAJECTORY'
JOINT.NAME       := 'PITMAN.REV'
ANGULAR.UNITS    := 'DEGREES'

```

UP

CREATE CURVE

```

NAME             := 'TIRE.COEFF'
TYPE.DATA        := 'PAIRED.XY'
SLOPE.LEFT      := '4.000'
SLOPE.RIGHT     := '0.000'
SCALE.X         := '1.0'
SCALE.Y         := '1.0'
START.X         := '0.0'
INCREMENT.X     := '0.0'
INTERPOLATION    := 'CUBIC'

```

DATA

0.000000000000000E+00	0.000000000000000E+00	0.200000000000000E-01	0.800000000000
0.400000000000000E-01	0.200000000000000	0.800000000000000E-01	0.49500000000
0.105000000000000	0.700000000000000	0.125000000000000	0.76000000000
0.165000000000000	0.795000000000000	0.220000000000000	0.79500000000
0.295000000000000	0.750000000000000	0.430000000000000	0.70000000000
1.000000000000000	0.600000000000000		

ENDDATA

UP

CREATE CURVE

```

NAME             := 'BIAS.TIRE.20PSI'
TYPE.DATA        := 'PAIRED.XY'
SLOPE.LEFT      := '666.7'
SLOPE.RIGHT     := '1600.000'
SCALE.X         := '1.0'
SCALE.Y         := '1.0'
START.X         := '0.0'
INCREMENT.X     := '0.0'
INTERPOLATION    := 'CUBIC'

```

DATA

0.000000000000000E+00	0.000000000000000E+00	0.100000000000000	66.670000000
0.200000000000000	125.000000000000	0.300000000000000	175.0000000
0.400000000000000	250.000000000000	0.500000000000000	375.0000000
0.600000000000000	475.000000000000	0.700000000000000	600.0000000
0.800000000000000	700.000000000000	1.000000000000000	975.0000000
1.200000000000000	1250.00000000000	1.400000000000000	1500.0000000
1.600000000000000	1800.00000000000	1.800000000000000	2100.0000000
2.000000000000000	2425.00000000000	2.200000000000000	2700.0000000
2.400000000000000	3125.00000000000	2.600000000000000	3350.0000000
2.800000000000000	3675.00000000000	3.000000000000000	3975.0000000
3.200000000000000	4300.00000000000		

ENDDATA

E-26

UP

CREATE CURVE

```

NAME             := 'BIAS.TIRE.30PSI'

```


DATA			
0.00000000000000E+00	0.00000000000000E+00	0.10000000000000	66.67000000
0.20000000000000	150.0000000000	0.30000000000000	225.000000
0.40000000000000	325.0000000000	0.50000000000000	475.000000
0.60000000000000	600.0000000000	0.70000000000000	725.000000
0.80000000000000	900.0000000000	1.00000000000000	1225.000000
1.20000000000000	1600.0000000000	1.40000000000000	1950.000000
1.60000000000000	2350.0000000000	1.80000000000000	2750.000000
2.00000000000000	3150.0000000000	2.20000000000000	3550.000000
2.40000000000000	3950.0000000000	2.60000000000000	4375.000000
2.80000000000000	4800.0000000000	3.00000000000000	5225.000000
3.20000000000000	5650.0000000000		

ۛۛۛ

```
NAME                := 'TRAJECTORY'
TYPE.DATA           := 'INCREMENTAL.X'
SLOPE.LEFT          := '0.0'
SLOPE.RIGHT         := '0.0'
SCALE.X             := '1.0'
SCALE.Y             := '1.0'
START.X             := '0.0'
INCREMENTAL.X       := '1000.0'
INTERPOLATION       := 'CUBIC'
```

[illegible]

ENDDATA

E-28

FILE: {AARDEMA.DADS3D.HMMUV.1037.HIGHCG.NATC}HMMUV_15MPH.INP

USER_INPUT FILE: HMMUV_15MPH.INP

TERRAIN: NATC Nevada Test Course May, 1987 Job# 2017-297

TIKE DATA: UMTRI (No Aligning Torque Data is available from UMTRI)

Roll Stiffness (lbs/rad) :

14692.0

Fore-Aft Offset used to give some distance before entering terrain
350.0

Vertical offset for each tire: (ZOFFSET(I), I=1:4 of tires)

13.38 13.38 13.38 13.38

Rotational Inertia of each wheel: (ROTINT(I), I=1:4 of wheels)

40.0 40.0 40.0 40.0

Run Flat Radius

12.50

Run Flat Stiffness

10000.0

Run Flat Damping

0.00

Trajectory Curve Name

TRAJECTORY

Speed Controller Command Vehicle Velocity:

264.00

Position error feedback gain PKP:

0.0

Velocity error feedback gain PKV:

0.0

Maximum output torque at each wheel @ 100% engine power TORMAX:

0.0

Rotation Point about global Z to get new vehicle orientation

0.0 0.0 0.0

Rotation Angle about global Z

0.0

Lateral Force versus slip and vertical force - 24PSI - UMTRI data

6 6

Slip Angle Data - 24 PSI - UMTRI data

0.0 0.01745 0.03491 0.06981 0.1396 0.2793

Vertical Force Data - 24PSI - UMTRI data

0.000 500.000 800.000 1700.000 2600.000 5000.000

Lateral Force Data - 24PSI - UMTRI data

0.0	0.0	0.0	0.0	0.0	0.0
0.0	84.500	157.500	271.000	367.500	416.500
0.0	139.000	254.500	424.500	577.000	642.500
0.0	277.500	511.000	880.500	1215.500	1378.000
0.0	313.000	578.000	1042.000	1580.000	1958.000
0.0	224.500	411.000	751.000	1397.500	2447.000

Lateral Force versus slip and vertical force - 24PSI - UMTRI data

6 6

Slip Angle Data - 24 PSI - UMTRI data

0.0 0.01745 0.03491 0.06981 0.1396 0.2793

Vertical Force Data - 24PSI - UMTRI data

0.000 500.000 800.000 1700.000 2600.000 5000.000

Lateral Force Data - 24PSI - UMTRI data

0.0	0.0	0.0	0.0	0.0	0.0
0.0	84.500	157.500	271.000	367.500	416.500

0.0	139.000	254.500	424.500	577.000	642.500
0.0	277.500	511.000	880.500	1215.500	1378.000
0.0	313.000	578.000	1042.000	1580.000	1958.000
0.0	224.500	411.000	751.000	1397.500	2447.000

Aligning Torque versus slip and vertical force - No Data from UMTRI

2 2

Slip Angle Data - No Data from UMTRI

0.0 1.000

Vertical Force Data - No Data from UMTRI

0.000 20000.00

Aligning Torque Data - No Data from UMTRI - Zero out the Torque

0.0 0.0

0.0 0.0

Aligning Torque versus slip and vertical force - No Data from UMTRI

2 2

Slip Angle Data - No Data from UMTRI

0.0 1.000

Vertical Force Data - No Data from UMTRI

0.000 20000.00

Aligning Torque Data - No Data from UMTRI - Zero out the Torque

0.0 0.0

0.0 0.0

GROUND SURFACE DATA: NATC Nevada Test Course Hwy, 1987 Job# 2017-297

2 72

X(I), I=1,NX (FORMAT SF10.4)

-108.0000 108.0000

Y(I), I=1,NY (FORMAT SF10.4)

0.0000	2.52	84.12	128.28	132.96	174.84	176.76	219.60
219.84	293.16	296.16	368.40	372.36	418.08	420.00	455.40
457.32	523.56	527.76	592.56	598.20	675.00	675.36	730.08
732.48	778.56	778.92	854.28	856.68	927.48	931.68	966.36
966.60	1023.24	1026.24	1081.68	1082.04	1132.80	1138.32	1201.56
1204.20	1236.96	1240.56	1276.68	1285.68	1378.44	1384.08	1460.40
1462.68	1496.76	1500.72	1543.92	1544.16	1621.80	1625.28	1690.20
1692.60	1760.40	1767.60	1805.40	1806.12	1864.44	1869.36	1946.88
1951.20	2000.00	3000.00	4000.00	5000.00	6000.00	7000.00	8000.00

Z(I), I=1,N

0.0000	-0.02	-0.60	7.80	9.18	21.51	22.08	11.76
11.72	-0.92	-1.44	8.04	8.87	18.44	18.84	9.72
9.43	-0.57	-1.20	-0.72	-0.09	8.48	8.52	19.90
20.40	8.76	8.72	0.15	-0.12	6.24	7.03	13.56
13.51	2.39	1.80	-0.84	-0.83	0.68	0.84	9.82
10.20	17.23	18.00	9.93	7.92	-0.11	-0.60	7.91
8.16	13.54	14.16	7.08	7.05	-2.28	-2.04	2.47
2.64	13.56	14.42	18.96	18.86	10.68	10.18	2.24
1.80	1.00	1.00	1.00	1.00	1.00	1.00	1.00

Z(I), I=1,N

1.13	1.08	-0.60	7.00	7.80	16.92	16.62	9.88
9.84	-0.12	0.27	9.57	10.08	14.40	14.08	8.12
7.80	-2.52	-2.32	0.70	0.96	6.84	6.90	16.56
16.29	11.20	11.16	0.12	0.40	8.52	9.00	14.72
14.76	5.16	4.91	0.27	0.24	1.32	1.99	9.72
10.40	18.84	18.80	9.60	8.73	-0.24	0.57	11.52
11.90	17.52	16.73	8.09	8.04	-2.76	-3.24	-0.60

E-30

-0.21	10.83	12.00	16.59	16.68	8.93	8.28	1.08
0.68	1.00	1.00	1.00	1.00	1.00	1.00	1.00

APPENDIX F
STATIC ANALYSIS INPUT DATA FILE

F-2

FILE: [AARDEMA.DADS3D.HMMWV.1037.REAR_SUSP.FORCE_XYZ]XYZFG_5000_JOINT.VB3
CREATE HEADER

THIS IS A MODEL OF THE RIGHT REAR SUSPENSION ELEMENTS
THE CHASSIS IS FIXED TO GROUND

THE SPHERICAL JOINT Z AXIS IS ALONG THE KINGPIN LINE
WHERE Z IS UPWARD AND X IS TO THE RIGHT

A CONSTANT X,Y,Z GLOBAL FORCE IS APPLIED TO THE WHEEL
TO DETERMINE THE FORCES IN THE OTHER ELEMENTS

ANALYSIS

CREATE SYSTEM.DATA

UNITS	:= 'ERG'
ANALYSIS.TYPE	:= 'DYNAMIC'
STARTING.TIME	:= '0.0'
ENDING.TIME	:= '1.0'
PRINT.INTERVAL	:= '0.05'
GRAVITY.SEAL.ELEVEL	:= '386.100'
1.GRAVITY	:= '0.0'
Y.GRAVITY	:= '0.0'
Z.GRAVITY	:= '-1.0'
SCALE.GRAVITY.COEFF	:= '1.0'
MATRIX.OPERATIONS	:= 'SPARSE'
REDUNDANCY.CHECK	:= 'TRUE'
LU.TOL	:= '1.0D-12'
ASSEMBLY.TOL	:= '1.0D-3'
BYPASS.ASSEMBLY	:= 'FALSE'
OUTPUT.FILE	:= 'BOTH'
REFERENCE.FRAME	:= 'GLOBAL'
DEBUG.FLAG	:= 'TRUE'

UP

CREATE DYNAMIC.DATA

REACTION.FORCES	:= 'TRUE'
FORCE.COORDINATES	:= 'JOINT'
PRINT.METHOD	:= 'INTERPOLATED'
MAX.INT.STEP	:= '0.05'
SOLUTION.TOL	:= '0.001'
INTEGRATION.TOL	:= '0.0001'

UP

UF

CONSTRAINTS

CREATE DISTANCE.CONSTRAINT

NAME	:= 'RAD-ROD.RR'
BODY.1.NAME	:= 'CHASSIS'
BODY.2.NAME	:= 'WHEEL.RR'
P.ON.BODY.1	:= (16.380, -161.980, 33.080)
P.ON.BODY.2	:= (32.327, -164.066, 30.405)
Q.ON.BODY.1	:= (16.380, -161.980, 34.080)
Q.ON.BODY.2	:= (32.327, -164.066, 31.405)
P.ON.BODY.1	:= (17.380, -161.980, 33.080)
P.ON.BODY.2	:= (33.327, -164.066, 30.405)
DISTANCE	:= '16.303798023773'
NODE.1	:= '0'
NODE.2	:= '0'

F-3

UP
UP
FORCE

CREATE TSDA

NAME	:= 'DUMMY_TSDA_1'
BODY.1.NAME	:= 'CHASSIS'
BODY.2.NAME	:= 'ARM.LRR'
SPRING.CONSTANT	:= '0.0'
FREE.LENGTH.SPRING	:= '0.0'
DAMPING.COEFFICIENT	:= '0.0'
ACTUATOR.FORCE	:= '0.0'
P.ON.BODY.1	:= (0.0, 0.0, 0.0)
P.ON.BODY.2	:= (0.0, 0.0, 0.0)
Q.ON.BODY.1	:= (0.0, 0.0, 1.0)
Q.ON.BODY.2	:= (0.0, 0.0, 1.0)
R.ON.BODY.1	:= (1.0, 0.0, 0.0)
R.ON.BODY.2	:= (1.0, 0.0, 0.0)
CURVE.SPRING	:= 'NONE'
CURVE.DAMPER	:= 'NONE'
CURVE.ACTUATOR	:= 'NONE'
NODE.1	:= '0'
NODE.2	:= '0'

UP

CREATE TSDA

NAME	:= 'DUMMY_TSDA_2'
BODY.1.NAME	:= 'CHASSIS'
BODY.2.NAME	:= 'ARM.LRR'
SPRING.CONSTANT	:= '0.0'
FREE.LENGTH.SPRING	:= '0.0'
DAMPING.COEFFICIENT	:= '0.0'
ACTUATOR.FORCE	:= '0.0'
P.ON.BODY.1	:= (0.0, 0.0, 0.0)
P.ON.BODY.2	:= (0.0, 0.0, 0.0)
Q.ON.BODY.1	:= (0.0, 0.0, 1.0)
Q.ON.BODY.2	:= (0.0, 0.0, 1.0)
R.ON.BODY.1	:= (1.0, 0.0, 0.0)
R.ON.BODY.2	:= (1.0, 0.0, 0.0)
CURVE.SPRING	:= 'NONE'
CURVE.DAMPER	:= 'NONE'
CURVE.ACTUATOR	:= 'NONE'
NODE.1	:= '0'
NODE.2	:= '0'

UP

CREATE TSDA

NAME	:= 'DUMMY_TSDA_3'
BODY.1.NAME	:= 'CHASSIS'
BODY.2.NAME	:= 'ARM.LRR'
SPRING.CONSTANT	:= '0.0'
FREE.LENGTH.SPRING	:= '0.0'
DAMPING.COEFFICIENT	:= '0.0'
ACTUATOR.FORCE	:= '0.0'
P.ON.BODY.1	:= (0.0, 0.0, 0.0)
P.ON.BODY.2	:= (0.0, 0.0, 0.0)
Q.ON.BODY.1	:= (0.0, 0.0, 1.0)

```

Q.ON.BODY.2           := ( 0.0, 0.0, 1.0 )
R.ON.BODY.1           := ( 1.0, 0.0, 0.0 )
R.ON.BODY.2           := ( 1.0, 0.0, 0.0 )
CURVE.SPRING          := 'NONE'
CURVE.DAMPER          := 'NONE'
CURVE.ACTUATOR        := 'NONE'
NODE.1                := '0'
NODE.2                := '0'

UP
CREATE TSDA
NAME                  := 'SPRING.RR'
BODY.1.NAME           := 'CHASSIS'
BODY.2.NAME           := 'ARM.LRR'
SPRING.CONSTANT        := '2108.00'
FREE.LENGTH.SPRING    := '15.030'
DAMPING.COEFFICIENT   := '0.0'
ACTUATOR.FORCE        := '0.0'
P.ON.BODY.1           := ( 19.747, -174.865, 40.868 )
P.ON.BODY.2           := ( 21.385, -174.597, 28.935 )
Q.ON.BODY.1           := ( 19.747, -174.865, 41.868 )
Q.ON.BODY.2           := ( 21.385, -174.597, 29.935 )
R.ON.BODY.1           := ( 20.747, -174.865, 40.868 )
R.ON.BODY.2           := ( 22.385, -174.597, 28.935 )
CURVE.SPRING          := 'NONE'
CURVE.DAMPER          := 'NONE'
CURVE.ACTUATOR        := 'NONE'
NODE.1                := '0'
NODE.2                := '0'

UP
CREATE TSDA
NAME                  := 'SHOCK.RR'
BODY.1.NAME           := 'CHASSIS'
BODY.2.NAME           := 'ARM.LRR'
SPRING.CONSTANT        := '0.0'
FREE.LENGTH.SPRING    := '0.0'
DAMPING.COEFFICIENT   := '0.0'
ACTUATOR.FORCE        := '0.0'
P.ON.BODY.1           := ( 19.598, -174.865, 43.492 )
P.ON.BODY.2           := ( 21.415, -174.597, 29.259 )
Q.ON.BODY.1           := ( 19.598, -174.865, 44.492 )
Q.ON.BODY.2           := ( 21.415, -174.597, 30.259 )
R.ON.BODY.1           := ( 20.598, -174.865, 43.492 )
R.ON.BODY.2           := ( 22.415, -174.597, 29.259 )
CURVE.SPRING          := 'NONE'
CURVE.DAMPER          := 'NONE'
CURVE.ACTUATOR        := 'NONE'
NODE.1                := '0'
NODE.2                := '0'

UP
UP
JOINTS
CREATE REVOLUTE.JOINT
NAME                  := 'REV.LRR'
BODY.1.NAME           := 'CHASSIS'

```

BODY.2.NAME	:= 'ARM.LRR'
P.ON.BODY.1	:= (12.09, -170.77, 30.770)
P.ON.BODY.2	:= (12.09, -170.77, 30.770)
Q.ON.BODY.1	:= (12.09, -169.77, 30.770)
Q.ON.BODY.2	:= (12.09, -169.77, 30.770)
R.ON.BODY.1	:= (13.09, -170.77, 30.770)
R.ON.BODY.2	:= (13.09, -170.77, 30.770)
NODE.1	:= '0'
NODE.2	:= '0'
UP	
CREATE REVOLUTE.JOINT	
NAME	:= 'REV.URR'
BODY.1.NAME	:= 'CHASSIS'
BODY.2.NAME	:= 'ARM.URR'
P.ON.BODY.1	:= (18.195, -162.380, 39.655)
P.ON.BODY.2	:= (18.195, -162.380, 39.655)
Q.ON.BODY.1	:= (18.195, -161.380, 39.655)
Q.ON.BODY.2	:= (18.195, -161.380, 39.655)
R.ON.BODY.1	:= (19.195, -162.380, 39.655)
R.ON.BODY.2	:= (19.195, -162.380, 39.655)
NODE.1	:= '0'
NODE.2	:= '0'
UP	
CREATE SPHERICAL.JOINT	
NAME	:= 'SPH.LRR'
BODY.1.NAME	:= 'ARM.LRR'
BODY.2.NAME	:= 'WHEEL.RR'
P.ON.BODY.1	:= (30.965, -169.370, 26.120)
P.ON.BODY.2	:= (30.965, -169.370, 26.120)
Q.ON.BODY.1	:= (28.170, -169.370, 39.270)
Q.ON.BODY.2	:= (28.170, -169.370, 39.270)
R.ON.BODY.1	:= (44.115, -169.370, 28.915)
R.ON.BODY.2	:= (44.115, -169.370, 28.915)
NODE.1	:= '0'
NODE.2	:= '0'
UP	
CREATE SPHERICAL.JOINT	
NAME	:= 'SPH.URR'
BODY.1.NAME	:= 'ARM.URR'
BODY.2.NAME	:= 'WHEEL.RR'
P.ON.BODY.1	:= (28.170, -169.370, 39.270)
P.ON.BODY.2	:= (28.170, -169.370, 39.270)
Q.ON.BODY.1	:= (25.375, -169.370, 52.420)
Q.ON.BODY.2	:= (25.375, -169.370, 52.420)
R.ON.BODY.1	:= (41.320, -169.370, 42.065)
R.ON.BODY.2	:= (41.320, -169.370, 42.065)
NODE.1	:= '0'
NODE.2	:= '0'
UP	
UP	
CREATE BODY	
NAME	:= 'CHASSIS'
CENTER.OF.GRAVITY	:= (0.585, -123.170, 63.064)
TYPE.ANGULAR.COORD	:= 'BRYANT'

ANGLE.1	::= '0.0'
ANGLE.2	::= '0.0'
ANGLE.3	::= '0.0'
FIXED.TO.GROUND	::= 'TRUE'
MASS	::= '20.049'
INERTIA.XXL	::= '41300.0'
INERTIA.YYL	::= '13900.0'
INERTIA.ZZL	::= '52300.0'
INERTIA.XYL	::= '0.0'
INERTIA.XZL	::= '0.0'
INERTIA.YZL	::= '0.0'
XG.FORCE	::= '0.0'
YG.FORCE	::= '0.0'
ZG.FORCE	::= '0.0'
XL.TORQUE	::= '0.0'
YL.TORQUE	::= '0.0'
ZL.TORQUE	::= '0.0'
CURVE.XGF	::= 'NONE'
CURVE.YGF	::= 'NONE'
CURVE.ZGF	::= 'NONE'
CURVE.XLT	::= 'NONE'
CURVE.YLT	::= 'NONE'
CURVE.ZLT	::= 'NONE'
SIGN.EO	::= 'POSITIVE'
ANGULAR.UNITS	::= 'DEGREES'
FLEXIBLE	::= 'FALSE'
SUPERELEMENT	::= 'FALSE'
UP	
CREATE BODY	
NAME	::= 'ARM.LRR'
CENTER.OF.GRAVITY	::= (21.5275, -170.77, 28.445)
TYPE.ANGULAR.COORD	::= 'BRYANT'
ANGLE.1	::= '0.0'
ANGLE.2	::= '13.84'
ANGLE.3	::= '0.0'
FIXED.TO.GROUND	::= 'FALSE'
MASS	::= '0.0932'
INERTIA.XXL	::= '1.0'
INERTIA.YYL	::= '1.0'
INERTIA.ZZL	::= '1.0'
INERTIA.XYL	::= '0.0'
INERTIA.XZL	::= '0.0'
INERTIA.YZL	::= '0.0'
XG.FORCE	::= '0.0'
YG.FORCE	::= '0.0'
ZG.FORCE	::= '0.0'
XL.TORQUE	::= '0.0'
YL.TORQUE	::= '0.0'
ZL.TORQUE	::= '0.0'
CURVE.XGF	::= 'NONE'
CURVE.YGF	::= 'NONE'
CURVE.ZGF	::= 'NONE'
CURVE.XLT	::= 'NONE'
CURVE.YLT	::= 'NONE'

CURVE.ZLT	:= 'NONE'
SIGN.EO	:= 'POSITIVE'
ANGULAR.UNITS	:= 'DEGREES'
FLEXIBLE	:= 'FALSE'
SUPERELEMENT	:= 'FALSE'
UP	
CREATE BODY	
NAME	:= 'ARM.URR'
CENTER.OF.GRAVITY	:= (23.1825, -165.875, 39.4625)
TYPE.ANGULAR.COORD	:= 'BRYANT'
ANGLE.1	:= '0.0'
ANGLE.2	:= '2.21'
ANGLE.3	:= '0.0'
FIXED.TO.GROUND	:= 'FALSE'
MASS	:= '0.0311'
INERTIA.XXL	:= '1.0'
INERTIA.YYL	:= '1.0'
INERTIA.ZZL	:= '1.0'
INERTIA.XYL	:= '0.0'
INERTIA.XZL	:= '0.0'
INERTIA.YZL	:= '0.0'
XG.FORCE	:= '0.0'
YG.FORCE	:= '0.0'
ZG.FORCE	:= '0.0'
XL.TORQUE	:= '0.0'
YL.TORQUE	:= '0.0'
ZL.TORQUE	:= '0.0'
CURVE.XGF	:= 'NONE'
CURVE.YGF	:= 'NONE'
CURVE.ZGF	:= 'NONE'
CURVE.XLT	:= 'NONE'
CURVE.YLT	:= 'NONE'
CURVE.ZLT	:= 'NONE'
SIGN.EO	:= 'POSITIVE'
ANGULAR.UNITS	:= 'DEGREES'
FLEXIBLE	:= 'FALSE'
SUPERELEMENT	:= 'FALSE'
UP	
CREATE BODY	
NAME	:= 'WHEEL.RR'
CENTER.OF.GRAVITY	:= (38.815, -169.37, 29.735)
TYPE.ANGULAR.COORD	:= 'BRYANT'
ANGLE.1	:= '0.0'
ANGLE.2	:= '0.0'
ANGLE.3	:= '-0.247'
FIXED.TO.GROUND	:= 'FALSE'
MASS	:= '0.5046'
INERTIA.XXL	:= '1.0'
INERTIA.YYL	:= '1.0'
INERTIA.ZZL	:= '1.0'
INERTIA.XYL	:= '0.0'
INERTIA.XZL	:= '0.0'
INERTIA.YZL	:= '0.0'
XG.FORCE	:= '2500.0'

YG.FORCE	::= '2500.0'
ZG.FORCE	::= '5000.0'
XL.TORQUE	::= '0.0'
YL.TORQUE	::= '-40887.5'
ZL.TORQUE	::= '0.0'
CURVE.XGF	::= 'NONE'
CURVE.YGF	::= 'NONE'
CURVE.ZGF	::= 'NONE'
CURVE.XLT	::= 'NONE'
CURVE.YLT	::= 'NONE'
CURVE.ZLT	::= 'NONE'
SIGN.EO	::= 'POSITIVE'
ANGULAR.UNITS	::= 'DEGREES'
FLEXIBLE	::= 'FALSE'
SUPERELEMENT	::= 'FALSE'
UP	
CREATE INITIAL.CONDITION	
NAME	::= 'INIT.KR'
BODY.1.NAME	::= 'WHEEL.KR'
BODY.2.NAME	::= 'NONE'
ELEMENT.NAME	::= 'NONE'
TYPE.INITIAL.COND	::= 'Z'
INITIAL.VALUE	::= '0.0'
TIME.DERIVATIVE	::= '0.0'
OMEGA.Y	::= '0.0'
OMEGA.Z	::= '0.0'
P.ON.BODY.1	::= (0.0, 0.0, 0.0)
P.ON.BODY.2	::= (0.0, 0.0, 0.0)
EXTRA.COORD	::= '0'
ANGULAR.UNITS	::= 'DEGREES'
UP	
%	

F-10

DISTRIBUTION LIST

	Copies
Commander	12
Defense Technical Information Center	
Bldg. 5, Cameron Station	
ATTN: DDAC	
Alexandria, VA 22304-9990	
Manager	2
Defense Logistics Studies	
Information Exchange	
ATTN: AMXMC-D	
Fort Lee, VA 23801-6044	
Commander	
U.S. Army Tank-Automotive Command	
ATTN: AMSTA-DDL (Technical Library)	2
AMSTA-CF (Mr. Orlicki)	1
AMSTA-R (Mr. Jackovich)	1
AMCPM-TV	3
AMSTA-UFA	8
AMSTA-RY	12
AMSTA-CR (Mr. Wheelock)	1
Warren, MI 48397-5000	
Director	
U.S. Army Materiel Systems Analysis	2
Activity (AMSAA)	
ATTN: AMSXY-CM (Mr. Fordyce)	
AMXSY-MP (Mr. Cohen)	
Aberdeen Proving Ground, MD 21005-5071	

DISTRIBUTION LIST (Continued)

	Copies
Superintendent US Military Academy ATTN: Dept. of Engineering Course Director for Autmv Engineering West Point, NY 10996	1
US Army Research Office P.O. Box 12211 ATTN: Dr. David Mann Research Triangle Park, NC 27709	1
HQDA Office of Dep Chief of Staff for Rsch Dev & Acquisition ATTN: Dir of Army Research, ARZ-A Dr. Lasser Washington D.C. 20310	1
Director US Army Human Engineering Lab Aberdeen Proving Grounds ATTN: Mr. Eckles APG, MD 21005	1
Commander US Army Military Equipment R&D Command ATTN: DRDME-RT Ft Belvoir, VA 22060	1
Director US Army Cold Regions Research & Engineering Lab P.O. Box 282 ATTN: Dr. Liston Library Hanover, NH 03755	1
Commander US Army Test & Evaluation Command Aberdeen Proving Grounds ATTN: AMSTE-BB AMSTE-TA APG, MD 21005	2

DISTRIBUTION LIST (Continued)

	Copies
Commander Rock Island Arsenal ATTN: SARRI-LR Rock Island, IL 61201	2
Commander US Army Yuma Proving Ground ATTN: STEYP-RPT STEYP-TE Yuma, AZ 85364	2
Director US Army Ballistic Research Lab Aberdeen Proving Grounds APG, MD 21005	1
Director US Army Corps of Engineers Waterways Experiment Station P.O. Box 631 ATTN: Mr. Nuttall Vicksburg, MS 39180	1
Director US Army Material Systems Analysis Agency Aberdeen Proving Grounds ATTN: Mr. Harold Burke APG, MD 21005	1
Director National Tillage Machinery Lab Box 792 Auburn, AL 36830	1
Director Keweenaw Research Center Michigan Technological Univ Houghton, MI 49931	1
HQ, DA ATTN: DAMA-AR DR. Herschner WASHINGTON, D.C. 20310	1

DISTRIBUTION LIST (Continued)

	Copies
Director Defense Advanced Research Projects Agency 1400 Wilson Boulevard Arlington, VA 22209	1
Commander US Army Materials and Mechanics Research Center ATTN: Mr. Adachi Watertown, MA 02172	1
General Research Corp 7655 Old Springhouse Road Westgate Research Park ATTN: Mr. A. Viilu McLean, VA 22101	1
President Army Armor and Engineer Board Fort Knox, KY 40121	1
Commander US Army Natic Laboratories ATTN: Technical Library Natick, MA 01760	1
Director USDA Forest Service Equipment Development Center 444 East Bonita Avenue San Dimes, CA 91773	1
Engineering Society Library 345 East 47th Street New York, NY 10017	1
HQ, DA Office of Dep Chief of Staff for Rsch, Dev & Acquisition ATTN: DAMA-AR Dr. Charles Church Washington, D.C. 20310	1

DISTRIBUTION LIST (Continued)

	Copies
Commander US Army Combined Arms Combat Developments Activity ATTN: ATCA-CCC-S Fort Leavenworth, KA 66207	1
Foreign Science & Tech Center 220 7th Street North East ATTN: AMXST-GEI Mr. Tim Nix Charlottesville, VA 22901	1
Commander US Army Development and Readiness Command 5001 Eisenhower Avenue ATTN: Dr. R.S. Wiseman Alexandria, VA 22333	1
Commander US Army Armament Research and Development Command ATTN: Mr. Rubin Dover, NJ 07801	1
US Marine Corps Mobility & Logistics Division Development and Ed Command ATTN: Mr. Hickson Quantico, VA 22134	1

END
DATE
FILMED

2-89

DTIC

